



UNIVERSITÀ
DEGLI STUDI
FIRENZE



ÉCOLE DOCTORALE
PRES I Bourgogne I Franche-Comté
Environnements - Santé

DOTTORATO DI RICERCA IN SCIENZE CHIMICHE

CICLO XXX

COORDINATORE Prof. Piero Baglioni

Extraction, purification, and structural analysis of glycosylated natural products, mimetics of native antigens involved in an immune response

Settore Scientifico Disciplinare Chimica Biorganica

Dottorando

Dott. Anne-Sophie CHAMPY-TIXIER

Tutore

Prof. Anna Maria Papini

Prof. Anne-Claire Mitaine-Offer

Coordinatore

Prof. Piero Baglioni

Anni 2014/2017

AKNOWLEDGEMENTS

My PhD project was performed in the context of a co-direction between the University of Firenze in Italy and the University of Bourgogne Franche-Comté in France. It was a real pleasure for me to discover two different research environments. I learnt a lot concerning research, language and life. It was really a unique and extraordinary experience. I had the opportunity to attend several national and international congresses and I could understand that research will have to be my future job. Now after three years of work, it is the end so I really would like to thank all people who help me during the PhD.

First, I would like to thank my two PhD directors:

- Pr. PAPINI Anna Maria Director of the Laboratory of Peptide and Protein Chemistry and Biology (Peptlab), University of Firenze, from the Chemistry Department “Ugo Schiff”, University of Firenze
- Pr. MITAINE-OFFER Anne-Claire, PEPITE EA4267 (Pathologies et épithéliums: prévention, innovation, traitement, évaluation), from the Laboratory of Pharmacognosy, University Bourgogne Franche-Comté.

They supported and helped me during the three years. Thanks to them, I am now finishing the PhD and I obtained a position as temporary teacher and researcher in Pharmacognosy at the University of Rouen in France.

I would like to thank Pr. LACAILLE-DUBOIS Marie-Aleth to welcome me in the Laboratory of Pharmacognosy in Dijon and also to transfer me all her knowledge in the field.

Then, a particular thank to my husband, my parents, my sister, my brother, my grandmother and all my family for their love, support, and patience.

Thanks to my friends and also my PhD friends (Carole, Christophe and Emilie); we spoke a lot about the PhD and we advanced together.

Thanks to the team of Pharmacognosy lab (Stéphanie YOUSFI, David PERTUIT) and to the team of Peptlab (Feliciana, Guiseppina, Mario, Francesca, Chiara, Fosca, Beatrice, Lorenzo...). You welcomed me, you helped me and it was a real pleasure to meet you.

Thanks to the University of Firenze and the University of Bourgogne Franche-Comté.

Thanks to the PhD school of the University of Firenze and the PhD school in health and environment (ES) of the University of Bourgogne France-Comté.

Thanks to the International Relationships and Erasmus office of the University of Firenze, Italy, for the Erasmus plus traineeship grant.

Thanks to the French association AROMAPRO, in particular to Dr Olivier TISSOT and Dr Marie-Alexandra SOLARI for their financial support and their trust.

Thank you very much for all. I hope I did not forget anyone. It was a real pleasure to do my PhD, to meet all of you and to be supported by each of you.

Abstract (English)

This PhD in co-direction between the Peptlab Laboratory of the University of Firenze (Italy) and the Laboratory of Pharmacognosy of the University of Bourgogne Franche-Comté (France), deals with extraction, purification and structural elucidation of saponins from plants as mimetic antigens involved in an immune response.

The phytochemical study of five species from three different families, *Wisteria frustecens*, *Wisteria floribunda* “macrobotrys” and *Wisteria floribunda* “rosea” from Fabaceae, *Weigela florida* “rumba” from Caprifoliaceae, and *Polygala acicularis* from Polygalaceae, allowed us to isolate sixteen natural glycosides: six with new structures, one analyzed for the first time in its native form, and nine which have been already described in the literature. These compounds were isolated using various chromatographic methods, and their structures were elucidated using mainly 2D NMR and mass spectrometry.

From the isolated glycosides, six were selected and tested as mimetics of native antigens involved in the immune response. Moreover, one flavonoid glycoside extracted from *Sophora japonica*, and one commercial triterpenic acid, ursolic acid, were also chosen as mimetics of native antigens. Immunoenzymatic assays (ELISA) were performed for each compound to evaluate their potential as mimetics of native antigens of multiple sclerosis and Rett syndrome. The IgM levels in sera of patients affected by multiple sclerosis and Rett syndrome were measured and compared to normal blood donors.

Concerning multiple sclerosis, no significant results were obtained for saponins, but in the case of Rett syndrome, interesting and surprising results were obtained. Indeed, the first hypothesis was that the glycosyl part of the molecule could be relevant for antibody recognition. In the case of Rett syndrome ursolic acid, an aglycone without any glycosidic part, demonstrated a good efficiency in IgM recognition. On the other hand, one triterpenic glycoside showed similar results. These results were discussed to define possible structure/activity relationships.

Keywords: Triterpene glycosides, NMR, ELISA tests, IgM, multiple sclerosis, Rett syndrome, antibodies

Abstract (French)

Cette thèse en cotutelle entre le Laboratoire Peptlab de l'Université de Florence en Italie et le Laboratoire de Pharmacognosie de l'Université de Bourgogne Franche-Comté en France, porte sur l'extraction, la purification et l'élucidation structurale de saponines d'origine végétale en tant que mimétiques d'antigènes impliqués dans une réponse immunitaire.

L'étude phytochimique de cinq espèces végétales appartenant à trois familles différentes, Fabaceae : *Wisteria frutescens*, *Wisteria floribunda* "macrobotrys", *Wisteria floribunda* "rosea", Caprifoliaceae : *Weigela florida* "rumba" et Polygalaceae : *Polygala acicularis*, a conduit à l'isolement de seize glycosides triterpéniques naturels parmi lesquelles six sont de structure nouvelle, une a été isolée sous sa forme native pour la première fois, et neuf déjà répertoriées dans la littérature. Les composés ont été isolés grâce à l'utilisation de différentes méthodes chromatographiques. Leurs structures ont été élucidées en utilisant principalement la RMN 2D et la spectrométrie de masse.

Parmi ces seize molécules, six ont été sélectionnées pour être testées en tant que mimétiques d'antigènes impliqués dans une réponse immunitaire. De plus, un flavonoïde glycosylé extrait de *Sophora japonica* et un acide triterpénique commercial, l'acide ursolique, ont eux aussi été choisis comme mimétiques d'antigènes. Des tests immunochimiques (ELISA) ont été réalisés afin d'évaluer leur potentiel en tant que mimétiques d'antigènes dans le sang de patients atteints de sclérose en plaque ou du syndrome de Rett. Le taux IgM dans le sérum des patients atteints de sclérose en plaque ou du syndrome de Rett a été mesuré et comparé à celui de donneurs sains.

Concernant la sclérose en plaque, les résultats sont peu significatifs concernant le potentiel des saponines en tant que mimétiques d'antigènes. Mais dans le cas du syndrome de Rett des résultats intéressants et surprenants ont été obtenus. En effet, l'hypothèse de départ était l'implication de la partie glycosylée dans la reconnaissance d'autoanticorps. Pour le syndrome de Rett, l'acide ursolique, qui est un aglycone, démontre une grande efficacité dans la reconnaissance d'IgM. Par contre, un triterpène glycosylé démontre lui aussi une efficacité semblable. Les résultats obtenus sont donc à analyser afin d'établir des relations structure/activité fiables.

Mots clés : Triterpènes glycosylés, RMN, tests ELISA, IgM, sclérose en plaque, syndrome de Rett, anticorps.

Abstract (Italian)

Questa tesi di dottorato in cotutela tra il laboratorio PeptLab dell'Università di Firenze e il laboratorio di farmacognosia dell'Université de Bourgogne Franche-Comté (Francia) tratta dell'estrazione, purificazione e caratterizzazione strutturale di saponine da piante, quali , mimetici di antigeni coinvolti nella risposta immunitaria.

Lo studio fitochimico di cinque specie da tre diverse famiglie la *Wisteria frustecens*, la *Wisteria floribunda* “macrobotrys” e la *Wisteria floribunda* “rosea” dalle Fabaceae, la *Weigela florida* “rumba” da Caprifoliaceae, e la *Polygala acicularis* da Polygalaceae, ci ha permesso di isolare sedici glicosidi naturali: sei con nuove strutture, uno caratterizzato per la prima volta nella sua forma nativa e nove che sono già stati repertoriati in letteratura. I composti sono stati isolati utilizzando varie tecniche cromatografiche e le loro strutture sono state elucidate essenzialmente tramite 2D NMR e spettrometria di massa.

Sei dei glicosidi isolati sono stati selezionati e utilizzati come mimetici di antigeni nativi coinvolti nella risposta immunitaria, così come un flavonoide glicoside estratto da *Sophora japonica*, e il triterpene derivato commerciale, l'acido ursolico. Test immunoenzimatici di tipo ELISA sono stati effettuati per ogni composto per valutare il loro potenziale quali antigeni che riconoscono anticorpi in sieri di pazienti affetti da sclerosi multipla e sindrome di Rett e il titolo in anticorpi è stato confrontato con quello in donatori sani.

Per quanto riguarda la sclerosi multipla non sono stati ottenuti risultati significativi con nessuna delle saponine, ma nel caso della sindrome di Rett, sono stati ottenuti risultati interessanti e sorprendenti. La prima ipotesi è che la parte glicosilica sia coinvolta nel riconoscimento di anticorpi. Ne caso della sindrome di Rett, l'acido ursolico, un aglicone senza porzione glicosidica ha mostrato una buona efficienza nel riconoscimento di IgM. D'altra parte un triterpene glicosidico ha mostrato risultati simili. Questi risultati sono stati discussi per tentare di stabilire una correlazione tra struttura e attività.

Keywords: Triterpeni glicosidici, NMR, ELISA, IgM, sclerosi multipla, sindrome di Rett, anticorpi

TABLE OF CONTENTS

GENERAL INTRODUCTION	2
Chapter 1: Immune-mediated diseases and diagnostics.....	5
1.1 Immune system	5
1.1.1 Innate and adaptative immunity	5
1.1.2 B and T lymphocytes	6
1.1.3 Autoimmunity.....	6
1.1.4 Antigens and antibodies	7
1.1 Multiple Sclerosis	9
1.2 Rett syndrome	10
1.3 Diagnostic methods.....	11
1.4 Research project.....	13
Chapter 2: Phytochemical study of five plants	17
2.1 Botanical study	17
2.1.1 Fabales order	17
2.1.2 Dipsacales order	21
2.2 Previous phytochemical works.....	24
2.2.1 Saponins	24
2.2.2 Isolated saponins from <i>Wisteria</i> genus	27
2.2.3 Isolated saponins from <i>Weigela</i> genus	33
2.2.4 Isolated saponins from <i>Polygala</i> genus.....	35
2.3 Materials and methods	37
2.3.1 Phytochemical study	37
2.3.1.1 Extraction and plant material.....	39
2.3.1.2 Analytic chromatographic methods	39
2.3.1.3 Preparative chromatographic methods	40
2.3.1.4 Lyophilisation	41
2.3.2 Structural elucidation	41
2.3.2.1 Mass spectrometry.....	41
2.3.2.2 Nuclear magnetic resonance (NMR)	43
2.4 Personal works	45
2.4.1 Extraction and isolation.....	45

2.4.2 Structural elucidation	53
Chapter 3: Peptide and glycopeptide synthesis and immunoenzymatic assays	107
3.1 Material and methods	107
3.1.1 Peptide and glycopeptide synthesis	107
3.1.2 Ursolic acid	107
3.1.3 Prosapogenin tenuifolin obtained by mild alkaline hydrolysis	107
3.1.4 Extraction of rutoside from <i>Sophora japonica</i>	108
3.1.5 Peptide synthesis.....	109
3.1.6 Immunoenzymatic assays with CSF114(Glc) and its unglucosylated analog	111
3.1.7 Immunoenzymatic assays of saponins, rutoside and ursolic acid.....	111
3.1.8 Statistical analysis.....	112
3.2 Personal works	112
3.2.1 Selection of molecules.....	112
3.2.2 Immunoenzymatic assays on multiple sclerosis patient sera	116
3.2.2.1 Selection of Multiple Sclerosis sera.....	116
3.2.2.2 SP-ELISA results	116
3.2.3 Immunoenzymatic assays on Rett syndrome patient sera	121
3.2.3.1 Selection of Rett syndrome sera	121
3.2.3.2 SP-ELISA results	121
GENERAL CONCLUSION.....	127
ABBREVIATIONS	129
LIST OF FIGURES AND TABLES	131
BIBLIOGRAPHY	135
LIST OF PERSONAL COMMUNICATIONS AND PUBLICATIONS	142
SUPPLEMENTARY DATA.....	144

GENERAL INTRODUCTION

GENERAL INTRODUCTION

Since a long time, people used plants to cure diseases. Nowadays, nature offers a large variety of active ingredients that have been characterized from plants. However, their synthesis is very often extremely complex. This is why it is important to continue performing phytochemical studies in order to discover new compounds with interesting pharmacological properties.

The laboratory of Pharmacognosy of the University of Bourgogne Franche-Comté in Dijon (France) has a long experience on extraction, purification and structural elucidation of saponins from plants. They discovered numerous new molecules and tested them to evaluate their biological properties. Saponins are amphiphilic glycosides, with many *in vitro* properties in various pharmacological fields. They are rarely used in their pure form in spite of various pharmacological activities *in vitro*, due to their potential toxicity. Plants, rich in saponins, are used in phytotherapy, in food and cosmetic industries.

A previous collaboration between the Laboratory of Pharmacognosy of the University of Bourgogne Franche-Comté (France) and the Laboratory of Peptide and Protein Chemistry and Biology (Peptlab) of the University of Firenze (Italy), on the use of saponins as antigens lead to interesting results. The Peptlab laboratory developed an N-glycosylated type I' beta-turn peptide structure termed CSF114 (Glc) that was demonstrated an efficient antigen to recognize autoantibodies in sera of patients affected by some autoimmune diseases. They assumed that the glucosyl moiety on an asparagine moiety was fundamental for antibody recognition with the idea in mind that an aberrant glycosylation could be triggered by a bacterial infection. This was recently published by the group. Therefore, the interest in glycosides gathered both laboratories. In particular, a collaboration was born around a common project aimed to use saponins as antigens for the recognition of different families of autoantibodies. Various triterpene glycosides were tested in case of patients affected by multiple sclerosis and interesting results were obtained which confirmed the potential role of glycosyl moieties.

According to these results, the aim of my PhD was to perform the extraction, purification and structural elucidation of new saponins from plants and testing them as mimetics of native antigens involved in an immune response. Two different diseases were chosen for the study: Multiple Sclerosis and Rett syndrome.

In this manuscript, I will present the phytochemical study of five plants rich in triterpenic glycosides: three species of the Fabaceae family: *Wisteria frutescens*, *Wisteria floribunda* “macrobotrys” and *Wisteria floribunda* “rosea”; one species of the Caprifoliaceae family: *Weigela florida* “rumba”, and one species of the Polygalaceae family: *Polygala acicularis*. Then, after selection of some isolated and characterized molecules, Enzyme Linked ImmunoSorbent Assays (ELISA tests) were performed using these saponins as mimetics of the native antigens to recognize antibodies in collections of patient sera and controls.

The present work is divided in three parts:

In the first part, I present generalities on the immune system, autoimmunity, multiple sclerosis and Rett syndrome.

In the second part, after some botanical data, a bibliographic synthesis on the family and the genus of the studied plants is realized. Then, the personal phytochemical study including techniques, methods and results are presented.

The third part is devoted to the results of the immunoenzymatic assays after selection of the molecules to demonstrate the potential role of saponins as mimetics of native antigens.

CHAPTER 1:

Immune-mediated diseases and diagnostics

Chapter 1: Immune-mediated diseases and diagnostics

The essential functions of the immune system are to maintain the coherence of the cells and tissues and to ensure their integrity by rejecting foreign aggressive substances or infectious agents that is, the “non-self”, and the “modified self” antigens while respecting the normal components of the host, that is, the “unmodified self-antigens” [1].

1.1 Immune system

Immunity is one of the most prominent examples of complex machinery merging together chemistry and biology to serve a very simple, yet complex purpose: protecting the organism against any form of external agents (Figure 1) [2].

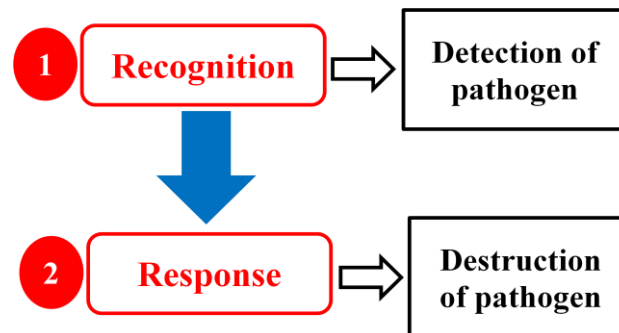


Figure 1: Function of the immune system

1.1.1 Innate and adaptative immunity

To preserve the immune system integrity and coherence there are two strategies:

- The innate immunity, also known as non adaptative immunity that is involved in the destruction of pathogen agents and prevents infections with an immediate non-specific response [3]. This system is present in almost all living organisms. The cells of the innate system are: the leukocytes (or white blood cells), the phagocytes (dendritic cells, monocytes, neutrophils, macrophages) and the Natural Killer cells (NK cells). These cells absorb pathogens to destroy them and release inflammatory mediators such as cytokines which stimulate other responses from the organism. Another part of the innate system is the complement system which is a biochemical cascade of reactions that can be activated to eliminate pathogens.
- The adaptative immunity which is much more specific can create immunological memory after an initial response to a specific pathogen, leading to an enhanced

response after encountering that pathogen. The adaptative response involves T lymphocytes and B lymphocytes derived from the same multipotent hematopoietic stem cells. B cells play a role in the humoral immune response contrary to T cells, which are involved in cell-mediated immune responses but both are produced in the bone marrow [2].

1.1.2 B and T lymphocytes

These cells carry on their surface highly diversified antigen-specific receptors, which are able to interact with a quasi-unlimited number of antigens, thanks to their structure diversity [3]. B cells through B cell receptors (BCRs) recognize linear or conformational epitopes on their own and bind intact antigens contrary to T cells, which specifically recognize and interact through T cell receptors (TCRs) with peptide fragments derived from antigens in association with major histocompatibility complex (MHC) molecules on the surface of antigen-presenting cells (APCs) [3].

Concerning T cells, we can distinguish the T helper cells also known as CD4+ T cells and the cytotoxic T cells also known as CD8+ T cells. Their interactions are different: CD4+ T helper cells interact with peptide-class-II-MHC compared to CD8+ cytotoxic T cells which interact with peptide-class-I-MHC [1].

1.1.3 Autoimmunity

Autoimmunity includes pathological manifestations that can develop when the immune system is abnormally overactivated because of a defective regulation function and trigger to a strong reaction against its unmodified components. The autoimmune response involves classical immune responses with T cells, B cells, APCs, inflammatory cells, antibodies and many other mediators of immunity such as cytokines (Figure 2) [1].

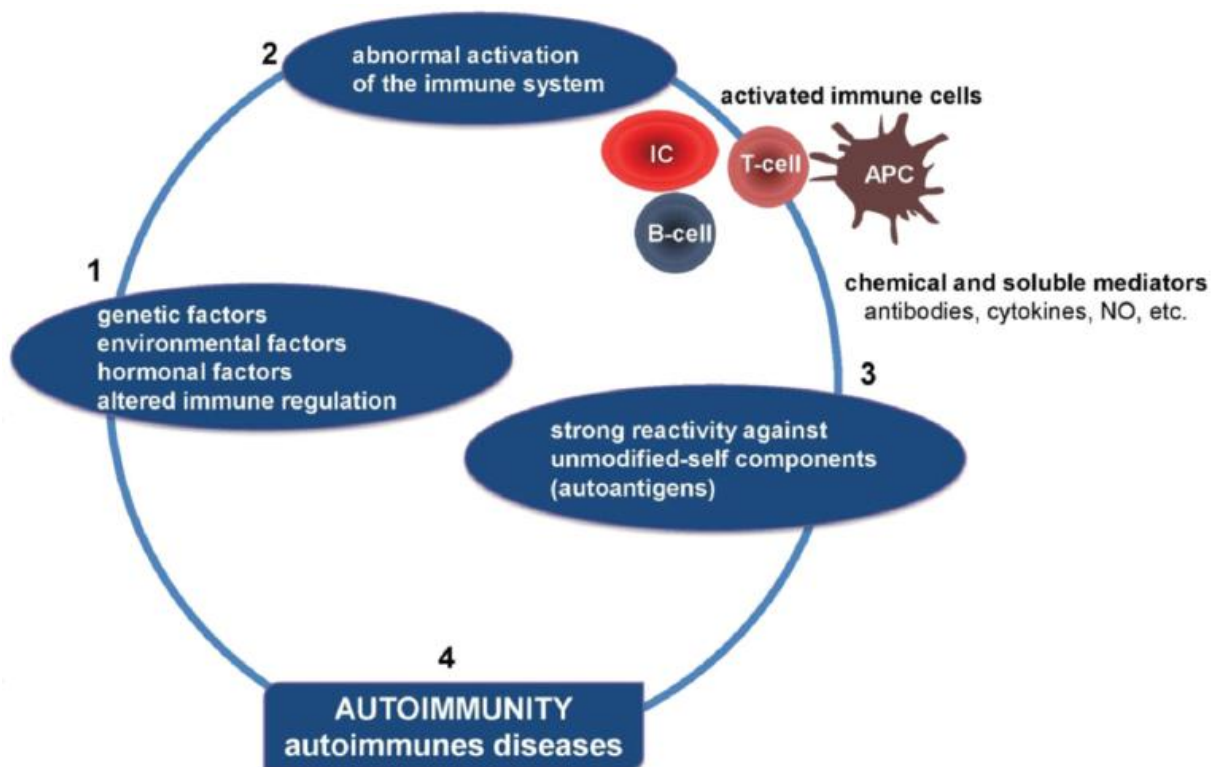


Figure 2: Pathological mechanisms of autoimmune diseases. IC (inflammatory cells); APC (antigen-presenting cell); NO (nitric oxide) [1]

Immune-mediated diseases are a group of different pathologies including autoimmune diseases affecting around 8% of the population with a predisposition higher for women than men. In our study, two diseases recognized as neurological, inflammatory, autoimmune disorders were chosen: Multiple Sclerosis (MS) and Rett syndrome (RTT).

1.1.4 Antigens and antibodies

Antigens (Ags) can be defined as substances that bind to antigen-specific receptors (BCRs and TCRs) of the immune system.

There are different types of antigens:

- Exogenous antigens: these Ags in the body come from outside usually by inhalation, ingestion or through the physical barriers.
- Endogenous antigens: these Ags are generated by the cells through the normal cellular metabolism and after bacterial and/or viral infections.
- Autoantigens: these Ags consist of native peptides or proteins that are recognized as targets by the immune system. This is the case of autoimmune diseases.

Antibodies (Abs) also known as immunoglobulins (Igs) have an Y-shaped protein, they are produced by plasma cells and used by the immune system to identify and neutralize Ags.

From a structural point of view, antibodies are glycoproteins with two distinct regions:

- The fragment antigen-binding (Fab) region, which is involved in Ag binding;
- The fragment crystallizable (Fc) region, which is involved in interactions with surface cell receptors of the immune system.

There are five different types of Abs, termed isotypes: IgG, IgM, IgA, IgE, and IgD. They have different biological properties and functional locations.

IgGs are the most important isotypes among the five generated by plasma B cells. They are present in blood and extracellular fluids and they are the most abundant (~75%) of serum immunoglobulins in humans. IgGs are large molecules of about 150kDa and they participate in the secondary immune response. IgGs are involved in the regulation of allergic reactions. IgG level measurements could be indicative of immune status to pathogens.

IgM is the largest isotype, it can be found in pentameric forms (~975 kDa), forming a “star” of Y-shaped Abs. IgMs are found in blood and consist of the very first response to initial exposure to antigens. They are produced by B cells. IgMs have the ability to activate the classical pathway of the complement leading to an immune response.

IgA isotype can be found in mucosal areas in monomeric or dimeric form that is the most prevalent. IgAs play a critical role in protection against pathogens.

IgE antibodies can be found in mucous membranes, lungs, and skin as monomers and are synthesized by plasma cells. IgE are the less common isotype of Abs in the organism. They have a function in immune response against allergens and parasitic worms.

IgDs are monomeric antibodies (185kDa) found in very small amounts in blood serum. IgD have important immunological functions such as B cells activation and elimination of B-lymphocytes, generating self-reactive autoantibodies [2].

1.1 Multiple Sclerosis

Multiple Sclerosis (MS) is a chronic, inflammatory, demyelinating disease of the central nervous system (CNS) [4] leading to a variety of sensory and motor disturbances [5]. It is characterized by the formation of sclerotic plaques in various areas of the CNS (Figure 3). The immune system is responsible to destroy protein components of myelin sheath. These plaques are the result of an inflammatory response most likely caused by activation of autoimmune Th-1 cell targeting oligodendrocytes and the myelin sheath together with activated monocytic cells. These highly immunologically active areas subsequently progress to form “scarring” plaques [2].

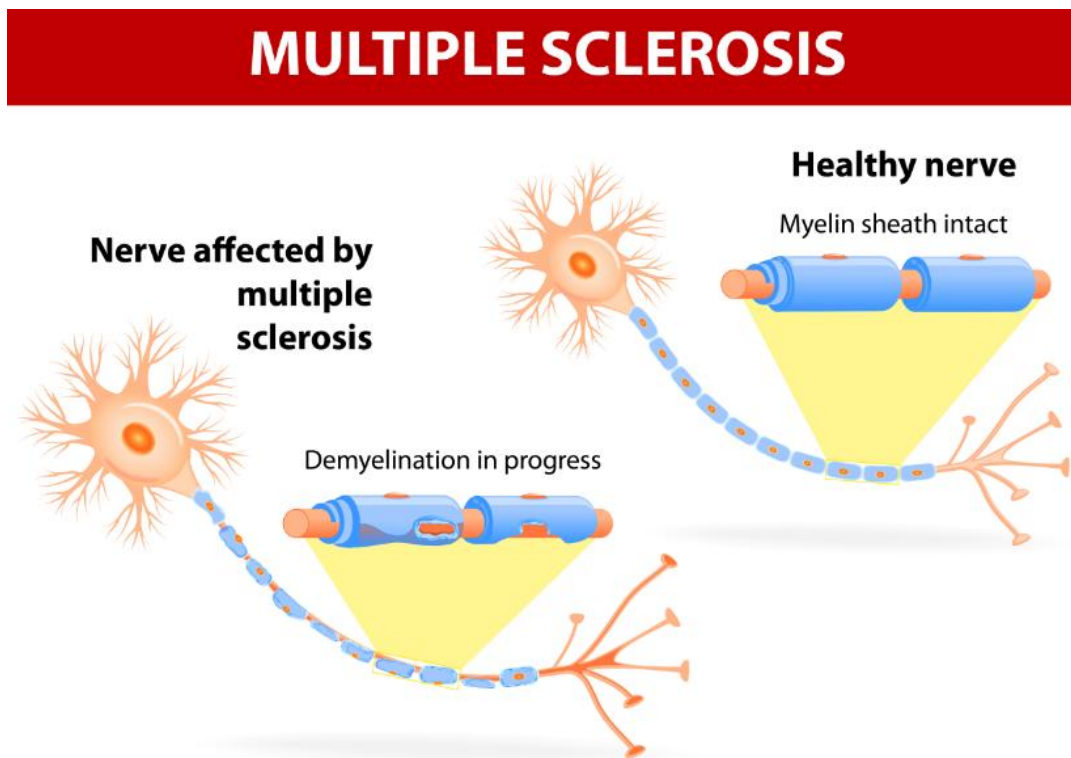


Figure 3: Multiple sclerosis: destruction of the myelin sheath
<http://www.iflscience.com>

Symptoms and signs can vary depending on the location and severity of the plaques. Generally, motor, sensor, visual, and cognitive disturbances are observed. This disease mostly affects women between 20-40 years old with a prevalence of 1/1000 [6].

CNS inflammation is the primary cause of the nervous system damage in MS. From a mechanistic point of view, MS is considered an inflammatory, multifactorial, autoimmune disease in which, genetic and environmental factors must be taken into consideration [4].

An early diagnose of MS is required in order to treat quickly the patients to avoid complications and severity of the disease. In the same time, the development of new and more specific drugs is in progress in pharmaceutical industries [7].

The conventional magnetic resonance imaging (MRI) is the gold standard in clinical diagnostics of MS. MRI is also used to follow up disease activity to monitor disease evolution [7]. With this technique, inflammation and demyelization can be evaluated. In fact, even if extremely expensive and not always available in clinical units, MRI is recognized as a diagnostic but also as a prognostic tool to help clinicians in therapeutic decisions [8].

It has been suggested that the adaptive immune system drives the early stages of MS and the innate immunity drives the progressive stage, although the degree to which the adaptive and the innate immune systems affect both stages is uncertain (Figure 4).

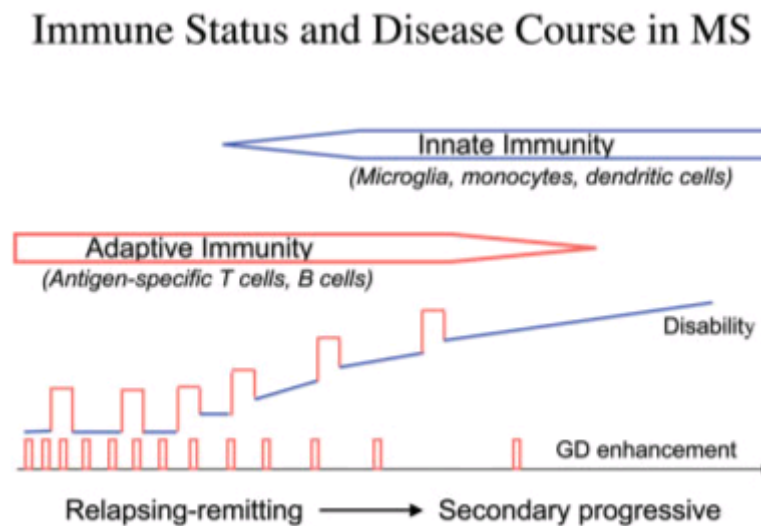


Figure 4: Immune status and disease course in MS [9]

1.2 Rett syndrome

Rett syndrome (RTT) is a progressive X-linked neurodevelopmental disorder and one of the most common causes of mental retardation in females with an estimated prevalence of 1:10000 to 15000 live births per year [10].

The disorder is characterized by a period of normal development during the first 6-18 months of life followed by gradual loss of skills already gained, such as speech and purposeful movement of the hands [11]. RTT girls lose their acquired cognitive, social, and motor skills in a typical four-stage neurological regression and develop autistic behavior accompanied by stereotypic hand movements. RTT in up to 95% children is mainly caused by mutations in the X-linked methyl-CpG-binding protein 2 gene (MeCP2) [12]. MeCP2 protein

from the methyl-CpG-binding protein (MBP) family [13] was the first discovered to selectively recognize and bind methylated DNA sequences [14]. MeCP2 is a key multifunctional protein in the brain (Figure 5) [15]. Hundreds of different MECP2 mutations have been associated with Rett syndrome [16] and mutations in other genes were also found.

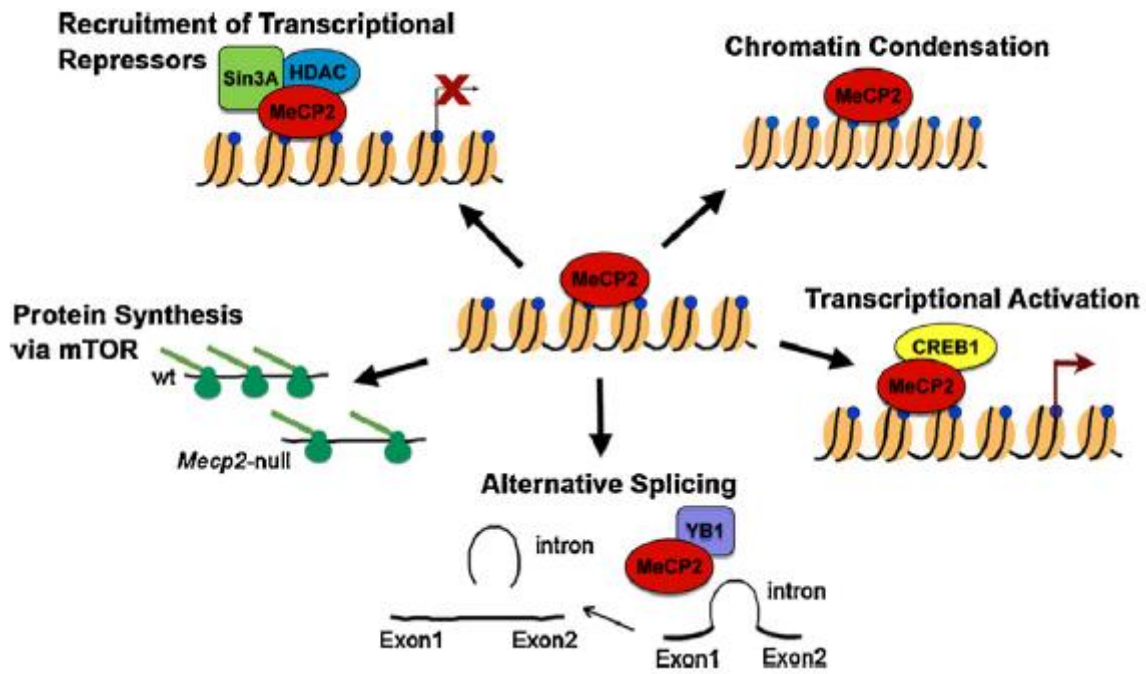


Figure 5: MeCP2 is a multifunctional protein.

MeCP2 functions reported so far have been schematically represented. Following a clockwise direction starting from the left upper cartoon, MeCP2 can function as a transcriptional repressor that recruits corepressors to silence methylated genes; it can mediate the formation of a highly compacted chromatin structure (in a methylation independent way); it may play a role in transcriptional activation mainly through its interaction with CREB1; it can be involved in mRNA alternative splicing (e.g. through its interactions with YB1) and eventually it can influence protein synthesis through modulation of the mTOR pathway [16].

RTT can be considered as a multi-systemic disease and is a brain pathology that includes the unique triad of increased biochemical signs of oxidative stress (OS) derangement [17].

1.3 Diagnostic methods

AIDs (autoimmune diseases) are a particular class of diseases, with complex mechanisms. Some diagnostic methods are available, but each AID is different and there are not specific diagnostic methods for each AID. Treatments for autoimmune diseases, when available, are extremely expensive and have huge secondary effects on the patients. So, it appears crucial to develop diagnostic methods to detect early the presence of the disease.

Most of these methods are based on the detection of inflammatory markers that are usually associated with the immune response; or on auto-Abs produced by the immune system [2].

Multiple Sclerosis is typically diagnosed on the presence of signs and symptoms, in combination with supporting MRI and laboratory testing. It can be difficult to confirm, especially early the disease. In fact signs and symptoms can be similar to those of other medical problems.

The most commonly used tools are neuroimaging and analysis of cerebrospinal fluid. Magnetic resonance imaging of the brain can show areas of destruction of the myelin sheath. Cerebrospinal fluid obtained by a lumbar puncture can provide evidence of chronic inflammation in the central nervous system. The cerebrospinal fluid is tested for oligoclonal bands of IgGs by electrophoresis. The oligoclonal bands are inflammation markers found in 75-85% of people with MS. The nervous system in MS may respond less actively to stimulation of the optic nerve and sensory nerves due to demyelization of such pathways.

Rett syndrome is typically diagnosed by a genotype-phenotype analysis to detect specific mutation of the X-linked methyl-CpG-binding protein 2 (MeCP2) gene. It can be difficult to confirm the diagnosis due to the multi-systemic disorder of RTT where other mutations in other genes can be found. Moreover, a series of biochemical processes and autoimmune components coexist with the clinical expression of the disease.

The aim of this PhD is to look for new classes of autoantibodies in patient sera. Therefore, we tried to find the best complex glycosidic antigens isolated from plants, otherwise difficult to be synthesized, and able to recognise specific antibodies in the case of patients affected by multiple sclerosis and rett syndrome.

Indirect enzyme-linked immunosorbent assays (ELISA) were performed to measure IgM levels in sera of patients affected by MS and RTT.

ELISA is one of the most commonly used immunoassay techniques. It is based on an enzyme-labeled antibody capable of detecting a serum antibody specifically recognizing an antigen immobilized to a solid surface composed of a 96-well plate. Antigens are coated on 96-well plate. Then, un-coated areas of the well are blocked using fetal bovine serum (FBS), a non-reactive protein solution. After that, diluted patient sera are added allowing the binding of the coated Ag to specific Abs present in sera. After washing the plate, a secondary enzyme-

coupled Ab is added. Secondary Abs are commonly labeled with alkaline phosphatase. The addition of a substrate specific to the secondary enzyme-coupled Ab, can reveal color change correlating to the amount of antibodies if present in the original serum sample (Figure 6).

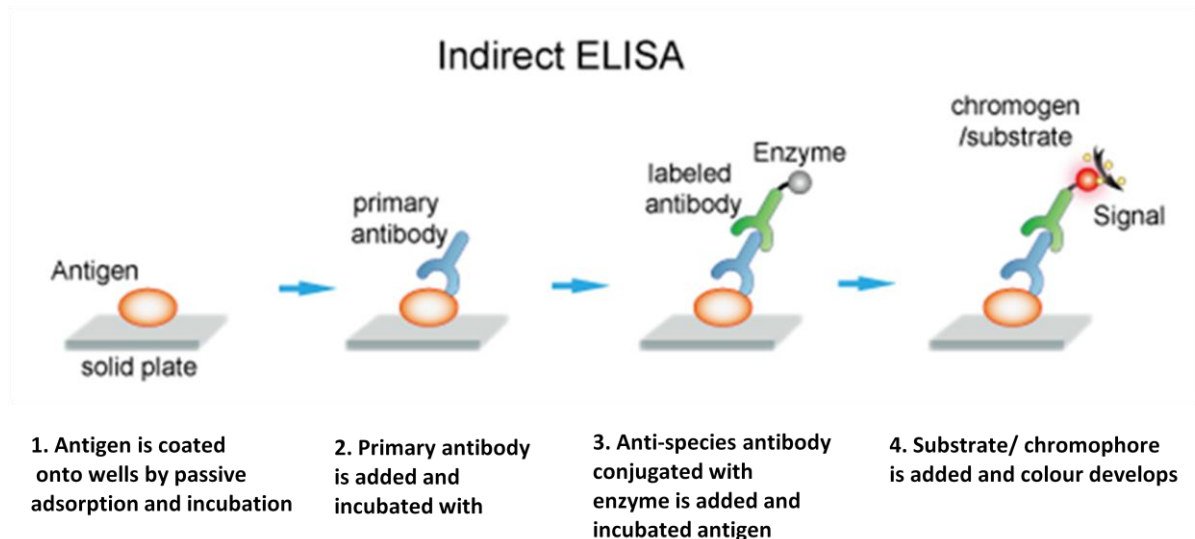


Figure 6: Indirect ELISA procedure
(<http://www.creative-diagnostics.com>)

This technique has several advantages:

- It is a simple and rapid technique to detect antigens attached to a solid surface;
- A large number of sera can be tested in a very short time;
- It is a relatively low cost technology.

ELISA offers commercial value in research laboratories, diagnostics of disease biomarkers and quality control in various industries.

1.4 Research project

Complex glycoconjugates, including glycolipids and glycoproteins, are commonly displayed on cell surfaces, where they play crucial role as mediator of extracellular communication and signaling networks [18-20]. Therefore, studies on glycan modification patterns of glycoconjugates are a great challenge in medical diagnostic research, offering insight into cellular and molecular mechanisms. Moreover, glyconjugates can be proposed as molecular biomarkers of disease activity and to understand molecular mechanisms of immune-mediated diseases [21-22]. Natural glycoconjugates are often complex mixtures of closely related materials very difficult to synthesize and analyze. In the field of autoimmunity different approaches are used to investigate the structures and functions of complex naturally

occurring glycoconjugates leading to the identification of autoantigens associated with different autoimmune diseases. In particular, in the context of Multiple Sclerosis and Rett syndrome, the identification of serum antibodies as biomarkers to be used for the diagnosis, monitoring, and prognosis of such heterogenous disease is a challenge because of the ambiguous identification of antigens (Ags) implicated in the disease.

MS pathogenesis has not been yet elucidated. Viral, immunological, and vascular hypotheses have been proposed [23]. Most of the putative Ags belongs to myelin protein family. Moreover, it is accepted that pathophysiological post-translational modifications of native Ags can trigger the immune system to generate autoantibodies escaping conventional diagnostic procedures. Thus, autoantibodies against aberrant glycosylations have been hypothesized as diagnostic biomarkers of MS [24-25]. In particular, the synthetic N-glycosylated peptide, a type I' beta-turn structure termed CSF114(Glc), that was specifically designed to detect anti-N-glycosylation disease-specific autoantibodies as biomarkers of MS, has been developed as a probe for the detection of autoAbs present in the serum of MS patients [26-27]. This probe is able to identify and measure MS-related autoAbs whose levels correlated with clinical assessment of MS activity and MRI profile of brain lesion [24]. The CSF114(Glc) peptide represents an unconventional approach since its structure is completely unrelated to any primary myelin protein structure and is not linked to any particular pathogenetic hypothesis. The main characteristic of CSF114(Glc) is its conformational β -turn structure exposing the sugar moiety on an asparagine residue, possibly the key element, for autoantibody recognition [28-29]. Different synthetic sugar moieties were assembled into the amino acid sequence of CSF114 and their reactivity studied in MS patient sera, confirming the role of N-glycosylation in autoantibody recognition [30]. Since the human glycoproteome repertoire lacks this uniquely modified amino acid, the attention was turned to bacteria, i.e., *Haemophilus influenzae*, expressing cell-surface adhesins including N-Glc, to establish a connection between *H. influenzae* infection and MS. We exploited the biosynthetic machinery from the opportunistic pathogen *H. influenzae* (and the homologous enzymes from *A. pleuropneumoniae*) was exploited to produce a unique set of defined glycosylated adhesin proteins. Interestingly we revealed that a hyperglycosylated protein domain, based on the cell-surface adhesin HMW1A, is preferentially recognized by antibodies from sera of an MS patient subpopulation. In conclusion, the hyperglycosylated adhesin is the first example of an N-glycosylated native antigen that can be considered a relevant candidate for triggering pathogenic antibodies in MS [31].

Rett syndrome (RTT) is an X-linked neurodevelopmental disorder affecting almost exclusively women is a multi-systemic disease. Indeed, researchers demonstrated that a single monogenic mutation of methyl-CpG binding protein 2 (MeCP2) is associated with Rett syndrome but other gene mutations are also listed. Besides, typical clinical features in approximately 80% of RTT patients can be considered for diagnosis of the disease. An increased biochemical sign of oxidative stress derangement can also be observed in case of Rett syndrome [17], and recently, in PeptLab at the University of Florence, they hypothesized the coexistence of a perturbation of the immune system in RTT patients. In particular, they demonstrated that the N-glycosylated structure based designed peptide CSF114(Glc) was a probe also for RTT patients. The IgM levels in RTT patient sera correlated with clinical features [32]. Therefore, it was confirmed for the first time the role of N-glycosylation in antibody recognition in Rett as first insight of an immune system disruption.

A previous collaborative study between Florence and Bourgogne Universities on the use of pure natural triterpene glycosides as mimetics of native antigens demonstrated that saponins tested on multiple sclerosis patient sera displayed a good capacity to recognize IgMs (sensitivity up to 38%) with a high specificity (88.9%) [33].

With these considerations in mind, we could envisage that structures containing naturally occurring glycosylations are attractive as possible antigenic probes mimicking native glycoconjugates. In particular, saponins are good candidates because their aglycon bears various glycosidic moieties, from single sugar to oligosaccharidic chains, as mono or bidesmosidic structures. Many of these compounds have been characterized during the last decades, and modern techniques of isolation from plants and structural elucidation are now available.

The aim of this PhD project was the selection of isolated natural saponins, i.e., triterpene-type saponins, as structures bearing different glycosyl moieties and their immunochemical characterization in MS and RTT patient sera in comparison with the structure-based designed glycopeptide CSF114(Glc) [34].

CHAPTER 2:

Phytochemical study of five plants

Chapter 2: Phytochemical study of five plants

2.1 Botanical study

Five species from three different families were studied: *Wisteria frutescens*, *Wisteria floribunda* “macrobotrys” and *Wisteria floribunda* “rosea” from Fabaceae, *Weigela florida* “rumba” from Caprifoliaceae, and *Polygala acicularis* from Polygalaceae. In this chapter, we describe the order, the family and the genus of each studied plant, and finally, the botanical characters of each species.

2.1.1 Fabales order

The Fabales are an order of flowering plants and form part of the nitrogen-fixing clade. According to the APG III classification, this order includes the Fabaceae or legumes, Quillajaceae, Polygalaceae and Surianaceae families (Figure 7) [35]. The Fabaceae is the most important plant family for production of food, containing most of the diversity of the Fabales.

Many Fabaceae host bacteria in their roots within structures called nodules. Nitrogen fixation is a classic example of a "tendency" or "predisposition". A number of genes involved in the establishment of the symbioses with both gram-negative and proteobacteria including *Rhizobium* and the gram-positive actinomycete *Frankia*, are the same as those involved in arbuscular mycorrhizal associations [36].

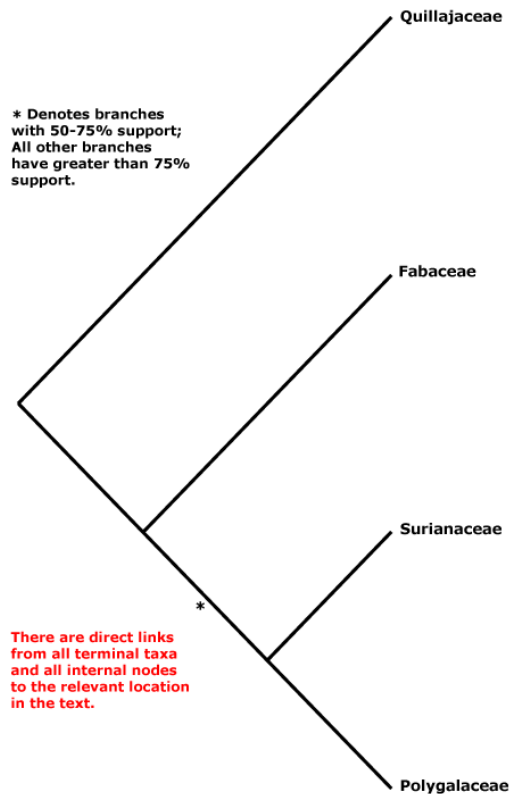


Figure 7: Phylogeny Fabales order [36]

Fabaceae family

The Fabaceae or Leguminosae are dicotyledonous plants belonging to the Fabales order. It is a large and important family of flowering plants. It includes trees, shrubs and herbaceous plants perennials or annuals. The main distinctive characteristic of this family is their fruit [37]. Indeed, according to their constituents (proteins, fat, carbohydrates, vitamins and microelements) they have been recognized as nutritive food [38].

That is why most of them are agricultural and food plants, such as *Glycine max* (Soybean), *Phaseolus* (beans), *Pisum sativum* (pea), *Cicer arietinum* (chickpeas), *Medicago sativa* (alfafa), *Arachis hypogaea* (peanut), *Lathyrus odoratus* (sweet pea), *Ceratonia siliqua* (carob), and *Glycyrrhiza glabra* (liquorice).

Wisteria genus

Wisteria Nutt, also called *Wistaria* Spreng. [39] is a genus of woody vines with alternate pinnately compound leaves and a large inflorescence of pendulous, showy purple, blue or white flowers. This is very appreciated in horticulture for a garden use.

Three different species were studied: *W. frutescens* (the American *Wisteria*) and two cultivars of *W. floribunda* (japanese *Wisteria*) “macrobotrys” and “rosea”.

W. frutescens (L.) Poir. is a toxic plant native to the United States (Figure 8). Its pods, seeds, and bark contain toxic principles, a glycoside named wisterin, and a resin.

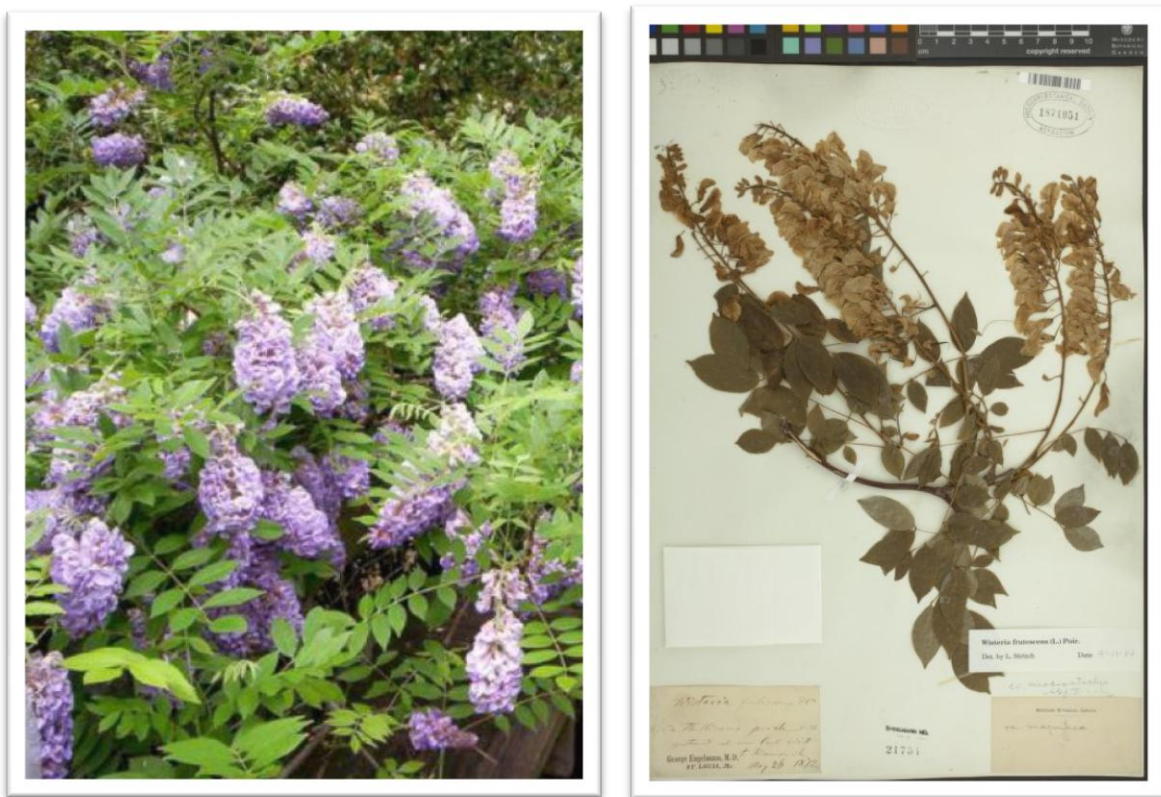


Figure 8: *Wisteria frutescens*

(<https://www.jardindupicvert.com>)

(<http://www.tropicos.org>)

W. floribunda (Willd.) DC occurs in Japan and Korea [40-41]. The cultivar “rosea” differs mainly by its pink flowers contrary to “macrobotrys” with huge purple and white flower grapes, which can measure until one meter (Figure 9).



Figure 9: *W. floribunda* “macrobotrys” and *W. Floribunda* “rosea”
(<https://www.jardindupicvert.com>)

Polygalaceae family

The Polygalaceae is the major angiosperm group of flowering plants in the Fabales order. These plants have a cosmopolite geographic distribution, with around 800 species spread over a limited number of 12 to 20 genera [42]. It is mostly composed of herbs, shrubs and trees. Under the Cronquist classification system, this family had their own order, Polygalales. Currently, according to the APG III classification, the family belongs to Fabales [35].

Polygala genus

Polygala is the most representative genus of flowering plants from the Polygalaceae family. This genus consists of more than 500 species from all over the world of which 39 species are distributed in China [43].

Several species of *Polygala* were used in traditional medicines as expectorant (*P. senega*, *P. tenuifolia* *P. japonica*), tonic and antihepatitis agent (*P. fallax*). This genus was largely studied during the last decades and was reported to contain triterpene glycosides [42].

P. acicularis Oliv.

Polygala acicularis also known as kikongo of “kienga” was chosen according chemotaxonomic criteria. It is used by Bakongo in the Kinshasa region (Badindingi) for wounds treatment (Figure 10) [44].



Figure 10: *Polygala acicularis*

(<http://www.tropicos.org>)

(<https://science.mnhn.fr/>)

2.1.2 Dipsacales order

The Dipsacales are an order of flowering plants of dicotyledons. In the APG III system of 2009, the order includes only two families, Adoxaceae and Caprifoliaceae (Figure 11) [35]. Some well-known members of Dipsacales are *Lonicera* (honeysuckle), *Viburnum* and *Valeriana offinalis*. The Dipsacales order is described as higher plants, herbs, vines and shrubs [45].

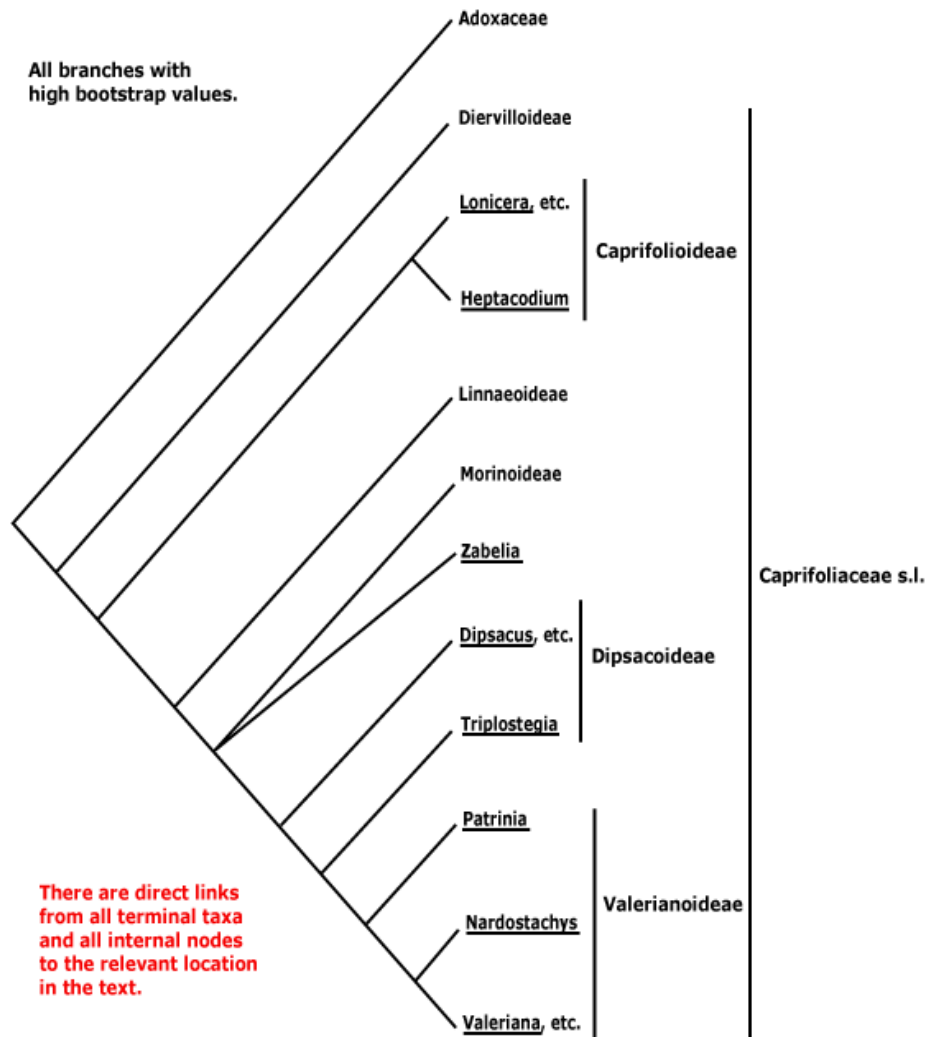


Figure 11: Phylogeny dipsacales order [36]

Caprifoliaceae family

The Caprifoliaceae family is represented by dicotyledonous flowering plants with 860 species and 36 genera, with a cosmopolitan distribution.

They are mostly herbs, perennial or annual, but also creepers or shrubs [45] including some ornamental garden plants in temperate regions.

The flowers have a 4- or 5-lobed calyx, which is usually small, and a 4- or 5-lobed corolla which often forms a substantial tube. The lobes may be equal, or formed into two lips with 4 lobes for the upper lip and one large lobe for the lower lip. The 4 or 5 stamens attach to the tube, alternating with the lobes, with the fruiting portion of the pistil below where the calyx and corolla lobes originate. The fruit, usually a fleshy berry, has 2 to 5 seed-forming divisions. The leaves are opposite and broad [46].

Weigela genus

Weigela or *Weigelia* is a genus of between 7 and 53 species of flowering plants, growing to 1-5m tall. All are natives of East Asia. The genus is named after the German scientist Christian Ehrenfried Weigel. The flowers of this genus are 2–4 cm long, with a five-lobed white, pink, or red corolla, which are produced in small corymbs of several together in early summer. Concerning the fruit it appears like a dry capsule containing numerous small winged seeds [46].

Historically, this genus contains ten species from Japan, China, Korea and Manchuria but many cultivars were produced [47].

Weigela florida (Bunge) A. DC. was the first species to be introduced and was widely cultivated in the 19th century [46]. It is deciduous shrub that typically grows to 6-10' tall. For our study, the cultivar *Weigela florida* “rumba”, an ornamental cultivar shrub of medium size with pink flowers was chosen according to chemotaxonomic criteria (Figure 12).



Figure 12: *Weigela florida* “rumba”
(<http://www.quebecmultiplants.com>)

2.2 Previous phytochemical works

After some generalities about the saponins, the triterpene glycosides already isolated and described in the literature, from the three genera, *Wisteria*, *Weigela*, and *Polygala*, are presented.

2.2.1 Saponins

Saponins are complex glycosides with a high molecular weight, which have a triterpene or steroid skeleton linked with sugar moieties. Saponins are used as detergents and they are known to have hemolytic activity [48]. In some cases, saponins can be toxic for example for fishes [49]. The majority of saponins are found in food or in medicinal plants. The word saponin comes from latin language (“sapo”) and means soap.

Saponins have very interesting pharmacological and biological properties. Researchers decided to work on them and in 1987, a lot of new structures have been elucidated thanks to new techniques that were developed. Saponins are principally found in higher plants and in sea animals such as sea cucumber [50] and sea stars [51] respectively.

Saponins are complex amphiphilic molecules. They are composed of a lipophilic aglycone (or genin) and hydrophilic oligosaccharidic chains linked to the aglycone by an ester or an *O*-heterosidic linkage. The genins are classified in two different groups: steroids and triterpenes.

Triterpenic structure

- Triterpenic genins are principally found in dicotyledonous Angiosperms as for example, in Caryophyllaceae [52] or in Asteraceae family [53]. These genins are obtained via cyclisation of the squalen moiety. There are four main types of pentacyclic skeletons: oleanane, ursane, lupane and dammarane (Figure 13).

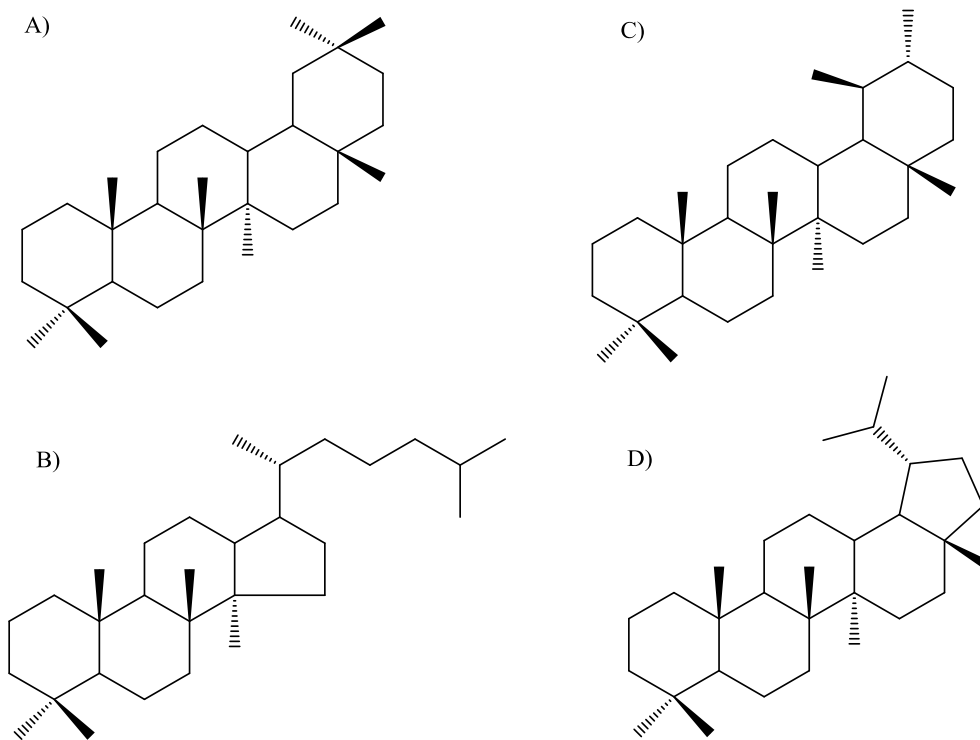


Figure 13: Triterpene skeleton: Oleanane (A), dammarane (B), ursane (C) and lupane (D) [54]

Steroidic structure

- Steroidic genins are principally found in monocotyledonous Angiosperms. There are two principal types of skeleton called spirostane and furostane (Figure 14).

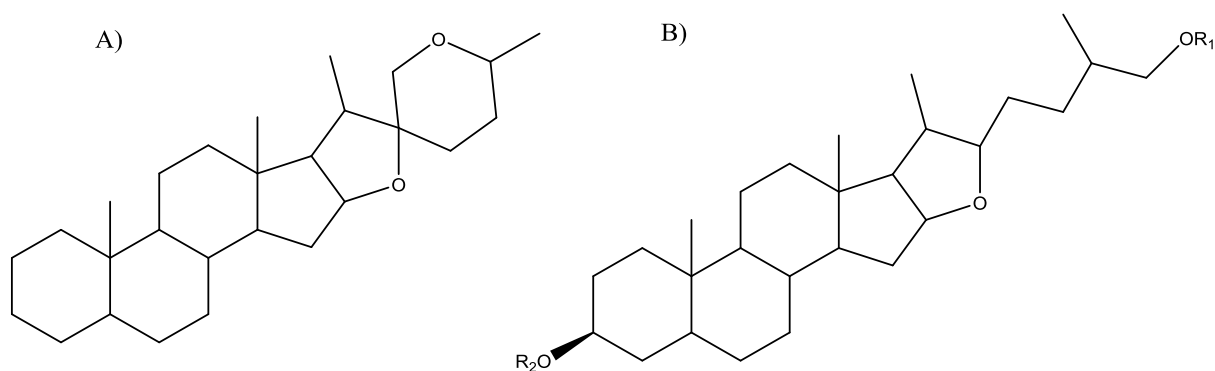


Figure 14: Steroidic skeleton: spirostane (A) and furostane (B) [54]

The genins can be substituted by one or several oligosaccharidic chains. For this reason, we can distinguish:

- Monodesmosidic saponins: they have only one oligosaccharidic chain generally linked at the C-3 position of the genin.
- Bidesmosidic saponins: they have two oligosaccharidic chains linked mainly at the C-3 and C-28 position of the genin for triterpenes, and at C-3 and C-26 for steroids.
- Tridesmosidic saponins: they are very unusual and possess three oligosaccharidic chains linked to the genin.

The osidic moieties are generally hexose, desoxy-hexose, ursonic acids and pentose. The most common ones found in saponins are presented below in Figure 15.

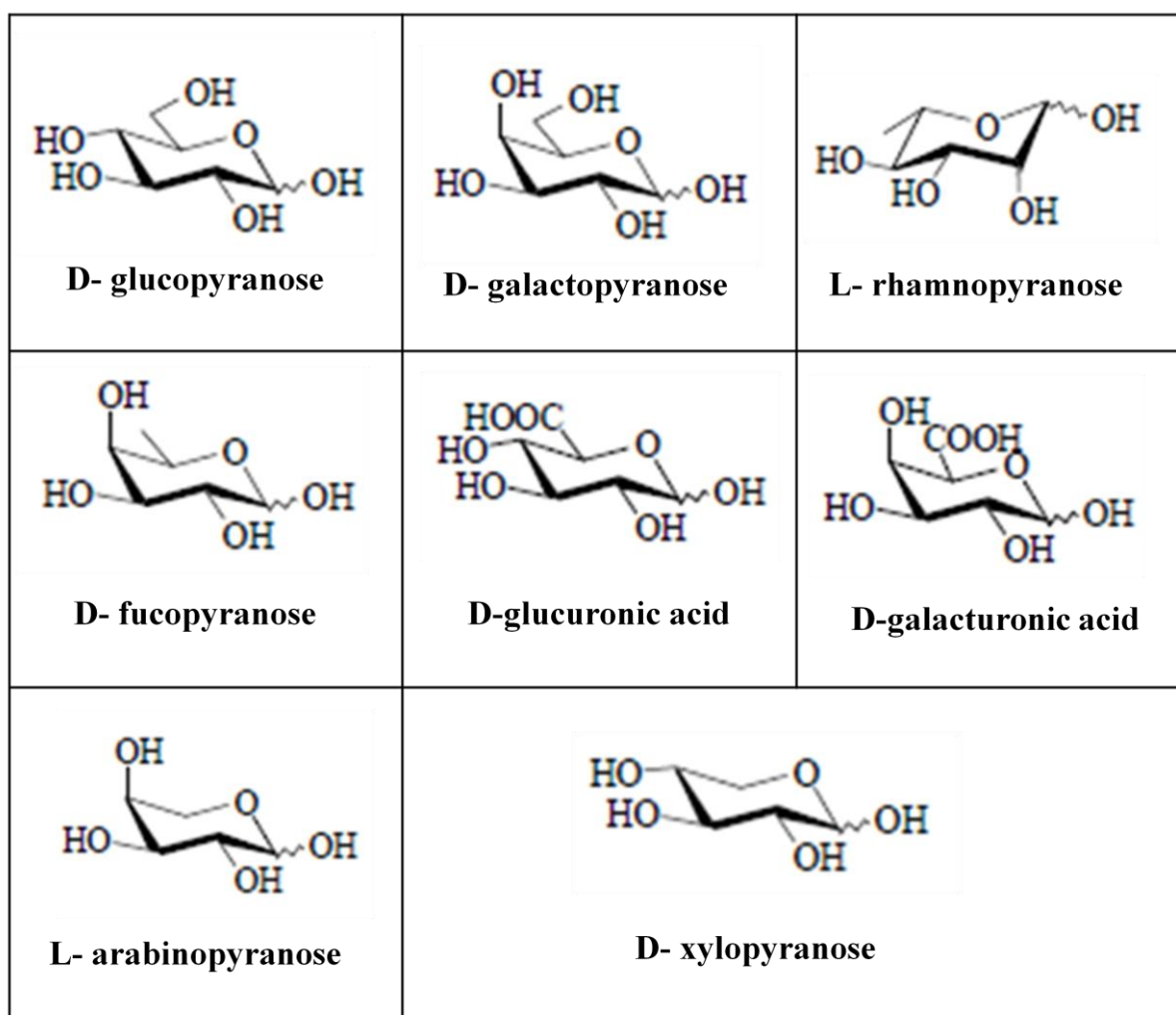


Figure 15: Most common osidic moieties found in saponins

Saponins are complex and amphiphilic molecules and it is very difficult to extract and purify them, but they have important properties in various fields such as biology, pharmacology, food and cosmetics. Moreover, saponins have shown anticarcinogenic, antimutagenic, hypoglycemic, hypocholesterolemic, hepatoprotective, immunomodulatory, neuroprotective, anticoagulant, anti-inflammatory and antioxidant activities in experimental in vivo animal models and in vitro models (Table 1) [55].

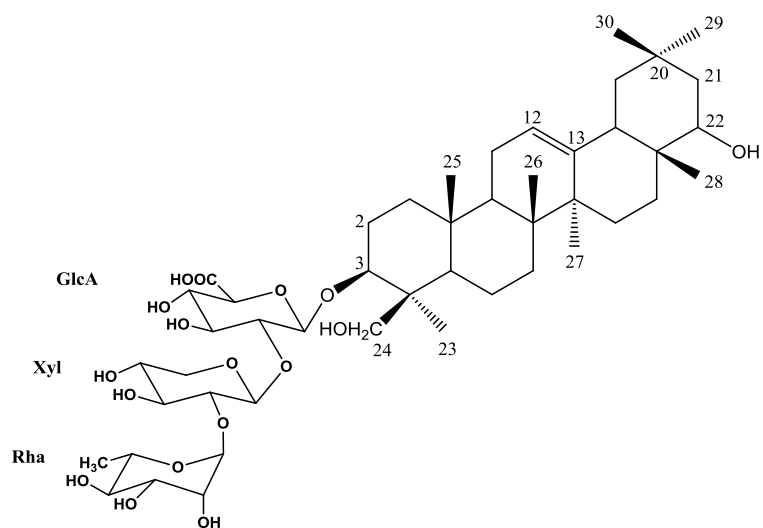
Health promoting activities/beneficial effects	Beneficial compounds	References
Anti-inflammatory effect	Soyasaponin Ab	Lin et al. (2016)
Immune modulatory activities	Soyasaponin Ab	Sun, Yan, Guo, and Zhao (2014)
Immunological adjuvants	Soyasaponins	Qiao, Liu, Meng, and Zhao (2014)
Inhibits HIV infection	Saponin B1	Nakashima et al. (1989)
Inhibits viral replication	Soyasaponins II	Hayashi et al. (1997)
Antiobesity effect	Soyasapogenol A and B	Kim et al. (2014)
Prevent hepatic lipid accumulation	Soyasaponin Af	Chávez-Santoscoy et al. (2014)
Protective effects on liver injury	Soyasapogenol A	Kuzuhara et al. (2000)
Hepatoprotective activity	Soyasaponins I, II, III, and IV	Kinjo et al. (1998)
Suppress tumour progression	Soyasapogenols	Du et al. (2014)
Colon Anticarcinogenic Activity	Soyasapogenol A and B	GurfinkeI and Rao (2003)
Suppress tumour progression.	Soyasapogenols	Du et al. (2014)
Chemoprevention and chemotherapy of cancer	Triterpenoidal saponins	Du et al. (2014)
Antimutagenic	Soyasapogenol B	Berhow et al. (2002)
Antioxidant and antiproliferative activities	Group B saponins	Guajardo-Flores et al. (2012)
Anticarcinogenic properties	Group B saponins, DDMP-saponinTotal saponins	Rao and Sung (1995) Oh and Sung (2001)
Free radical scavenging activity	DDMP saponin	Yoshiki and Okubo (1995)
Antioxidant, anti-inflammatory and anti-diabetic properties	Saponins along with other phytochemicals	Luo et al. (2016)
Antiallergic activity	Sandosaponin A and B	Yoshikawa et al. (1997)
Lowers plasma cholesterol and increases fecal bile acids	Group B saponins	Lee et al. (1999)
Hypocholesterolaemic	Saponins	Rochfort and Panozzo (2007)
Controls dietary hypercholesterolaemia	Saponins	Oakenfull and Sidhu (1984)
Reduces serum cholesterol and triglycerides	Saponins	
Cytoprotective effect against alternariol (mycotoxin)	Soyasaponin I	Vila-Donat, Fernández-Blanco, Sagratini, Font, and Ruiz (2014)
Sialyltransferase inhibitor	Soyasaponin I	Wu, Hsu, Chen, and Tsai (2001)

Table 1. Health promoting activities of saponins [55]

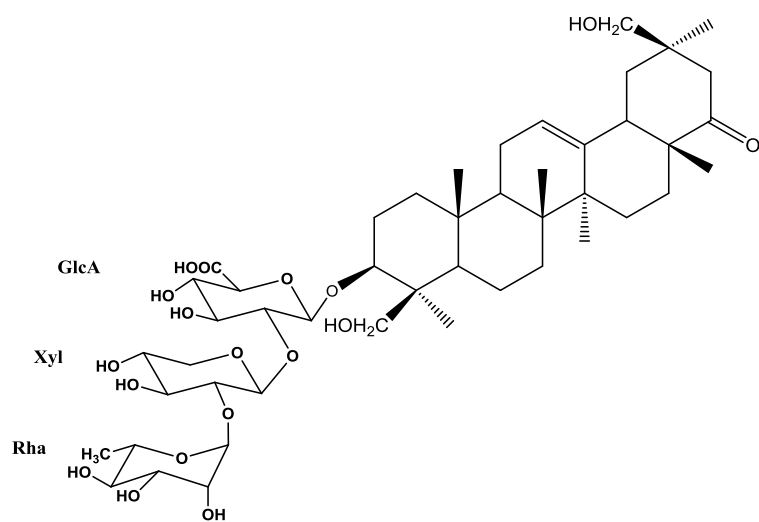
Saponins are used as emulsifying and foaming agents in cosmetology. Besides, as the example of licorice, *Glycyrrhiza glabra* (Fabaceae), they are traditionally used in the treatment of cough. In fact, it is now employed by food industry for its sweetening power [54].

2.2.2 Isolated saponins from *Wisteria* genus

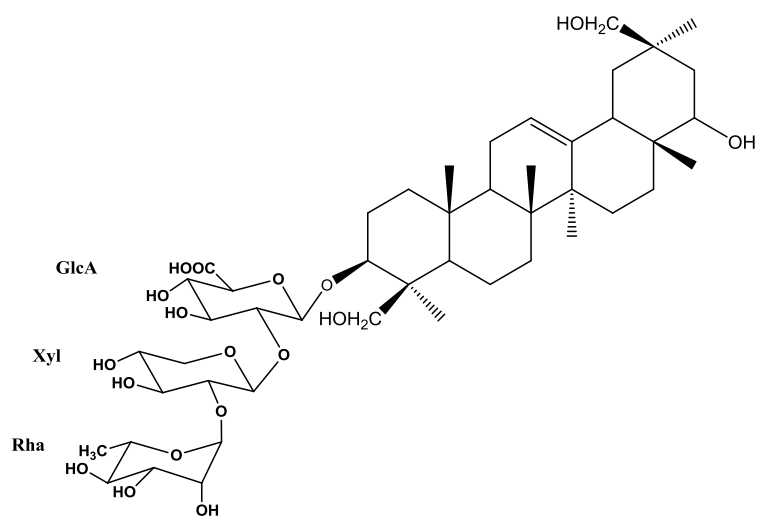
From a structural point of view, these molecules are all C-3 monodesmosidic oleanane-type glycosides. They possess unusual primary alcohol and carboxyl functions at the C-30 position, and a rare ketone function at the C-22 position. The structure of the oligosaccharidic chain linked to the C-3 is always the same as Rha-(1-2)-Xyl-(1-2)-GlcA.



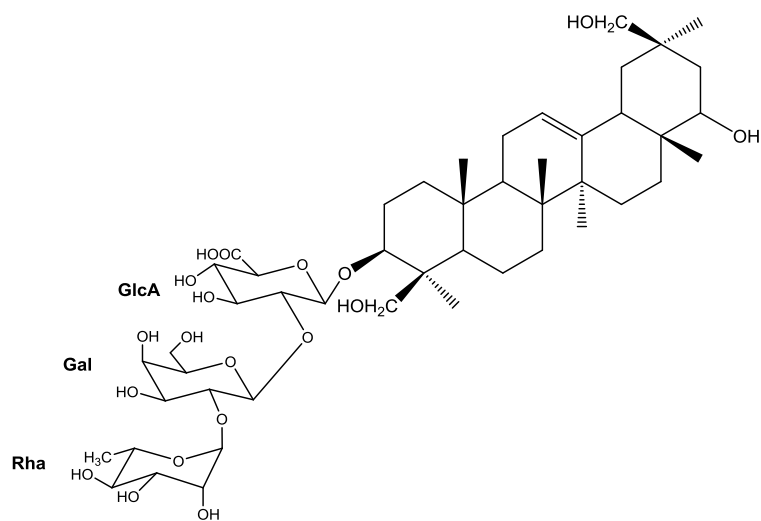
Soyasaponin II [56]



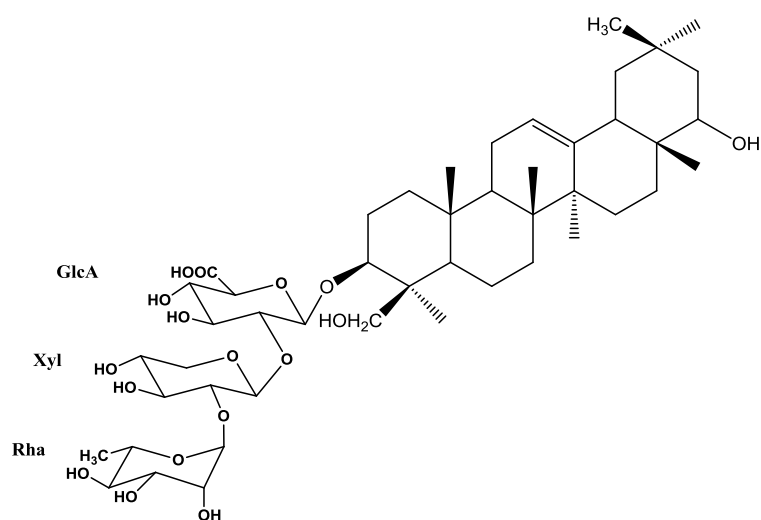
Wistariasaponin A [57]



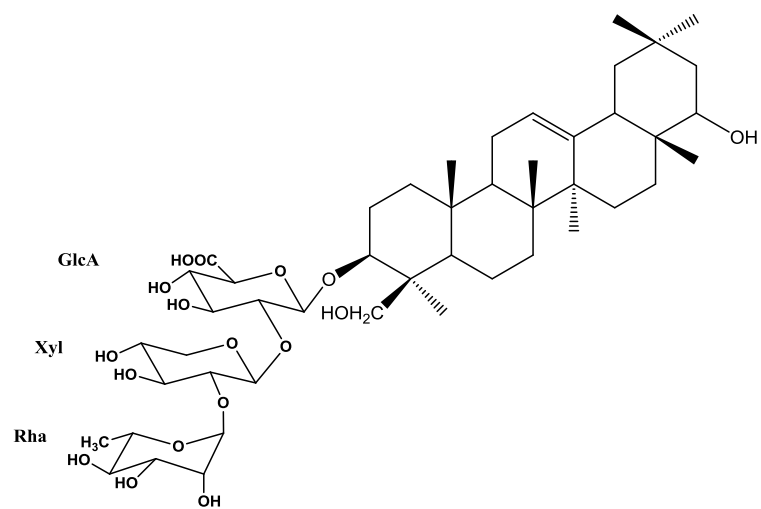
Wistariasaponin B1 [57]



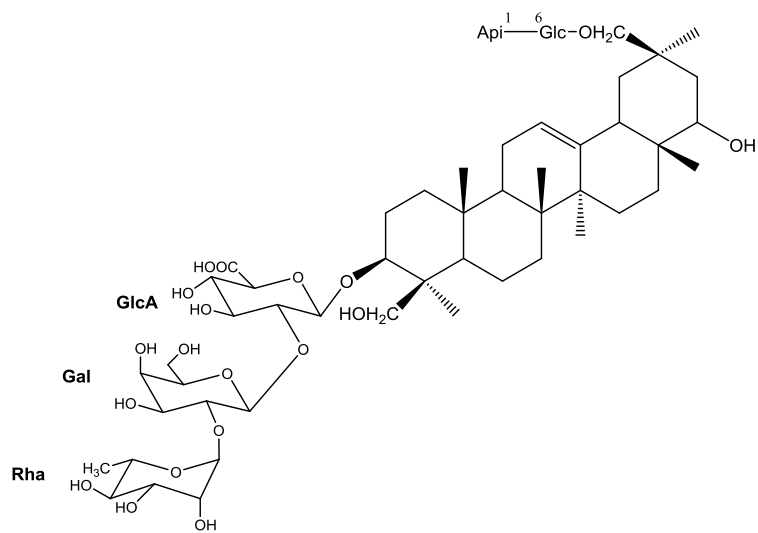
Wistariasaponin B2 [57]



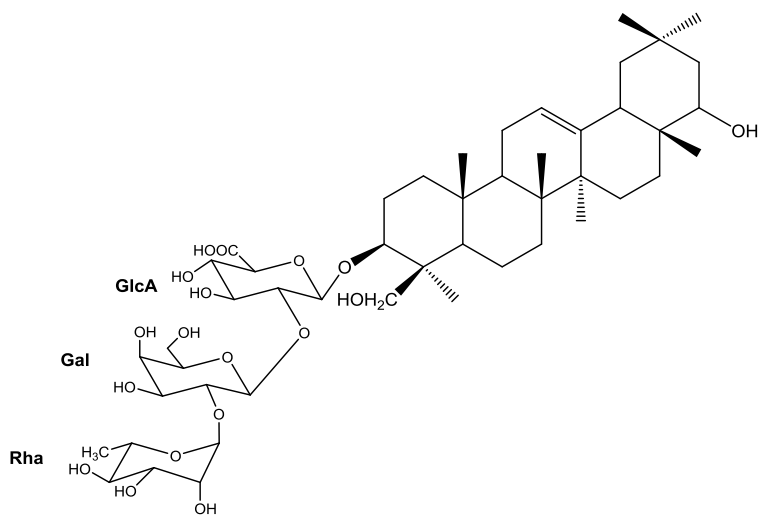
Wistariasaponin C [57]



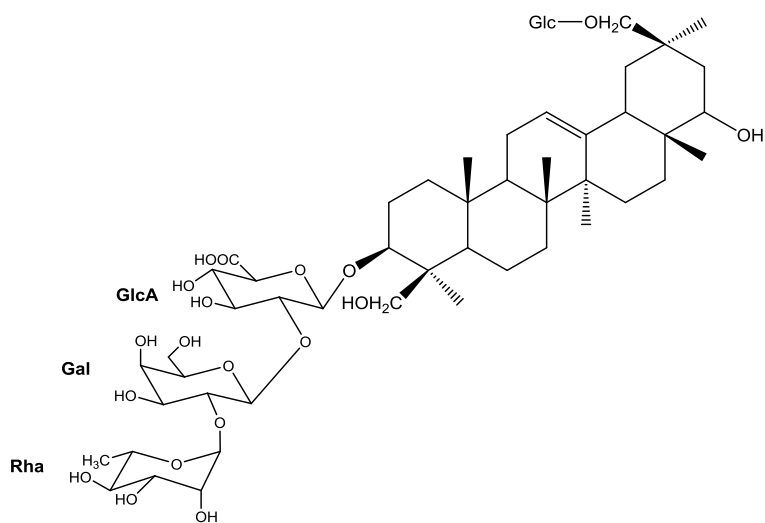
Astragaloside VIII [58]



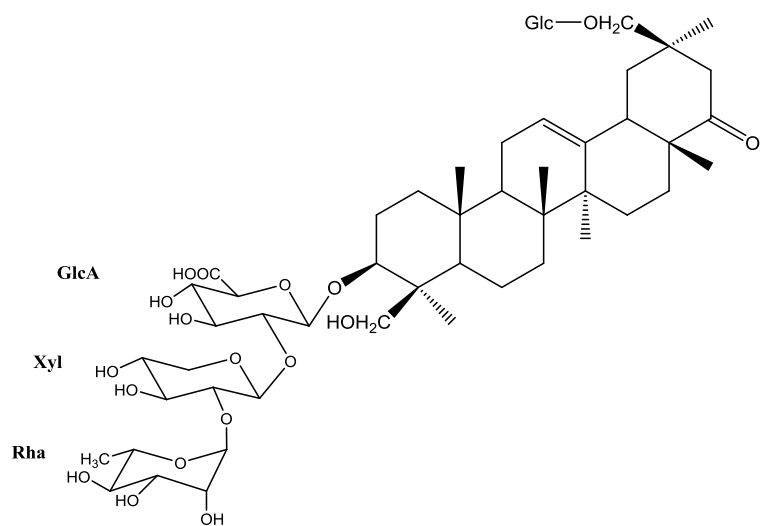
Robinioside I [58]



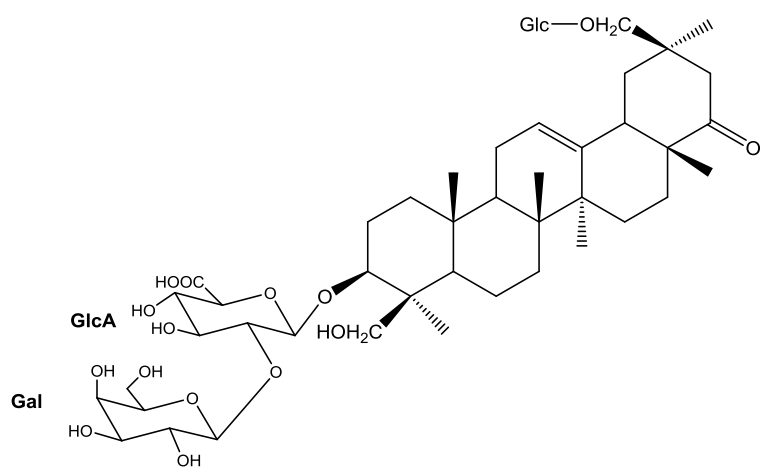
Soyasaponin I [58]



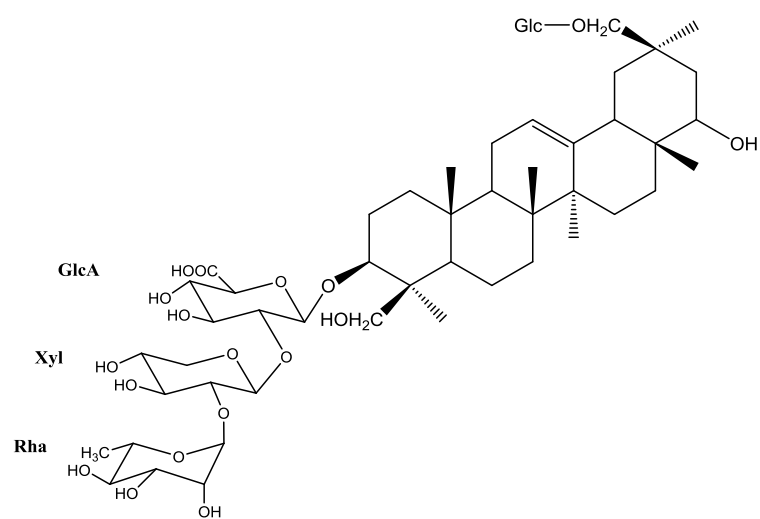
Subproside V [58]



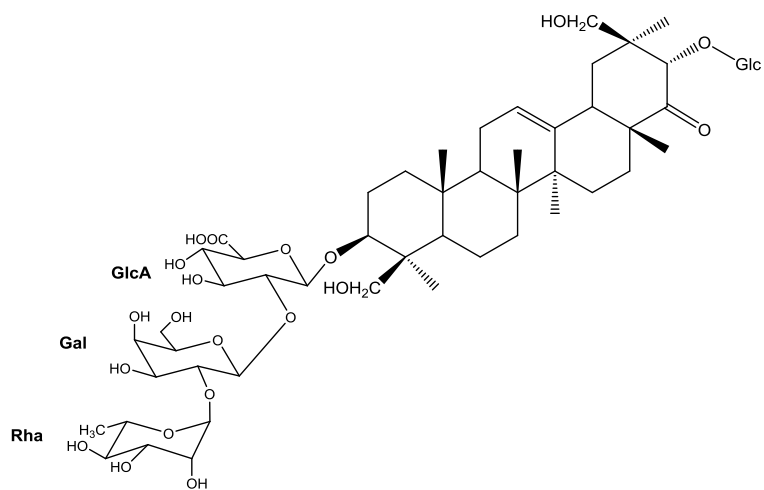
Wistariasaponin A2 [58]



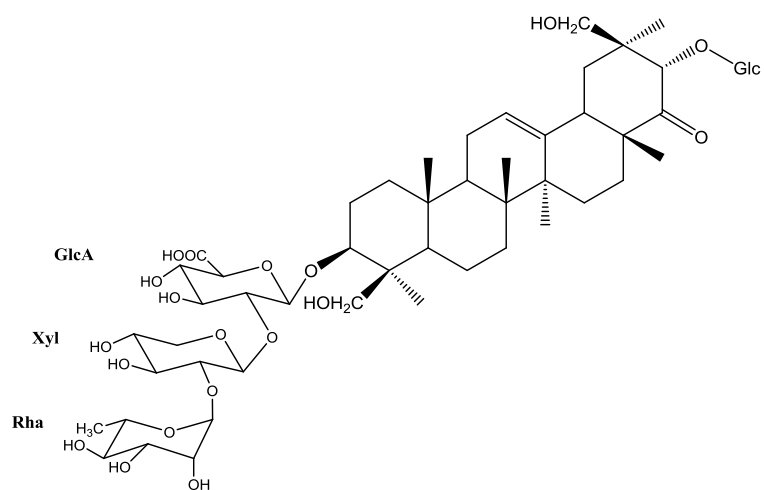
Wistariasaponin A3 [58]



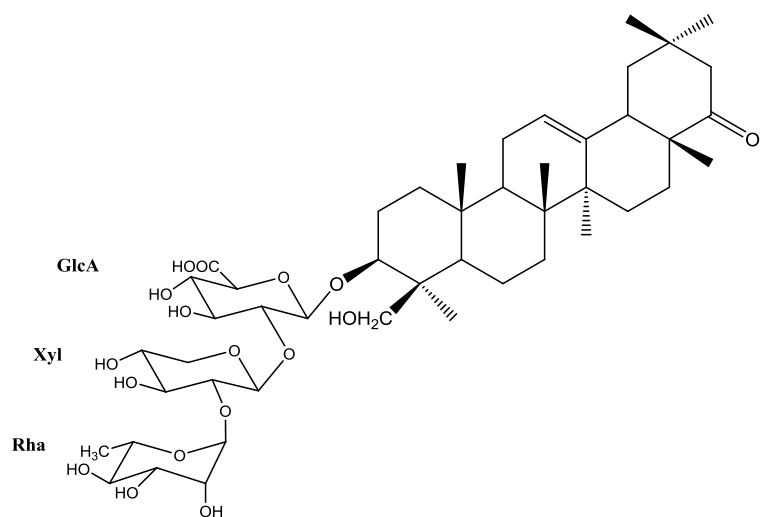
Wistariasaponin B3 [58]



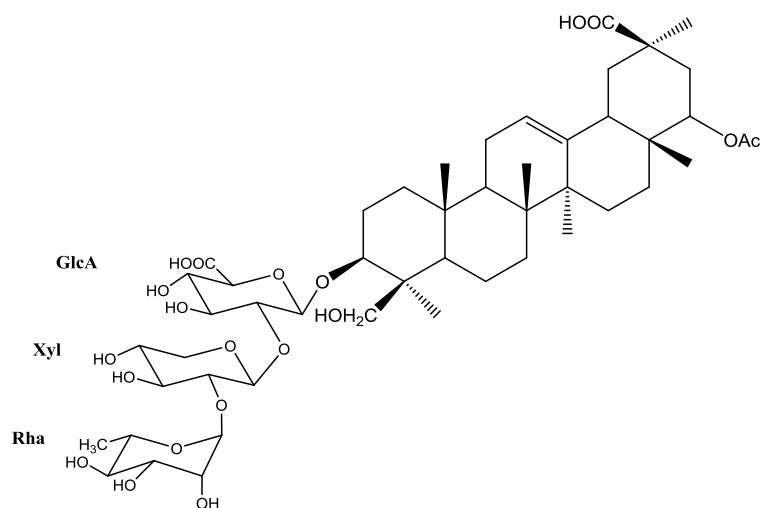
Wistariasaponin YC2 [58]



Wistariasaponin YC1 [58]



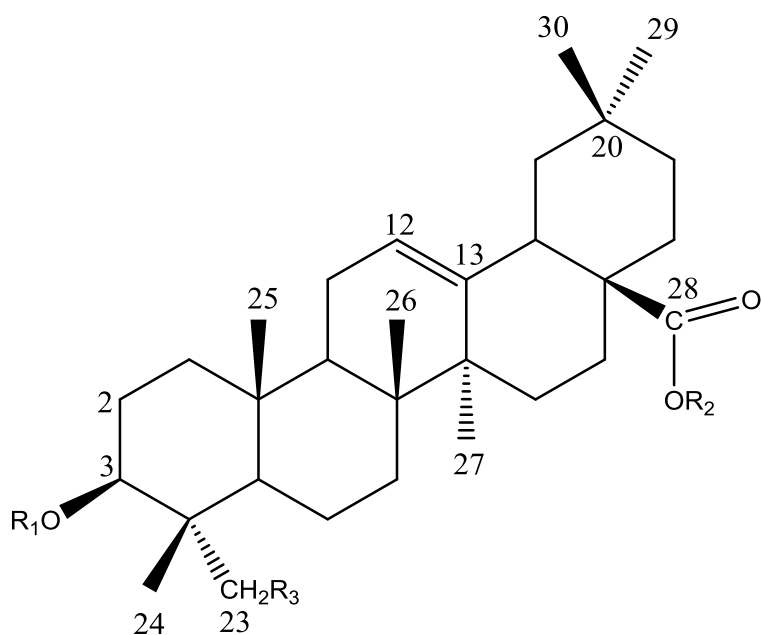
Wistariasaponin D [59]



Wistariasaponin G [59]

2.2.3 Isolated saponins from *Weigela* genus

The saponins isolated from *Weigela hortensis* and *W. stelzneri* are mono-, bidesmosidic oleanolic acid or hederagenin glycosides (Tables 2a and 2b) [47, 60].



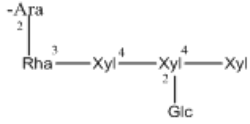
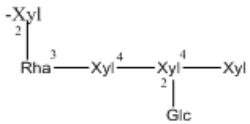
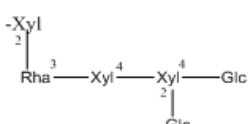
Name	R1 group in C-3 position	R2 group in C-28 position	R3 group in C-23 position	Reference
Hederagenin 3- <i>O</i> - α -L-rhamnopyranosyl-(1 \rightarrow 2)- α -L-arabinopyranosyl-28- <i>O</i> - β -D-glucopyranosyl-(1-6)- β -D-glucopyranoside	-Rha ² —Ara	-Glc ⁶ —Glc	-OH	[60]
Oleanolic acid 3- <i>O</i> - α -L-rhamnopyranosyl-(1-2)- α -L-arabinopyranosyl-28- <i>O</i> - β -D-glucopyranosyl-(1-6)-3-acetyl- β -D-glucopyranoside	-Rha ² —Ara	*Glc ⁶ —3AcGlc	-OH	[60]
3- <i>O</i> - β -D-glucopyranosyl-(1 \rightarrow 2)-[β -D-xylopyranosyl-(1 \rightarrow 4)]- β -D-xylopyranosyl-(1 \rightarrow 4)- β -D-xylopyranosyl-(1 \rightarrow 3)- α -L-rhamnopyranosyl-(1 \rightarrow 2)- α -L-arabinopyranosyloleanolic acid		-H	-H	[47]
3- <i>O</i> - β -D-glucopyranosyl-(1 \rightarrow 2)-[β -D-xylopyranosyl-(1 \rightarrow 4)]- β -D-xylopyranosyl-(1 \rightarrow 4)- β -D-xylopyranosyl-(1 \rightarrow 3)- α -L-rhamnopyranosyl-(1 \rightarrow 2)- β -D-xylopyranosyloleanolic acid		-H	-H	[47]
3- <i>O</i> - β -D-glucopyranosyl-(1 \rightarrow 2)-[β -D-glucopyranosyl-(1 \rightarrow 4)]- β -D-xylopyranosyl-(1 \rightarrow 4)- β -D-xylopyranosyl-(1 \rightarrow 3)- α -L-rhamnopyranosyl-(1 \rightarrow 2)- β -D-xylopyranosyloleanolic acid		-H	-H	[47]

Table 2a: Saponins isolated from *Weigela genus*

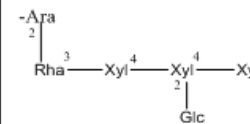
Name	R1 group in C-3 position	R2 group in C-28 position	R3 group in C-23 position	Reference
3- <i>O</i> - β -D-glucopyranosyl-(1 \rightarrow 2)-[β -D-xylopyranosyl-(1 \rightarrow 4)]- β -D-xylopyranosyl-(1 \rightarrow 4)- β -D-xylopyranosyl-(1 \rightarrow 3)- α -L-rhamnopyranosyl-(1 \rightarrow 2)- α -L-arabinopyranosyloleanolic acid 28- <i>O</i> - β -D-glucopyranosyl-(1 \rightarrow 6)- β -D-glucopyranosyl ester		-Glc ⁶ —Glc	-H	[47]
3- <i>O</i> - β -D-glucopyranosyl-(1 \rightarrow 2)- α -L-arabinopyranosylhederagenin 28- <i>O</i> - β -D-xylopyranosyl-(1 \rightarrow 6)-[α -L-rhamnopyranosyl-(1 \rightarrow 2)]- β -D-glucopyranosyl ester	-Ara ² —Glc	-Glc ⁶ —Xyl Rha	-OH	[47]
3- <i>O</i> - α -L-arabinopyranosyloleanolic acid 28- <i>O</i> - β -D-xylopyranosyl-(1 \rightarrow 6)-[α -L-rhamnopyranosyl-(1 \rightarrow 2)]- β -D-glucopyranosyl ester	-Ara	-Glc ⁶ —Xyl Rha	-OH	[47]
3- <i>O</i> - α -L-arabinopyranosyloleanolic acid 28- <i>O</i> - β -D-glucopyranosyl-(1 \rightarrow 6)-[α -L-rhamnopyranosyl-(1 \rightarrow 2)]- β -D-glucopyranosyl ester	-Ara	-Glc ⁶ —Glc Rha	-OH	[47]
3- <i>O</i> - α -L-arabinopyranosyloleanolic acid 28- <i>O</i> - β -D-glucopyranosyl-(1 \rightarrow 6)- β -D-glucopyranosyl ester	-Ara	-Glc ⁶ —Glc	-OH	[47]

Table 2b: Saponins isolated from *Weigela genus*

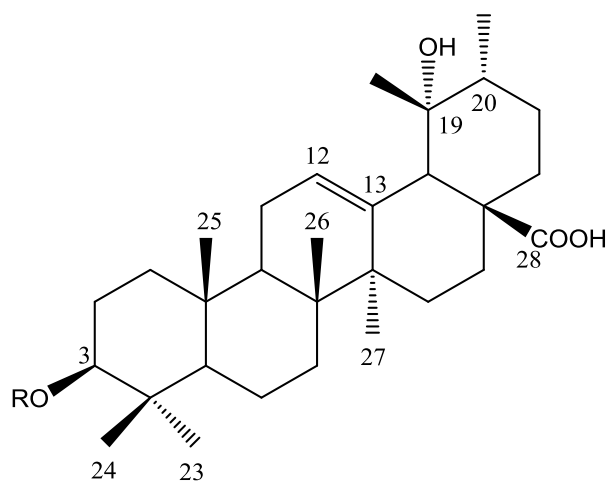
2.2.4 Isolated saponins from *Polygala* genus

Polygala genus was extensively studied and several species were reported to contain triterpene glycosides. Presenegenin, bayogenin, polygalagenin, medicagenic acid, hederagenin and preatroxigenin were reported as characteristic aglycons from this genus [42].

The sequence 3-*O*- β -D-glucopyranosylpresenegenin 28-*O*- β -D-xylopyranosyl-(1 \rightarrow 4)- α -L-rhamnopyranosyl-(1 \rightarrow 2)- β -D-fucopyranosyl ester often encountered in these genera, represents a chemotaxonomic marker for the Polygalaceae family. During the period 2005-2012, around sixty triterpene saponins were isolated from several species of the Polygalaceae family. From the *Polygala* genus [43]:

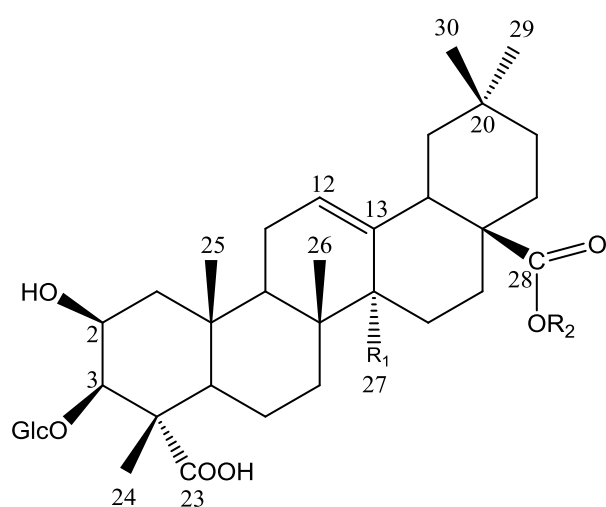
- From *P. ruwenzoriensis*, *P. arenaria*, *P. tenuifolia* and *P. japonica*, twenty two are presenegenin glycosides;
- From *P. crotalarioides*, two with an unusual aglycone, 2-oxo-olean-12-ene-3 β , 27-dihydroxy-23,28-dioic acid;
- From *P. japonica*, three having unusual aglycones as 11-oxo-olean-12-ene-2 β ,3 β ,27-trihydroxy-23,28-dioic acid, 2-oxo-olean-12-ene-23,28-dioic acid glycoside, 3 β ,23,27,29-tetrahydroxy-olean-12-en-28-oic acid, three bayogenin glycosides and three saponin derivatives of medicagenic acid;
- From *P. micrantha*, three medicagenic acid glycosides were also isolated.

Since 2013, new glycosides were isolated from the *Polygala* genus, mainly from *P. sibirica* and *P. flavescens* [61-62]. The structures of the isolated compounds are summarized in Tables 3a and 3b.



Name	R group	Plant	Reference
3 β , 19 α -dihydroxyurso-12-ene-23,28-dioic acid 3-O- β -D-glucuronopyranoside	-Glc	<i>Polygala sibirica L.</i> (aerial parts)	[61]
Pomolic acid 3-O-(3-O-sulfo)- α -L-arabinopyranoside	-(3-O-sulfo)Ara	<i>Polygala sibirica L.</i> (aerial parts)	[61]
Pomolic acid 3-O-(4-O-sulfo)- β -D-xylopyranoside	-(4-O-sulfo)Xyl	<i>Polygala sibirica L.</i> (aerial parts)	[61]
Pomolic acid 3-O-(2-O-acetyl-3-O-sulfo)- α -L-arabinopyranoside	-(2-O-acetyl-3-O-sulfo)Ara	<i>Polygala sibirica L.</i> (aerial parts)	[61]

Table 3a: Saponins isolated from *Polygala* genus



Name	R1 group	R2 group	Plant	Reference
3- <i>O</i> -β-D-glucopyranosyl medicagenic acid 28- <i>O</i> -β-D-galactopyranosyl-(1→4)-β-D-xylopyranosyl-(1→4)-α-L-rhamnopyranosyl-(1→2)-(4- <i>O</i> -acetyl)-[β-D-apiofuranosyl-(1→3)]-β-D-fucopyranosyl ester	-CH ₃		<i>Polygala sibirica</i> (aerial parts)	[61]
3- <i>O</i> -β-D-glucopyranosyl medicagenic acid 28- <i>O</i> -[α-L-rhamnopyranosyl-(1→2)-[(-[β-D-apiofuranosyl-(1→3)]-[4- <i>O</i> -acetyl])]-β-D-fucopyranosyl ester	-CH ₃		<i>Polygala flavescens</i> ssp. (aerial parts)	[62]
3- <i>O</i> -β-D-glucopyranosyl presenegenin 28- <i>O</i> -[β-D-galactopyranosyl-(1→4)-β-D-xylopyranosyl-(1→4)-α-L-rhamnopyranosyl-(1→2)-[β-D-glucopyranosyl-(1→3)]-[4- <i>O</i> -acetyl]]-β-D-fucopyranosyl ester	-CH ₂ OH		<i>Polygala flavescens</i> ssp. (aerial parts)	[62]
3- <i>O</i> -β-D-glucopyranosyl medicagenic acid 28- <i>O</i> -[β-D-galactopyranosyl-(1→4)-β-D-xylopyranosyl-(1→4)-α-L-rhamnopyranosyl-(1→2)-[β-D-glucopyranosyl-(1→3)]]-β-D-fucopyranosyl ester	-CH ₃		<i>Polygala flavescens</i> ssp. (aerial parts)	[62]

Table 3b: Saponins isolated from *Polygala* genus

2.3 Materials and methods

2.3.1 Phytochemical study

NMR spectra were performed using two different equipments: a Varian INOVA 600 (Agilent Technologies) at the operating frequency of 600 MHz. The operating conditions were as follows: ¹H: frequency, 600 MHz; sweep width, 8 kHz; sampling point, 66 k; spectral width, 7804 Hz, accumulation, 32 pulses; temperature, 304 K. ¹³C: frequency, 150 MHz; sweep width, 32 kHz; sampling point, 160 k; spectral width, 30000 Hz, accumulation, 8000 pulses; temperature, 304 K. Each sample was dissolved in C₅D₅N (200μL) using 5 mm micro-sample tube (SHIGEMI Co., Ltd., Japan). Chemical shifts were referenced to solvent signal (δ_H 7.22, δ_C 123.87). Conventional pulse sequences were used for gMQF-COSY, TOCSY, NOESY, gHSQC, and gHMBC. The mixing time in the NOESY experiment was set to 500 ms. TOCSY spectra were acquired using the standard MLEV17 spin-locking sequence and 60 ms mixing time. TOCSY, NOESY and HSQC spectra were recorded using phase-sensitive mode. The size of the acquisition data matrix was 2048 x 256 words in f2 and f1, respectively, and zero filling up to 2k in f1 was made prior to Fourier transformation. Sine-bell or Shifted

sine-bell window functions, with the corresponding shift optimized for every spectrum, were used for resolution enhancement and baseline correction was applied in both dimensions.

The second one is a Varian VNMR-S 600 MHz spectrometer equipped with 3 mm triple resonance inverse and 3 mm dual broadband probeheads. Spectra are recorded in pyridine-*d*₅. Solvent signals were used as internal standard (pyridine-*d*₅: $\delta_{\text{H}} = 7.21$, $\delta_{\text{C}} = 123.5$ ppm), and all spectra were recorded at T = 35°C. The carbon type (CH₃, CH₂, CH) was determined by DEPT and coupling constants (*J*) were measured in Hz.

HR-ESIMS (positive-ion mode) was carried out on a Bruker micrOTOF mass spectrometer and ESIMS (negative-ion mode) on a Finnigan LCQ Deca.

Optical rotation values were recorded on an AA-10R automatic polarimeter.

A R.E.U.S ultrasonic apparatus was used for the extraction. Isolation of compounds were carried out using column chromatography (CC) on Sephadex LH-20 (550 mm x 20 mm, GE Healthcare Bio-Sciences AB), and vacuum liquid chromatography (VLC) on reversed-phase RP-18 silica gel (75-200 μm , Silicycle). Medium-pressure liquid chromatography (MPLC) was performed on silica gel 60 (Merck, 15-40 μm) with a Gilson M 305 pump (25 SC head pump, M 805 manometric module), a Büchi glass column (460 mm x 25 mm and 460 mm x 15 mm), and a Büchi precolumn (110 mm x 15 mm). HPLC was performed on a 1260 Agilent instrument, equipped with a degasser, a quaternary pump, an autosampler, and an UV detector at 210 nm. Chromatographic separation for analytical part was carried out on a C18 column (250 mm \times 4.6 mm id, 5 μm ; Phenomenex LUNA) at room temperature and protected by a guard column. The mobile phase constituted of (A) 0.01% (*v/v*) aqueous trifluoroacetic acid and (B) acetonitrile delivered at 1 ml/min according to the gradient. The injection volume was 10 μl at the concentration of 1 mg/ml. Semi preparative part: Chromatographic separation was carried out on a C-18 column (250 mm x 10 mm id, 5 μm ; Phenomenex LUNA) at room temperature and protected by a guard column. The gradient was the same at 3 ml/min. The injection volume was 0.3 ml at the concentration of 10 mg/ml. Thin-layer chromatography (TLC, Silicycle) and high-performance thin-layer chromatography (HPTLC, Merck) were carried out on precoated silica gel plates 60F₂₅₄, solvent system CHCl₃/MeOH/H₂O/AcOH. The spray reagent for saponins was vanillin reagent (1% vanillin in EtOH/H₂SO₄, 50:1).

2.3.1.1 Extraction and plant material

Extractions were performed by an ultrasound-assisted method. *Wisteria frutescens* voucher specimen N° 20111002 was provided in 2011 from Botanic® (Quétigny, France). *W. floribunda* “macrobotrys” voucher specimen N°20151001 and for *W. floribunda* “rosea” voucher specimens, N°20151002 were provided in 2015 from Botanic® (Quétigny, France). *Weigela florida* “rumba” voucher specimen (N° 20121101) was provided in 2012 from Jardiland® (Chenôve, France). Each sample was deposited in the herbarium of the Laboratory of Pharmacognosy, Université de Bourgogne Franche-Comté, Dijon, France. *Polygala acicularis* was picked up by Pr Delaude from the Liège University (Belgium), in Democratic Republic of Congo and was authenticated by Dr Breyne. A sample was deposited in the Botanical Laboratory, Université de Louvain, Belgium and in the National Botanical Garden of Bruxelles, Belgium.

2.3.1.2 Analytic chromatographic methods

At each step of the protocol of purification by chromatographic methods, the composition of the obtained fractions is checked by thin layer chromatography.

Thin layer chromatography (TLC)

TLC analyses are performed on normal silicagel. The migration is made in glass tanks with an appropriate eluent. The mobile phase is usually a mix of three or four solvents.

Solid support: Normal silica glass plate; (Silica Plate TLC), silicycle Ultra pure silicagel, 10-12 µm.

Revelation: Reagent with sulfuric vanillin, heating at 110°C.

This reagent highlights saponins even if they don't have UV chromophore groups. 100 mL of solution composed of 1g vanillin, 2mL sulfuric acid and ethanol 95% is prepared. An UV observation at 254nm and 365nm is made before revelation to detect flavonoids or compounds with chromophore groups.

High performance thin layer chromatography (HPTLC)

The size of the silica gel in HPTLC is thinner than in TLC. These plates are more precise. The purity of compounds can be verified by this technique.

Solid support: HPTLC plate; Merck, type kieselgel 60 F₂₅₄, 5-6 µm

2.3.1.3 Preparative chromatographic methods

Vacuum liquid chromatography (VLC) in normal and reversed phase

The VLC is a chromatographic technique used for preliminary purification. It is carried out with a funnel gooch and a vacuum pump. The funnel gooch is full of silica gel (normal or reverse phase). The elution can be realized using an isocratic mode or a gradient. The polarity of the eluent is chosen according to the polarity of the sample. Before using, conditioning is performed with the first solvent of the gradient and the sample is dissolved in the same solvent.

VLC normal phase

A chloroform/methanol/water eluent is used because of high polarity of the silica gel and the amphiphilic nature of the saponins. This step allows to eliminate the tannins and to do a first fractionation of the saponins.

Stationary phase: Silicagel 60 (60-200 μ m) silicycle

Mobile phase: Isocratic elution by trays with chloroform/methanol/water mixture in different proportions (80:20:2, 70:30:5, 60:32:7)

VLC reverse phase

A methanol/water mixture is used with this apolar silica gel grafted with hydrophobic groups (C-18). This step allows to eliminate free sugars from the crude extract.

Stationary phase: Silicagel RP-18 (75-200 μ m) silicycle

Mobile phase: Isocratic elution by trays with methanol/water eluent in different proportions

Size exclusion chromatography

This chromatographic method is used to separate compounds according to their molecular weight through a dextran gel. The molecules are eluted in the order of their decreasing molecular masses. In our case, the order of elution is the following: Tannins>Saponins>Flavonoids>Free sugars.

Stationary phase: Sephadex gel LH-20, GE Healthcare, Biosciences AB

Mobile phase: methanol

Column: Glass column

Collector: Pharmacia Biotech-Super Frac

Medium pressure liquid chromatography (MPLC)

This is a chromatographic technique more precise to purify compounds because of the low particle size of the silica gel. A methanol/water mixture is used for reverse phase MPLC and a chloroform/methanol/water mixture for normal phase MPLC. The elution is carried out with a flow between 2 mL and 5 mL and a maximum pressure of 20 bars. Then, fractions with the same chromatographic profile are mixed together and evaporated.

Stationary phase: silicagel60 F₂₅₄ (15-40 µm) Merck, or RP-18 (75-200µm) silicycle

Mobile phase: MeOH/H₂O in different proportions (reverse phase)

CHCl₃/MeOH/H₂O in different proportions (normal phase)

Column: Büchi glass column (230 x 15 mm and 460 x 15 mm)

Pump: Pump manager C-615, Büchi

Pump module C-601, Büchi

Collector: Fraction Collector C-660, Büchi

High performance liquid chromatography (HPLC)

This is the most precise chromatographic technique. The problem is the lack of chromophores in saponins and so the use of an UV detector at 201nm.

Analytic column: C18 column (250 mm × 4.6 mm id, 5 µm; Phenomenex LUNA)

Semi-preparative column: C-18 column (250 mm x 10 mm id, 5 µm; Phenomenex LUNA)

Mobile phase: 0.01% (v/v) aqueous trifluoroacetic acid and acetonitrile in gradient mode

Pump: Quaternary pump Büchi® with autosampler and UV detector at 201nm.

Collector: Büchi® Fraction Collector C-660

2.3.1.4 Lyophilisation

This method is based on the sublimation of the water to obtain powder of the product. It is dissolved in water, and then frozen before lyophilisation. The resulting powder is easier to manipulate and store.

2.3.2 Structural elucidation

2.3.2.1 Mass spectrometry

Mass spectrometry is used to detect and identify molecules with measurements of their mass and fragmentation to characterize their structure. The principle is the separation of charged molecules in gas phase in function of the mass-to-charge ratio.

Electro-Spray Ionization (ESI)

This technique, very useful for saponins, instead of electronic impact, consists of the transfer of ionic species from solution into the gas phase. A continuous stream of the sample solution is passed through a capillary tube, which is maintained at a high voltage (e.g. 2.5 - 6.0 kV). A mixture of highly charged droplets with the same polarity as the capillary voltage is generated. A nebulising gas (e.g. nitrogen) is applied. The generated charged droplets pass down a pressure and potential gradient toward the analyzer region of the mass spectrometer. With an ESI-source temperature and/or another stream of nitrogen drying gas, the charged droplets are continuously reduced in size by evaporation of the solvent, leading to an increasing charge density at the surface. Finally, the electric field strength within the charged droplet reaches a critical point at which it is kinetically and energetically possible for ions at the surface of the droplets to be ejected into the gaseous phase. The emitted ions are sampled and are then accelerated into the mass analyzer for analysis of molecular mass and measurement of ion intensity. (Figure 16) [63].

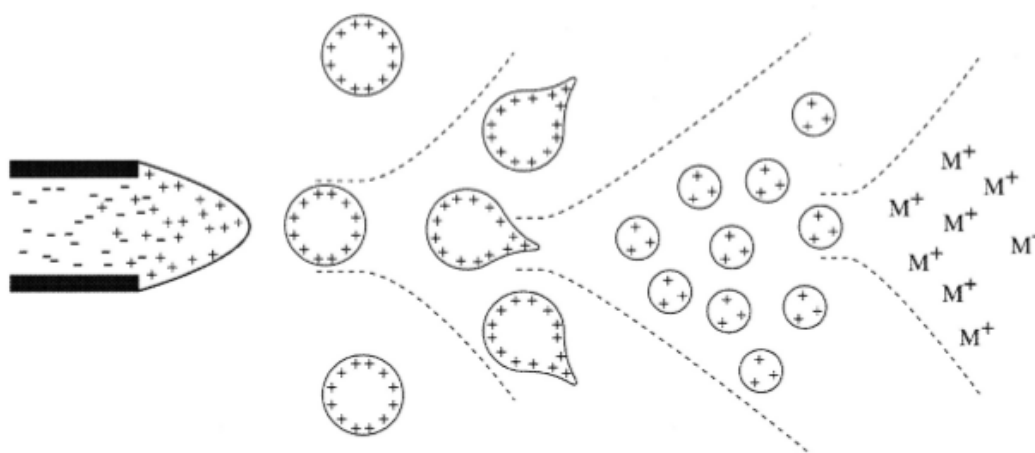


Figure 16: Mechanism of electro-spray ionization [63]

This technique is sensitive, robust, and reliable to investigate, at femto-mole quantities in microliter sample volumes of bio-molecules that couldn't be analyzed by other conventional techniques.

2.3.2.2 Nuclear magnetic resonance (NMR)

The NMR is the most efficient technology to investigate saponin structures. It gives informations about the genin, the conformation and configuration of the sugar moieties, the interglycosidic linkages, and the position of the sugars on the skeleton.

These informations are obtained with mono- and bi-dimensional spectra. 2D-NMR allows to observe correlation between different spins in the molecule. The total assignment of the protons and carbons of the saponin can be achieved.

1D- and 2D-NMR spectra HSQC (Heteonuclear Single Quantum Correlation), HMBC (Heteonuclear Multiple Bond Correlation), COSY (COrelated SpectroscopY), TOCSY (Total Correlation SpectroscopY), and NOESY (Nuclear Overhauser Effect SpectroscopY) or ROESY (Rotating-frame Overhauser Effect SpectroscopY), are performed for each molecule. Measurements are made in pyridine d_5 (C_5D_5N) and chemical shifts δ are expressed in ppm.

2.3.2.2.1 1D NMR: 1H and ^{13}C NMR spectra

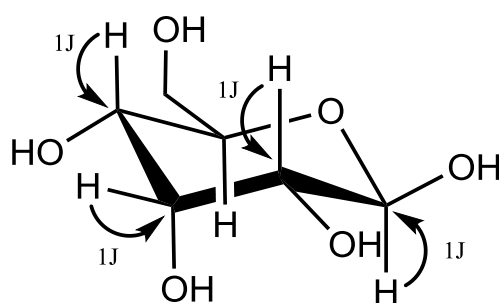
1H NMR and ^{13}C NMR spectra revealed mainly the signals of methyls, methylenes and methines of the aglycon, double bonds, and osidic groups with their anomeric position.

With NMR ^{13}C spectra register in DEPT (Distortionless Enhanced Polarization Transfer), primary and tertiary carbons can be differentiated from secondary.

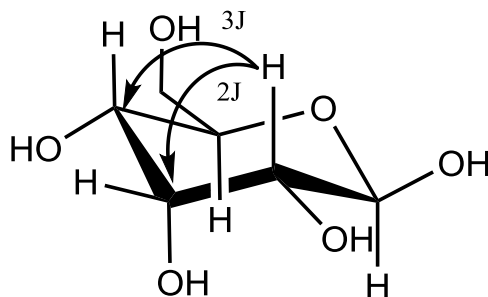
2.3.2.2.2 2D NMR: Homo- and heteronuclear correlations

Heteronuclear correlations $^1H/^{13}C$

HSQC: This experiment allows to see a direct coupling (1J) between carbon and proton.

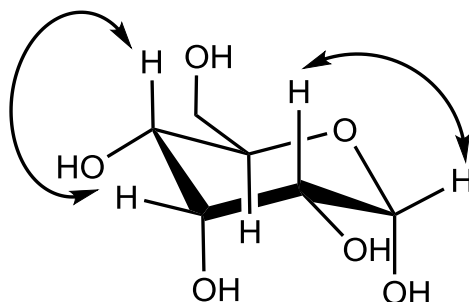


HMBC: It is an experiment to see long-range heteronuclear coupling $^1\text{H}/^{13}\text{C}$ (2J and 3J). It is essential to determine the structure of aglycon, sugar moieties, interglycosidic linkages and skeleton/oligosaccharidic chain linkages.

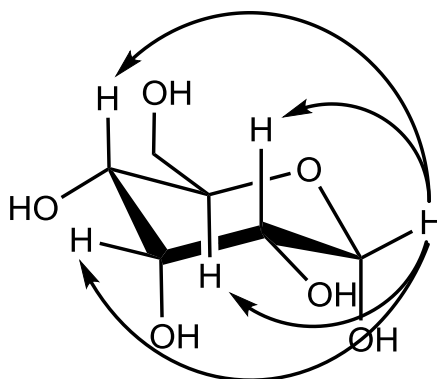


Homonuclear correlations

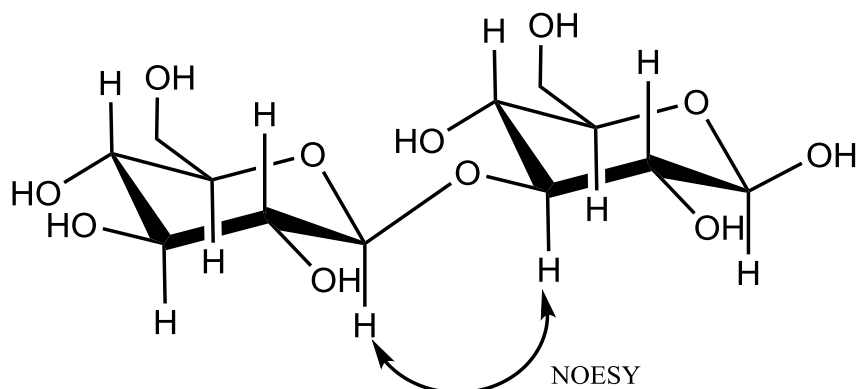
COSY: Homonuclear 2J and 3J coupling between two protons in the same spin system is used to see neighbor protons in the molecule.



TOCSY: This experiment also called HOHAHA (HOmonuclear HARTmann-HAhn spectroscopy) is very useful to see protons in the same spin system. We can see all protons in one sugar.



NOESY: It is an experiment, which shows dipolar interactions for protons separated by less than 3,5 Å. With NOESY spectra spatial proximity can be found for some part of the molecule. It's very useful to determine linkage between different parts of the molecule. The ROESY spectrum can be also used.

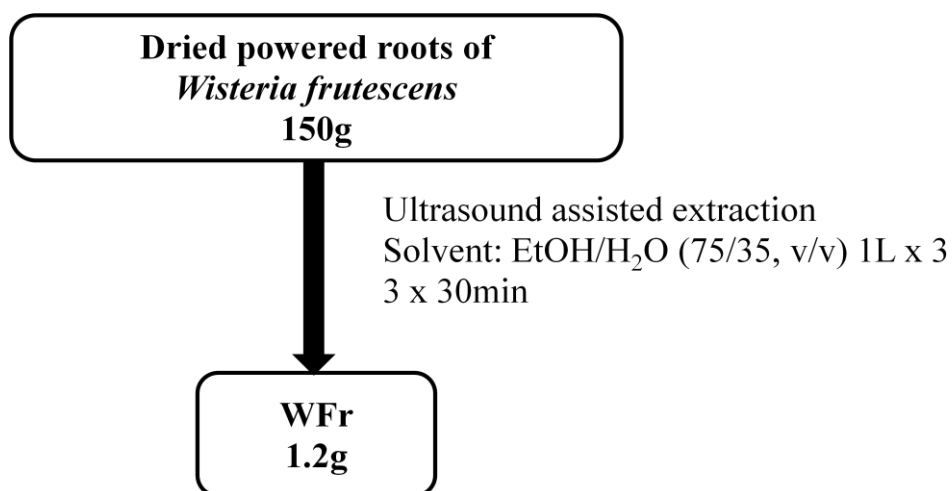


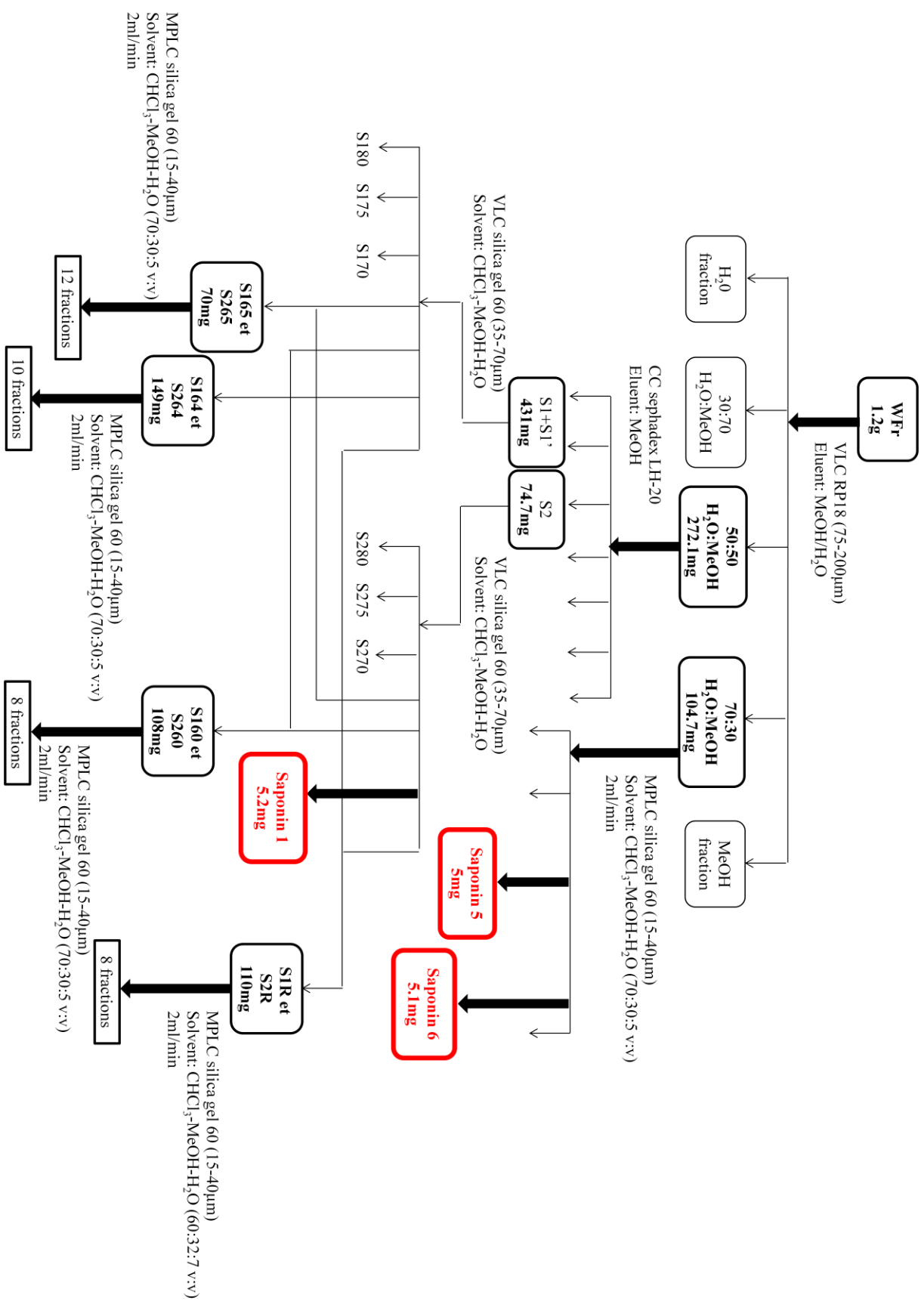
2.4 Personal works

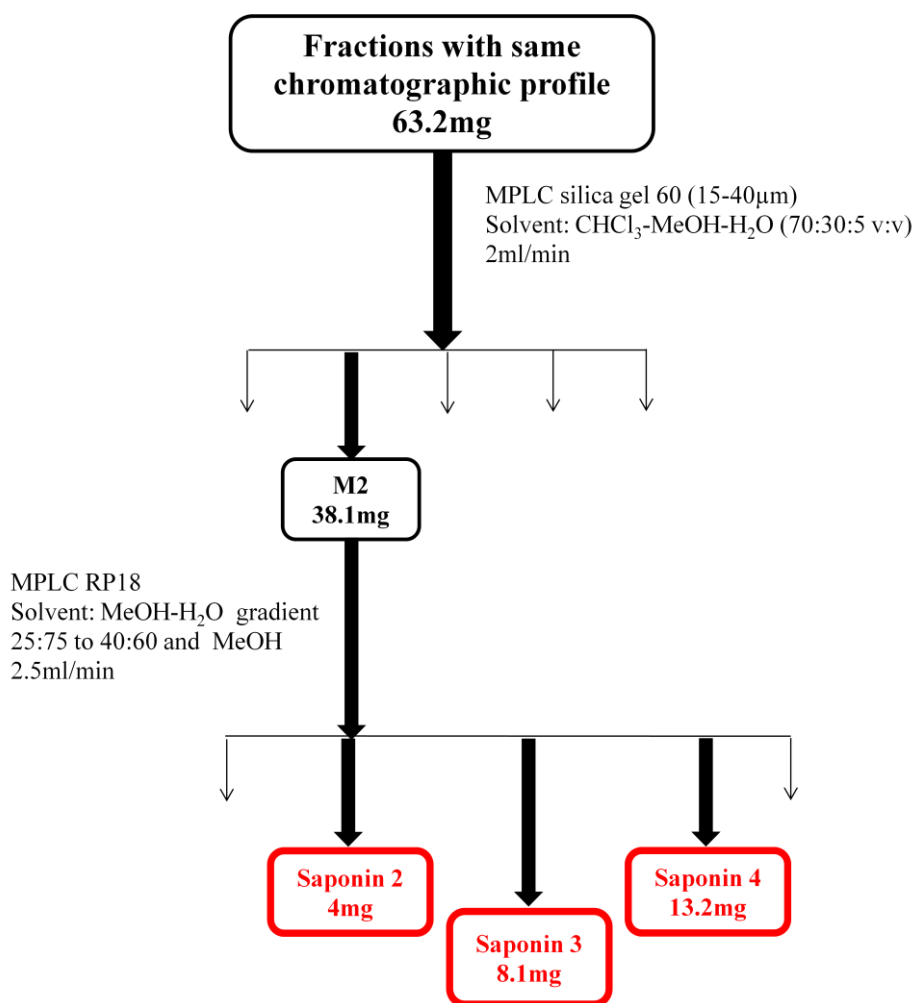
2.4.1 Extraction and isolation

W. frutescens

The roots of *W. frutescens* were studied. Six triterpene glycosides (**1-6**) were isolated using various chromatographic methods: two previously undescribed, one described in its native form for the first time, and three known ones already reported in the literature. Extraction and isolation of these compounds are summarized below:

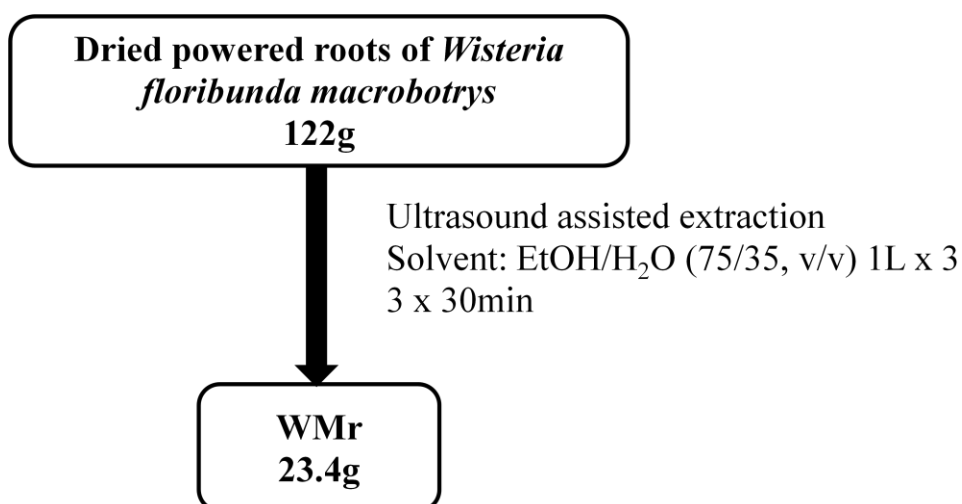


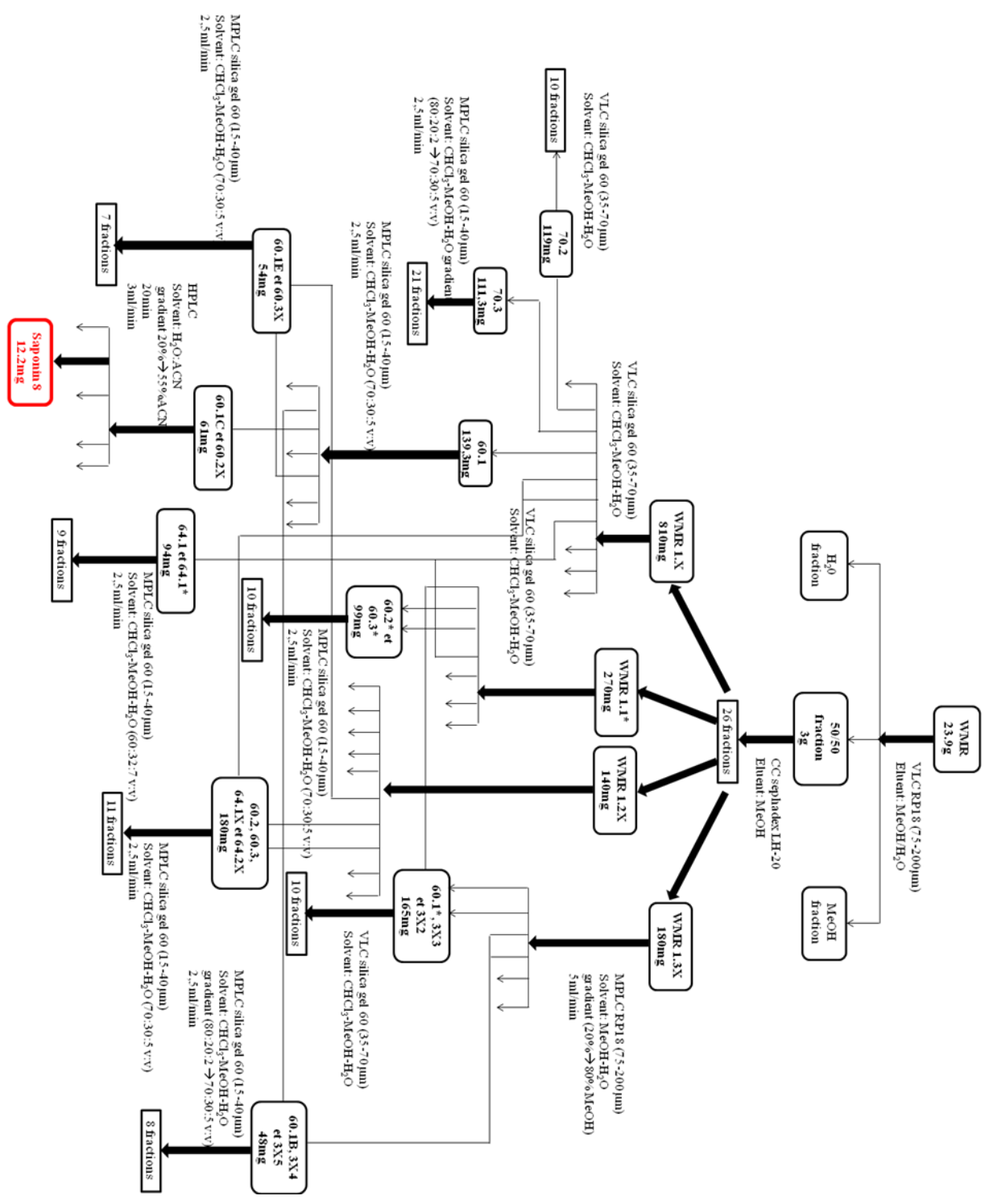


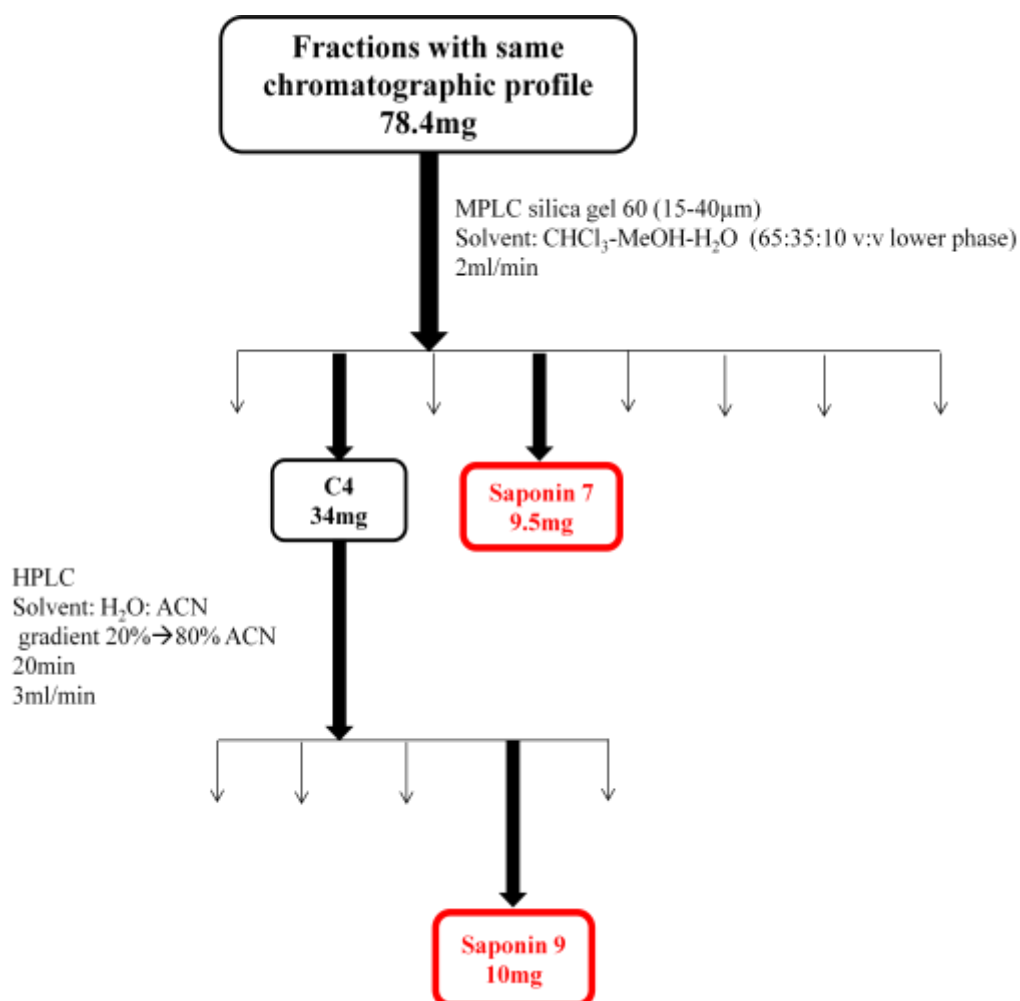


W. floribunda “macrobotrys”

The roots of *W. floribunda* “macrobotrys” were analysed. Three saponins (7-9) were extracted and purified: one new oleanane-type glycoside and two known ones:

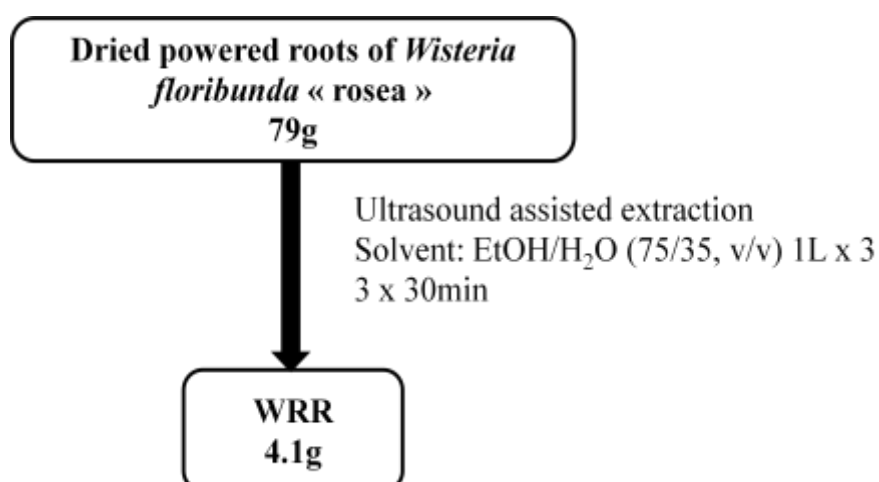


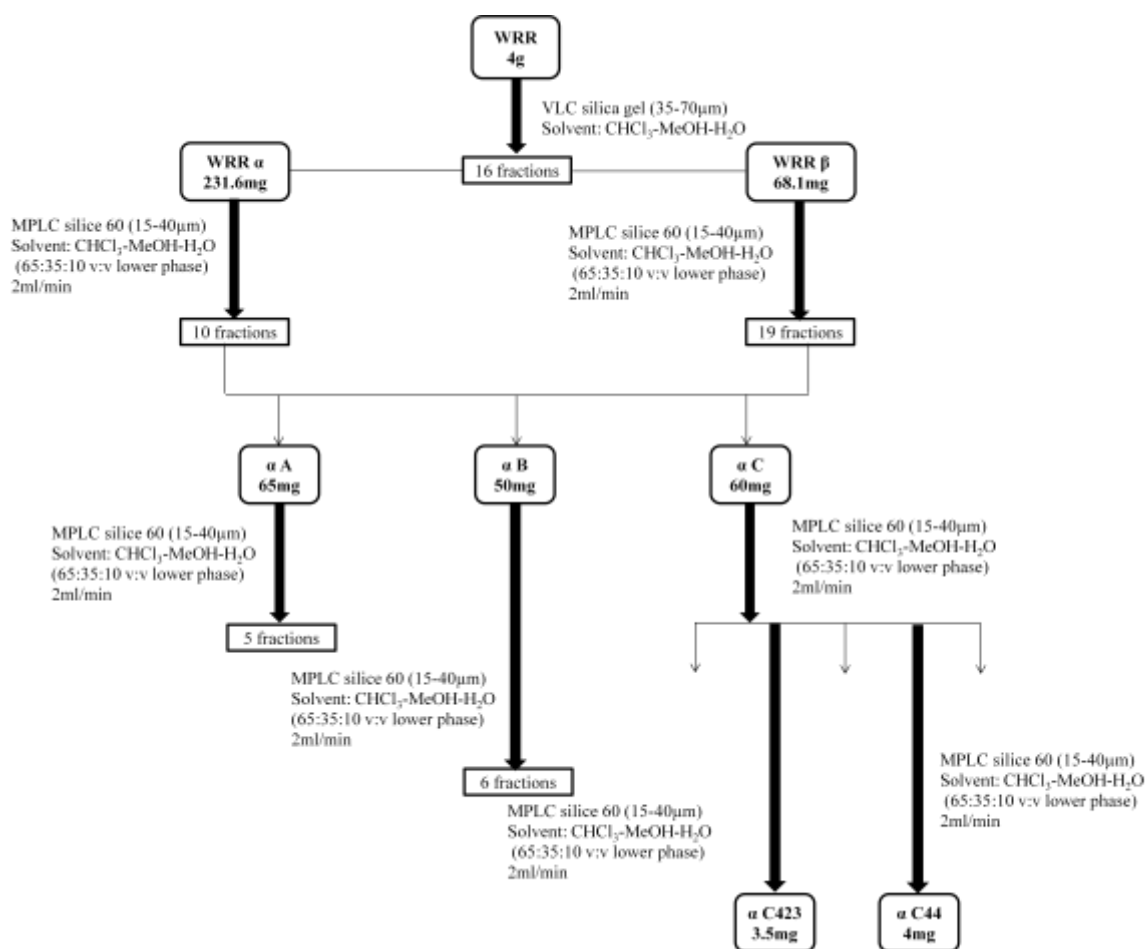




W. floribunda “rosea”

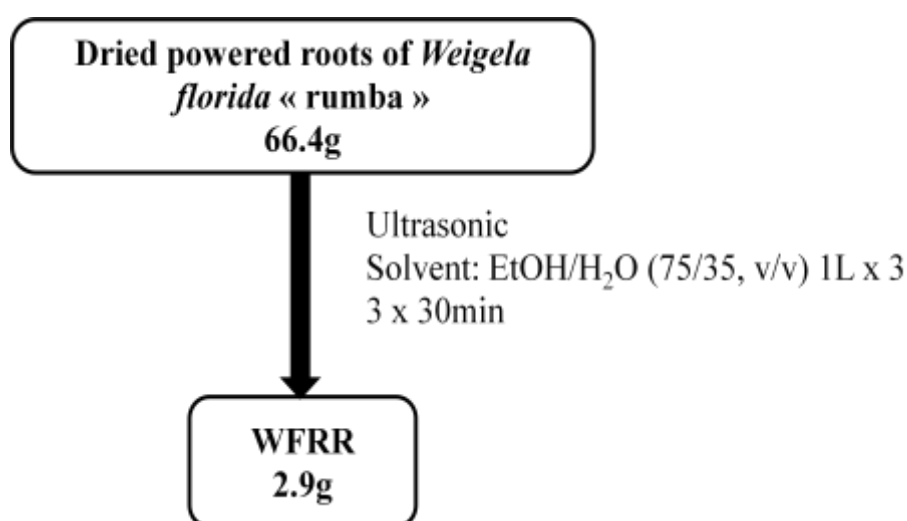
The roots of *W. floribunda* “rosea” were extracted. Two known saponins (**10**, **11**) were obtained by chromatographic methods:

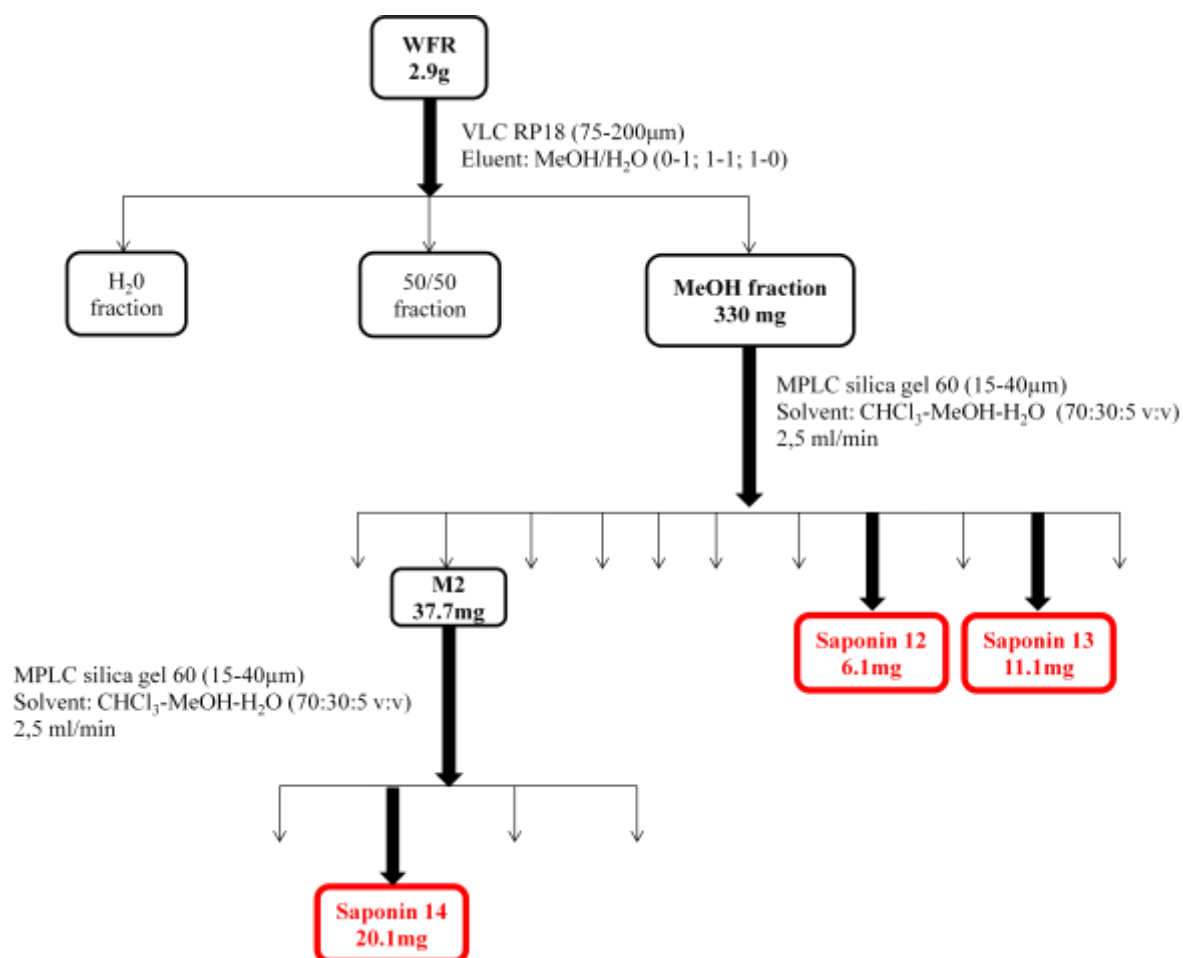




W. Florida “rumba”

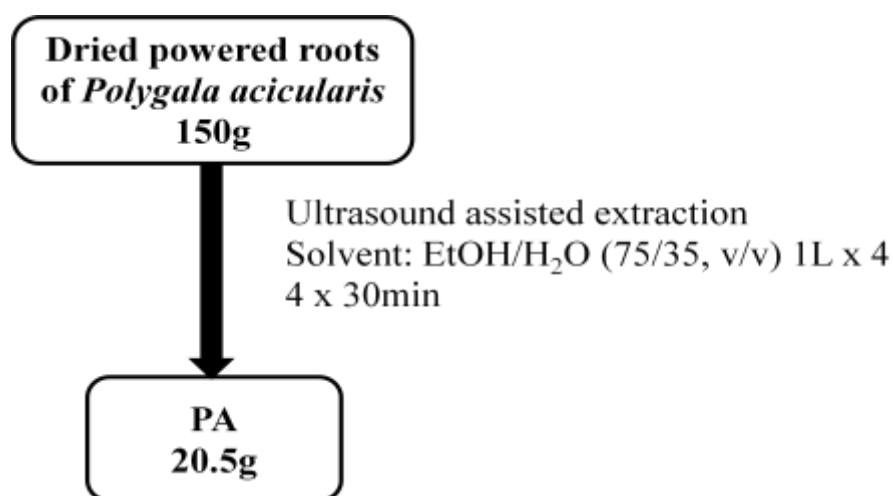
From the roots of *W. florida* “rumba”, three new saponins (**12-14**) were isolated. Extraction and isolation are presented:

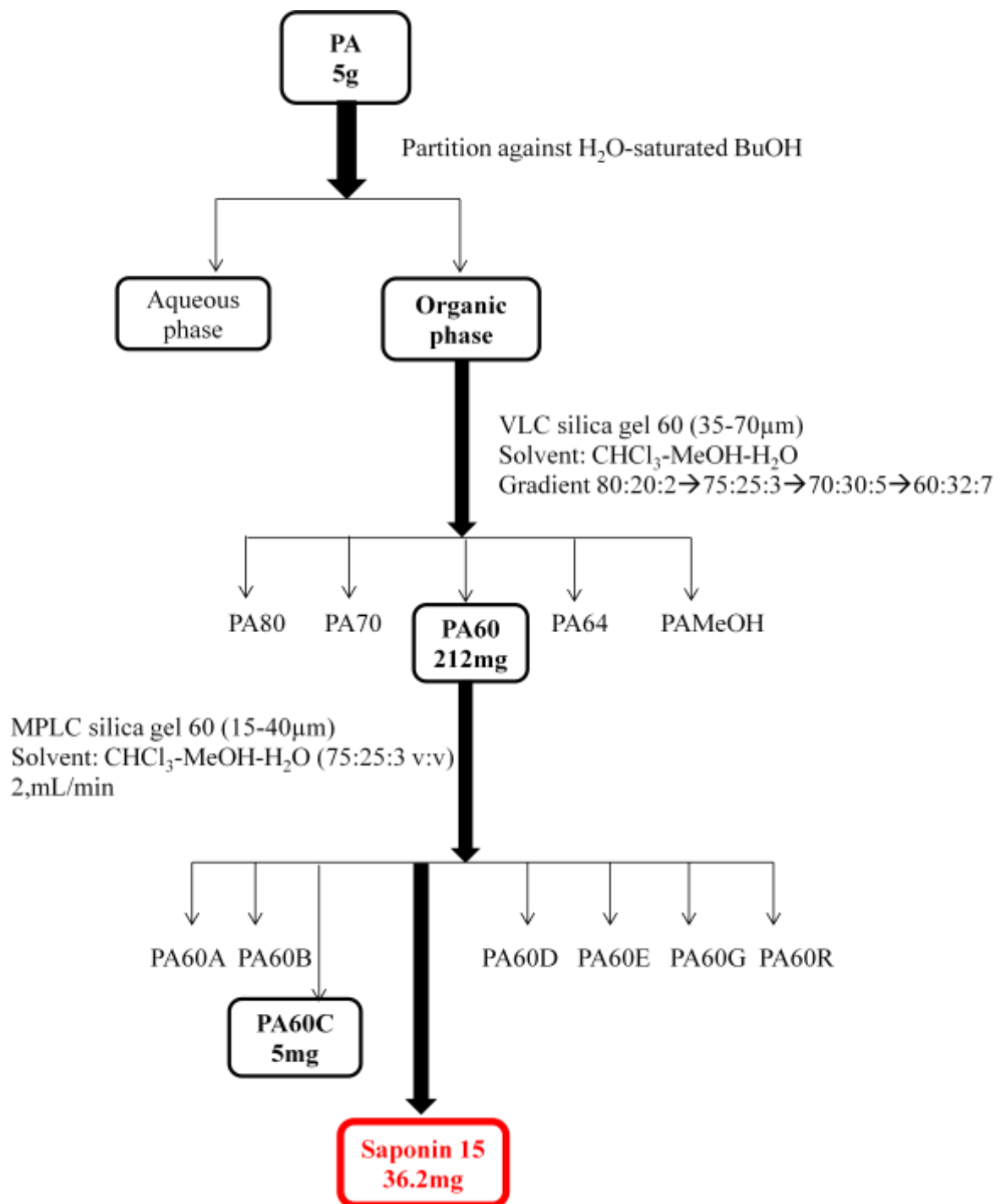


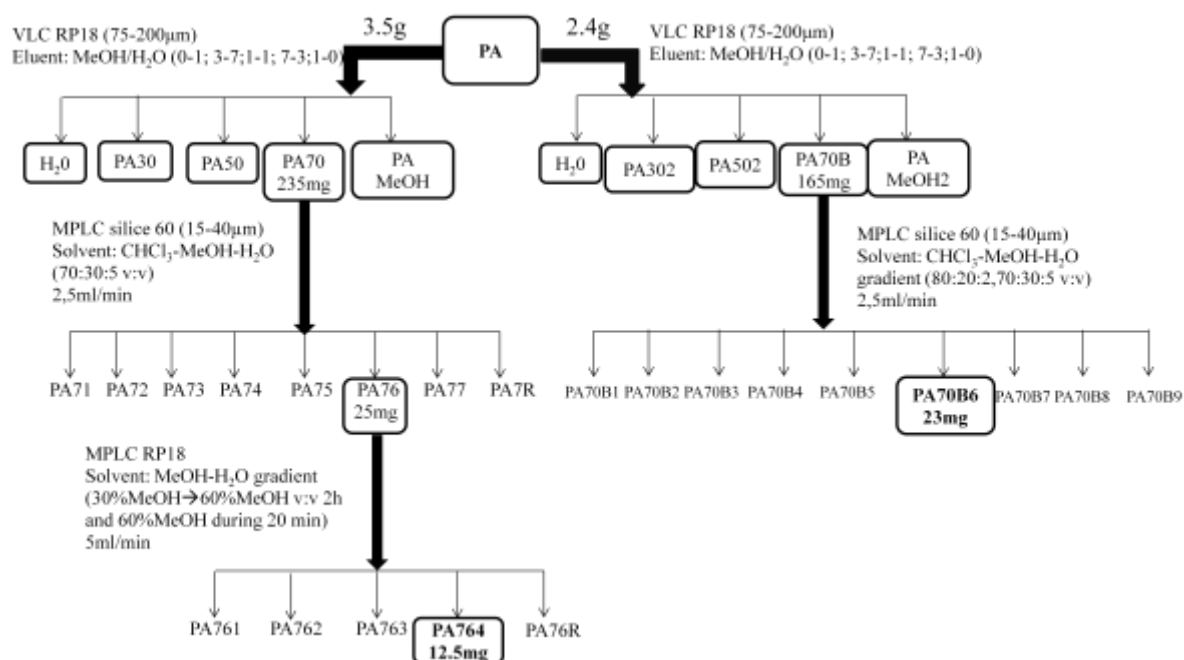


Polygala acicularis

From the roots of *Polygala acicularis* two presenegenin glycosides (**15**, **16**) previously described in literature were isolated. The protocol is described below:







2.4.2 Structural elucidation

W. frutescens

Six oleanane-type saponins from the roots of *W. frutescens* were isolated. Their structures were established by a detailed 600 MHz NMR analysis including 1D and 2D NMR (^1H , ^{13}C NMR, COSY, TOCSY, NOESY, HSQC, HMBC) experiments and mass spectrometry as two previously undescribed triterpenoid saponins (**1**, **2**) and four known ones (**3-6**). The structural analysis of the native form of wistariasaponin G (**3**) is described for the first time.

The saponins **1-3** were isolated from an aqueous-ethanolic extract of the roots of *W. frutescens* by various solid/liquid chromatographic methods: vacuum liquid chromatography (VLC) on normal and reverse phase RP-18 silica gel, medium pressure liquid chromatography (MPLC) and size exclusion chromatography on Sephadex LH-20.

The HR-ESIMS (positive-ion mode) spectrum of compound **1** established its molecular formula as $\text{C}_{51}\text{H}_{80}\text{O}_{20}$ with a pseudo-molecular peak at m/z 1035.5150 $[\text{M} + \text{Na}]^+$ (calcd 1035.5141). Its ESIMS (negative-ion mode) displayed a quasi-molecular ion peak at m/z 1011 $[\text{M} - \text{H}]^-$, indicating a molecular weight of 1012 (Figure 17).

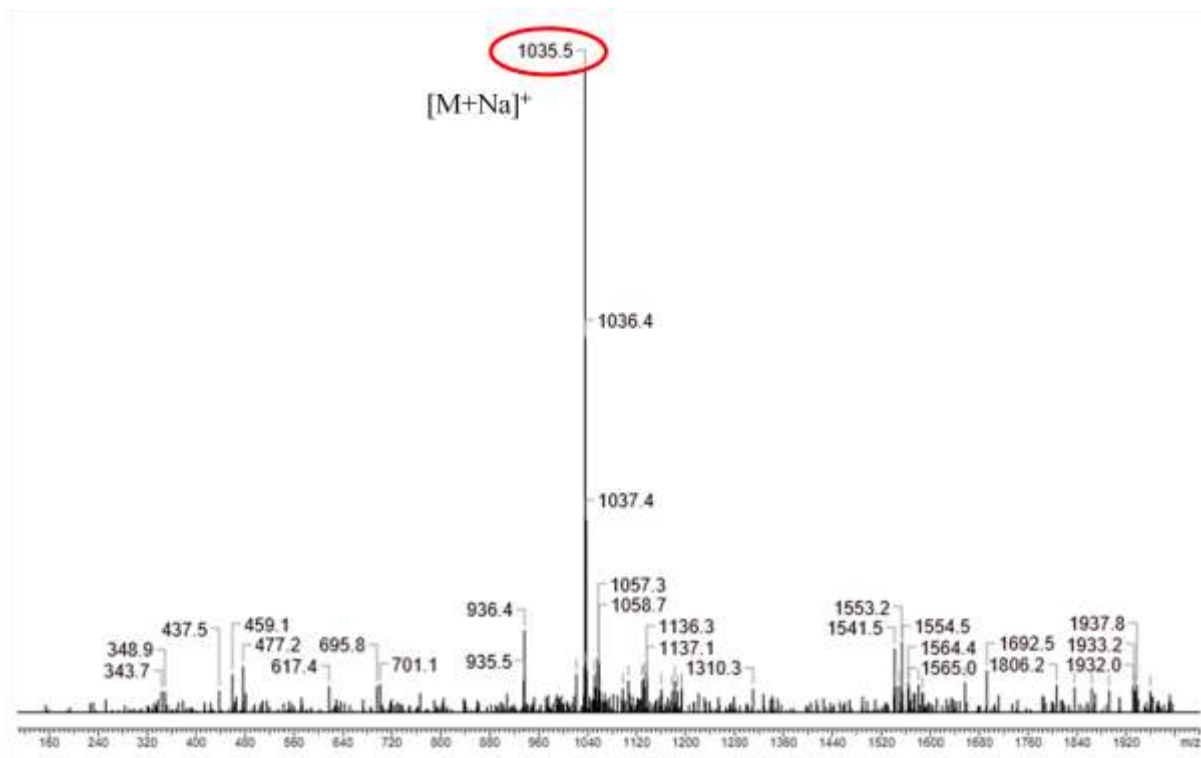


Figure 17: Positive ESIMS of saponin **1**

The ^1H NMR spectrum of the aglycone part of **1** displayed signals assignable to seven angular methyl groups at δ_{H} 0.75, 0.85, 0.98, 1.01, 1.07, 1.22 and 1.28 (3H s, each), one olefinic proton at δ_{H} 5.28 (1H, br t, $J = 3.0$, H-12), three oxygen bearing methine protons at δ_{H} 3.23 (1H, dd, $J = 12.0, 3.8$ Hz, H-3_{ax}), 4.53 (1H, dd, $J = 12.4, 4.0$ Hz, H-16_{ax}) and 6.10 (1H, br s, H-22_{eq}), and one primary alcoholic function at δ_{H} 4.23 (1H, d, $J = 12.4$ Hz, H-28_{aeq}), 4.86 (1H, d, $J = 12.4$ Hz, H-28_{beq}) (Table 4). In the ^{13}C NMR spectrum, signals at δ_{C} 170.3 and 171.1 suggested two ester functions. Furthermore, HMBC correlations at δ_{H} 2.01 (3H, s) / δ_{C} 171.1 and δ_{H} 2.09 (3H, s) / δ_{C} 170.3 revealed the presence of two acetyl groups. A HMBC cross-peak at δ_{H} 1.65 (1H, dd, $J = 13.3, 4.0$ Hz, H-15_{eq}) / δ_{C} 141.7 (C-13) and a COSY correlation between δ_{H} 1.65 (1H, dd, $J = 13.3, 4.0$ Hz, H-15_{eq}), 2.24 (1H, dd, $J = 13.3, 12.4$ Hz, H-15_{ax}) and 4.53 (1H, dd, $J = 12.4, 4.0$ Hz, H-16_{ax}), allowed the location of a secondary alcoholic function at the C-16 position. A HMBC correlation between a deshielded signal at δ_{H} 4.23 (1H, d, $J = 12.4$ Hz, H-28_{aeq}) and δ_{C} 66.4 (C-16) proved the location of the primary alcoholic function at C-28. Other HMBC correlations of δ_{H} 1.07 (3H, s, H₃-30_{ax}) and 0.85 (3H, s, H₃-29_{eq}) with δ_{C} 37.7 (C-21), and a COSY correlation between δ_{H} 1.74 (H-21_{ax}) and 6.10 (1H, br s, H-22_{eq}) confirmed the location of another secondary alcoholic function at C-22. The configurations of C-3 and C-16 of the aglycone were determined by the correlations

observed in the NOESY spectrum between H-3 α -axial and H₃-23 α -equatorial, and between H-16 α -axial and H₃-27 α -axial, respectively. The α -equatorial orientation of H-22 was deduced by its coupling constant as a br s and by the NOESY connectivity with α -axial H-16. The structure of the aglycone of **1** was thus recognized to be the unusual olean-12-ene-3 β ,16 β ,22 β -28-tetrol, a stereoisomer of the camelliagenin A (Table 4). The deshielded values of H-22_{eq} at δ_{H} 6.10 and H-28_{aeq} and H-28_{beq} at δ_{H} 4.23, 4.86, respectively, suggested an acetylation at these two positions (Table 4, Figure 18). The HMBC correlation between δ_{H} 4.23 (H-28_{aeq}) and δ_{C} 171.1 (OCO) allowed the location of the first acetyl group at C-28 and thus the location of the other acetyl group at C-22.

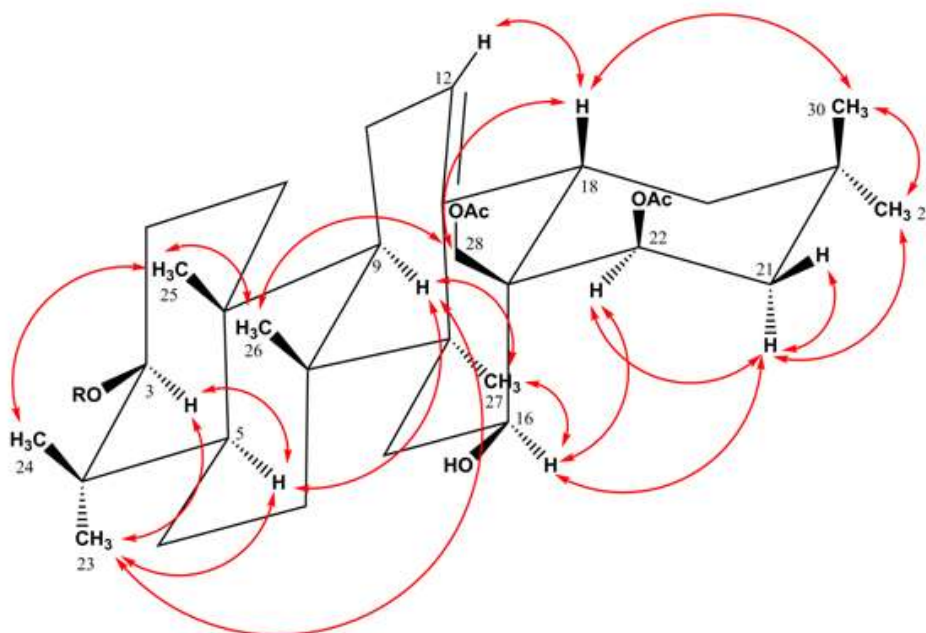


Figure 18: Significant NOE correlations in NOESY experiment of compound **1**.

The HSQC spectrum of **1** displayed signals of three anomers at δ_{H} 5.53 (1H, d, $J = 7.3$ Hz) / δ_{C} 102.1, δ_{H} 4.83 (1H, d, $J = 6.9$ Hz) / δ_{C} 104.8, and δ_{H} 6.20 (1H, br s) / δ_{C} 101.6 (Figures 19, 20 and 21). The ring protons of the monosaccharide residues were assigned starting from the readily identifiable anomeric protons by means of the ^1H - ^1H COSY, TOCSY, HSQC, and HMBC experiments and by GC (see experimental). Units of one β -D-glucuronopyranosyl (GlcA), one β -D-xylopyranosyl (Xyl), and one α -L-rhamnopyranosyl (Rha) were thus identified (Table 5). The monodesmosidic structure was suggested by the HMBC cross-peak at δ_{H} 4.83 (1H, d, $J = 6.9$ Hz, GlcA-1) / δ_{C} 89.6 (C-3) and the NOESY cross-peak at δ_{H} 4.83 (1H, d, $J = 6.9$ Hz, GlcA-1) / δ_{H} 3.23 (1H, dd, $J = 12.0, 3.8$ Hz, H-3_{ax})

(Figure 22). Other HMBC correlations at δ_H 4.23 (1H, dd, $J = 8.0, 6.9$ Hz, GlcA-2) / δ_C 102.1 (Xyl-1) and at δ_H 4.14 (1H, dd, $J = 8.8, 7.3$ Hz, Xyl-2) / δ_C 101.6 (Rha-1) suggested a α -L-rhamnopyranosyl-(1 \rightarrow 2)- β -D-xylopyranosyl-(1 \rightarrow 2)- β -D-glucuronopyranosyl sequence (Table 5).

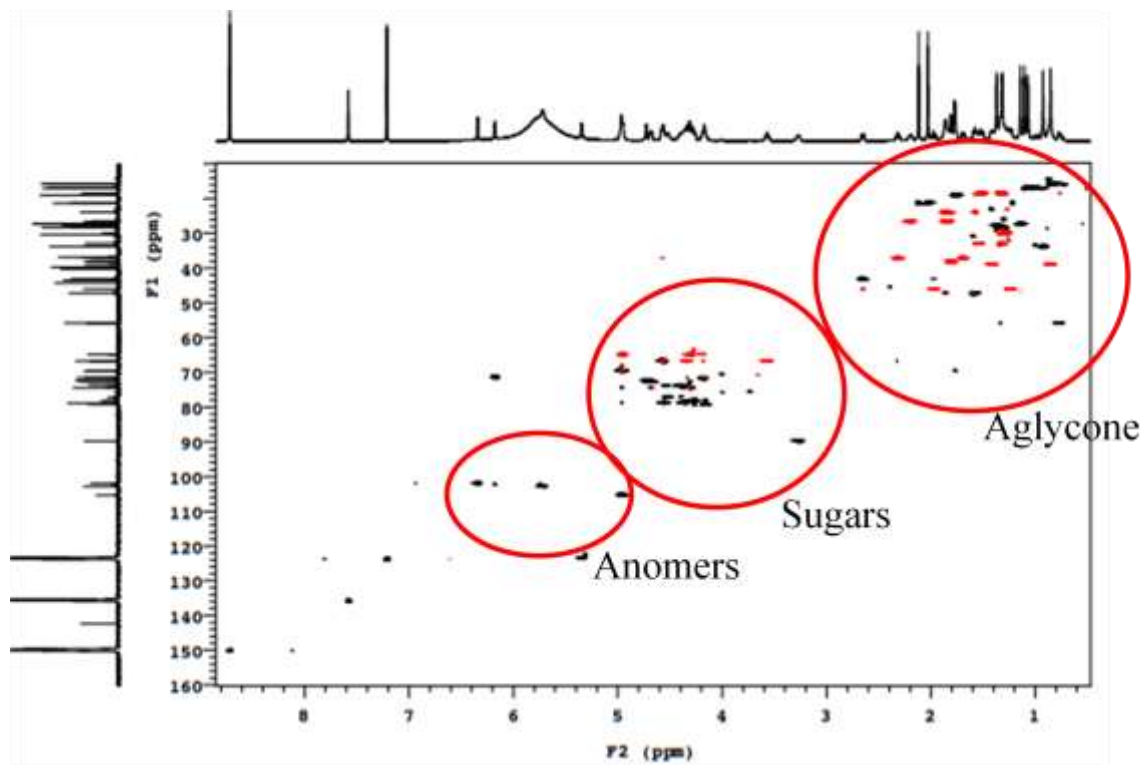


Figure 19: General HSQC of saponin 1

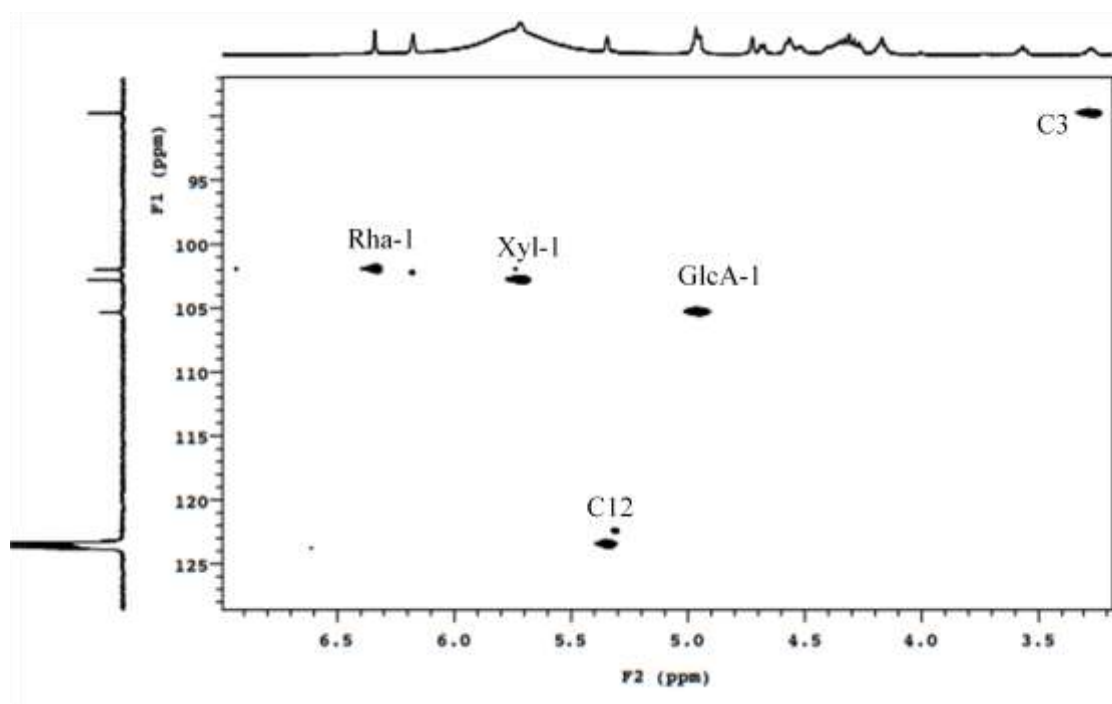


Figure 20: HSQC anomers zone of saponin 1

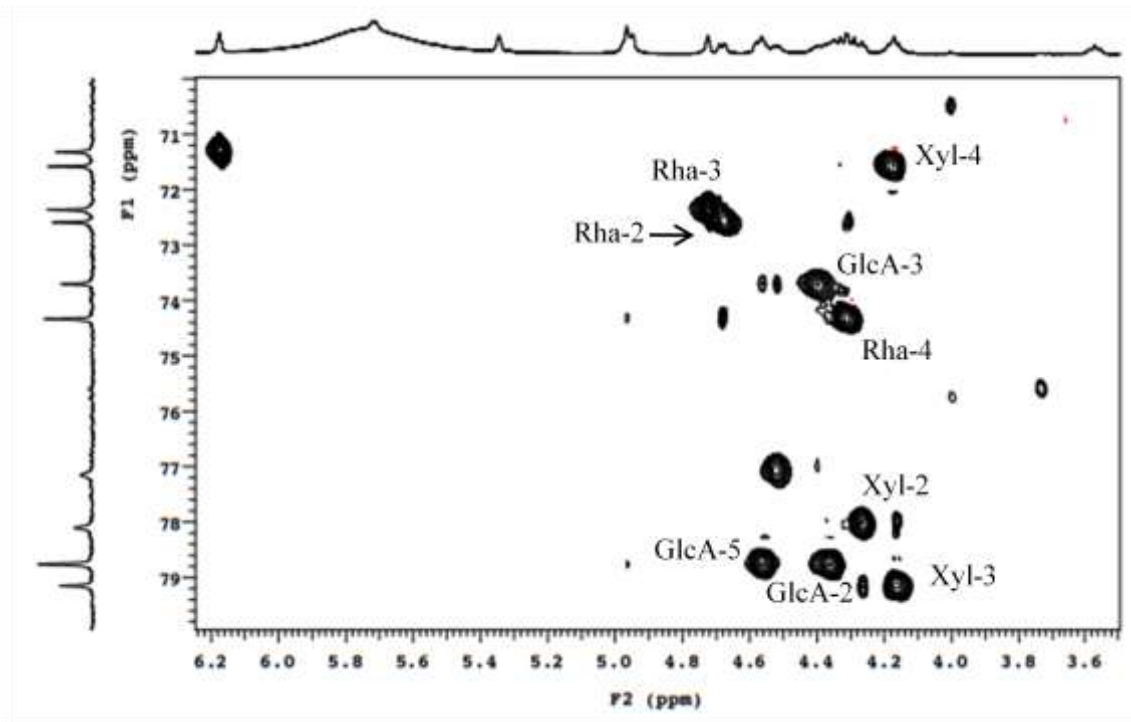


Figure 21: HSQC spectrum of saponin 1

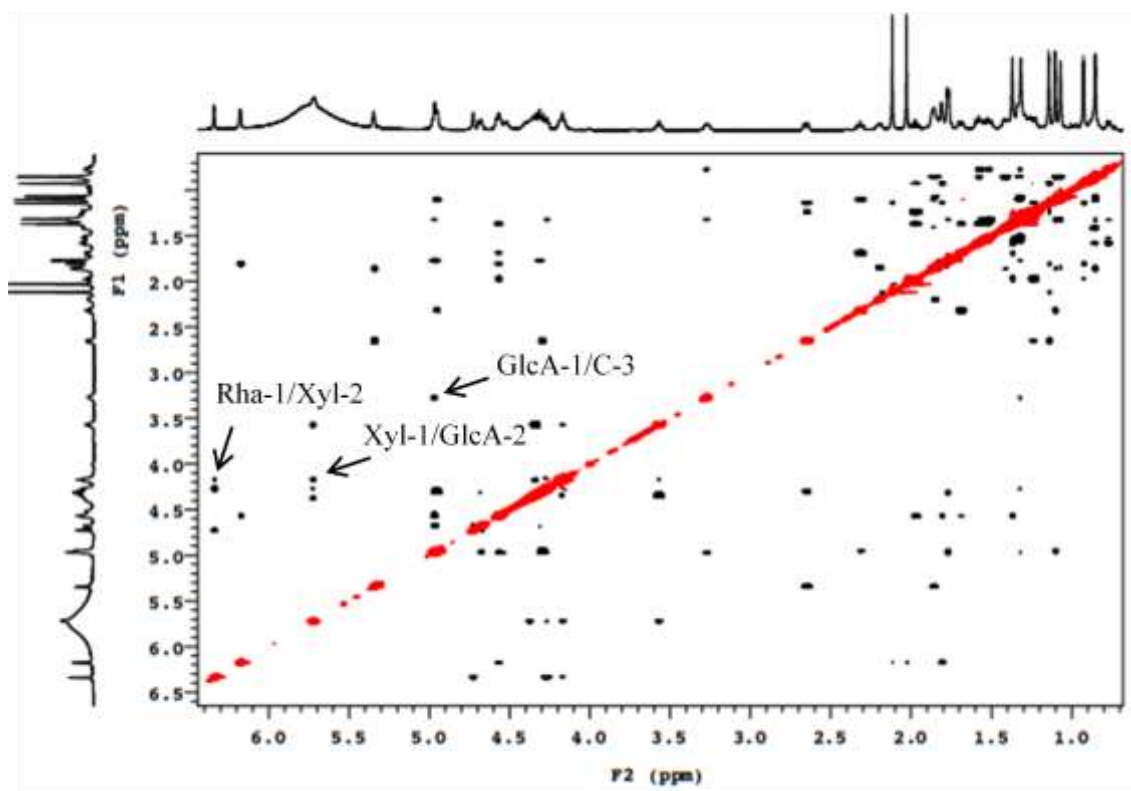


Figure 22: ROESY spectrum of saponin 1

The monosaccharides obtained by acid hydrolysis of **1** were identified by comparison on TLC with authentic samples as glucuronic acid, xylose and rhamnose. The absolute configurations of the sugars were determined to be D for GlcA and Xyl, and L for Rha by GC analysis according to a method previously described [64]. The large $^1J_{H-1,C-1}$ value of the Rha (167 Hz) confirmed that the anomeric proton was equatorial (α -pyranoid anomeric form). The relatively large $^3J_{H-1,H-2}$ value of GlcA and Xyl (6.9 and 7.3 Hz, respectively) in their pyranose form indicated their β anomeric orientation. The same protocol was used for the identification of the monosaccharides of **2** and **3**.

On the basis of the above results, the structure of **1** was elucidated as the new 3-*O*- α -L-rhamnopyranosyl-(1 \rightarrow 2)- β -D-xylopyranosyl-(1 \rightarrow 2)- β -D-glucuronopyranosyl-22,28-*O*-diacetylolean-12-ene-3 β ,16 β ,22 β ,28-tetrol (**1**).

The HR-ESIMS (positive-ion mode) spectrum of compound **2** showed a pseudo-molecular ion peak at m/z 1023.5269 [$M + Na$] $^+$ (calcd 1023.5141) ascribable to the molecular formula $C_{50}H_{80}O_{20}$. Its ESIMS (positive-ion mode) displayed a quasi-molecular ion peak at m/z 1023 [$M + Na$] $^+$, indicating a molecular weight of 1000 (Figure 23).

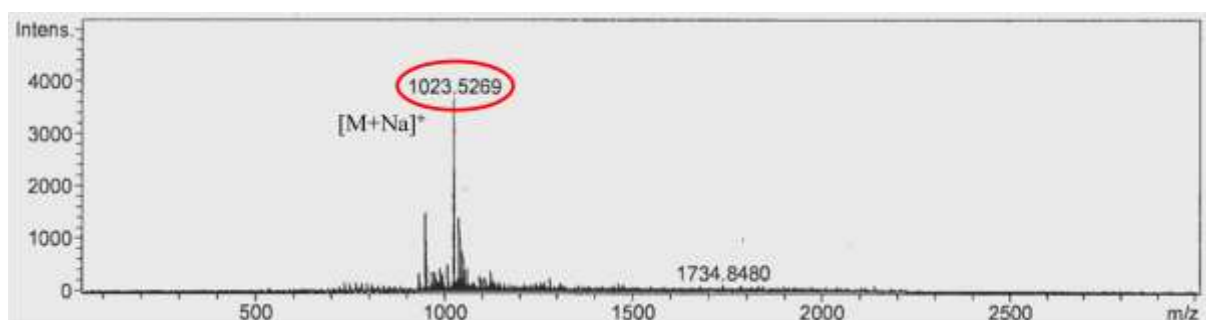


Figure 23: Positive ESIMS of saponin **2**

The 1H NMR spectrum of the aglycone part of **2** displayed signals assignable to seven angular methyl groups at δ_H 0.74, 0.83, 0.92, 1.01, 1.03, 1.22 and 1.28 (3H, s, each), one olefinic proton at δ_H 5.22 (1H, br t, $J = 3.1$, H-12), three oxygen bearing methine protons at δ_H 3.21 (1H, dd, $J = 11.9, 3.6$ Hz, H-3 $_{ax}$), 4.53 (1H, dd, $J = 12.5, 4.1$ Hz, H-16 $_{ax}$) and 6.24 (1H, br s, H-22 $_{eq}$), and one free primary alcoholic function at δ_H 4.25 (1H, d, $J = 12.3$ Hz, H-28 $_{aeq}$), 4.93 (1H, d, $J = 12.3$ Hz H-28 $_{beq}$) / δ_C 63.0. In the ^{13}C NMR spectrum, a signal at δ_C 170.2 suggested an ester function and a HSQC correlation at δ_H 2.07 (3H, s) / δ_C 21.0 revealed the

presence of only one acetyl group. These signals suggested that the aglycone of **2** is a 22-*O*-acetylated derivative of the aglycone of **1** (Table 4).

The HSQC spectrum of **2** displayed signals of three anomers at δ_{H} 4.81 (1H, d, $J = 7.1$ Hz) / δ_{C} 104.8, 5.50 (1H, d, $J = 7.4$ Hz) / δ_{C} 101.9, and 6.18 (1H, br s) / δ_{C} 101.6. According to the same protocol as for compound **1**, units of one β -D-glucuronopyranosyl, one β -D-glucopyranosyl, and one α -L-rhamnopyranosyl were identified (Table 5, Figures 24 and 25). NOESY correlations were mainly used to establish the structure of the oligosaccharidic chain, between δ_{H} 4.81 (1H, d, $J = 7.1$ Hz, GlcA-1) / δ_{H} 3.21 (1H, dd, $J = 11.9, 3.6$ Hz, H-3_{ax}), δ_{H} 5.50 (1H, d, $J = 7.4$ Hz, Glc-1) / δ_{H} 4.44 (1H, dd, $J = 8.1, 7.1$ Hz, GlcA-2), and δ_{H} 6.18 (1H, br s, Rha-1) / δ_{H} 4.12 (1H, dd, $J = 8.4, 7.4$ Hz Glc-2) (Figure 26).

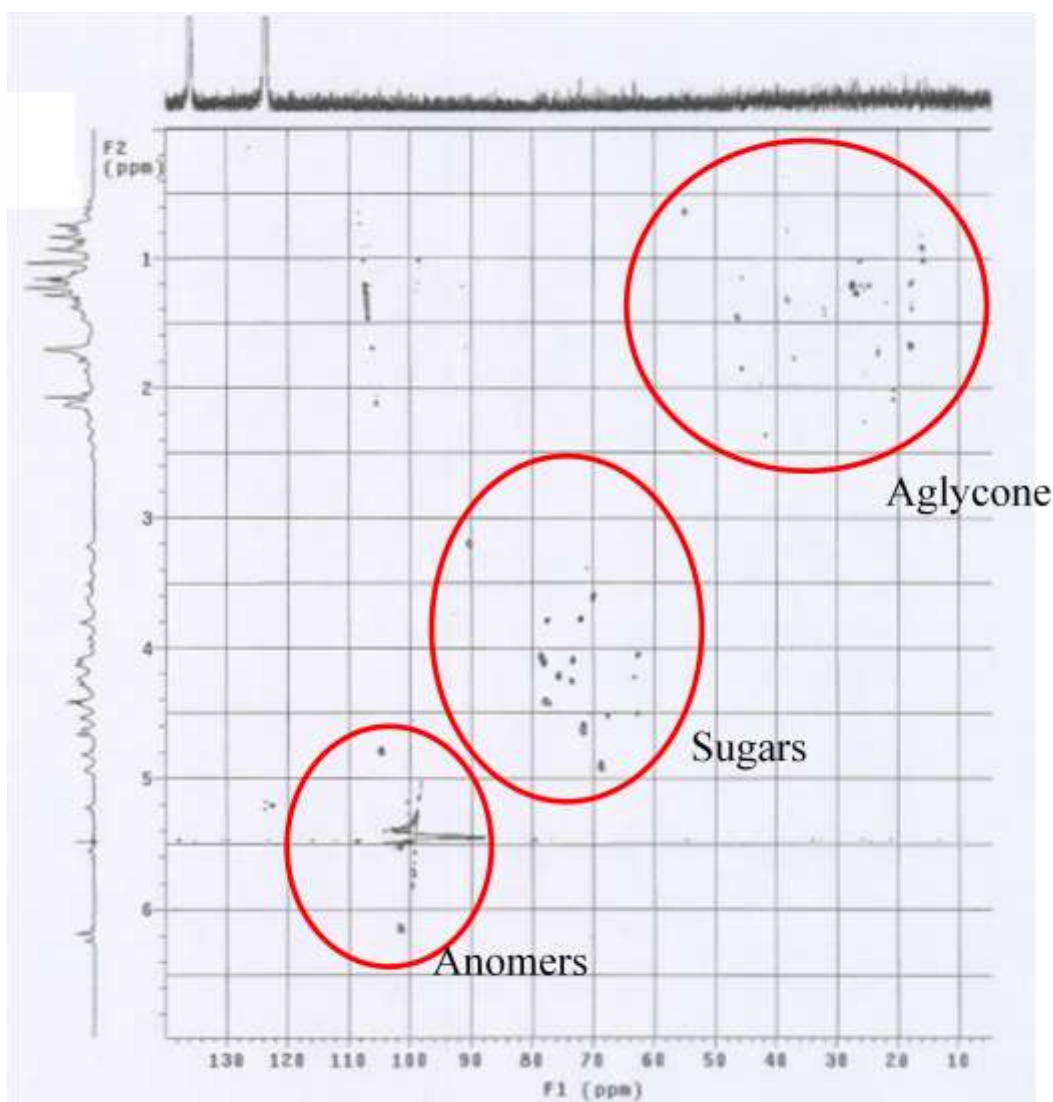


Figure 24: General HSQC spectrum of saponin **2**

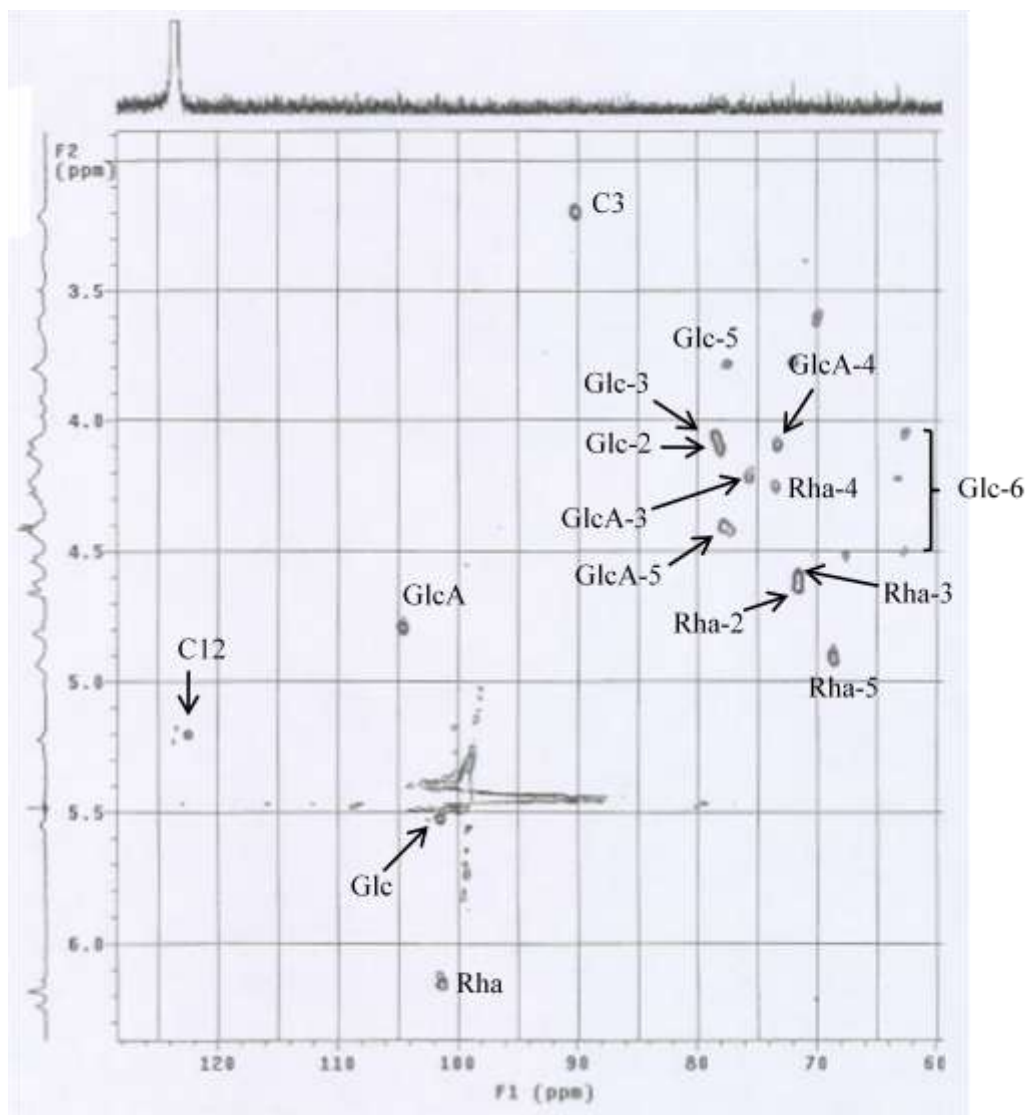


Figure 25: HSQC anomers zone of saponin 2

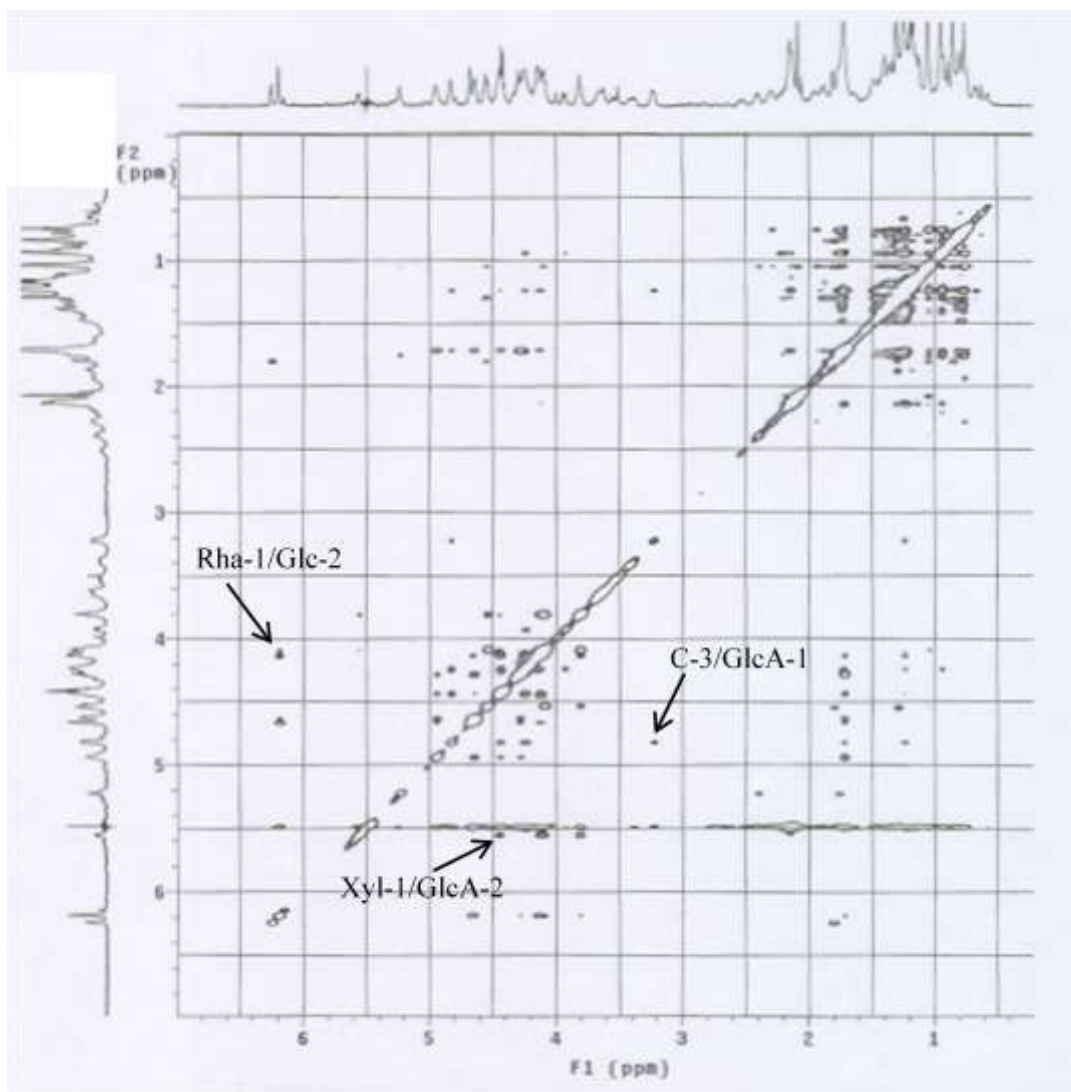


Figure 26: NOESY spectrum of saponin **2**

The structure of the new natural compound **2** was thus established as 3-*O*- α -L-rhamnopyranosyl-(1 \rightarrow 2)- β -D-glucopyranosyl-(1 \rightarrow 2)- β -D-glucuronopyranosyl-22-*O*-acetylolean-12-ene-3 β ,16 β ,22 β ,28-tetrol (**2**).

The HR-ESIMS (positive-ion mode) spectrum of compound **3** established its molecular formula as $C_{49}H_{76}O_{20}$ with a pseudo-molecular peak at m/z 1007.4881 [$M + Na$] $^+$ (calcd 1007.4828). Its ESIMS (positive-ion mode) displayed a quasi-molecular ion peak at m/z 1007 [$M + Na$] $^+$, indicating a molecular weight of 984 (Figure 27).

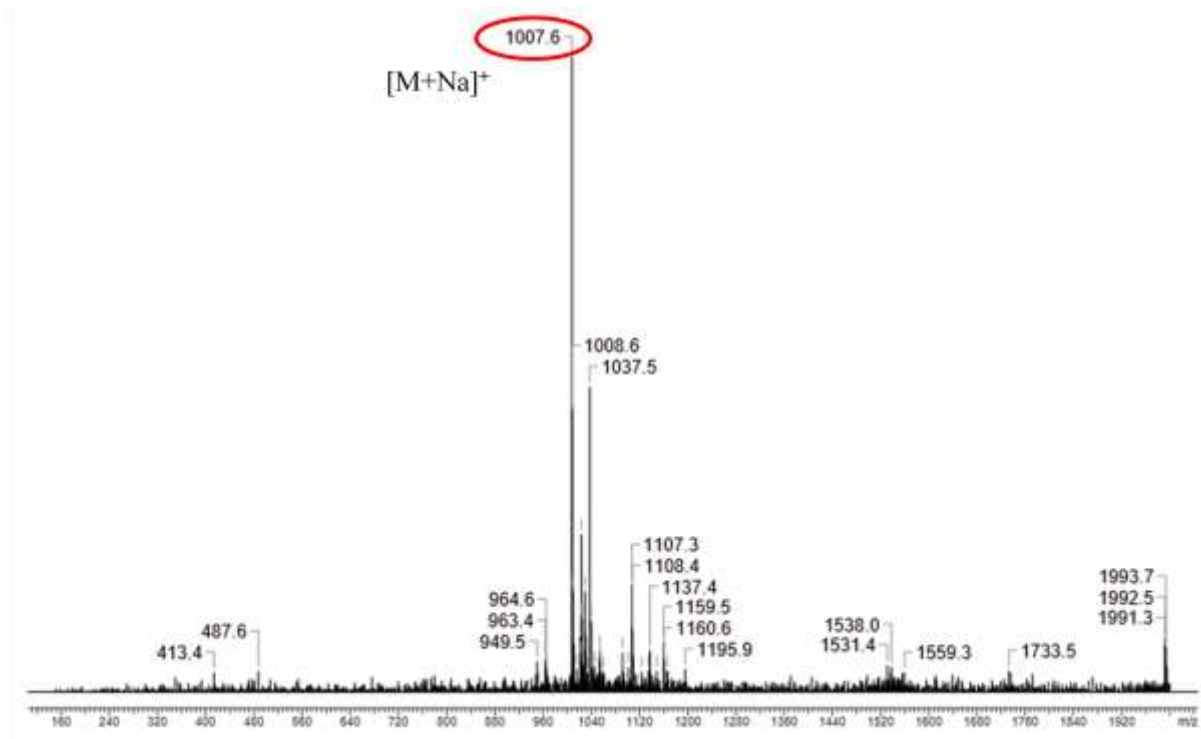


Figure 27: Positive ESIMS of saponin **3**

The NMR signals of compound **3** sugar portion were superimposable to those of **1** (Table 4). Moreover, the oligosaccharidic chain 3-*O*- α -L-rhamnopyranosyl-(1 \rightarrow 2)- β -D-xylopyranosyl-(1 \rightarrow 2)- β -D-glucuronopyranosyl was linked at the C-3 position of the aglycone according to the NOESY cross-peak at δ_{H} 3.37 (1H, dd, $J = 12.0, 3.7$ Hz H-3_{ax}) / δ_{H} 4.79 (1H, d, $J = 6.9$ Hz, GlcA-1) (Figures 28, 29, 30 and 31). The ^1H NMR spectrum area corresponding to the aglycone part of **3** showed six tertiary methyl groups as singlets at δ_{H} 0.59, 0.83, 0.91, 1.23, 1.26, 1.39, (3H, s, each), one olefinic proton at δ_{H} 5.46 (1H, br t, $J = 3.0$ Hz, H-12), three oxygen bearing methine protons at δ_{H} 3.37 (1H, dd, $J = 12.0, 3.7$ Hz H-3_{ax}) and 4.77 (1H, br s, H-22_{eq}), and one free primary alcoholic function at δ_{H} 3.35 (1H, d, $J = 11.2$ Hz, H-24_{ax}), 4.20 (H-24_{bax}) / δ_{C} 62.6. In the ^{13}C NMR spectrum, a signal at δ_{C} 180.5 suggested a free carboxylic acid group and another signal at δ_{C} 170.9, an ester function. The HSQC correlation at δ_{H} 2.09 (3H, s) / δ_{C} 21.1 confirmed the presence of one acetyl group.

A HMBC correlation between δ_{H} 0.91 (3H, s, H₃-28_{eq}) and δ_{C} 78.1 (C-22) allowed the location of one secondary alcoholic function at C-22. The deshielded value of the C-22 signal was in accordance with an acetylation as described in the previous compounds **1** and **2**. In the

same way, a HMBC cross-peak at δ_{H} 1.39 (3H, s, H₃-23_{eq}) and δ_{C} 62.6 (C-24) placed the primary alcoholic function at the C-24 position. NOESY correlations between H₃-23 α -equatorial and H-3 α -axial and H-5 α -axial confirmed the location of the CH₂OH group at the 24 β -axial position. The configuration of C-22 was determined by the connectivity observed in the NOESY spectrum between H-22 α -equatorial and H₃-27 α -axial. The lack of NOESY correlations between H₃-30 β_{ax} and H-18 β_{ax} and H₃-28 β_{eq} suggested the location of the carboxylic acid group at the C-30 position. The structure of the aglycone was thus recognized as an acetylated derivative of the 3 β ,22 β ,24-trihydroxyolean-12-en-30-oic acid (Table 4).

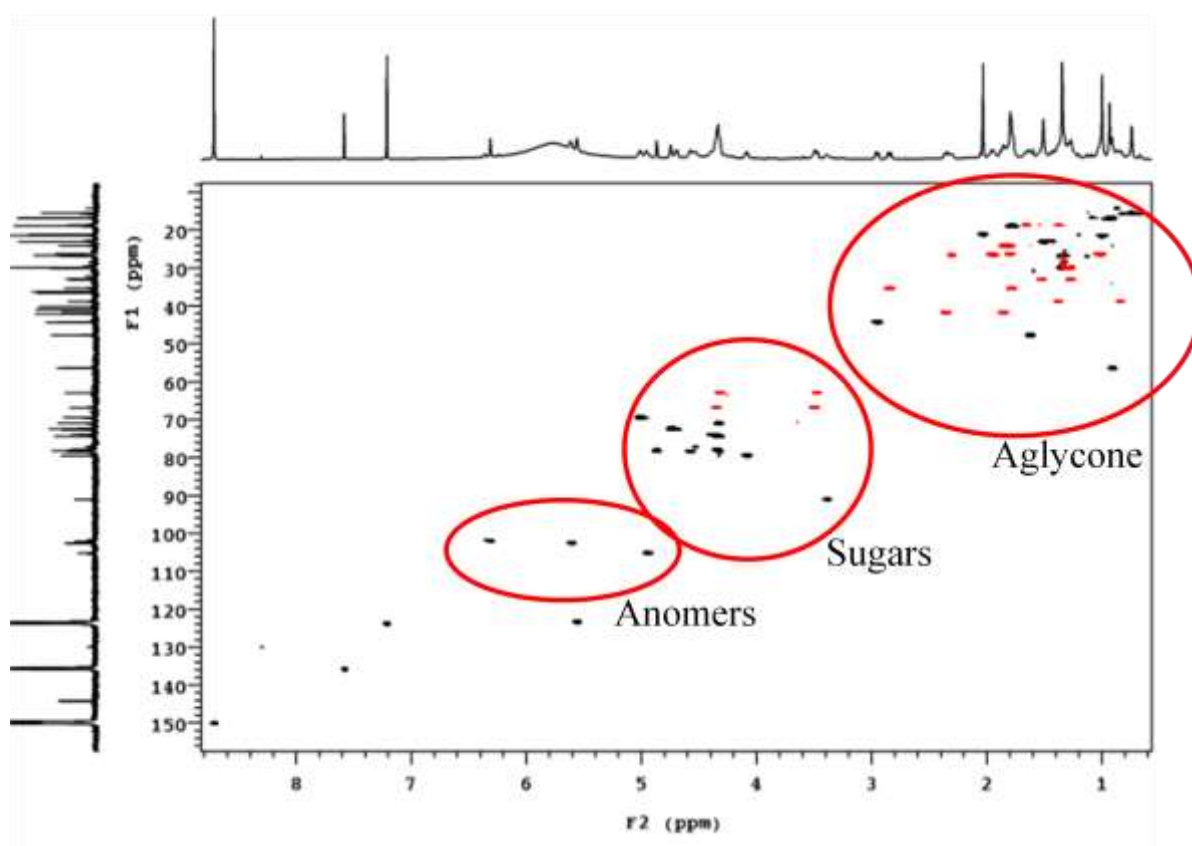


Figure 28: General HSQC of saponin 3

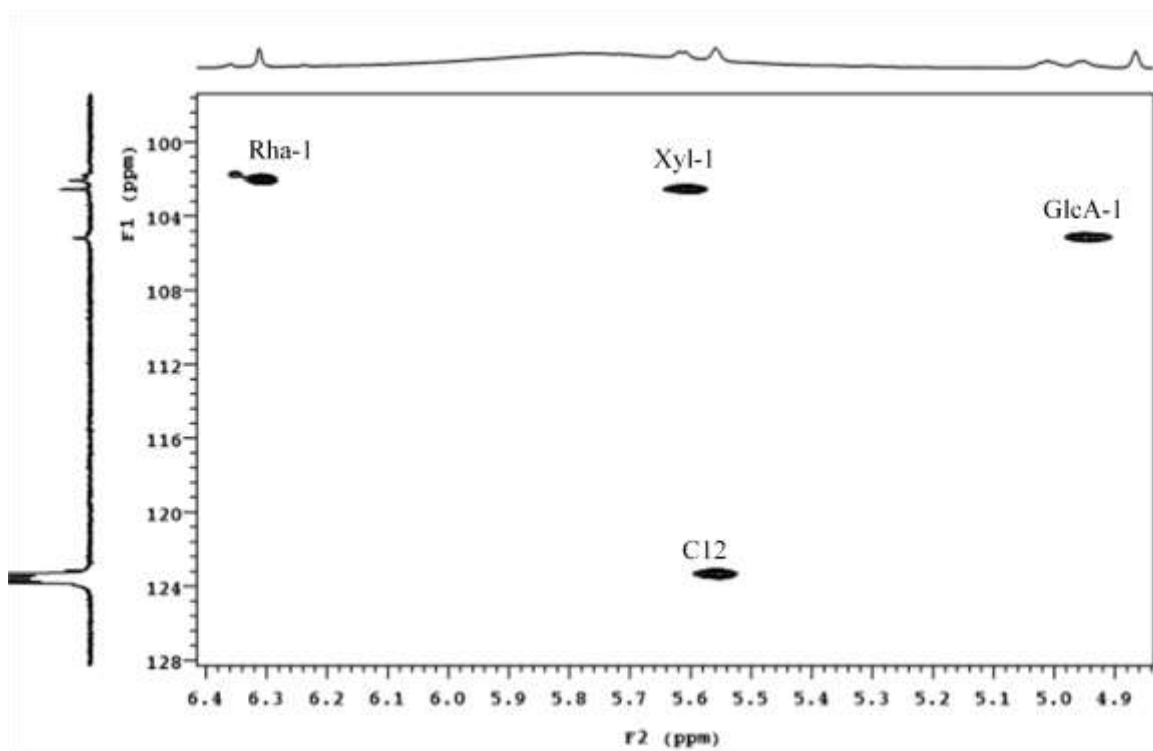


Figure 29: HSQC anomers zone of saponin 3

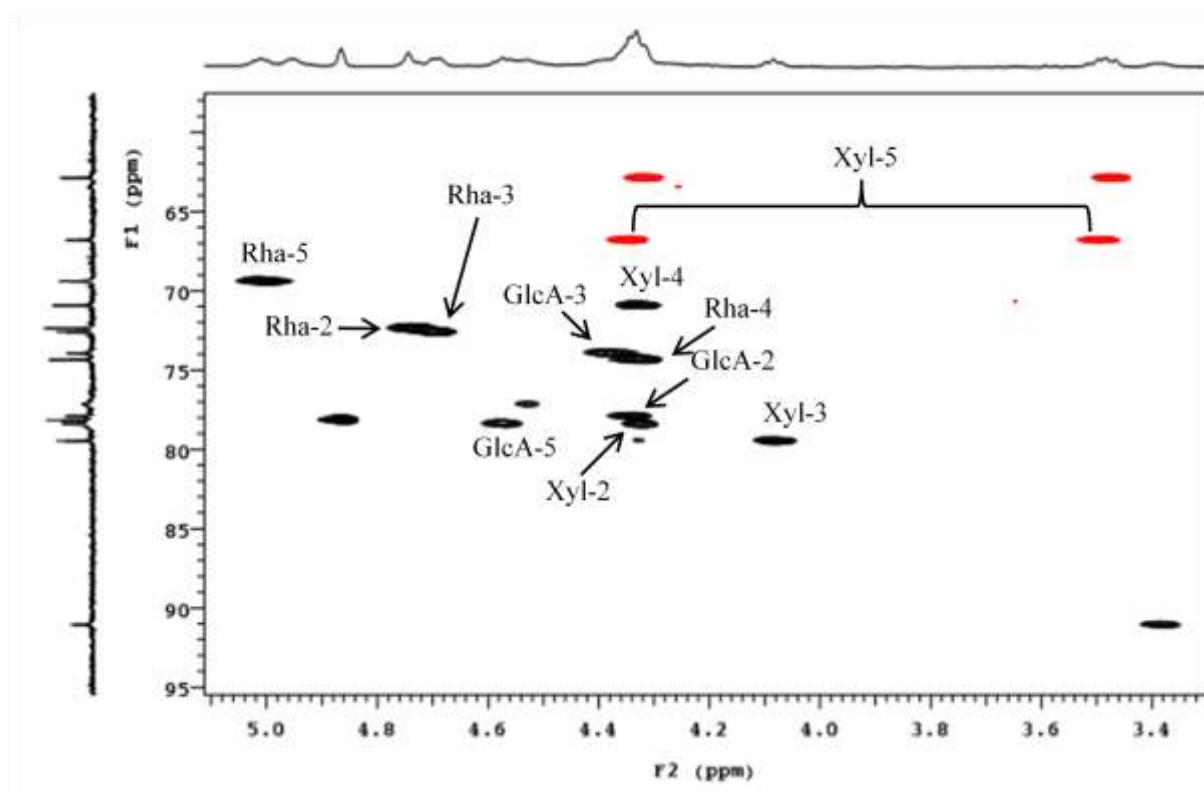


Figure 30: HSQC spectrum of saponin 3

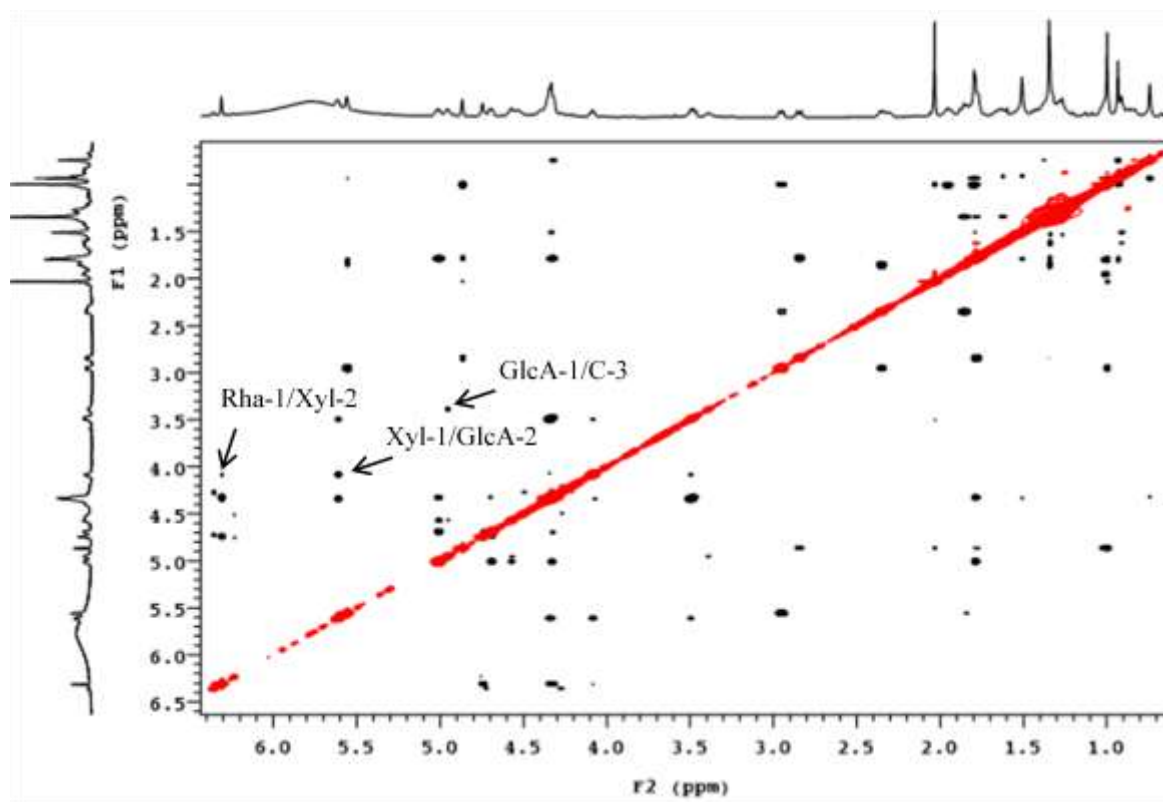


Figure 31: ROESY spectrum of saponin **3**

On the basis of these results and the literature data, the structure of compound **3** was elucidated as 3-*O*- α -L-rhamnopyranosyl-(1 \rightarrow 2)- β -D-xylopyranosyl-(1 \rightarrow 2)- β -D-glucuronopyranosyl-22-*O*-acetyl-3 β ,22 β ,24-trihydroxyolean-12-en-30-oic acid (**3**). This saponin, named wistariasaponin G, was already isolated from *Wisteria brachybotrys* but its structural analysis was performed after methylation. For the first time, we have described the structural elucidation of its native form.

After 1D and 2D NMR analysis, structures of **1-3** were elucidated as: 3-*O*- α -L-rhamnopyranosyl-(1 \rightarrow 2)- β -D-xylopyranosyl-(1 \rightarrow 2)- β -D-glucuronopyranosyl-22,28-*O*-diacetylolean-12-ene-3 β ,16 β ,22 β ,28-tetrol (**1**), 3-*O*- α -L-rhamnopyranosyl-(1 \rightarrow 2)- β -D-glucopyranosyl-(1 \rightarrow 2)- β -D-glucuronopyranosyl-22-*O*-acetylolean-12-ene-3 β ,16 β ,22 β ,28-tetrol (**2**) and 3-*O*- α -L-rhamnopyranosyl-(1 \rightarrow 2)- β -D-xylopyranosyl-(1 \rightarrow 2)- β -D-glucuronopyranosyl-22-*O*-acetyl-3 β ,22 β ,24-trihydroxyolean-12-en-30-oic acid (**3**) (Figure 32) and three known oleanane-type glycosides were identified as: 3-*O*- α -L-rhamnopyranosyl-(1 \rightarrow 2)- β -D-xylopyranosyl-(1 \rightarrow 2)- β -D-glucuronopyranosyl wistariasapogenol A (wistariasaponin A) (**4**) [56], 3-*O*- α -L-rhamnopyranosyl-(1 \rightarrow 2)- β -D-xylopyranosyl-(1 \rightarrow 2)- β -D-glucuronopyranosyl soyasapogenol B (wistariasaponin C) (**5**) [56], and 3-*O*- α -L-

rhamnopyranosyl-(1→2)-β-D-glucopyranosyl-(1→2)-β-D-glucuronopyranosyl soyasapogenol B (azukisaponin V) (**6**) [65] (Figure 33).

Table 4. ¹³C NMR and ¹H NMR data of the aglycones of compounds **1-3** in Pyridine-*d*₅/D₂O (δ ppm, *J* in Hz)

Position	1		2		3	
	δ_C	δ_H	δ_C	δ_H	δ_C	δ_H
1	38.6	0.82 (1H, m) 1.34 (1H, m)	38.7	0.78 (1H, m) 1.33 (1H, m)	38.5	0.79 (1H, m) 1.29 (1H, m)
2	26.1	1.81 (1H, m) 2.33 (1H, m)	26.1	1.92 (1H, m) 2.25 (1H, m)	26.2	1.86 (1H, m) 2.45 (1H, m)
3	89.6	3.23 (1H, dd, 12.0, 3.8)	90.6	3.21 (1H, dd, 11.9, 3.6)	90.9	3.37 (1H, dd, 12.0, 3.7)
4	39.4	-	39.4	-	43.7	-
5	55.5	0.67 (1H, br d, 10.8)	55.5	0.65 (1H, br d, 10.5)	55.9	0.79 (1H, br d, 10.8)
6	18.3	1.22 (1H, m)	18.2	1.18 (1H, m)	18.4	1.21 (1H, m)
7	32.3	1.39 (1H, m) 1.20 (1H, m) 1.40 (1H, m)	32.8	1.39 (1H, m) 1.20 (1H, m) 1.40 (1H, m)	32.5	1.52 (1H, m) 1.17 (1H, m) 1.38 (1H, m)
8	40.0	-	39.9	-	39.8	-
9	47.3	1.46 (1H, dd, 14.0, 7.0)	47.0	1.46 (1H, dd, 14.0, 6.9)	47.3	1.48 (1H, dd, 13.9, 6.8)
10	36.3	-	36.5	-	36.1	-
11	23.5	1.66 (1H, m) 1.75 (1H, m)	23.8	1.70 (1H, m) 1.74 (1H, m)	23.7	1.62 (1H, m) 1.68 (1H, m)
12	123.3	5.28 (1H, br t, 3.0)	122.3	5.22 (1H, br t, 3.1)	123.1	5.46 (1H, br t, 3.0)
13	141.7	-	141.5	-	144.5	-
14	42.8	-	43.1	-	41.7	-
15	36.5	1.65 (1H, dd, 13.3, 4.0) 2.24 (1H, dd, 13.3, 12.4)	37.0	1.72 (1H, dd, 13.4, 4.1) 2.17 (1H, dd, 13.4, 12.5)	25.9	1.70 (1H, m) 1.88 (1H, m)
16	66.4	4.53 (1H, dd, 12.4, 4.0)	68.0	4.53 (1H, dd, 12.5, 4.1)	26.2	0.96 (1H, m) 1.80 (1H, m)
17	46.7	-	46.2	-	36.0	-
18	43.1	2.57 (1H, dd, 13.4, 3.4)	42.2	2.38 (1H, dd, 13.0, 3.0)	44.5	2.84 (1H, dd, 12.8, 3.6)
19	45.8	1.18 (1H, dd, 13.6, 3.4) 1.91 (1H, dd, 13.6, 13.4)	46.3	1.16 (1H, dd, 13.3, 3.0) 1.86 (1H, dd, 13.3, 13.0)	41.7	1.72 (1H, dd, 13.2, 3.6) 2.30 (1H, dd, 13.2, 12.8)
20	29.9	-	30.0	-	43.7	-
21	37.7	1.74 (overlapped) 2.86 (1H, br d, 13.6)	37.6	1.75 (overlapped) 2.90 (1H, br d, 14.0)	35.2	1.63 (overlapped) 2.81 (1H, br d, 13.6)
22	71.3	6.10 (1H, br s)	70.2	6.24 (1H, br s)	78.1	4.77 (1H, br s)
23	27.9	1.22 (3H, s)	28.0	1.22 (3H, s)	22.5	1.39 (3H, s)
24	16.7	0.98 (3H, s)	16.2	1.01 (3H, s)	62.6	3.35 (1H, d, 11.2) 4.20 (overlapped)
25	15.2	0.75 (3H, s)	15.1	0.74 (3H, s)	15.2	0.59 (3H, s)
26	16.7	1.01 (3H, s)	16.3	0.92 (3H, s)	16.5	0.83 (3H, s)
27	27.3	1.28 (3H, s)	27.2	1.28 (3H, s)	26.3	1.23 (3H, s)

28	64.7	4.23 (1H, d, 12.4) 4.86 (1H, d, 12.4)	63.0	4.25 (1H, d, 12.3) 4.93 (1H, d, 12.3)	21.1	0.91 (3H, s)
29	33.4	0.85 (3H, s)	34.0	0.83 (3H, s)	29.9	1.26 (3H, s)
30	26.9	1.07 (3H, s)	27.9	1.03 (3H, s)	180.5	
at C-22						
$\underline{\text{COCH}}_3$	170.3		170.2		170.9	
$\underline{\text{CH}}_3\text{CO}$	21.1	2.09 (3H, s)	21.0	2.07 (3H, s)	21.1	2.09 (3H, s)
at C-28						
$\underline{\text{COCH}}_3$	171.1					
$\underline{\text{CH}}_3\text{CO}$	20.9	2.01 (3H, s)				

Table 5. ^{13}C NMR and ^1H NMR data of the sugar moieties of compounds **1-3** in Pyridine- d_5 / D_2O (δ ppm, J in Hz)

Position	1		2		3	
	δ_{C}	δ_{H}	δ_{C}	δ_{H}	δ_{C}	δ_{H}
GlcA-1	104.8	4.83 (1H, d, 6.9)	104.8	4.81 (1H, d, 7.1)	104.7	4.79 (1H, d, 6.9)
2	78.4	4.23 (1H, dd, 8.0, 6.9)	77.8	4.44 (1H, dd, 8.1, 7.1)	77.3	4.17 (1H, dd, 8.1, 6.9)
3	75.7	4.22 overlapped	75.9	4.22 (1H, dd, 8.1, 7.0)	75.7	4.22 overlapped
4	73.8	4.12 (1H, dd, 8.3, 6.9)	73.5	4.10 (1H, dd, 8.3, 7.0)	73.7	4.13 (1H, dd, 8.3, 6.9)
5	78.4	4.44 (1H, d, 8.3)	78.0	4.42 (1H, d, 8.3)	77.8	4.42 (1H, d, 8.3)
6	172.7	-	173.0	-	172.8	-
Xyl-1	102.1	5.53 (1H, d, 7.3)			102.2	5.42 (1H, d, 7.4)
2	77.5	4.14 (1H, dd, 8.8, 7.3)			78.4	4.19 (1H, dd, 8.5, 7.4)
3	78.7	4.07 (1H, dd, 8.8, 7.6)			78.8	3.99 (1H, dd, 8.5, 6.9)
4	70.5	4.31 m			70.3	4.31 m
5	66.3	3.47 (1H, dd, 11.2, 10.2) 4.24 (1H, dd, 11.2, 5.3)			66.3	3.38 (1H, dd, 11.9, 9.5) 4.29 (1H, dd, 11.9, 5.2)
Glc-1			101.9	5.50 (1H, d, 7.4)		
2			78.1	4.12 (1H, dd, 8.4, 7.4)		
3			78.2	4.08 (1H, t, 9.1)		
4			70.6	4.28 (1H, t, 9.0)		
5			77.4	3.80 m		
6			62.6	4.05 (1H, dd, 10.5, 4.5) 4.52 (1H, dd, 10.5, 1.7)		
Rha-1	101.6	6.20 (1H, br s)	101.6	6.18 (1H, br s)	101.7	6.14 (1H, br s)
2	71.8	4.66 (1H, br s)	72.0	4.68 (1H, br s)	71.8	4.67 (1H, br s)
3	71.9	4.63 (1H, dd, 9.2, 2.5)	72.0	4.62 (1H, dd, 9.0, 2.5)	71.9	4.61 (1H, dd, 9.1, 2.4)
4	73.8	4.27 (1H, t, 9.2)	73.8	4.26 (1H, t, 9.0)	73.3	4.27 (1H, t, 9.1)
5	69.1	4.91 (1H, dq, 9.2, 6.6)	69.0	4.95 (1H, dq, 9.0, 6.2)	68.9	4.92 (1H, dq, 9.1, 6.0)
6	18.5	1.71 (1H, d, 6.6)	18.0	1.70 (1H, d, 6.2)	18.4	1.72 (1H, d, 6.0)

Overlapped proton signals are reported without designated multiplicity.

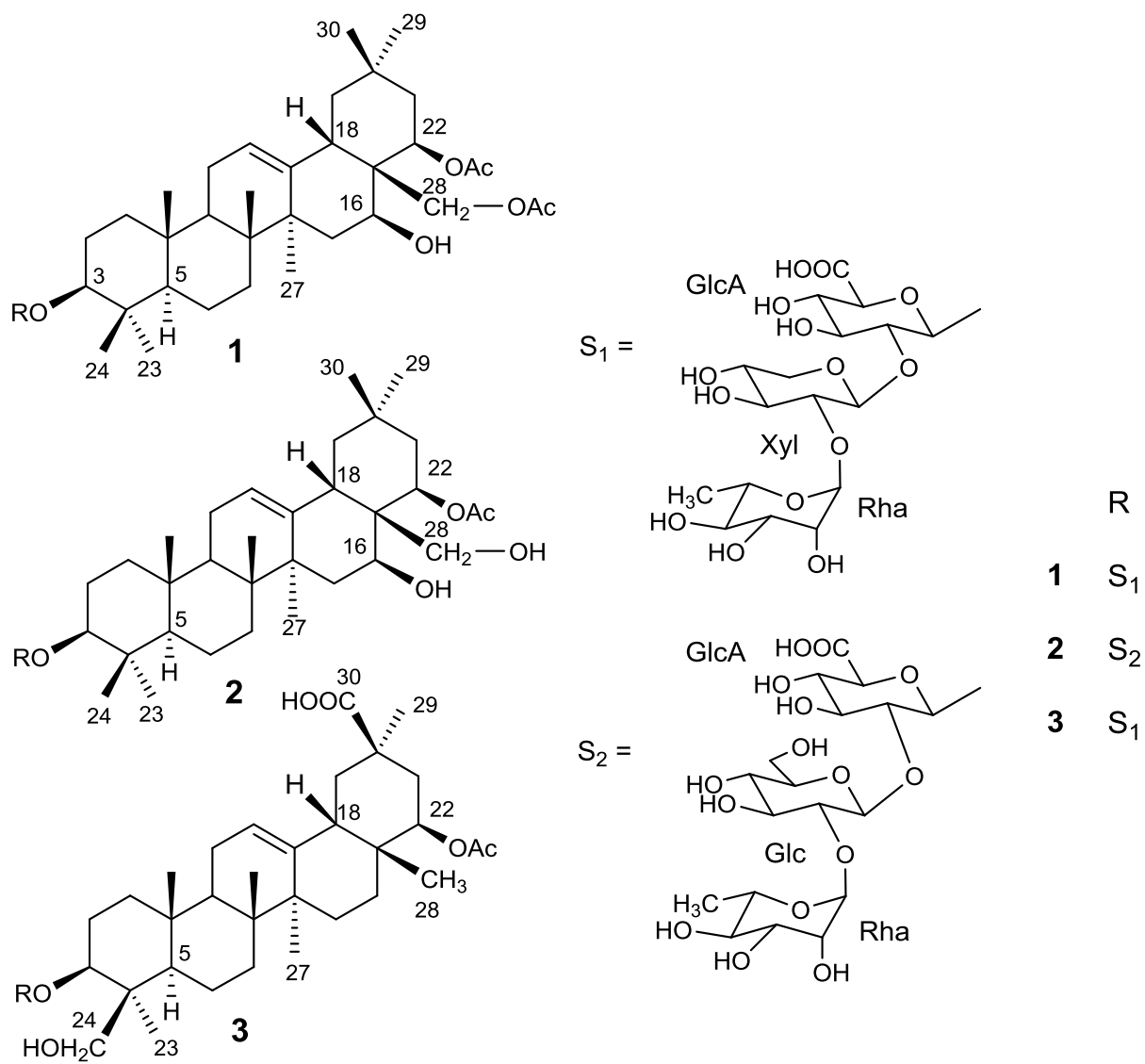


Figure 32: Structure of saponins 1-3

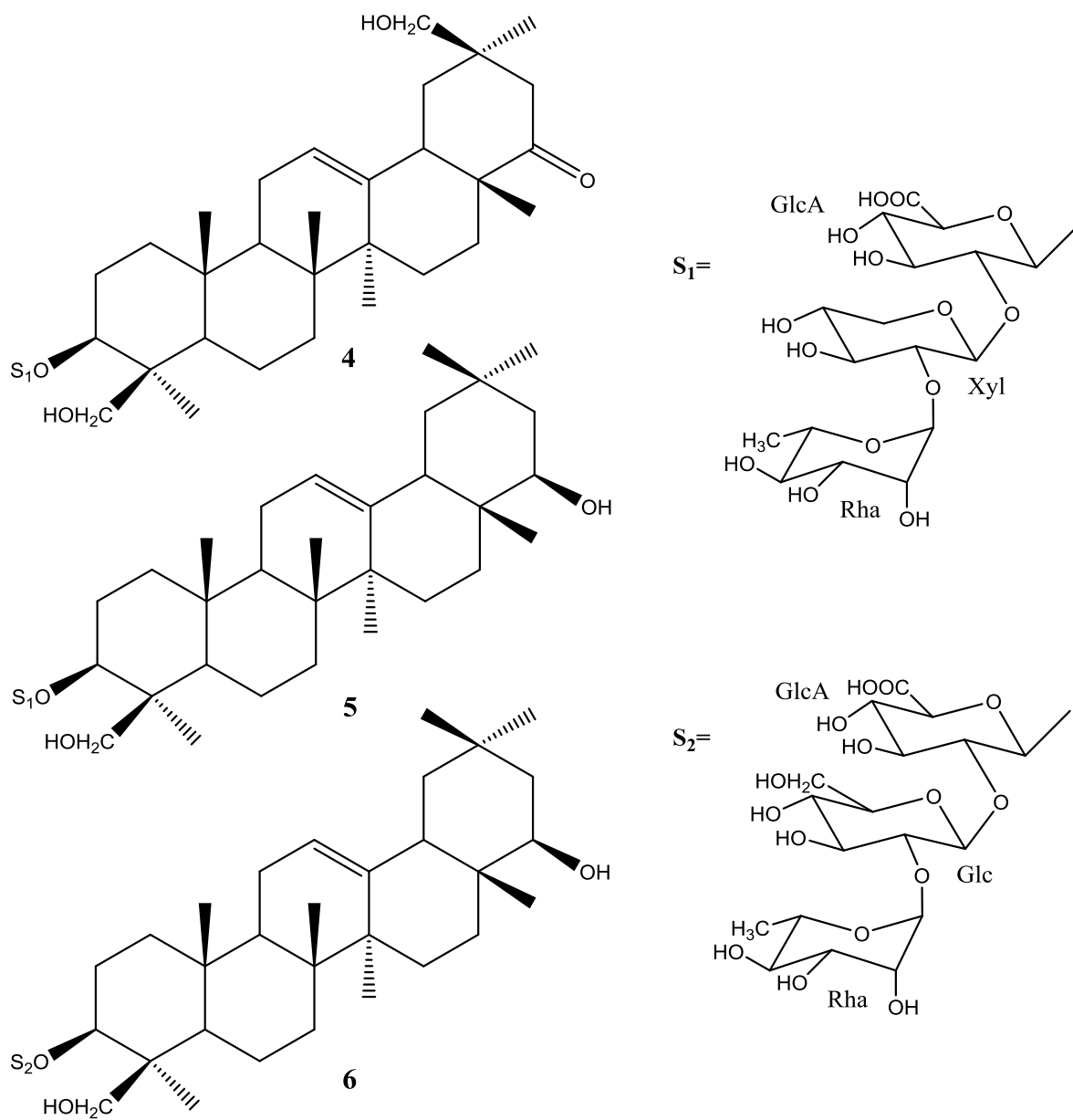


Figure 33: Structure of saponins 4-6

W. floribunda “macrobotrys” and “rosea”

From the roots of *W. floribunda* “macrobotrys”, a previously undescribed saponin (**7**) was isolated, together with two known ones (**8**, **9**), and its structure was elucidated. From the roots of *W. floribunda* “rosea”, two known ones were identified (**10**, **11**).

The HR-ESIMS (positive-ion mode) of **7** established its molecular formula as $C_{43}H_{66}O_{16}$ with a pseudo-molecular ion peak at m/z 861.4268 $[M + Na]^+$ (calcd 861.4249). Its ESIMS (negative-ion mode) displayed a quasi-molecular ion peak at m/z 837 $[M - H]^-$, indicating a molecular weight of 838 (Figure 34).

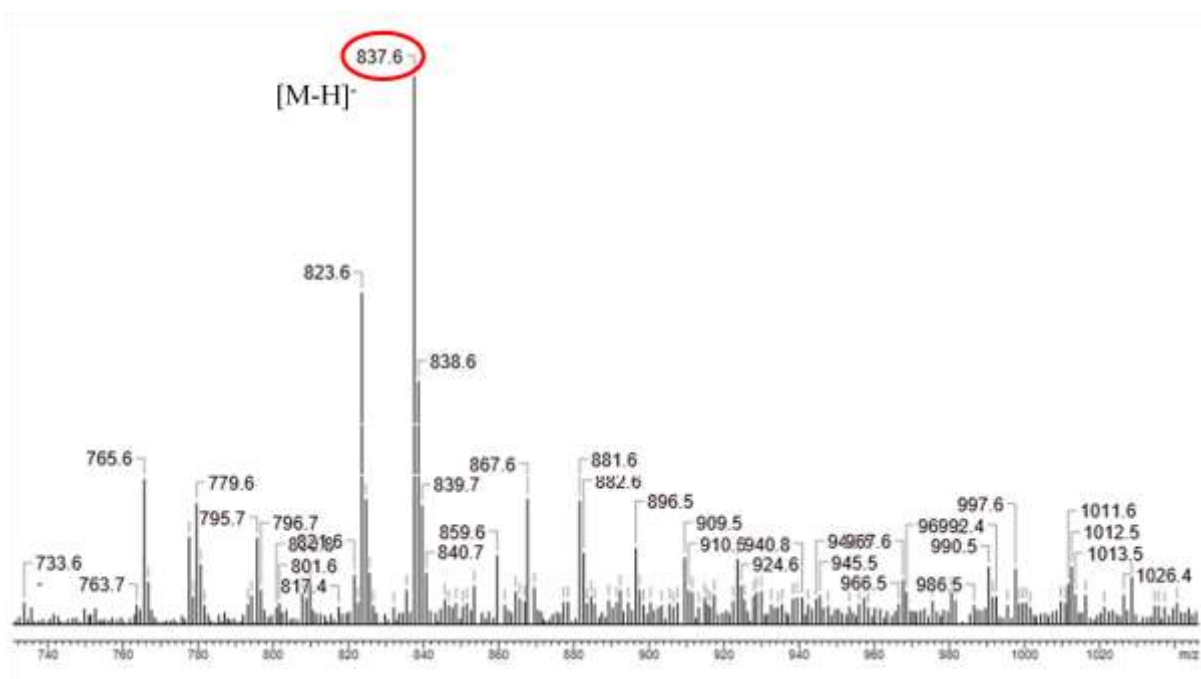


Figure 34: Negative ESIMS of saponin **7**

The 1H NMR spectrum of the aglycon part displayed signals assignable to six angular methyl groups as singlets at δ_H 0.82 (H₃-25), 0.91 (H₃-26), 0.93 (H₃-28), 1.26 (H₃-27), 1.27 (H₃-29), 1.36 (H₃-23), one olefinic proton at δ_H 5.46 (br t, $J = 3.0$ Hz) (H-12), two oxygen-bearing methine protons at δ_H 3.46 (H-3) and 4.75 (br s) (H-22), and one primary alcoholic function at δ_H 3.48 (d, $J = 11.2$ Hz), 4.25 (d, $J = 11.2$ Hz) (H₂-24) (Table 7). A signal in the ^{13}C NMR spectrum at δ_C 179.2 suggested a carbonyl function of a free carboxylic acid group. Another one at δ_C 170.2 suggested a carbonyl function of an acetyl group, which was confirmed by a HMBC cross-peak at δ_H 2.07 (s)/ δ_C 170.2, and a HSQC correlation at δ_H 2.07 (s)/ δ_C 21.1. The HMBC correlation between an angular methyl group at δ_H 1.36 (s, H₃-23) and δ_C 89.9 (C-3), allowed the location of the first secondary alcoholic function at C-3.

The second one was located at C-22, by observation of a HMBC correlation at $\delta_{\text{H}} 0.93$ (s, H-28)/ $\delta_{\text{C}} 77.8$ (C-22). The deshielded chemical shift of H-22 at $\delta_{\text{H}} 4.75$ suggested an acetylation at the C-22 position. In the HMBC spectrum, a cross-peak between $\delta_{\text{H}} 1.36$ (H₃-23) and $\delta_{\text{C}} 62.7$ (C-24) allowed the location of the primary alcoholic function at C-24 position. More correlations were observed between $\delta_{\text{H}} 1.27$ (s, H₃-29), 1.74 (dd, $J = 13.6, 3.0$, H-21), and 1.79 (dd, $J = 13.5, 3.4$, H-19), and $\delta_{\text{C}} 179.2$, to find the location of the free carboxylic group at the C-30 position. The lack of ROESY correlations between H₃-30 β_{ax} and H-18 β_{ax} and H₃-28 β_{eq} suggested the location of the carboxylic acid group at the C-30 position. The configuration of C-3 was determined by the interactions observed in the ROESY spectrum between H-3 α -axial and H₃-23 α -equatorial. Moreover, the multiplicity of the H-22 at $\delta_{\text{H}} 4.75$ as a (br s), confirmed the α -equatorial orientation of the H-22.

The structure of the aglycon of **7** was thus recognized to be the 22-*O*-acetyl-3 β , 22 β , 24-trihydroxyolean-12-en-30-oic acid, previously described in *W. frutescens* [66], *W. brachybotrys* [56-59] and *Millettia speciosa* Champ. Ex Benth. [67] (Table 7, Figure 35).

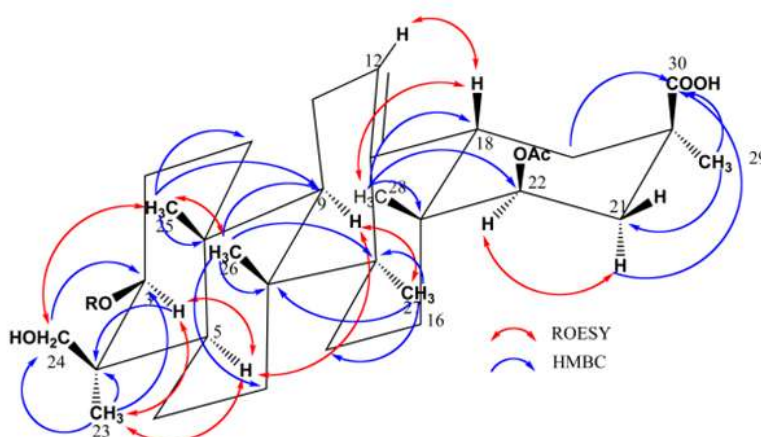


Figure 35: Key HMBC and ROESY correlations for the aglycon of **7**.

In the osidic region, the HSQC spectrum of **7** displayed two anomeric signals at $\delta_{\text{H}} 4.77$ (1H, d, $J = 7.6$ Hz)/ $\delta_{\text{C}} 104.3$ and $\delta_{\text{H}} 5.21$ (d, $J = 6.9$ Hz)/ $\delta_{\text{C}} 105.2$ (Figure 36, 37 and 38). The ring protons of the monosaccharide residues were assigned starting from the readily identifiable anomeric protons by means of the ¹H-¹H COSY, TOCSY, HSQC, and HMBC experiments. The monosaccharides obtained by acid hydrolysis of **7** were identified by comparison on TLC with authentic samples as glucuronic acid (GlcA) and xylose (Xyl). The absolute configurations of the sugars were determined to be D for GlcA and Xyl by GC analysis according to a method previously described. The relatively large ³ $J_{\text{H-1,H-2}}$ value of the GlcA and Xyl (7.6, 6.9 Hz) in their pyranose form indicated a β anomeric orientation for

GlcA and Xyl. Units of one β -D-glucuronopyranosyl and one β -D-xylopyranosyl were thus identified (Table 6). The 3-*O*-heterosidic linkage was suggested by a HMBC cross-peak δ_{H} 4.77 (d, $J = 7.6$ Hz, GlcA-1)/ δ_{C} 89.9 (C-3), and a ROESY cross-peak at δ_{H} 4.77 (GlcA-1)/ δ_{H} 3.46 (H-3). The HMBC correlations at δ_{H} 5.21 (d, $J = 6.9$ Hz, Xyl-1)/ δ_{C} 81.1 (GlcA-2) and the ROESY correlation at δ_{H} 5.21 (Xyl-1)/ δ_{H} 4.00 (dd, $J = 8.4, 7.6$, GlcA-2) proved a β -D-xylopyranosyl-(1 \rightarrow 2)- β -D-glucuronopyranosyl sequence (Table 6, Figure 39).

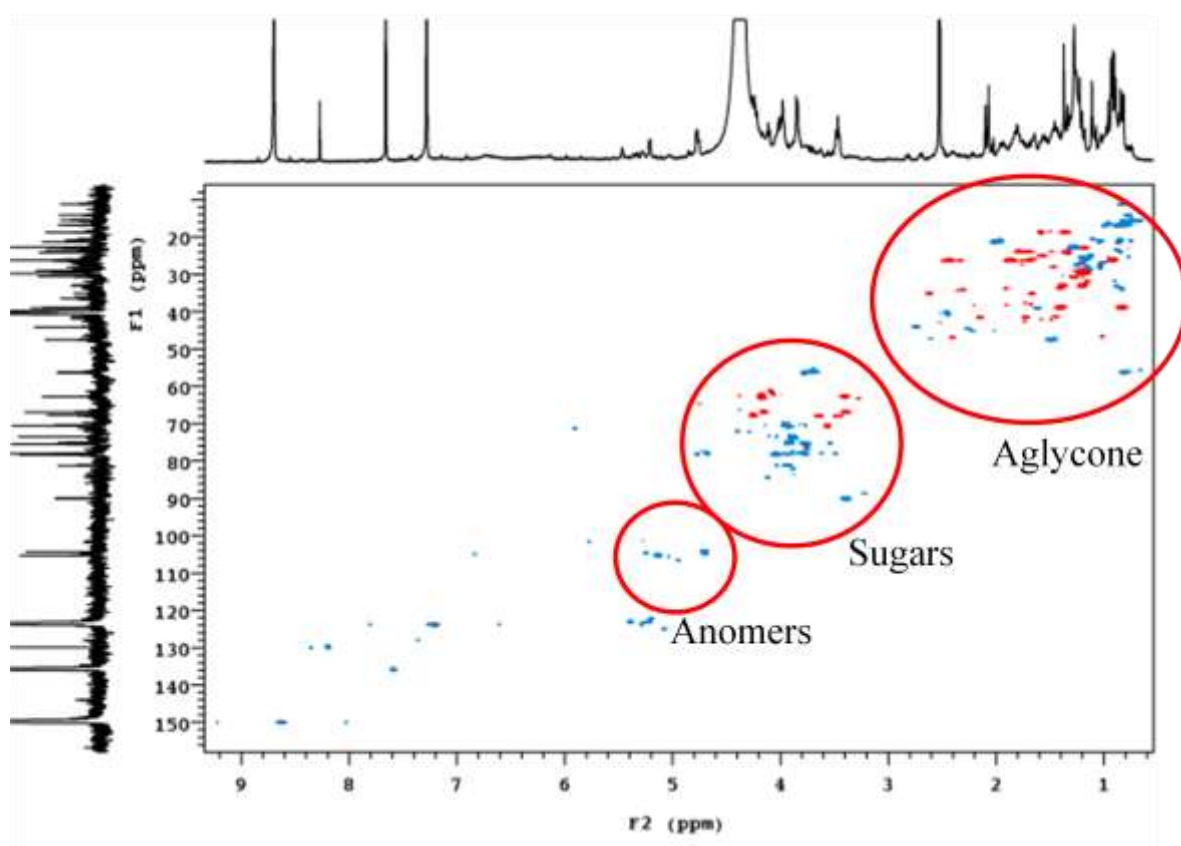


Figure 36: General HSQC of saponin 7

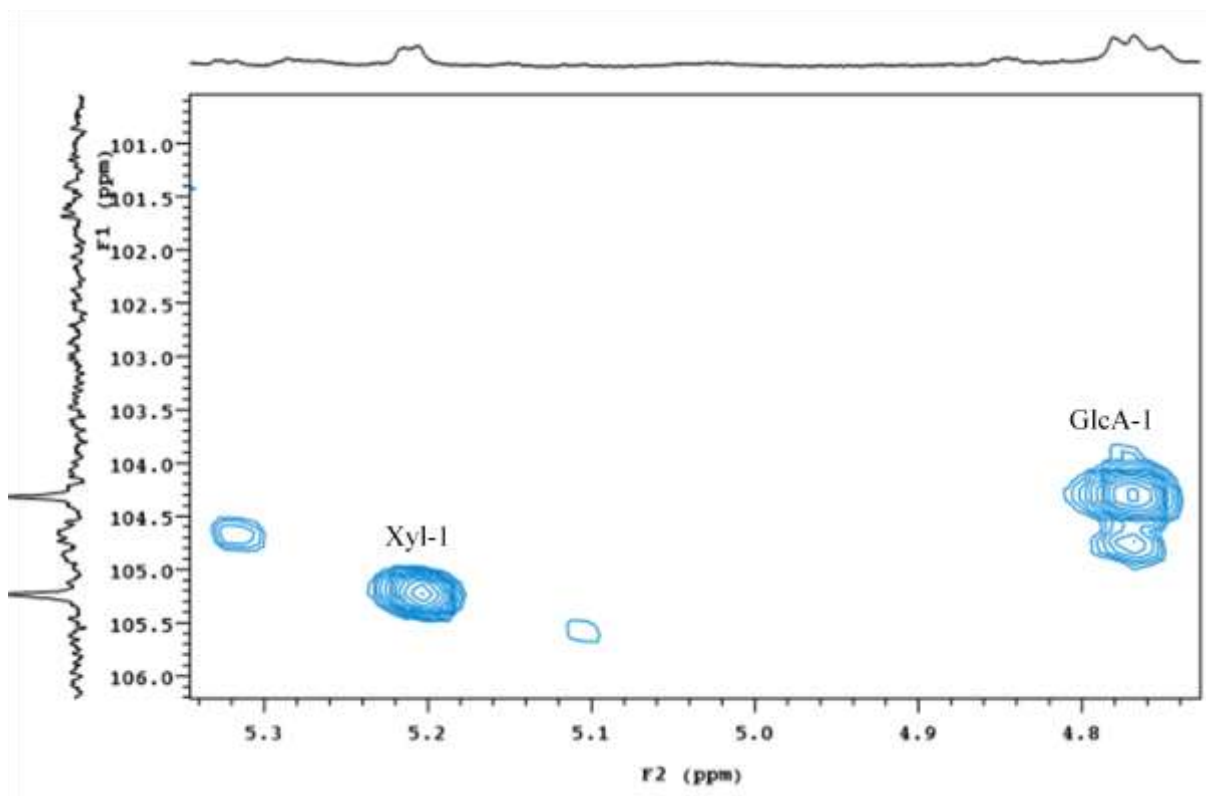


Figure 37: HSQC anomers zone of saponin 7

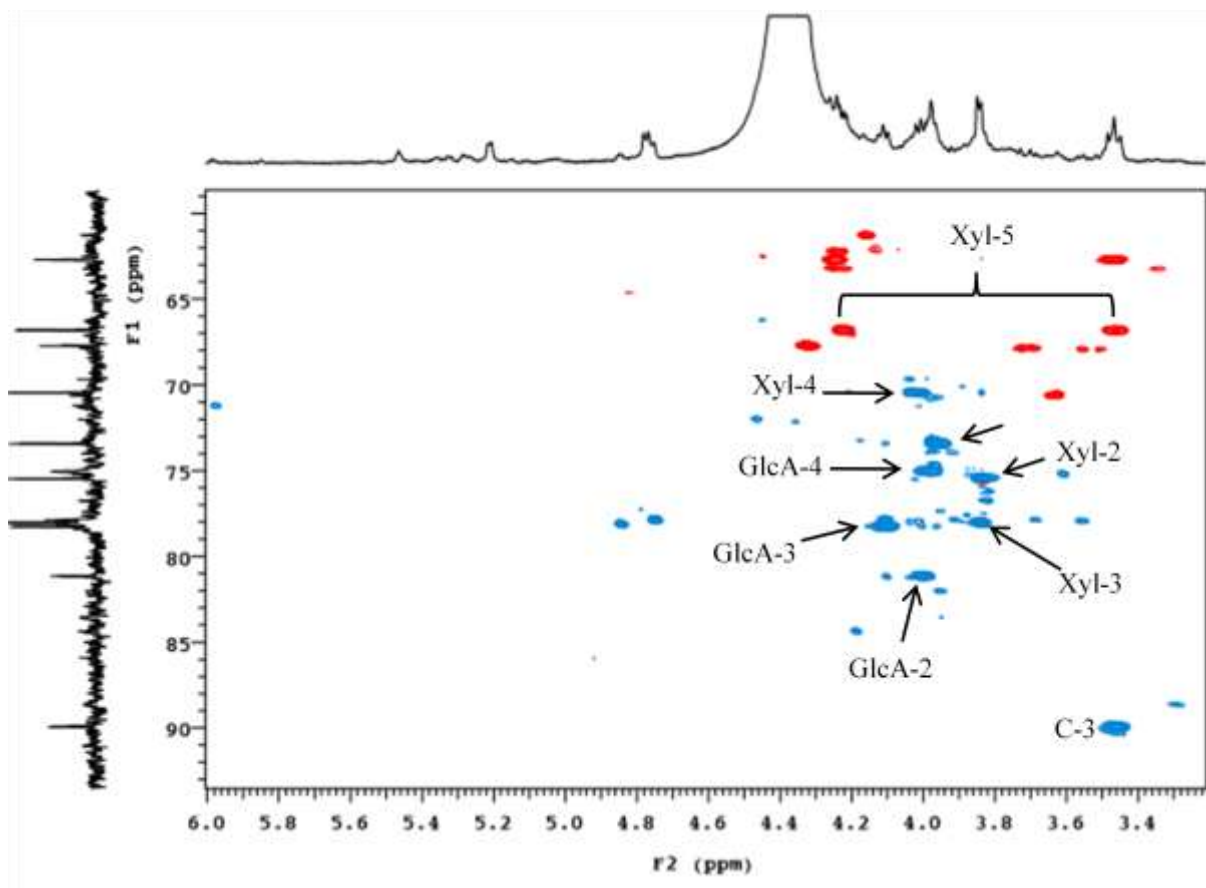


Figure 38: HSQC spectrum of saponin 7

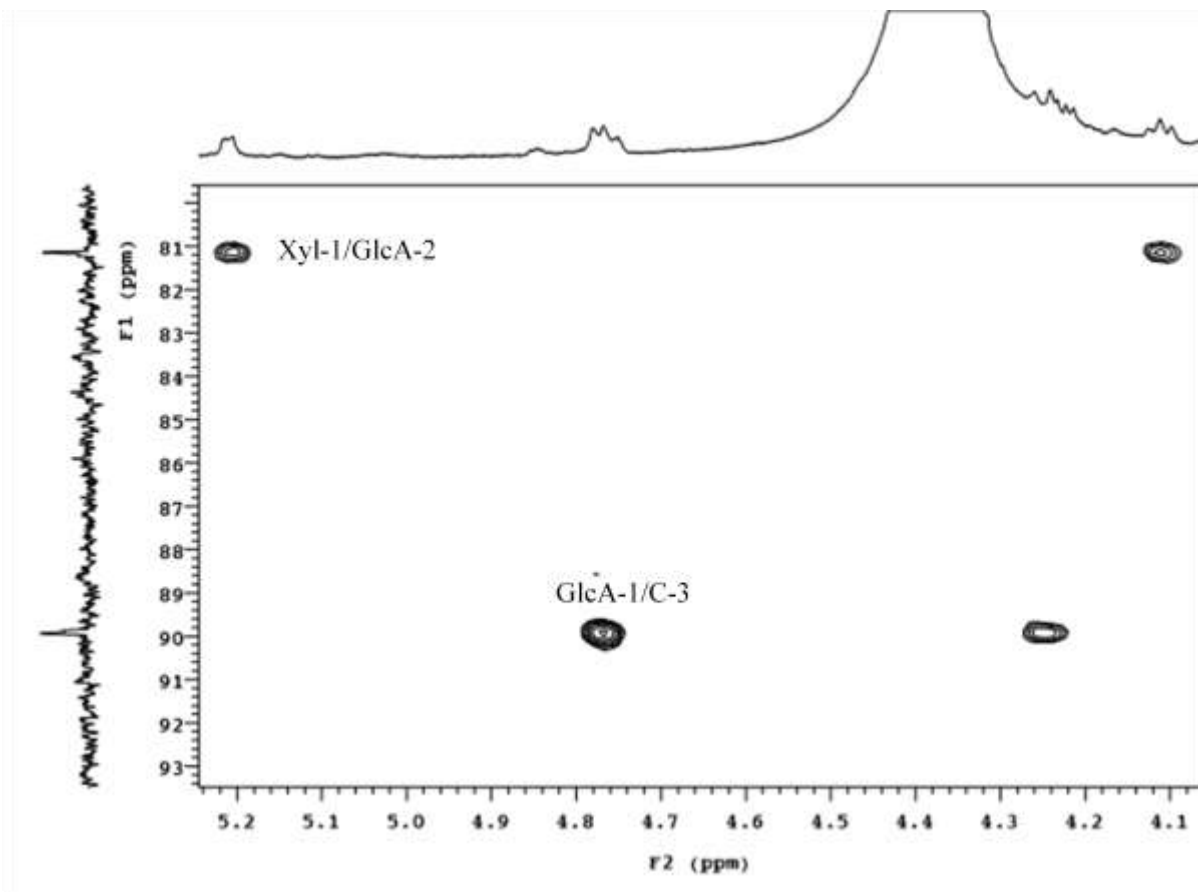


Figure 39: HMBC spectrum of saponin **7**

On the basis of the above results, the structure of **7** was elucidated as 3-*O*- β -D-xylopyranosyl-(1 \rightarrow 2)- β -D-glucuronopyranosyl-22-*O*-acetyl-3 β ,22 β ,24-trihydroxyolean-12-en-30-oic acid (**7**) (Figure 40).

From *W. floribunda* “macrobotrys”, the known molecules were already isolated from *W. frutescens* [66] as 3-*O*- α -L-rhamnopyranosyl-(1 \rightarrow 2)- β -D-xylopyranosyl-(1 \rightarrow 2)- β -D-glucuronopyranosyl-22-*O*-acetyl-3 β ,22 β ,24-trihydroxyolean-12-en-30-oic acid (**8**), and 3-*O*- α -L-rhamnopyranosyl-(1 \rightarrow 2)- β -D-xylopyranosyl-(1 \rightarrow 2)- β -D-glucuronopyranosyl-22,28-*O*-diacetylolean-12-ene-3 β ,16 β ,22 β ,28-tetrol (**9**). From the roots of *W. floribunda* “rosea”, the two known saponins were identified as 3-*O*- α -L-rhamnopyranosyl-(1 \rightarrow 2)- β -D-xylopyranosyl-(1 \rightarrow 2)- β -D-glucuronopyranosyl-olean-12-ene-3 β ,22 β ,24-triol (**10**) (Astragaloside VIII) [68], and 3-*O*- α -L-rhamnopyranosyl-(1 \rightarrow 2)- β -D-galactopyranosyl-(1 \rightarrow 2)- β -D-glucuronopyranosyl-22-*O*-acetyl-3 β ,22 β ,24-trihydroxyolean-12-en-30-oic acid (**11**) (Millettiasaponin A) [67] (Figure 40).

A literature survey of other *Wisteria* species [56-59, 66] and other genera of the Fabaceae [69] such as *Astragalus* L. [70-72], *Glycine* Willd. [73] or *Medicago* L. [74] for example, showed that monodesmosidic oleanane-type saponins with glucuronic acid linked at the C-3 position are very common to this family. More specifically, the sequence 3-*O*- β -D-glucuronopyranosyl-22-*O*-acetyl-3 β ,22 β ,24-trihydroxyolean-12-en-30-oic acid is found in saponins isolated from *Wisteria* [56-59, 66], *Derris* Wall. [75], and *Millettia* Wight & Arn. [67] genera, which belong to the subfamily Faboideae. This may represent a chemotaxonomic marker of this subfamily.

Table 6. ^{13}C NMR and ^1H NMR data of the sugar moiety of compound **7** in Pyridine- d_5 (δ in ppm)

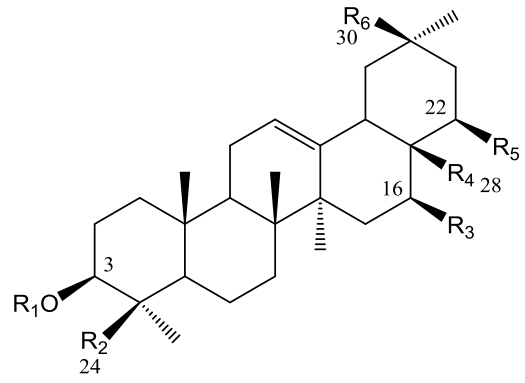
Position	δ_{C}	δ_{H} (J in Hz)
GlcA-1	104.3	4.77 d (7.6)
2	81.1	4.00 dd (8.4, 7.6)
3	78.2	4.11 dd (8.4, 8.0)
4	73.4	3.97
5	75.0	3.98
6	174.7	-
Xyl-1	105.2	5.21 d (6.9)
2	75.4	3.84
3	78.0	3.83
4	70.4	4.02
5	66.8	3.47 (dd, $J = 12.0, 10.0$), 4.22 (dd, $J = 12.0, 5.6$)

Overlapped proton signals are reported without designated multiplicity.

Table 7. ^{13}C NMR and ^1H NMR data of compound **7** in Pyridine- d_5 (δ in ppm)

Position	δ_{C}	δ_{H} (J in Hz)
Aglycone		
1	38.8	0.91 (m), 1.47 (m)
2	26.2	1.94 (m), 2.49 (m)
3	89.9	3.46
4	44.0	-
5	56.2	0.88 (br d, $J = 10.5$)
6	18.7	1.43(m), 1.66(m)
7	32.8	1.26(m), 1.45(m)
8	39.9	-
9	47.5	1.58 (d, $J = 14.0, 6.8$)
10	36.4	-
11	23.8	1.78 m, 1.82 m
12	123.3	5.46 (br t, $J = 3.0$)
13	144.0	-
14	41.7	-
15	26.1	1.78 (m), 1.90 (m)
16	25.9	0.98 (m), 1.76 (m)
17	36.0	-
18	44.0	2.82(dd, $J = 12.8, 3.4$)
19	41.5	1.79 (dd), $J = 13.5, 3.4$), 2.22(dd, $J = 13.5, 12.8$)
20	40.6	-
21	35.0	1.74(dd, $J = 13.6, 3.0$), 2.69 (brd, $J = 13.6$)
22	77.8	4.75 (br s)
23	22.6	1.36 (s)
24	62.7	3.48(d, $J = 11.2$), 4.25 (d, $J = 11.2$)
25	15.4	0.82(s)
26	16.7	0.91(s)
27	26.2	1.26(s)
28	21.2	0.93 (s)
29	29.7	1.27(s)
30	179.2	-
Acetyl at C-22		
CO	170.2	-
CH ₃	21.1	2.07 (s)

Overlapped proton signals are reported without designated multiplicity.



	7	8	9	10	11
R₁	S ₁	S ₂	S ₂	S ₂	S ₃
R₂	CH ₂ OH	CH ₂ OH	CH ₃	CH ₂ OH	CH ₂ OH
R₃	H	H	OH	H	H
R₄	CH ₃	CH ₃	CH ₂ OAc	CH ₃	CH ₃
R₅	OAc	OAc	OAc	OH	OAc
R₆	COOH	COOH	CH ₃	CH ₃	COOH

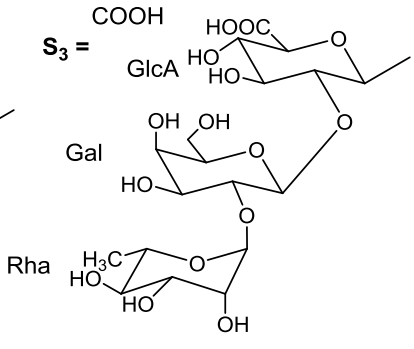
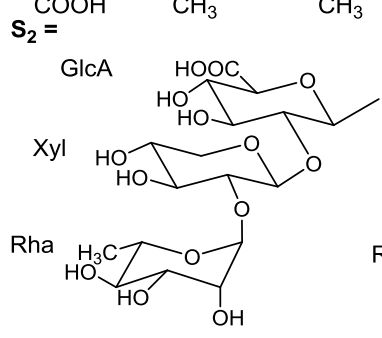
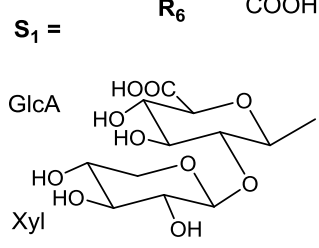


Figure 40: Structure of saponins 7-11

Weigela florida “rumba”

Three new triterpene glycosides **12-14** were isolated from an aqueous-ethanolic extract of the roots of *Weigela florida* “rumba” (Bunge) A. DC., by various solid/liquid chromatographic methods. Their structures were determined by 2D NMR and mass spectrometry as follow.

The HR-ESIMS (positive-ion mode) spectrum of compound **12** established its molecular formula as $C_{61}H_{98}O_{27}$ with a pseudo-molecular peak at m/z 1285.5334 $[M + Na]^+$ (calcd 1285.6193 $[M + Na]^+$) indicating a molecular weight of 1262 (Figure 41).

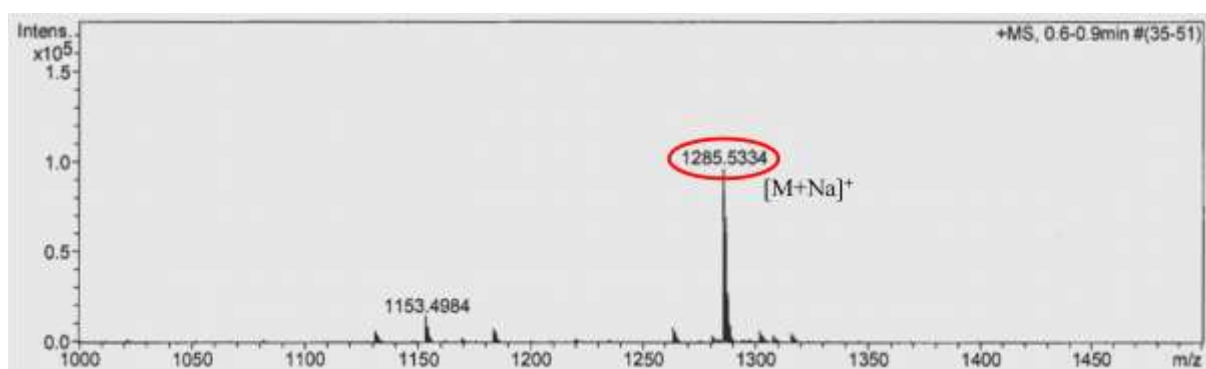


Figure 42: Positive ESIMS of saponin **12**

The 1H NMR spectrum of the aglycone part of **12** displayed signals assignable to seven angular methyl groups at δ_H 0.76, 0.89, 0.90, 0.93, 1.03, 1.21 and 1.23(s, each), one olefinic proton at δ_H 5.42(H-12) and one oxygen-bearing methine protons at δ_H 3.23 (H-3). The HMBC spectrum showed 2J and 3J couplings from the methyl protons (23, 24, 25, 26, 27, 29 and 30), which allowed the assignments of most carbons and protons of this aglycon. The deshielded chemical shift of C-28 observed at δ_C 180.2 suggested the presence of a carbonyl group of a carboxylic acid function. According to the literature data, this genin was identified as oleanolic acid, already described in saponins from *Weigela stelzneri* [47] (Table 8).

The HSQC spectrum of **12** displayed signals of six anomers at δ_H 4.78 (d, $J = 7.8$ Hz)/ δ_C 102.4, δ_H 4.80 (d, $J = 6.2$ Hz) / δ_C 104.7, δ_H 4.86 (d, $J = 6.9$ Hz)/ δ_C 102.1, δ_H 5.19 (d, $J = 7.1$ Hz)/ δ_C 106.3, δ_H 5.36 (d, $J = 6.9$ Hz)/ δ_C 104.6, and δ_H 6.06 (br s)/ δ_C 101.1 (Figure 42, 43 and 44). The ring protons of the monosaccharide residues were assigned starting from the readily identifiable anomeric protons by means of the 1H - 1H COSY, TOCSY, HSQC and

HMBC experiments. The monosaccharides obtained by acid hydrolysis of **12** were identified by comparison on TLC with authentic samples as xylose, arabinose and rhamnose. The absolute configurations were determined to be D for xylose, and L for arabinose and rhamnose by GC analysis according to a method previously described [64]. The relatively large $^3J_{\text{H-1,H-2}}$ value of the Xyl and Ara (6.2-7.8 Hz) in their pyranose form indicated a β anomeric orientation for Xyl, and an α anomeric orientation for Ara. The large $^1J_{\text{H-1,C-1}}$ value of the Rha (166 Hz) confirmed that the anomeric proton was equatorial (α -pyranoid anomeric form).

Units of one α -L-arabinopyranosyl, one α -L-rhamnopyranosyl and four β -D-xylopyranosyl were thus identified (Table 9). The monodesmosidic structure was elucidated by using mainly HMBC and NOESY spectra: the HMBC correlation at δ_{H} 4.80 (Ara-1) / δ_{C} 88.5 (C-3) and the NOESY correlation at δ_{H} 4.80 (Ara-1) / δ_{H} 3.23 (H-3) confirmed the *O*-heterosidic linkage between Ara and C-3 of the aglycon. The HMBC cross-peak at δ_{H} 6.06 (Rha-1)/ δ_{C} 75.2 (Ara-2) and the NOESY cross-peak at δ_{H} 6.06 (Rha-1)/ δ_{H} 4.46 (dd, 6.7, 6.2)(Ara-2) proved the (1 \rightarrow 2) linkage between Rha and Ara. The correlation at δ_{H} 5.19 (Xyl I-1)/ δ_{C} 82.0 (Rha-3) in the HMBC spectrum, and at δ_{H} 5.19 (Xyl I-1)/ δ_{H} 4.62 (dd, 9.5, 2.3) (Rha-3) in the NOESY spectrum, confirmed the (1 \rightarrow 3) linkage between Xyl I and Rha. The HMBC cross-peak at δ_{H} 4.78 (Xyl II-1)/ δ_{C} 76.6 (Xyl I-4) and the NOESY cross-peak at δ_{H} 4.78 (Xyl II-1)/ δ_{H} 4.10 (Xyl I-4) proved the (1 \rightarrow 4) linkage between Xyl II and Xyl I. Finally, the structure analysis of the terminal sequence β -D-xylopyranosyl-(1 \rightarrow 2)-[β -D-xylopyranosyl-(1 \rightarrow 4)]- β -D-xylopyranosyl was based upon the HMBC correlation at δ_{H} 5.36 (Xyl IV-1)/ δ_{C} 81.2 (Xyl II-4), the NOESY correlation at δ_{H} 5.36 (Xyl IV-1)/ δ_{H} 4.20 (Xyl II-4) and the HMBC cross-peak at δ_{H} 3.93 (dd, 8.1, 7.8)(Xyl II-2) / δ_{C} 102.1 (Xyl III-1) (Table 9, Figure 45).

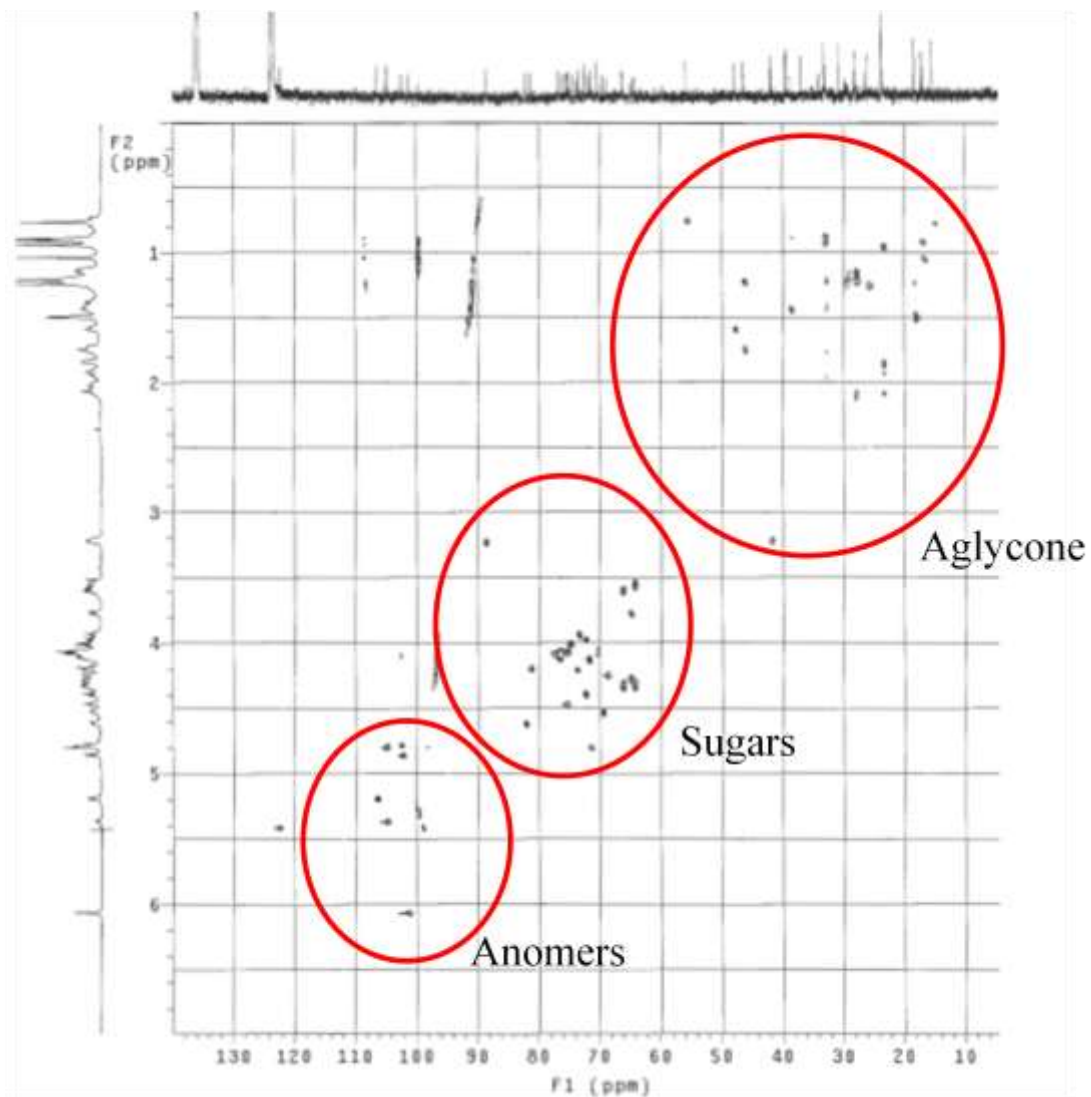


Figure 42: General HSQC of saponin 12

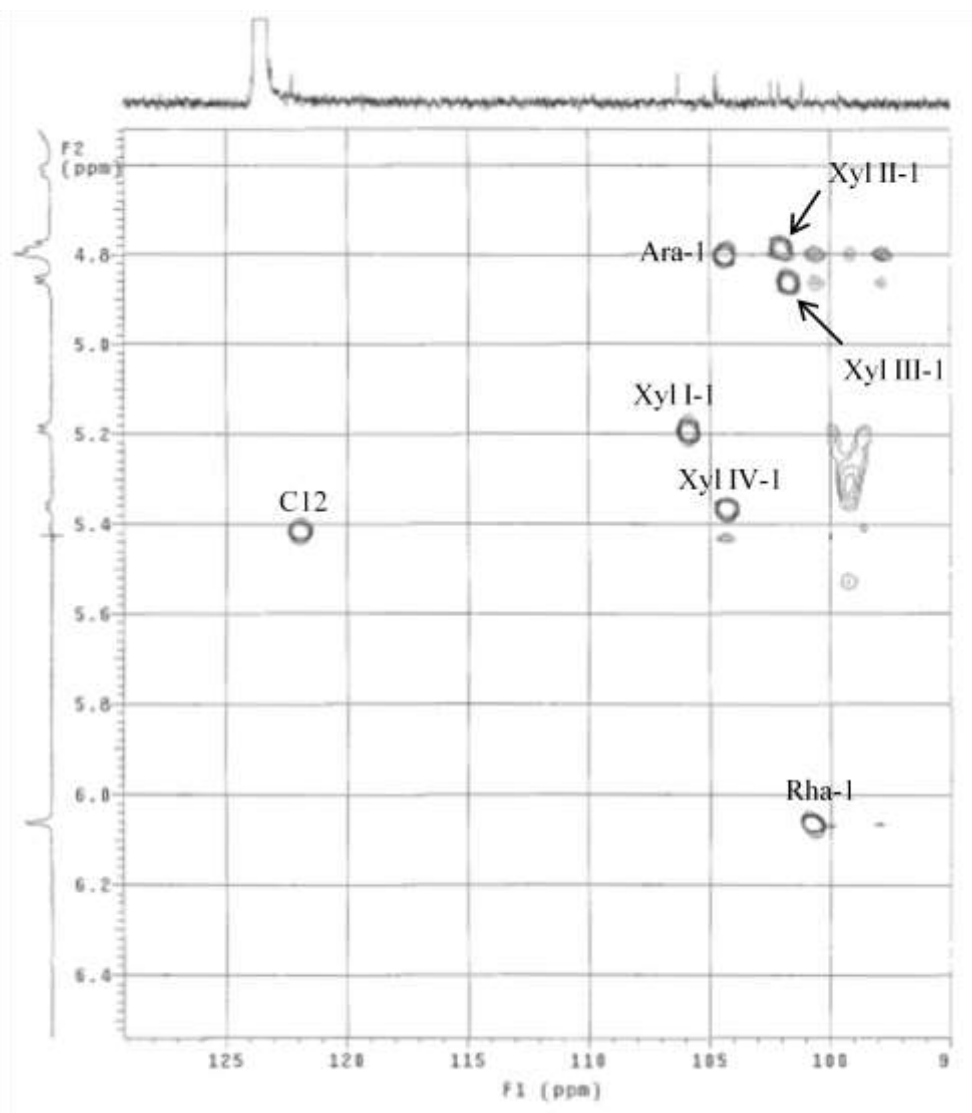


Figure 43: HSQC anomers zone of saponin 12

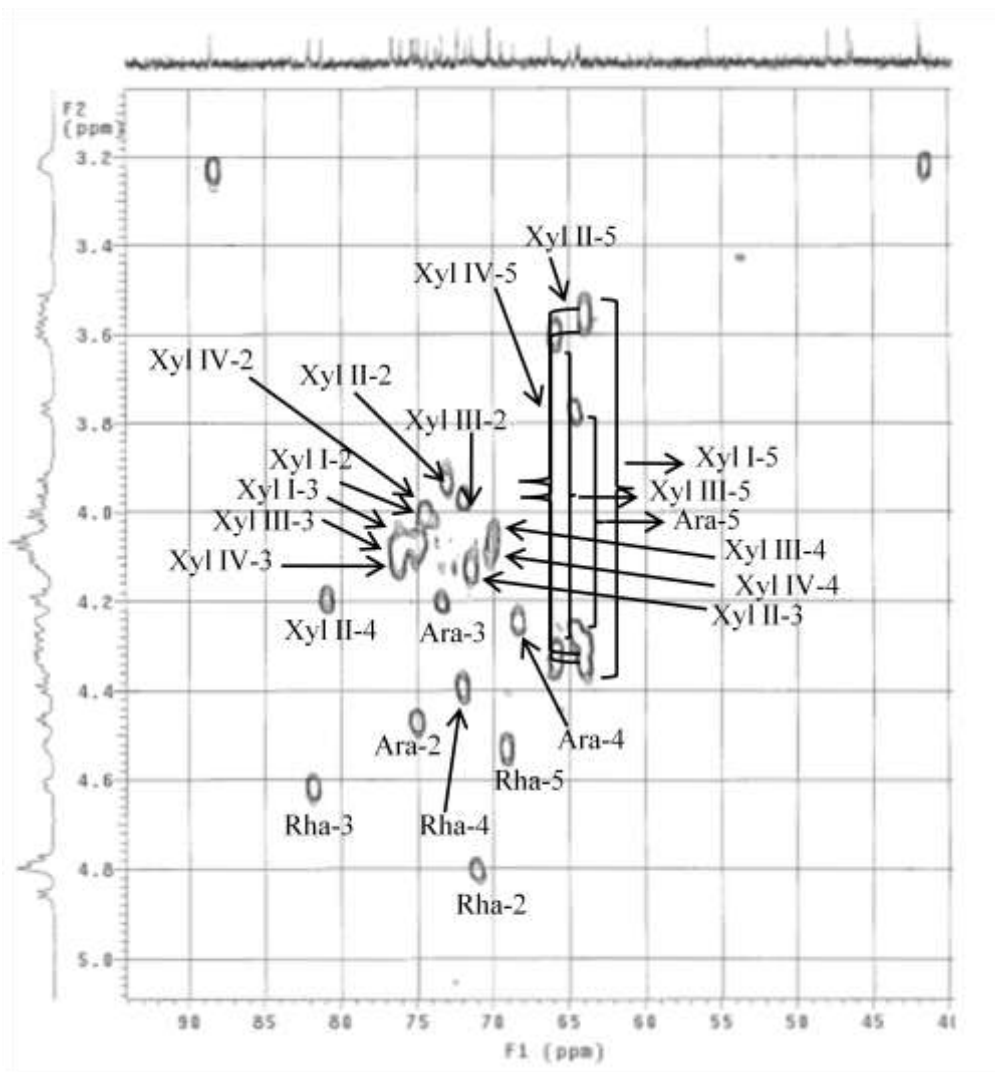


Figure 44: HSQC spectrum of saponin 12

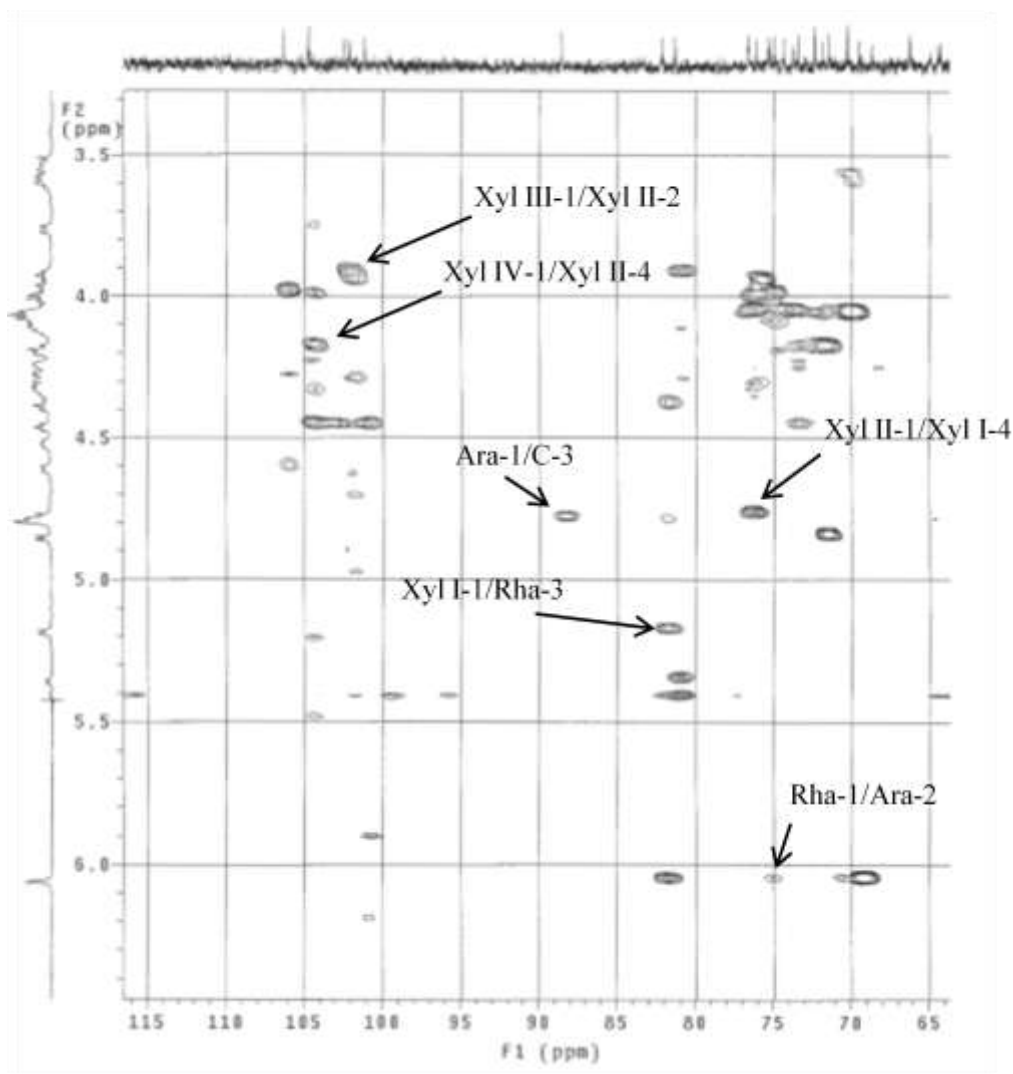


Figure 45: HMBC spectrum of saponin **12**

On the basis of the above results, the structure of the previously undescribed compound **12** was elucidated as 3-*O*- β -D-xylopyranosyl-(1 \rightarrow 2)-[β -D-xylopyranosyl-(1 \rightarrow 4)]- β -D-xylopyranosyl-(1 \rightarrow 4)- β -D-xylopyranosyl-(1 \rightarrow 3)- α -L-rhamnopyranosyl-(1 \rightarrow 2)- α -L-arabinopyranosyloleanolic acid (**12**).

The HR-ESIMS (positive-ion mode) spectrum of compound **13** established its molecular formula as $C_{62}H_{100}O_{28}$, as compound **12**. Its ESIMS (positive-ion mode) showed a pseudo-molecular peak at m/z 1315.5336 [$M + Na$] $^+$ (calcd 1315.6299[$M + Na$] $^+$) indicating a molecular weight of 1292, differing from **12** from 30 uma (Figure 46).

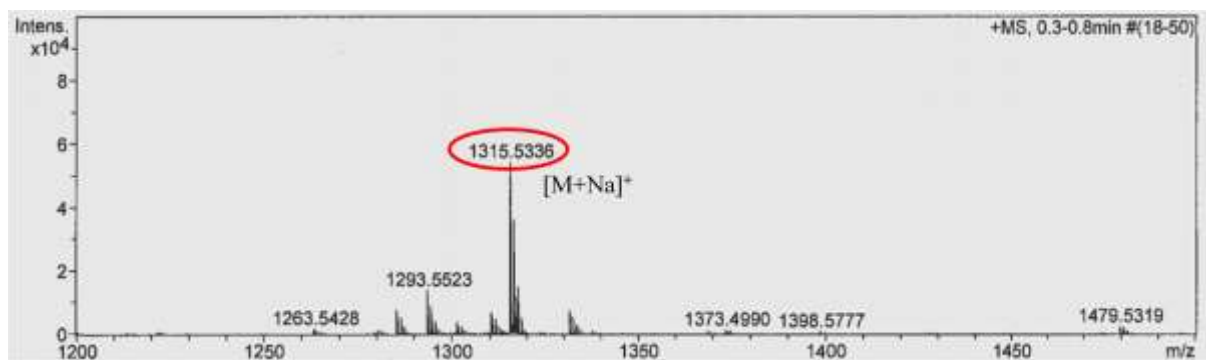


Figure 46: Positive ESIMS of saponin **13**

The ^1H and ^{13}C NMR signals of compounds **12** and **13** were almost surimposable excepted for the terminal hexose linked at the C-4 position of Xyl II. The full NMR assignments of this remaining sugar and the GC MS data, led to the identification of a β -D-glucopyranosyl moiety. The NOESY correlation at δ_{H} 5.27 (Glc-1)/ δ_{H} 4.23 (Xyl II-4) established the structure of the previously undescribed compound **13** as 3-O- β -D-xylopyranosyl-(1 \rightarrow 2)-[β -D-glucopyranosyl-(1 \rightarrow 4)]- β -D-xylopyranosyl-(1 \rightarrow 4)- β -D-xylopyranosyl-(1 \rightarrow 3)- α -L-rhamnopyranosyl-(1 \rightarrow 2)- α -L-arabinopyranosyloleanolic acid (**13**) (Figure 47, 48, 49 and 50).

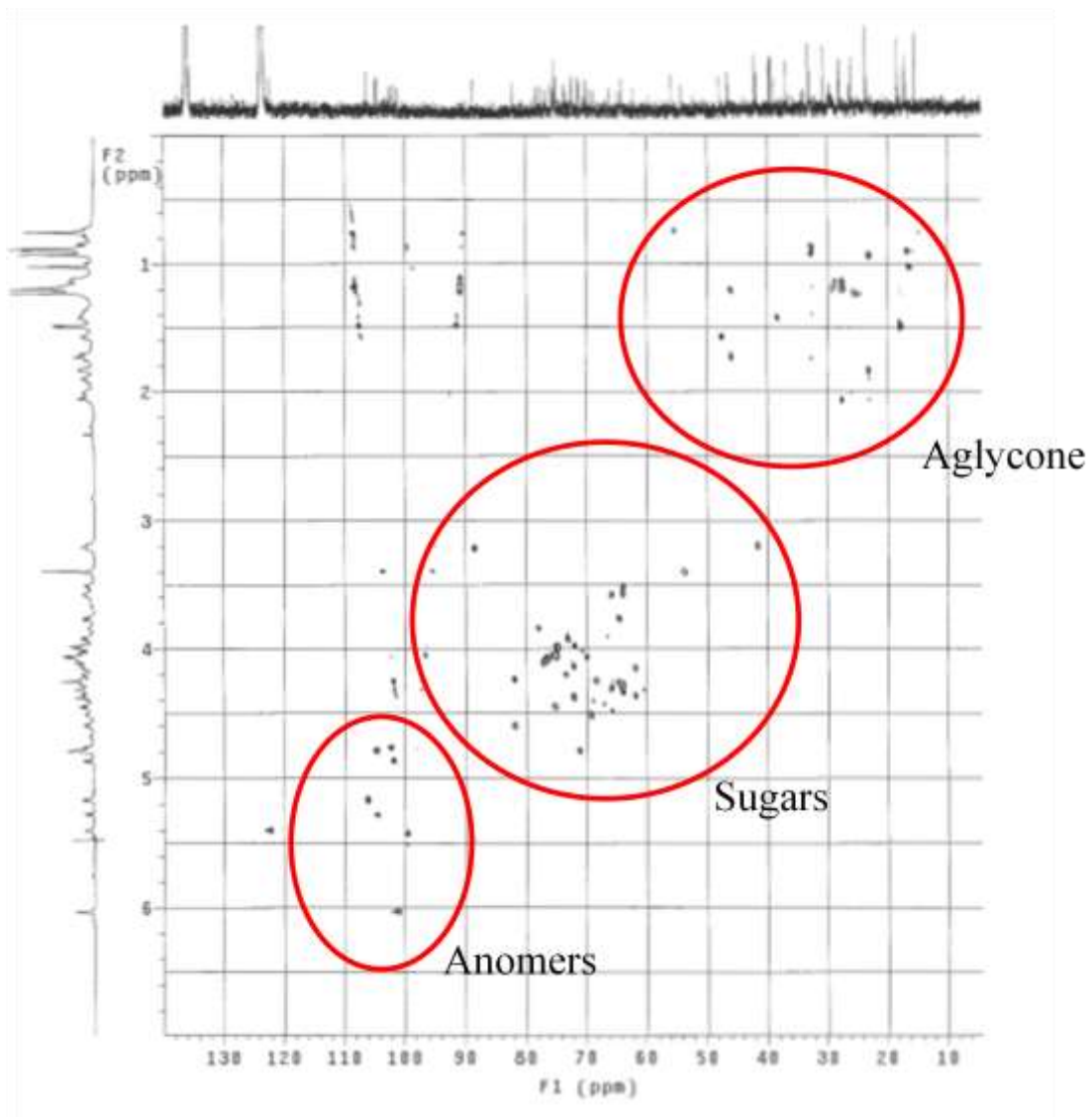


Figure 47: General HSQC spectra of saponin 13

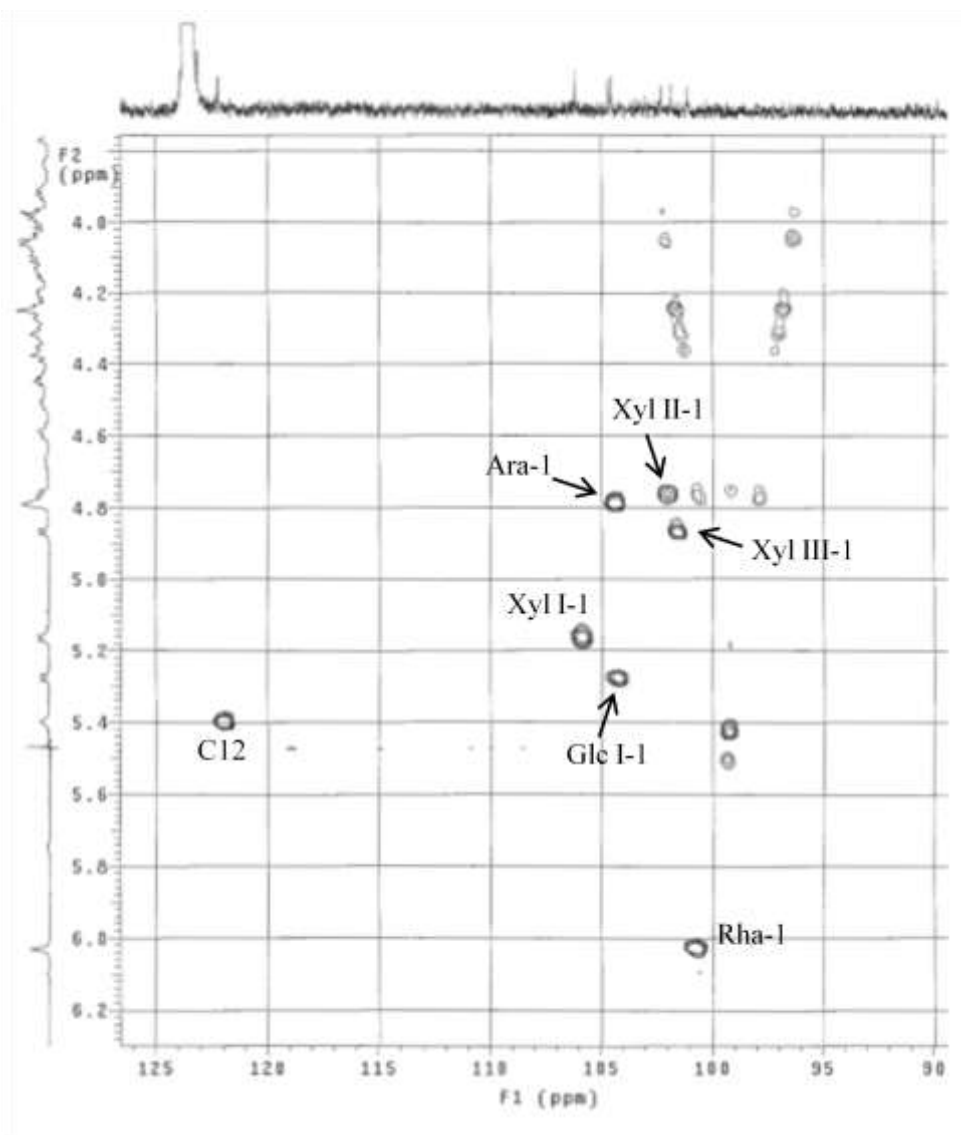


Figure 48: HSQC anomers zone of saponin 13

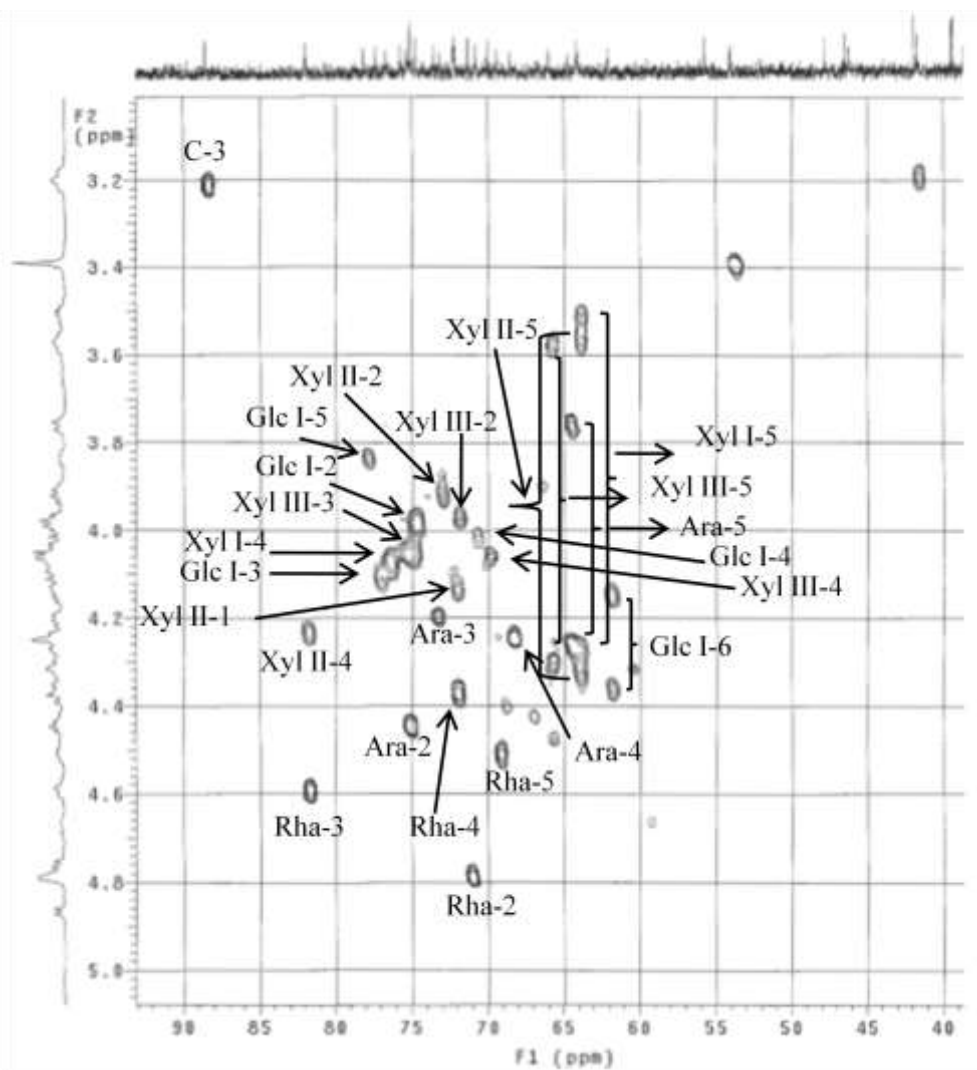


Figure 49: HSQC spectrum of saponin 13

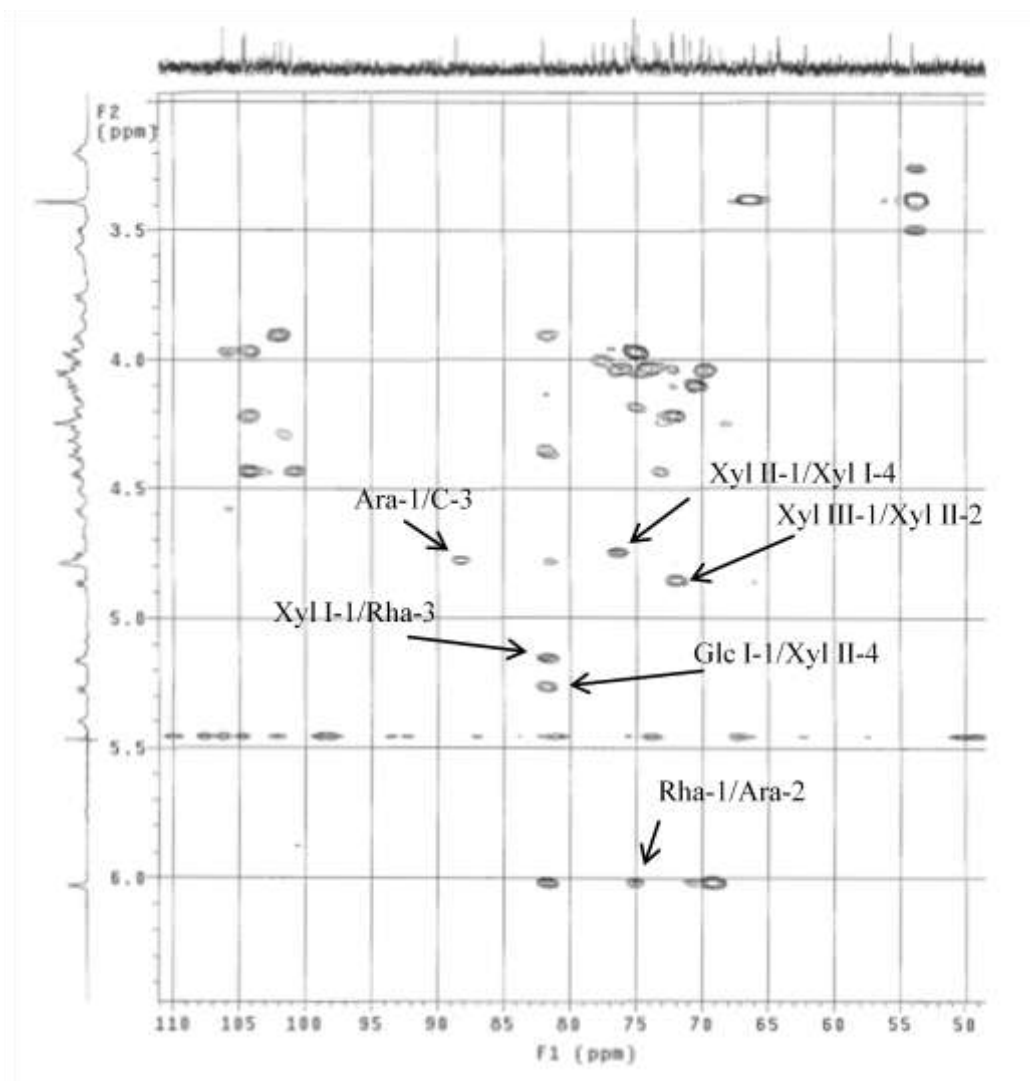


Figure 50: HMBC spectrum of saponin **13**

The HR-ESIMS (positive-ion mode) spectrum of compound **14** established its molecular formula as $C_{46}H_{74}O_{15}$. Its ESIMS (positive-ion mode) showed a pseudo-molecular peak at m/z 889.4410 $[M + Na]^+$ (calcd 889.4925 $[M + Na]^+$) indicating a molecular weight of 866 (Figure 51).

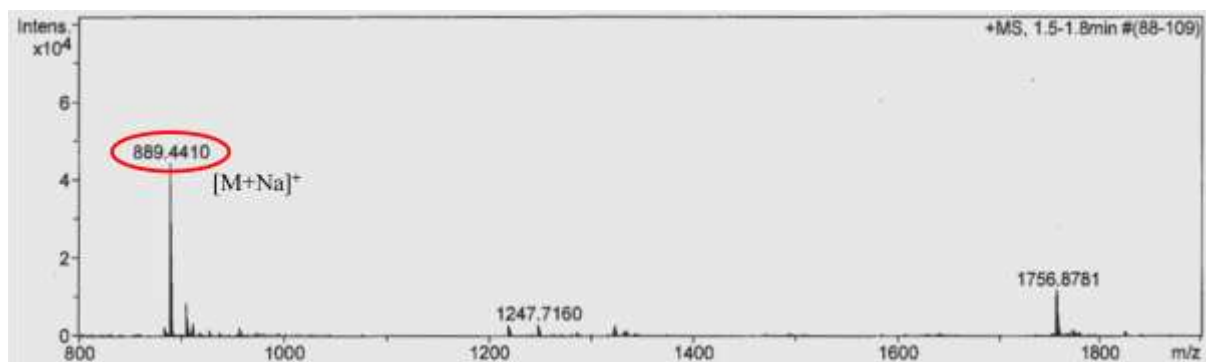


Figure 51: Positive ESIMS of saponin **14**

The ^1H NMR spectrum of the aglycone part of **14** displayed signals assignable to seven angular methyl groups at δ_{H} 0.76, 0.88, 0.90, 0.94, 1.03, 1.22 and 1.24 (s, each), one olefinic proton at δ_{H} 5.44 (br t, 3.1), and one oxygen-bearing methine protons at δ_{H} 3.22 (H-3). In the ^{13}C NMR spectrum, a signal at δ_{C} 180.2 suggested a carboxylic acid function (C-28). As for **12** and **13**, the genin of **14** was identified as oleanolic acid [47] (Table 8).

The HSQC spectrum of **14** displayed signals of three anomers at δ_{H} 4.79 (d, 6.0)/ δ_{C} 104.7, δ_{H} 5.22 (d, 7.6)/ δ_{C} 106.6, and δ_{H} 6.08 (br s)/ δ_{C} 101.0 (Figure 52, 53 and 54). By 2D NMR and GC analysis, units of one α -L-arabinopyranosyl, one α -L-rhamnopyranosyl and one β -D-xylopyranosyl were identified (Table 9). The structural analysis of the oligosaccharidic chain linked at the C-3 of the aglycon was realized using mainly HMBC and NOESY spectra. The HMBC correlation at δ_{H} 4.79 (Ara-1)/ δ_{C} 88.5 (C-3) and the NOESY correlation at δ_{H} 4.79 (Ara-1)/ δ_{H} 3.22 (H-3) confirmed the *O*-heterosidic linkage between Ara and C-3. The HMBC cross-peak at δ_{H} 6.08 (Rha-1)/ δ_{C} 75.1 (Ara-2) and the NOESY cross-peak at δ_{H} 6.08 (Rha-1)/ δ_{H} 4.47 (d, 6.9, 6.0) (Ara-2) proved the (1 \rightarrow 2) linkage between Rha and Ara. The correlation at δ_{H} 5.22 (Xyl I-1)/ δ_{C} 82.0 (Rha-3) in the HMBC spectrum and at δ_{H} 5.22 (Xyl I-1)/ δ_{H} 4.63 (dd, 9.5, 2.9) (Rha-3) in the NOESY spectrum, confirmed the (1 \rightarrow 3) linkage between Xyl I and Rha (Table 9, Figures 55 and 56).

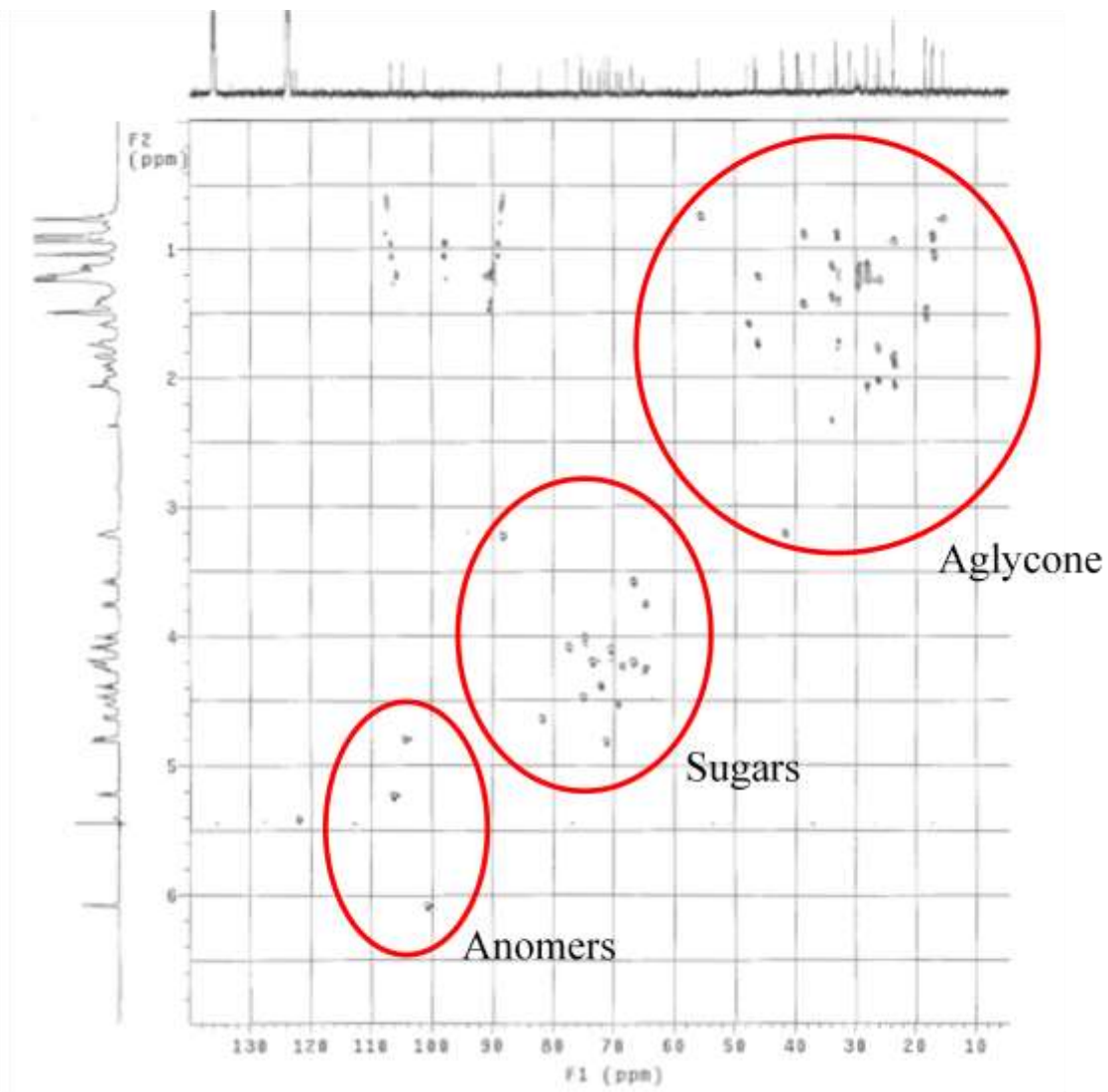


Figure 52: General HSQC spectrum of saponin 14

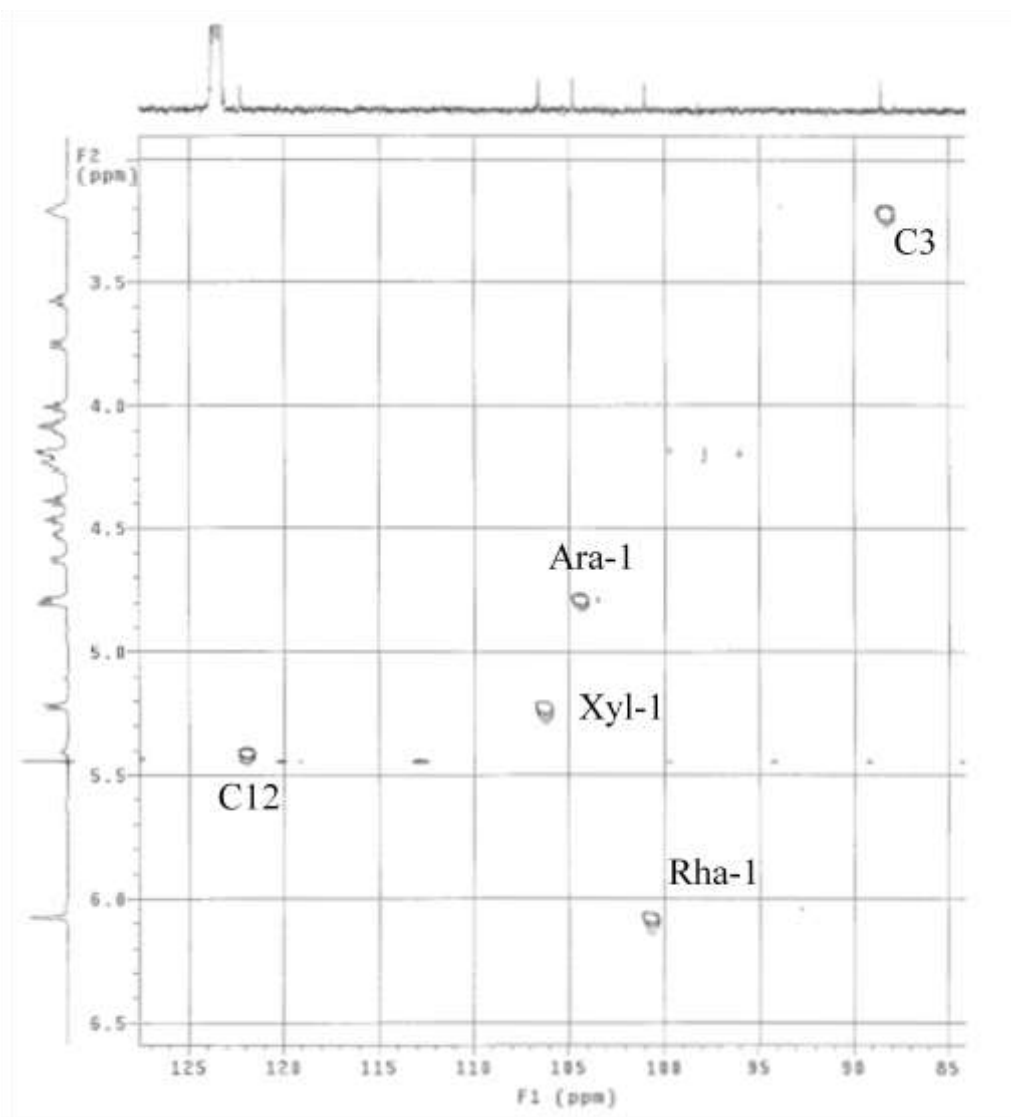


Figure 53: HSQC anomers zone of saponin 14

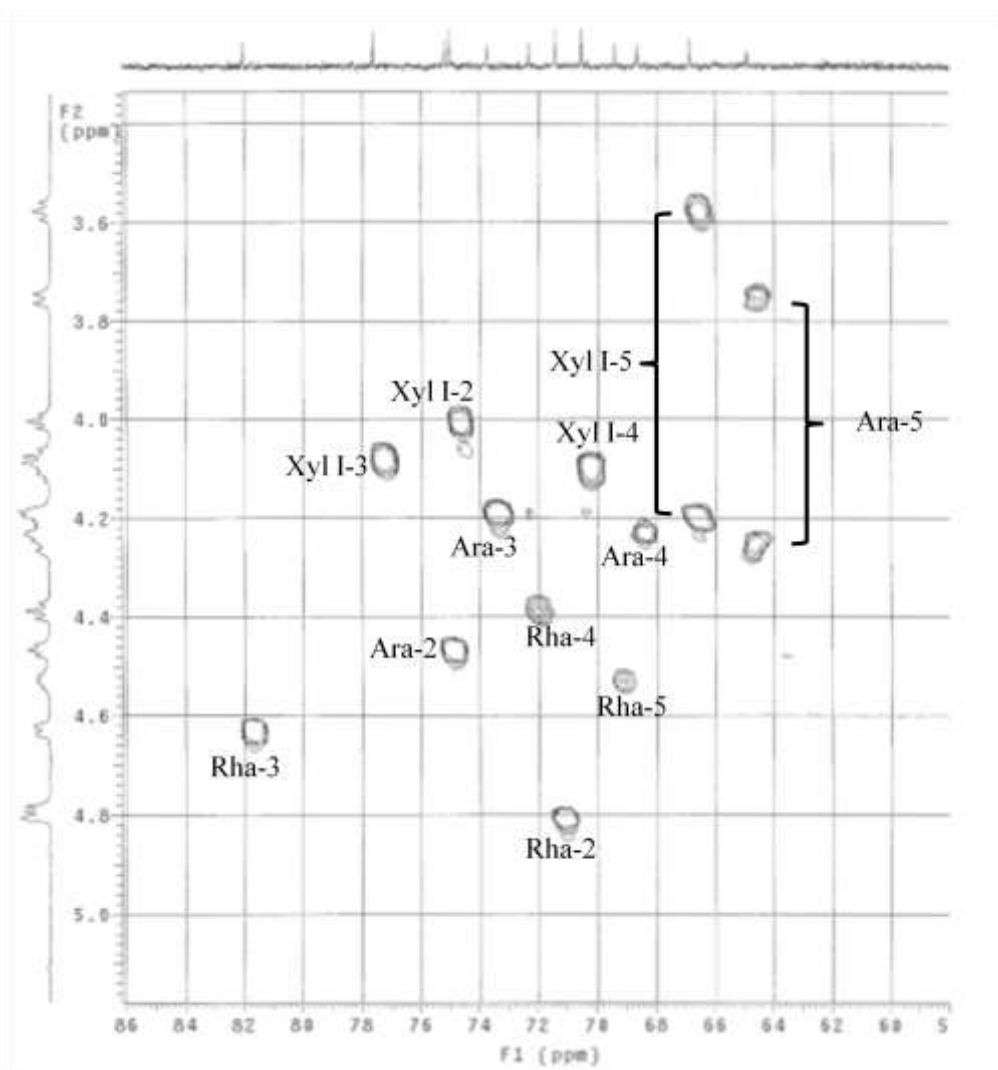


Figure 54: Sugar moieties of saponin 14

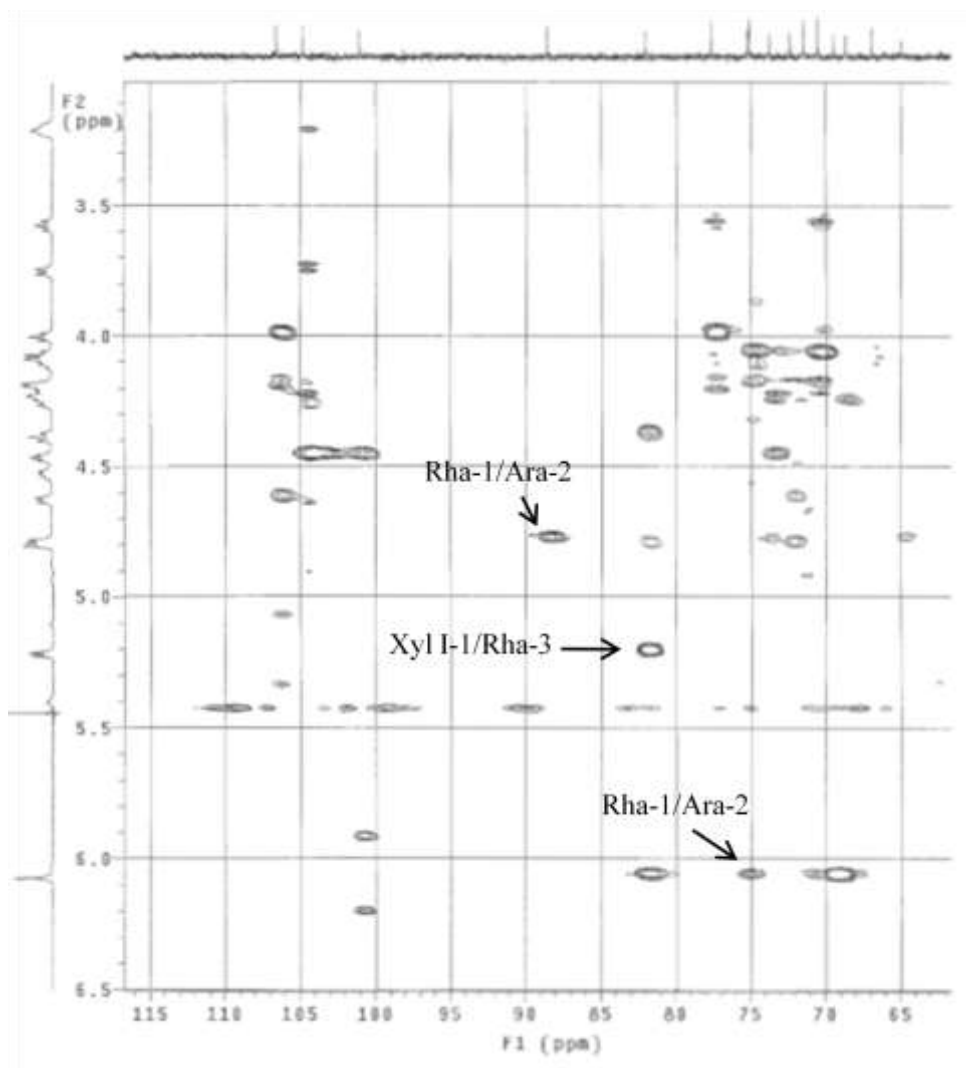


Figure 55: HMBC spectrum of saponin 14

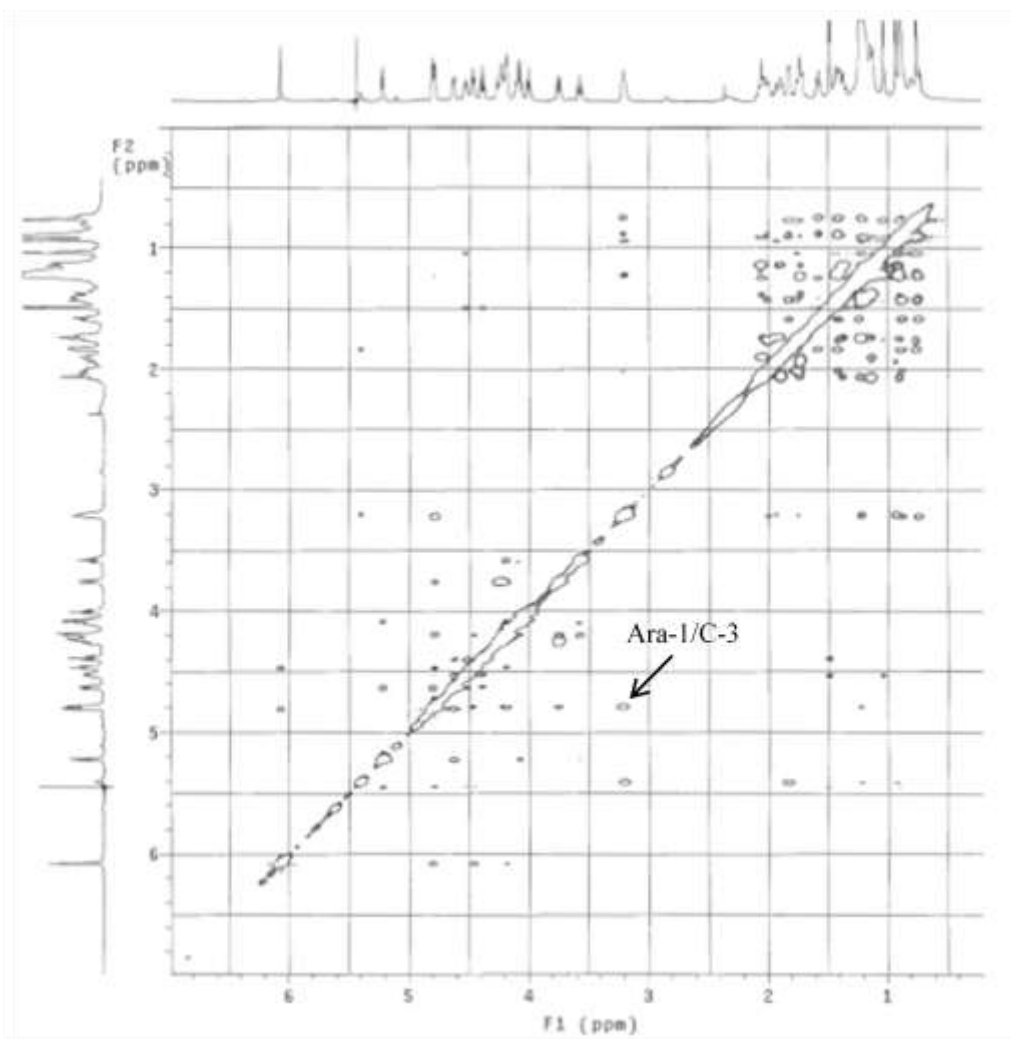


Figure 56: NOESY spectrum of saponin **14**

On the basis of the above results, the structure of the previously undescribed compound **14** was elucidated as 3-*O*- β -D-xylopyranosyl-(1 \rightarrow 3)- α -L-rhamnopyranosyl-(1 \rightarrow 2)- α -L-arabinopyranosyloleanolic acid (**14**). This sequence was already found in saponins from *Weigela stelzneri* [47]. Other species should be investigated to confirm this sequence as a chemotaxonomic marker of the genus *Weigela*.

From the roots of *Weigela florida* “rumba”, three new triterpene glycosides were identified as 3-*O*- β -D-xylopyranosyl-(1 \rightarrow 2)-[β -D-xylopyranosyl-(1 \rightarrow 4)]- β -D-xylopyranosyl-(1 \rightarrow 4)- β -D-xylopyranosyl-(1 \rightarrow 3)- α -L-rhamnopyranosyl-(1 \rightarrow 2)- α -L-arabinopyranosyloleanolic acid (**12**), 3-*O*- β -D-xylopyranosyl-(1 \rightarrow 2)-[β -D-glucopyranosyl-(1 \rightarrow 4)]- β -D-xylopyranosyl-(1 \rightarrow 4)- β -D-xylopyranosyl-(1 \rightarrow 3)- α -L-rhamnopyranosyl-(1 \rightarrow 2)- α -L-arabinopyranosyloleanolic acid (**13**) and 3-*O*- β -D-xylopyranosyl-(1 \rightarrow 3)- α -L-rhamnopyranosyl-(1 \rightarrow 2)- α -L-arabinopyranosyloleanolic acid (**14**) (Figure 57).

Table 8. ^{13}C NMR and ^1H NMR data of the aglycones of compounds **12-14** in Pyridine- d_5 (δ in ppm, J in Hz)

No	12		13		14	
	δ_{C}	δ_{H}	δ_{C}	δ_{H}	δ_{C}	δ_{H}
1	38.6	0.88 (m), 1.43 (m)	38.5	0.84 (m), 1.42 (m)	38.6	0.88 (m), 1.42 (m)
2	26.3	1.78 (m), 2.02 (m)	26.2	1.74 (m), 2.00 (m)	23.3	1.88 (m), 2.04
3	88.5	3.23	88.5	3.22	88.5	3.22
4	39.2	-	39.2	-	39.4	-
5	55.7	0.73 (br d, 12.2)	55.6	0.71 (br d, 11.6)	55.7	0.72 (br d, 12.2)
6	18.2,	1.23, 1.47 (m)	18.2	1.20, 1.45 (m)	18.1	1.45, nd
7	32.8,	1.22, 1.43 (m)	32.9	1.19, 1.40 (m)	32.8	1.17, 1.38 (m)
8	39.4	-	39.3	-	39.2	-
9	47.7	1.57 (dd, 14.1, 8.1)	47.7	1.55 (dd, 15.0, 9.0)	47.7	1.57 (dd, 14.0, 8.6)
10	36.6	-	36.7	-	36.7	-
11	23.5	1.83 (m), 1.91	23.4	1.82 (m), 1.86	23.5	1.82 (m), 1.86
12	122.2	5.42	122.2	5.40 (br t, 3.0)	122.2	5.44 (br t, 3.1)
13	144.5	-	144.4	-	144.5	-
14	41.8	-	41.8	-	41.8	-
15	28.0	1.14 (m), 2.08 (m)	27.8	1.13 (m), 2.03 (m)	28.0	1.12 (m), 2.06 (m)
16	23.3	1.91, 2.06(m)	23.3	1.89 (m), 2.05 (m)	26.3	1.75 (m), 2.01 (m)
17	46.4	-	46.4	-	46.4	-
18	41.7	3.23	41.6	3.20	41.6	3.20
19	46.2	1.22, 1.73	46.1	1.20, 1.72	46.2	1.19, 1.74
20	30.6	-	30.6	-	30.6	-
21	33.9	1.11 (m), 1.35 (m)	nd	nd	33.9	1.12 (m), 1.37 (m)
22	32.8	1.70, 1.89	32.8	1.73, nd	32.8	1.71 1.78
23	27.9	1.21 (s)	27.8	1.19 (s)	27.9	1.22 (s)
24	16.8	1.03 (s)	16.7	1.01 (s)	16.8	1.03 (s)
25	15.2	0.76 (s)	15.2	0.75 (s)	15.2	0.76 (s)
26	17.1	0.90 (s)	17.0	0.89 (s)	17.1	0.90 (s)
27	25.9	1.23 (s)	25.8	1.22 (s)	25.9	1.24 (s)
28	180.2	-	180.3	-	180.2	-
29	33.0	0.89 (s)	33.8	0.88 (s)	33.0	0.88 (s)
30	23.5	0.93 (s)	23.4	0.92 (s)	23.5	0.94 (s)

Overlapped proton signals are reported without designated multiplicity.

Table 9. ^{13}C NMR and ^1H NMR data of the sugar moieties of compounds **12-14** in Pyridine- d_5 (δ_{H} ppm, J in Hz)

No	12		13		14	
	δ_{C}	δ_{H}	δ_{C}	δ_{H}	δ_{C}	δ_{H}
Ara-1	104.7	4.80 (d, 6.2)	104.6	4.79 (d, 6.2)	104.7	4.79 (d, 6.0)
2	75.2	4.46 (dd, 6.7, 6.2)	75.1	4.45 (dd, 6.9, 6.2)	75.1	4.47 (dd, 6.9, 6.0)
3	73.7	4.21	73.5	4.20	73.7	4.19
4	68.6	4.24 (m)	68.5	4.24 (m)	68.6	4.23 (m)
5	64.8	3.77 (br d, 10.7), 4.26	64.7	3.76 (br d, 9.8), 4.27	64.9	3.75 (br d, 10.7), 4.25
Rha-1	101.1	6.06 (br s)	101.0	6.03 (br s)	101.0	6.08 (br s)
2	71.4	4.80 (br s)	71.3	4.79 (br s)	71.4	4.80 (br s)
3	82.0	4.62 (dd, 9.5, 2.3)	82.0	4.59 (dd, 9.3, 2.7)	82.0	4.63 (dd, 9.5, 2.9)
4	72.2	4.39 (dd, 9.5, 9.3)	72.2	4.37	72.3	4.39 (t, 9.5)
5	69.4	4.53 (dq, 9.3, 6.0)	69.4	4.51 (dq, 9.5, 6.0)	69.4	4.53 (dq, 9.5, 6.2)
6	18.1	1.49 (d, 6.0)	18.0	1.49 (d, 6.0)	18.1	1.48 (d, 6.2)
Xyl I-1	106.3	5.19 (d, 7.1)	106.1	5.16 (d, 7.4)	106.6	5.22 (d, 7.6)
2	74.3	4.01 (dd, 7.8, 7.1)	74.7	3.99	75.0	4.01 (dd, 8.6, 7.6)
3	75.3	4.07	75.2	4.05	77.6	4.08 (dd, 8.6, 8.3)
4	76.6	4.10	76.6	4.07	70.5	4.10 (m)
5	64.4	3.52 (t, 10.7), 4.28	64.1	3.50 (t, 10.0), 4.28	66.8	3.58 (t, 10.5), 4.20
Xyl II-1	102.4	4.78 (d, 7.8)	102.3	4.76 (d, 7.4)		
2	73.3	3.93 (dd, 8.1, 7.8)	73.1	3.92 (dd, 8.6, 7.4)		
3	71.7	4.12	72.2	4.14		
4	81.2	4.20	82.0	4.23		
5	64.2	3.58, 4.34	64.1	3.56, 4.34		
Xyl III-1	102.1	4.86 (d, 6.9)	101.8	4.87 (d, 6.7)		
2	72.2	3.96 (dd, 7.4, 6.9)	72.2	3.98		
3	76.1	4.09	75.7	4.06		
4	70.1	4.07	69.9	4.07		
5	66.1	3.60, 4.30	65.9	3.58, 4.30		
Xyl IV-1	104.6	5.36 (d, 6.9)				
2	74.3	4.02				
3	76.6	4.08				
4	70.1	4.07				
5	66.1	3.60, 4.34				
Glc I-1			104.5	5.27 (d, 7.9)		
2			74.7	3.98		
3			77.6	4.11		
4			70.8	4.01		
5			78.1	3.84 (m)		
6			62.0	4.14, 4.37		

Overlapped proton signals are reported without designated multiplicity.

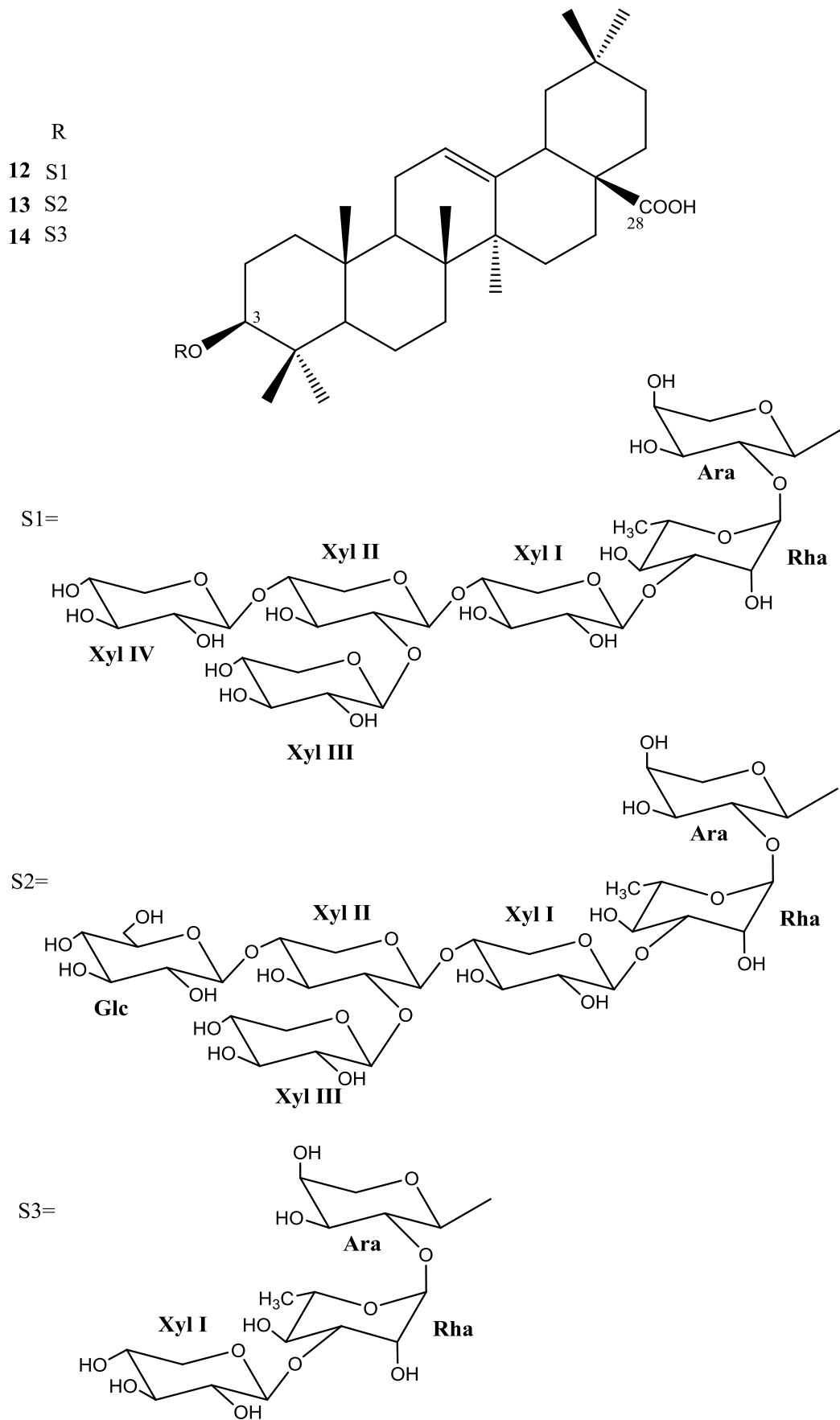


Figure 57: Structure of saponins 12-14

Polygala acicularis

Two triterpene glycosides were isolated from the roots of *Polygala acicularis*. They were identified mainly by 2D NMR spectroscopic analysis (COSY, TOCSY, NOESY, HSQC, HMBC) and mass spectrometry, as 3-*O*- β -D-glucopyranosyl-presenegenin-28-*O*- β -D-xylopyranosyl-(1 \rightarrow 4)- α -L-rhamnopyranosyl-(1 \rightarrow 2)-(3,4-di-*O*-acetyl)- β -D-fucopyranosyl ester (**15**), and 3-*O*- β -D-glucopyranosyl-presenegenin-28-*O*- β -D-xylopyranosyl-(1 \rightarrow 4)- α -L-rhamnopyranosyl-(1 \rightarrow 2)-[4-*O*-(*E*)-3,4-dimethoxycinnamoyl]- β -D-fucopyranosyl ester (**15**).

Compound **15**, a white amorphous powder, showed in HR ESIMS (positive-ion mode) a quasimolecular ion peak $[M + Na]^+$ at m/z 1373.5808 indicating a molecular weight of 1350, compatible with a molecular formula of $C_{63}H_{98}O_{31}$ (Figure 58).

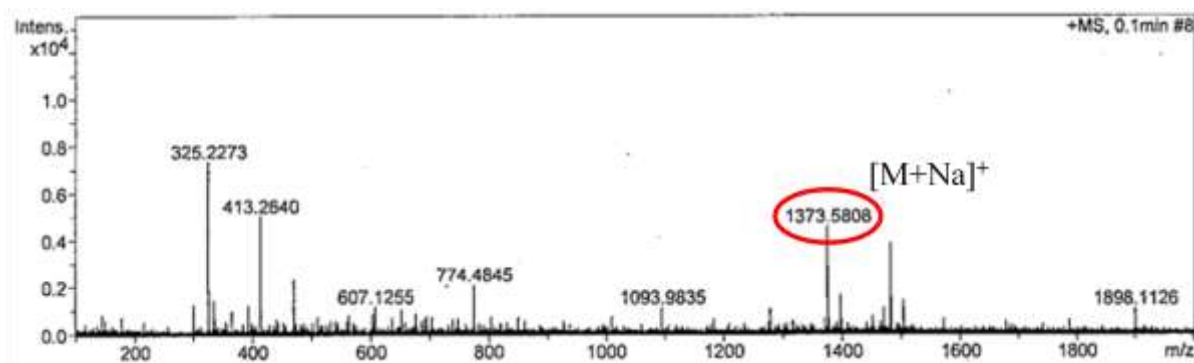


Figure 58: Positive ESIMS of saponin **15**

The spectroscopic NMR data of the prosapogenin of **15** were in good agreement with those of tenuifolin (3-*O*- β -D-glucopyranosyl-presenegenin), commonly encountered in the Polygalaceae family [42-43]. The 1H NMR spectrum of **15** displayed signals for five anomeric protons at δ_H 6.40 (br s), 6.06 (d, $J = 8.1$ Hz), 5.04 (d, $J = 7.0$ Hz), 4.93 (d, $J = 7.6$ Hz), 4.84 (d, $J = 7.0$ Hz), which gave correlations, in the HSQC spectrum, with carbon signals at δ_C 102.0, 94.2, 104.5, 103.9, and 106.9 respectively (Figures 59 and 60). The ring protons of the monosaccharide residues were assigned starting from the readily identifiable anomeric protons by means of the COSY, TOCSY, HSQC, HMBC experiments (Tables 10 and 11). Evaluation of spin-spin couplings and chemical shifts allowed the identification of one β -fucopyranose (Fuc), one α -rhamnopyranose (Rha), one β -glucopyranose (Glc), one β -xylopyranoses (Xyl), and one β -galactopyranose (Gal) units. The common D-configuration for Fuc, Glc, Xyl, and Gal, and the L-configuration for Rha were assumed by GC MS as

previously described. Correlations observed in the HMBC spectrum between signals at δ_{H} 5.04 (Glc-1) and δ_{C} 86.9 (C-3), and in the ROESY spectrum between δ_{H} 5.04 (Glc-1) and δ_{H} 4.62 (H-3), confirmed the substitution at the C-3 position of the presenegenin by a 3-*O*- β -D-glucopyranose. After subtraction of the anomeric signals of the glucosyl moiety, the signals of four sugars linked to the aglycon by an ester linkage remained. In the HMBC spectrum, a correlation between signals at δ_{H} 6.06 (d, $J = 8.1$ Hz, Fuc-1) and δ_{C} 176.5 (C-28) proved a glycosidic ester linkage to the C-28 of the aglycon. A ROESY correlation between signals at δ_{H} 6.40 (Rha-1) and δ_{H} 4.71 (dd, $J = 8.8, 8.1$ Hz) (Fuc-2) revealed the (1 \rightarrow 2) linkage between these two sugars. The signals at δ_{H} (Fuc-3) and δ_{H} (Fuc-4) were shifted downfield at δ_{H} 5.54 and δ_{H} 5.52 respectively and the presence of two acetyl methyl signals at δ_{H} 2.06 (s) and δ_{H} 2.10 (s) suggested the Fuc-3 and Fuc-4 substitution by two acetyl groups. According to the HMBC correlation between δ_{H} 4.21 (Rha-4) and δ_{C} 106.9 (Xyl-1), and a reverse one between δ_{H} 4.84 (Xyl-1) and δ_{C} 86.2 (Rha-4), we concluded that saponin **15** presented the sequence 3-*O*- β -D-glucopyranosyl-presenegenin-28-*O*- β -D-xylopyranosyl-(1 \rightarrow 4)- α -L-rhamnopyranosyl-(1 \rightarrow 2)-(3,4-di-*O*-acetyl)- β -D-fucopyranosyl ester (Figure 61), which has been already encountered in four Polygalaceae, *Polygala fallax* [76], *Polygala renii* [77], *Carpolobia alba* [78] and *Carpolobia lutea* [78]. Moreover, the assignments of the ^1H and ^{13}C NMR signals of a terminal β -D-galactopyranose were deduced from the TOCSY, HSQC, HMBC and ROESY spectra. A HMBC cross-peak at δ_{H} 4.93 (Gal-1) / δ_{C} 77.2 (Xyl-4), and a ROESY cross-peak at δ_{H} 4.93 (Gal-1) / δ_{H} 4.36 (Xyl-4), suggested a substitution of the position 4 of the xylose by this terminal galactose.

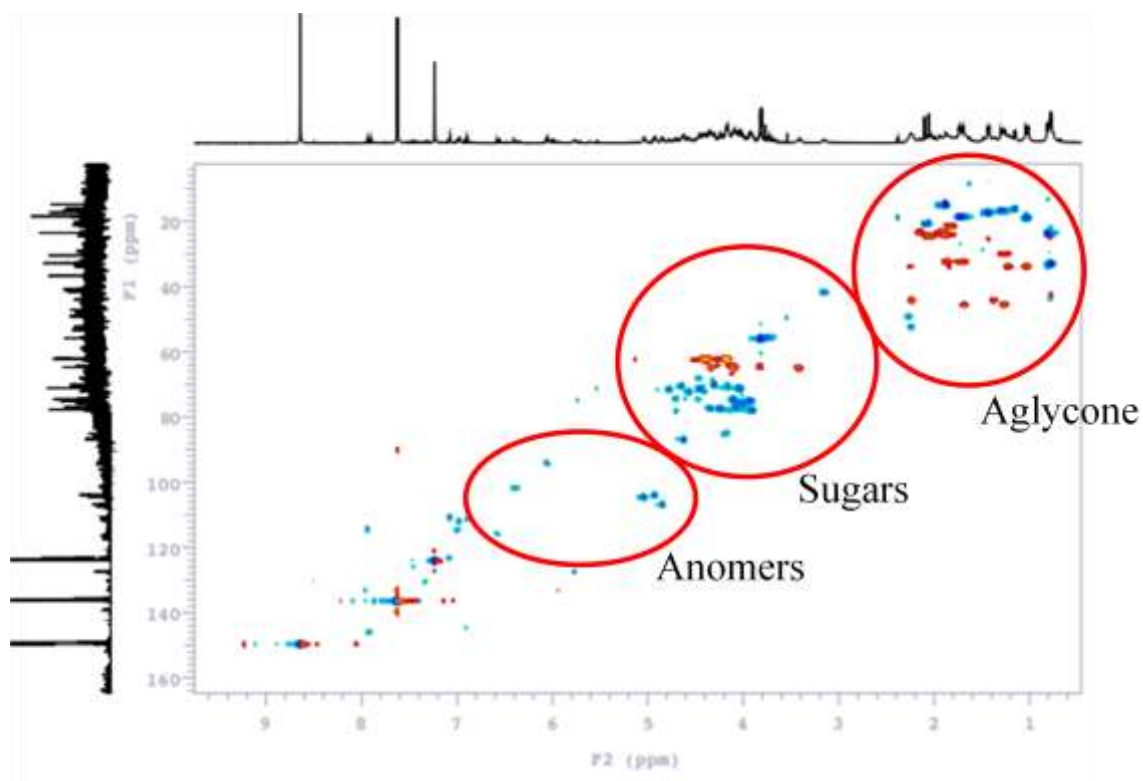


Figure 59: General HSQC of saponin 15

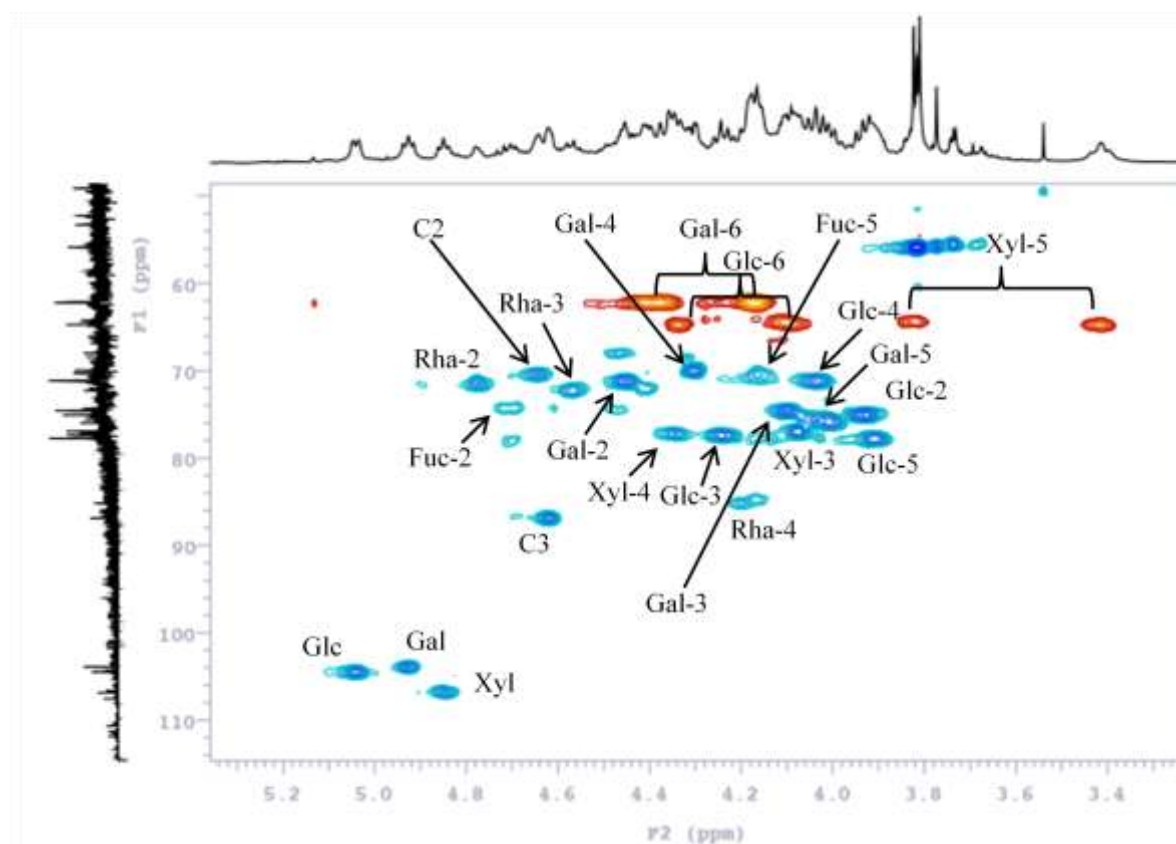


Figure 60: HSQC spectrum of saponin 15

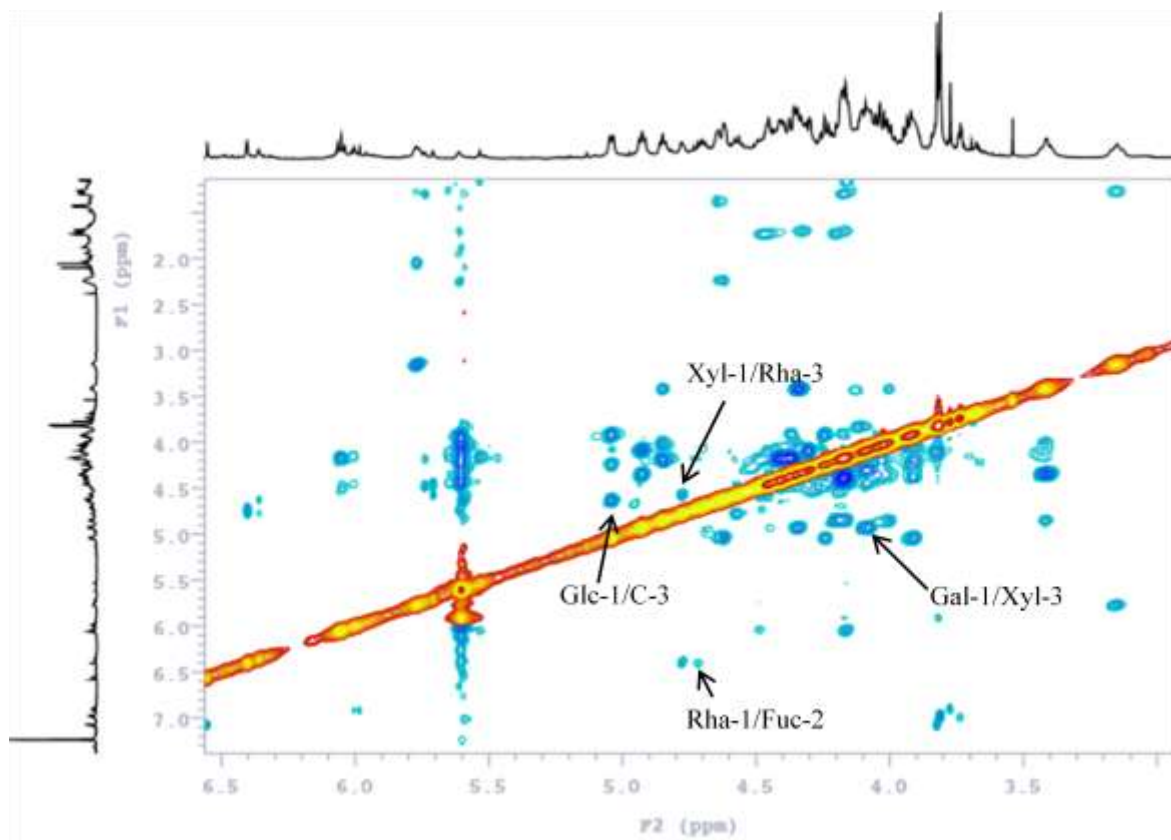


Figure 61: ROESY spectrum of saponin **15**

The structure of **15** was thus established as 3-*O*- β -D-glucopyranosyl-presenegenin-28-*O*- β -D-galactopyranosyl-(1 \rightarrow 3)- β -D-xylopyranosyl-(1 \rightarrow 4)- α -L-rhamnopyranosyl-(1 \rightarrow 2)-(3,4-di-*O*-acetyl)- β -D-fucopyranosyl ester (**15**) (Figure 62). This molecule was already isolated from another species of *Polygala*, *P. fallax*, and named Polygalasaponin XXXV [76].

The ^1H - and ^{13}C -NMR signals of **16** assigned from the 2D spectra, were almost superimposable on those of **15** excepted for the β -D-fucopyranosyl moiety (Tables 10 and 11). The downfield shifts observed in the HSQC spectrum for the H-C(4)/(C4) resonances of the Fuc at δ_{H} 5.68/ δ_{C} 74.7 proved the secondary alcoholic function at the 4 position of the Fuc to be acylated. The Fuc-4 position was substituted by a (*E*)-3,4-dimethoxycinnamoyl. This acyl moiety appeared as two doublets at δ_{H} 6.53 and 7.88 (1H each, $J = 16$ Hz). The full assignments of the carbons and protons of the 3,4-dimethoxycinnamoyl unit obtained by further 2D-NMR investigations, were in good agreement with those described in literature [79] (Table 10).

This molecule was identified as 3-*O*- β -D-glucopyranosyl-presenegenin-28-*O*- β -D-galactopyranosyl-(1 \rightarrow 3)- β -D-xylopyranosyl-(1 \rightarrow 4)- α -L-rhamnopyranosyl-(1 \rightarrow 2)-[4-*O*-(*E*)-3,4-dimethoxycinnamoyl]- β -D-fucopyranosyl ester (**16**) (Figure 62), previously isolated from *Polygala senega* [79], and named senegin II.

In conclusion, we found in this plant two saponins possessing a common sequence 3-*O*- β -D-glucopyranosylpresenegenin 28-*O*- β -D-galactopyranosyl-(1 \rightarrow 4)- β -D-xylopyranosyl-(1 \rightarrow 4)- α -L-rhamnopyranosyl-(1 \rightarrow 2)- β -D-fucopyranosyl ester, with additional acylations of the Fuc-4 and/or Fuc-3 positions. A chemotaxonomic marker has already been identified in the Polygalaceae which is 3-*O*- β -D-glucopyranosylpresenegenin 28-*O*- β -D-xylopyranosyl-(1 \rightarrow 4)- α -L-rhamnopyranosyl-(1 \rightarrow 2)- β -D-fucopyranosyl ester [42-43]. These results corroborated those previously described for saponins isolated from this family.

The structural analysis of three other isolated molecules, identified as sucrose esters, is in progress.

Table 10. ^{13}C NMR and ^1H NMR data of the aglycones of compounds **15** and **16** in Pyridine- d_5 /D $_2$ O (δ ppm, J in Hz)

Position	15		16	
	δ_{C}	δ_{H}	δ_{C}	δ_{H}
1	44.0	1.37, 2.23	44.2	1.33, 2.19
2	71.0	4.64	71.0	4.58
3	89.9	4.62	87.0	4.56
4	53.3	-	53.1	-
5	52.2	2.22	52.4	2.19
6	21.2	1.80, 1.86	20.1	1.90, 2.08
7	33.7	1.02, 1.21	33.9	1.00, 1.19
8	40.9	-	41.2	-
9	49.1	2.27	49.3	2.23
10	36.6	-	36.8	-
11	23.4	nd	23.4	nd
12	127.4	5.80 (br t, 3.0)	127.3	5.73 (br t, 3.0)
13	139.2	-	139.5	-
14	47.8	-	48.0	-
15	24.0	1.70, 2.06	23.0	1.90, 2.10
16	23.5	nd	23.5	nd
17	47.0	-	46.9	-
18	41.6	3.15 (dd, 13.6, 3.1)	41.8	3.11 (dd, 13.5, 3.0)
19	45.2	1.26, 1.69	45.2	1.22, 1.65
20	30.5	-	30.6	-
21	33.5	1.84, 2.25	33.9	2.17, nd
22	32.1	1.73, 1.88	nd	nd
23	184.8		185.0	
24	14.8	1.87 (s)	14.6	1.82 (s)
25	17.2	1.43 (s)	17.4	1.39 (s)
26	18.4	1.03 (s)	19.0	0.96 (s)
27	64.1	3.84, 4.10	64.1	3.77, 4.08
28	176.5		176.5	
29	32.8	0.78 (s)	33.1	0.75 (s)
30	23.5	0.81 (s)	23.4	0.77 (s)

Nd : Not determined

Table 11. ^{13}C NMR and ^1H NMR data of the sugar moieties and the 3,4-dimethoxycinnamoyl group of compounds **15** and **16** in Pyridine- d_5 /D $_2$ O (δ ppm, J in Hz)

Position	15		16	
	δ_{C}	δ_{H}	δ_{C}	δ_{H}
Glc-1	104.5	5.04 (d, $J = 7.0$)	104.3	4.99 (d, $J = 7.2$)
2	76.0	3.93	74.8	3.87
3	77.3	4.24	76.9	4.19
4	71.1	4.04	70.9	3.98
5	77.7	3.91 m	77.1	3.86 m
6	62.2	4.16, 4.36	61.9	4.12, 4.34
Fuc-1	94.2	6.06 (d, $J = 8.1$)	93.9	6.02 (d, $J = 8.1$)
2	74.5	4.71 (dd, $J = 8.8, 8.1$)	74.0	4.66 (dd, $J = 8.8, 8.1$)
3	76.3	5.54	74.1	4.42
4	72.3	5.52	74.7	5.68
5	70.3	4.17	70.5	4.11
6	15.9	1.14 (d, $J = 6.4$)	16.3	1.26 (d, $J = 6.2$)
Ac at Fuc-3	171.1			
	20.3	2.06 (s)		
Ac at Fuc-4	170.4			
	20.5	2.10 (s)		
Rha-1	102.0	6.40 (br s)	101.4	6.35 (br s)
2	71.2	4.79 (br s)	71.2	4.73 (br s)
3	72.3	4.58	72.3	4.58
4	86.2	4.21	85.1	4.15
5	68.0	4.47	67.8	4.30
6	18.4	1.73 (d, $J = 5.9$)	18.4	1.65 (d, $J = 5.7$)
Xyl-1	106.9	4.84 (d, $J = 7.0$)	106.7	4.80 (d, $J = 7.0$)
2	75.5	4.04	75.3	3.97
3	76.9	4.09	76.4	4.02
4	77.2	4.36	76.7	4.30
5	64.7	3.42 (t, $J = 8.2$), 4.34	64.5	3.37 (t, $J = 8.8$), 4.30
Gal-1	103.9	4.93 (d, $J = 7.6$)	103.7	4.89 (d, $J = 7.1$)
2	71.2	4.44	70.9	4.40
3	75.0	4.10	74.4	4.05
4	69.9	4.32	69.8	4.27
5	76.0	4.01 m	76.4	4.02
6	62.2	4.18, 4.42	61.9	4.12, 4.36
3,4-dimethoxycinnamoyl				
C(α)			167.6	
CH(β)			115.6	6.53 (d, $J=16.0$)

CH(γ)	146.0	7.88 (d, $J=16.0$)
C(1)	127.3	
CH(2)	110.6	7.04 (s)
C(3)	149.0	
C(4)	151.8	
CH(5)	111.7	6.93 (d, $J=8.3$)
CH(6)	123.1	7.03 (d, $J=8.3$)
MeO-C(3)	55.6	3.76 (s)
MeO-C(4)	55.6	3.78 (s)

Nd : Not determined

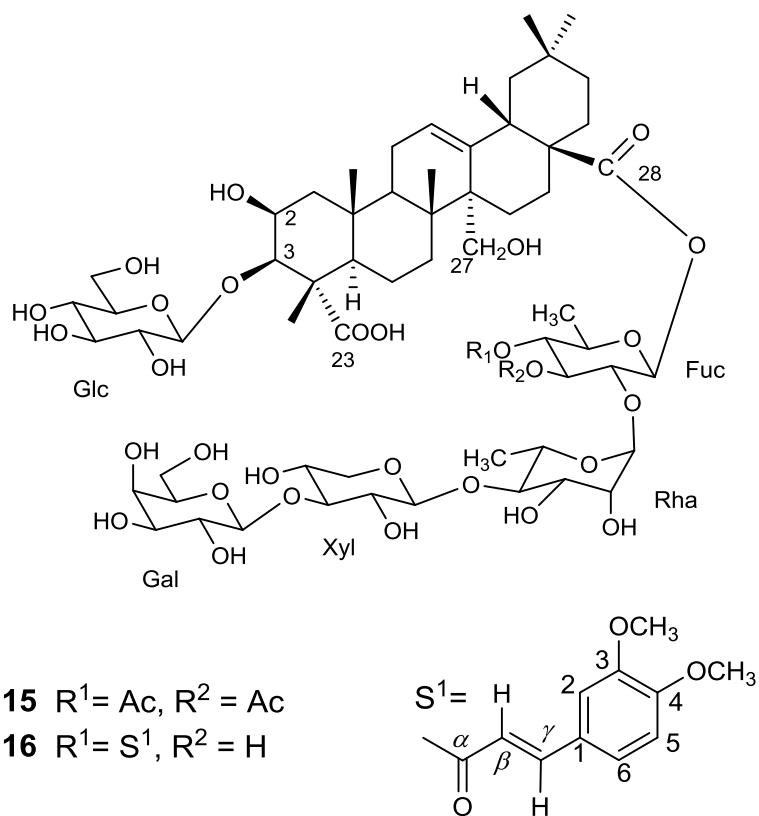


Figure 62: Structure of saponins **15** and **16**

CHAPTER 3:

Peptide and glycopeptide synthesis and immunoenzymatic assays

Chapter 3: Peptide and glycopeptide synthesis and immunoenzymatic assays

3.1 Material and methods

3.1.1 Peptide and glycopeptide synthesis

The N-glucosylated peptide CSF114(Glc) and its unglucosylated analog were prepared by a microwave-assisted solid-phase peptide synthesis. Peptides were purified by solid-phase extraction and high pressure liquid chromatography (HPLC) and further characterized by mass spectrometry and analytical HPLC.

3.1.2 Ursolic acid

Ursolic acid $\geq 90\%$, a triterpenic acid was purchased to Sigma Aldrich (Figure 63).

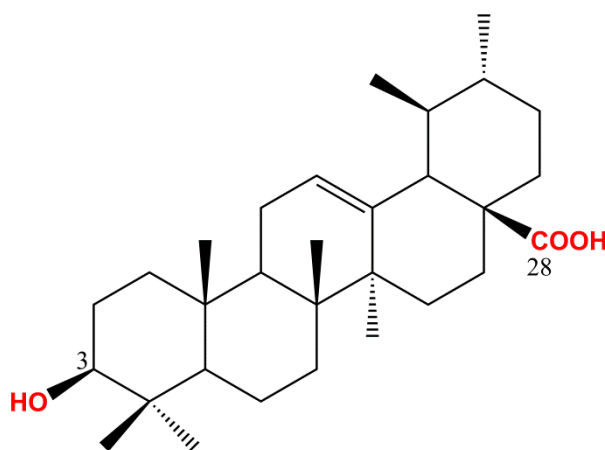


Figure 63: Structure of ursolic acid (17)

3.1.3 Prosapogenin tenuifolin obtained by mild alkaline hydrolysis

A crude saponin extract from *Polygala acicularis* (15mg) was refluxed with 5% aqueous KOH solution (50ml) for 2h. The mixture was adjusted to pH 7 with diluted HCl solution and then extracted with H₂O-saturated BuOH (3x50ml). The combined BuOH extracts were washed with H₂O and concentrated to dryness to obtain the prosapogenin named tenuifolin (Figure 64).

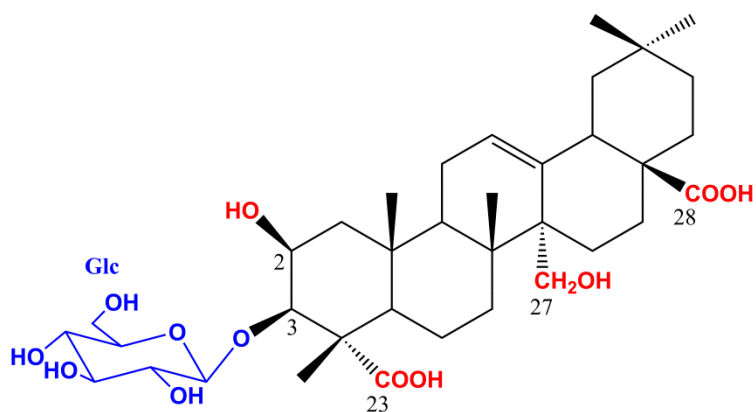


Figure 64: Structure of prosapogenin tenuifolin (**18**)

3.1.4 Extraction of rutoside from *Sophora japonica*

Sophora japonica L. is a majestic Chinese tree from the Fabaceae family (Figure 65). It can measure until 25 meter and it is used as ornamental tree in European gardens. In the past, Chinese people used flower buds to dye the silk in yellow and now flower buds are extracted because they contain around 15-20% of a flavonoid glycoside, named rutoside or rutin. This flavonoid is a quercetin diglycoside, which possess interesting pharmacological properties (Figure 66) [80-82].



Figure 65: *Sophora japonica*

<http://mon-herbier.teznet.fr/planches/DP0208>

The protocol used to obtain rutoside from the flower buds of *Sophora japonica* was described in the literature [80]. 10 g of dried flower buds were crushed and mixed with 100 ml of methanol. The mixture was either refluxed during 1h, then it was filtered and the solvent removed. The dry residue was dissolved in water to convert it into the hydrated form, which precipitates from solution. The mixture was extracted with diethylether to remove chlorophyll and the precipitate in the aqueous phase was collected by vacuum filtration and dried in an oven at 70°C.

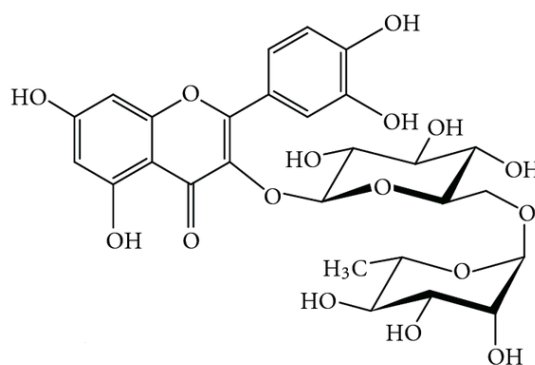


Figure 66: Structure of rutoside (19)

3.1.5 Peptide synthesis

Sequence CSF114:

Thr-Pro-Arg-Val-Glu-Arg-Asn-Gly-His-Ser-Val-Phe-Tyr-Gly-Trp-Met-Val-Lys

The resin is swollen for 30 min with DMF (2 mL/100 mg of resin) before use. Each amino-acid cycle is characterized by the following four steps:

First Fmoc-deprotection: Resin is stirred (1 × 5 min) with a solution of 20% piperidine in DMF (1 mL/100 mg of resin). Washing: DMF (2 × 3 min).

Second Fmoc-deprotection: Resin is stirred (1 × 15 min) with a solution of 20% piperidine in DMF (1 mL/100 mg of resin). Washing: DMF (2 × 3 min), DCM (2 x 3min), DMF (1 x 3min).

Coupling reaction: Fmoc-protected amino acids (5 eq), TBTU (5 eq) and DIPEA (74μL) were dissolved in DMF with a final dilution of 1 mL DMF for 100 mg of resin. Couplings were performed for 30 min at room temperature. Washing: DMF (2 × 3 min) and DCM (2 × 3 min). After DCM washing each coupling reaction is monitored by Kaiser test. After the last Fmoc-removal the resin is washed with DCM and dried under vacuum.

Kaiser test:

To a small amount of peptide-resin placed in a test tube, three drops for each of the following solutions were added: ninhydrine (5 g) in ethanol (100 mL); phenol (80 g) in ethanol (20 mL); KCN (2 mL of 1 mM aqueous solution) in pyridine (98 mL). The tube is heated at 100 °C for 5 min. A positive test (resin beads and solution appears strongly blue-violet) states the presence of at least 5% free amino groups.

Cleavage:

Cleavages from the resin and side chain deprotection were performed using a cleavage mixture depending on the sequence and modified amino acids introduced, as indicated for each compound. The peptide-resin is treated for 3 h with cleavage mixture (1 mL × 100 mg of resin) at room temperature. The resin is filtered off and the solution is concentrated flushing with N₂. The peptide is precipitated from cold diethylether, centrifuged and lyophilized.

Purification:

Peptides are purified by Spot Liquid Chromatography Flash (SLCF) to remove salts and impurities. It is performed on RP-C18 LiChroprep columns on an automatic Armen Instrument. Fractions are checked by analytical RP-HPLC ESI-MS or RP-UPLC ESI-MS, product-containing homogeneous ones are pooled together. All peptides are further purified by semi-preparative RP-HPLC. All the peptides were obtained with a purity $\geq 95\%$ to be used for autoantibody detection.

Sequence CSF114(Glc) :

Thr-Pro-Arg-Val-Glu-Arg-Asn(Glc)-Gly-His-Ser-Val-Phe-Tyr-Gly-Trp-Met-Val-Lys

The protocol is the same as the unglucosylated sequence except for the addition of asparagine glucosylated. The modified amino acid Fmoc-Asn[Glc(OAc)₄] is manually introduced. Couplings are performed with an excess of 2.5 eq of modified amino acid, 2.5 eq of HATU as activator, and 3.5 eq of DIPEA, for 1 hour at room temperature. Deprotection of the hydroxyl functions of sugar moieties linked to the N-glycosylated peptides was performed in basic conditions (pH 11-12) using a fresh sodium methanolate solution.

Purification was performed by Spot Liquid Chromatography Flash (SLCF) to remove salts and impurities. It is performed on RP-C18 LiChroprep columns on an automatic Armen Instrument. Fractions are checked by analytical RP-HPLC ESI-MS or RP-UPLC ESI-

MS, product-containing homogeneous ones are pooled together. Peptide is further purified by semi-preparative RP-HPLC. CFS114(Glc) with a purity $\geq 95\%$ was used for autoantibody detection.

3.1.6 Immunoenzymatic assays with CSF114(Glc) and its unglucosylated analog

The peptide was coated on 96-well activated polystyrene ELISA plates (NUNC Maxisorb) using a solution 10 $\mu\text{l/ml}$ in pure carbonate buffer 0.05 M at pH 9.6 (100 $\mu\text{l/well}$) and incubated at $+4^\circ\text{C}$ overnight. After three washes with 150 mM NaCl solution containing 0.05% Tween 20 (washing buffer), non-specific binding sites were blocked with 10% fetal bovine serum (FBS) in washing buffer (100 $\mu\text{l/well}$) at room temperature for 60 min. Sera diluted 1:100 in 10% FBS in washing buffer were incubated at $+4^\circ\text{C}$ overnight. After three washes, 100 μl of alkaline phosphatase conjugated with anti-human IgM (diluted 1:1200 in 10% FBS in washing buffer) were added to each well. After 3h incubation at room temperature and three washes, 100 $\mu\text{l/well}$ of 1 $\text{mg}\cdot\text{ml}^{-1}$ p-nitrophenylphosphate (Sigma-Aldrich) in carbonate buffer (pH 9.6) was added. After 30min, the reaction was stopped with 1 M NaOH (50 $\mu\text{l/well}$), and the absorbance was read in a multichannel ELISA reader (Tecan Sunrise, Männedorf, Switzerland) at 405 nm. ELISA plates, coating conditions, reagent dilutions, buffers, and incubation times were preliminary tested. Antibody levels are expressed as absorbance in arbitrary units at 405 nm (sample dilution 1:100).

3.1.7 Immunoenzymatic assays of saponins, rutoside and ursolic acid

Saponins, rutoside and ursolic acid were coated on 96-well microplates BD FalconTM separately using a solution 10 $\mu\text{g/ml}$ in pure ethanol (100 $\mu\text{l/well}$). The plates were then incubated at $+4^\circ\text{C}$ overnight. The non-specific binding sites were blocked with 10% fetal bovine serum (FBS) in 150 mM NaCl solution without surfactant at room temperature for 60 min. Sera diluted 1:100 in 10% FBS in 150 mM NaCl were incubated at $+4^\circ\text{C}$ overnight (100 $\mu\text{L/well}$). After three washes, 100 μl of alkaline phosphatase conjugated anti-human IgM (Invitrogen) (diluted 1:1500 in 10% FBS washing buffer) were added to each well. After 3h incubation at room temperature and three washes, 100 $\mu\text{l/well}$ of 1 $\text{mg}\cdot\text{ml}^{-1}$ p-nitrophenyl phosphate (Sigma-Aldrich) in carbonate buffer (pH 9.6) with 10 mM MgCl_2 solution was added. After 30min, the reaction was stopped with 1M NaOH (50 $\mu\text{l/well}$), and the absorbance was read in a multichannel ELISA reader (Tecan Sunrise, Männedorf, Switzerland) at 405 nm. ELISA plates, coating conditions, reagent dilutions, buffers, and incubation times were

preliminary tested. Antibody levels are expressed as absorbance in arbitrary units at 405 nm (sample dilution 1:100).

3.1.8 Statistical analysis

Statistical analysis was performed using GraphPad prism 6. Mann-Whitney tests were used to evaluate the predictive antibody values; two-tailed p-values and receiver operating characteristic (ROC) curves were calculated. Cut-off values were established.

3.2 Personal works

3.2.1 Selection of molecules

The aim of this PhD thesis was the selection of natural glycosides with different structures, bearing different glycosyl moieties and aglycones. Their immunochemical characterization in MS and RTT patient sera was thus performed.

For our study, eight glycosides (**4**, **8**, **13**, **14**, **16**, **17**, **18** and **19**) were chosen to perform immunoenzymatic assays in order to measure IgM level in MS patients' and RTT patients' sera to try to establish structure / activity relationships. Compounds were selected according to their structure, seven from natural source (**4**, **8**, **13**, **14**, **16**, **18** and **19**) and one commercial, ursolic acid (**17**). The obtained results with these molecules were compared to the synthetic peptide CSF114 (Glc), which has already shown its efficiency in the recognition of IgM in patients affected by Multiple Sclerosis and Rett syndrome.

- Compounds **4** and **8** (Figure 67), monodesmosidic glycosides, possess the same oligosaccharidic chains at the C-3 position, as 3-*O*- α -L-rhamnopyranosyl-(1 \rightarrow 2)- β -D-xylopyranosyl-(1 \rightarrow 2)- β -D-glucuronopyranosyl. But their aglycons are different: compound **8** has a primary alcoholic function at C-23, one acetyl group at C-22, and one carboxylic group at C-30, while **4** has two primary alcoholic functions at C-23 and C-30, and a rare ketone group at C-22.

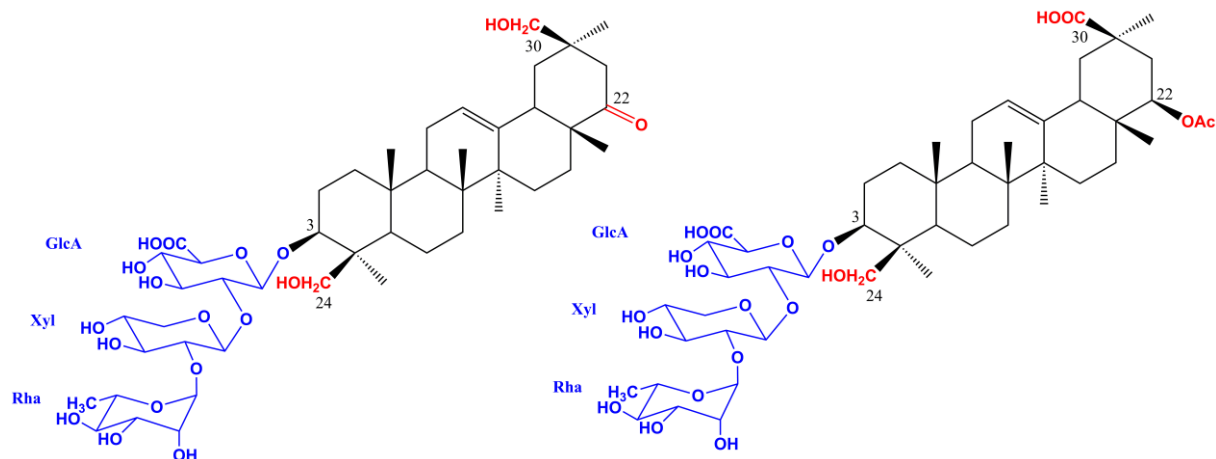


Figure 67: Structure of saponins **4** and **8**

- Compounds **13** and **14** (Figure 68), monodesmosidic, have the same aglycone, oleanolic acid, but they differ by the structure, and so by the length, of the oligosaccharidic chain at C-3: 3-*O*- β -D-xylopyranosyl-(1 \rightarrow 3)- α -L-rhamnopyranosyl-(1 \rightarrow 2)- α -L-arabinopyranosyl for **14**, and 3-*O*- β -D-xylopyranosyl-(1 \rightarrow 2)-[β -D-glucopyranosyl-(1 \rightarrow 4)]- β -D-xylopyranosyl-(1 \rightarrow 4)- β -D-xylopyranosyl-(1 \rightarrow 3)- α -L-rhamnopyranosyl-(1 \rightarrow 2)- α -L-arabinopyranosyloleanolic acid for **13**.

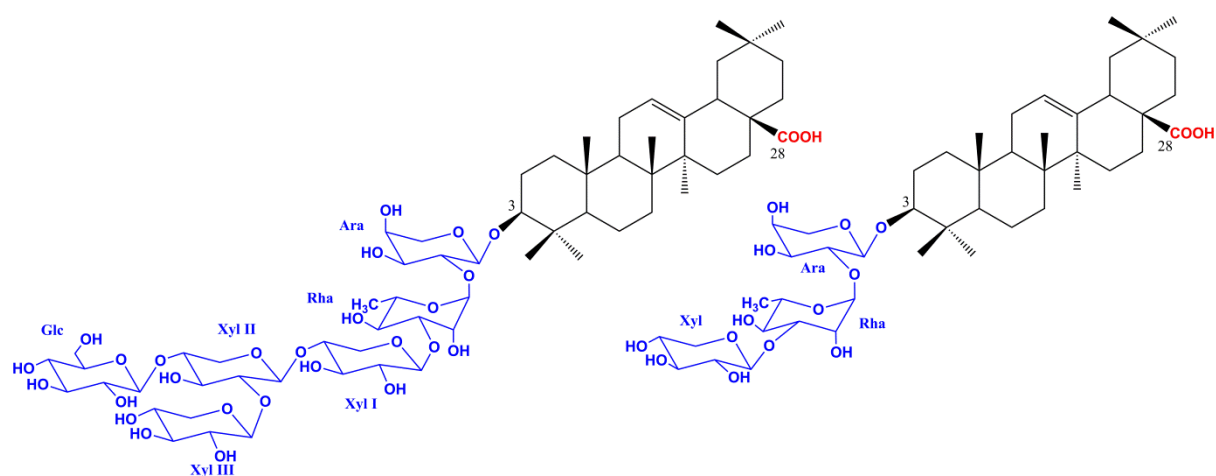


Figure 68: Structure of saponins **13** and **14**

- Compound **16** is a bidesmosidic saponin (Figure 69), with a *O*-heterosidic linkage at C-3 with a 3-*O*- β -D-glucopyranosyl moiety and an ester linkage at C-28 with the oligosaccharidic chain β -D-galactopyranosyl-(1 \rightarrow 3)- β -D-xylopyranosyl-(1 \rightarrow 4)- α -L-rhamnopyranosyl-(1 \rightarrow 2)-[4-*O*-(*E*)-3,4-dimethoxycinnamoyl]- β -D-fucopyranosyl. The acylation with a 3,4-dimethoxycinnamoyl moiety is often encountered in the Polygalaceae

family. The aglycone, the presenegenin, possesses many free oxygenated groups which is not so usual: two secondary alcoholic functions at C-2 and C-3 positions, one primary alcoholic function at C-27, and two carboxylic functions at C-23 and C-28.

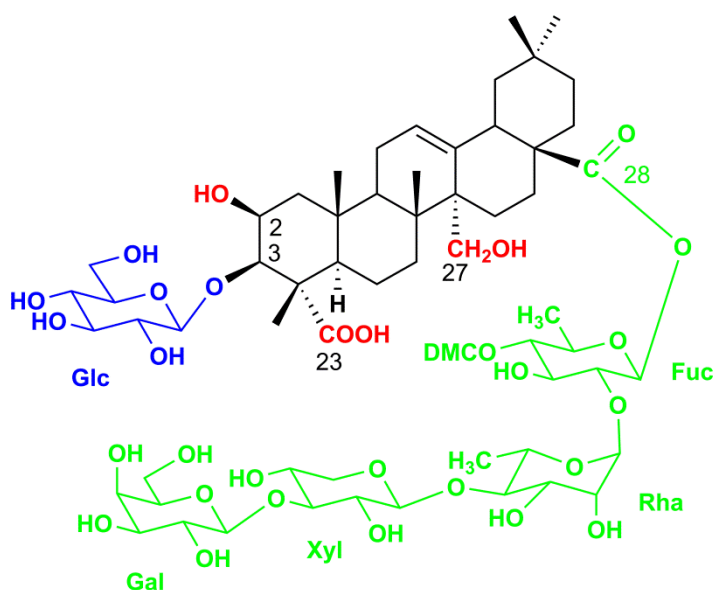


Figure 69: Structure of saponin 16

- Compound 18 (figure 70), a monodesmosidic saponin, was chosen because of the only one β -D-glucopyranosyl moiety linked at C-3 position (tenuifolin).

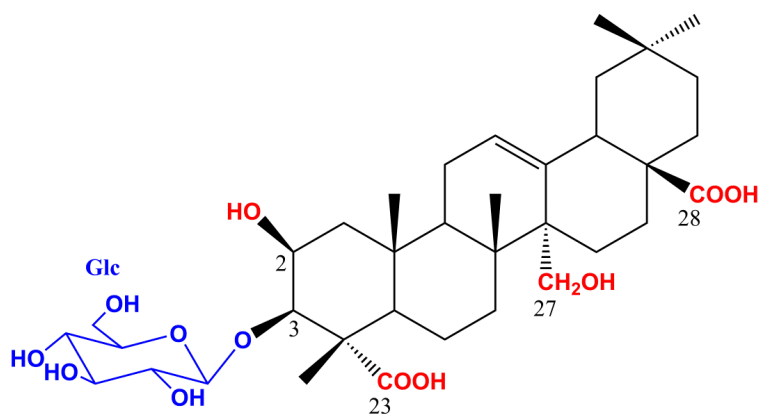


Figure 70: Structure of saponin 18

- An aglycon was chosen, a commercial triterpenic acid, ursolic acid (**17**), as a negative control for the immunoenzymatic assays because of the lack of osidic part in the molecule (Figure 71).

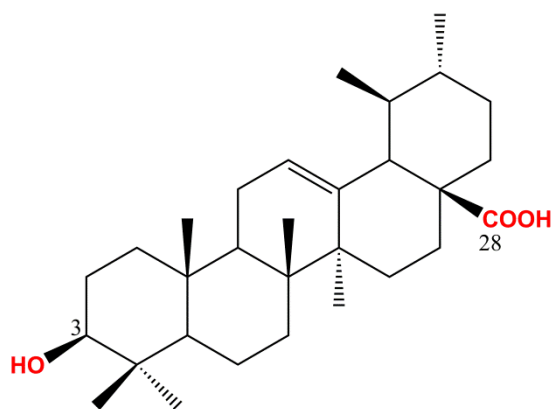


Figure 71: Structure of the ursolic acid (**17**)

- Finally, a flavonoid glycoside, rutoside (**18**) was tested to see if the triterpenic nature of the aglycon could play a key role in the assays (Figure 72).

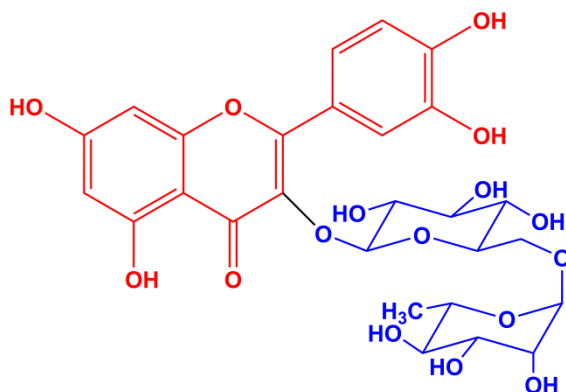


Figure 72: Structure of the rutoside (**19**)

All these eight compounds were tested as mimetics of native antigens to detect an immune response performing ELISA tests to measure IgM levels in MS patient and RTT patient sera and normal blood donors. The synthetic N-glycosylated peptide, CSF114(Glc) was used as positive control for the recognition of IgMs in Multiple Sclerosis and Rett syndrome.

3.2.2 Immunoenzymatic assays on multiple sclerosis patient sera

3.2.2.1 Selection of Multiple Sclerosis sera

Sera from 19 Multiple Sclerosis patients collected at diagnosis and 11 healthy blood donors were obtained for diagnostic purposes and stored at -20°C until use. Multiple Sclerosis (MS) patient sera samples were collected in two Multiple Sclerosis Centers: The Multiple Sclerosis Clinical Care and Research Centre, Department of Neurosciences, Reproductive Sciences and Odontostomatology, Federico II University (Naples, Italy) and the Azienda Ospedaliera Universitaria Careggi, Clinica Neurologica, University of Florence (Florence, Italy). All patients and healthy donors gave their informed consent. Multiple Sclerosis patients were previously diagnosed after a lumbar puncture, MRI examination, and cerebrospinal analysis. Samples were pre-selected depending on their reactivity to CSF114(Glc). Antibody responses were determined in SP-ELISA.

3.2.2.2 SP-ELISA results

Below are shown the results of ELISA. Experiments were carried out as described in the Experimental part. The sera were used in triplicate with a dilution of 1:100. Data distribution of IgM antibodies responses to compounds **4**, **8**, **13**, **14**, **16**, **17**, **18** and **19** in the sera of MS patients and normal blood donors (NBDs) determined by ELISA will be presented:

Saponins **4** and **8** which are monodesmosidic ones with the same oligosaccharidic chain and a different aglycone demonstrate a difference in the recognition of IgM in MS patients. Indeed, Mann-Whitney tests were used to evaluate the predictive IgM antibody values and p values of 0.0202 and 0.0052 were found respectively. In this case, the results (Figure 73) are not relevant but the different functions on the aglycone could also be responsible of IgM recognition.

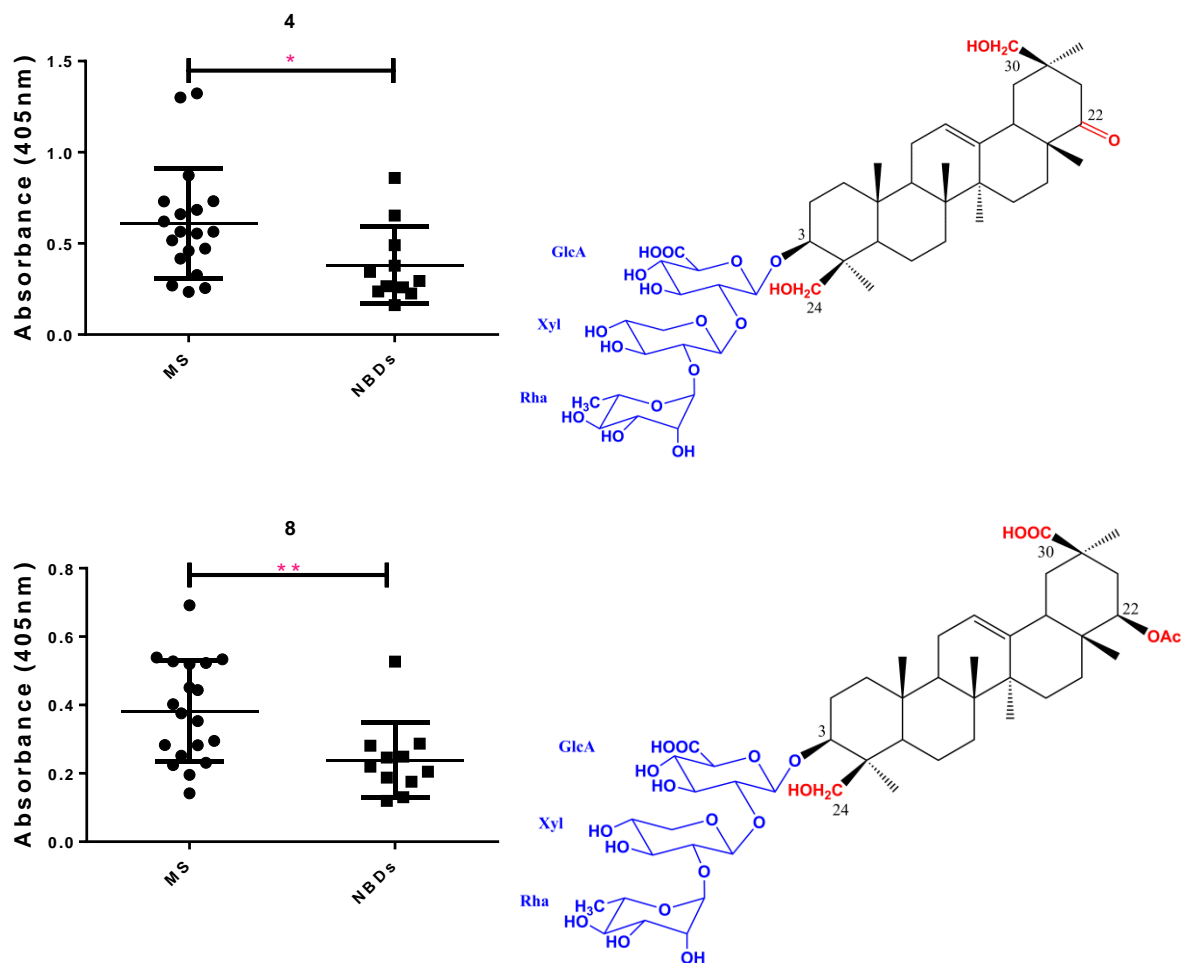


Figure 73: Data distribution of IgM antibody response to saponins **4** and **8** in MS sera and NBDs determined by ELISA. Data are reported as absorbance at 405nm of sera diluted 1:100. Statistical analysis was performed using Graph prism 6 software. Mann-Whitney tests were used to evaluate the predictive antibody values and two-tailed p values were calculated (P value < 0.001=****, P value > 0.001=**, P value >0.01=*)

Concerning saponins **13** and **14** which are monodesmosidic saponins with the same aglycone and an oligosaccharidic chain of different length, no significant results were obtained (Figure 74). It appears that these saponins are not able to recognize IgMs in MS sera.

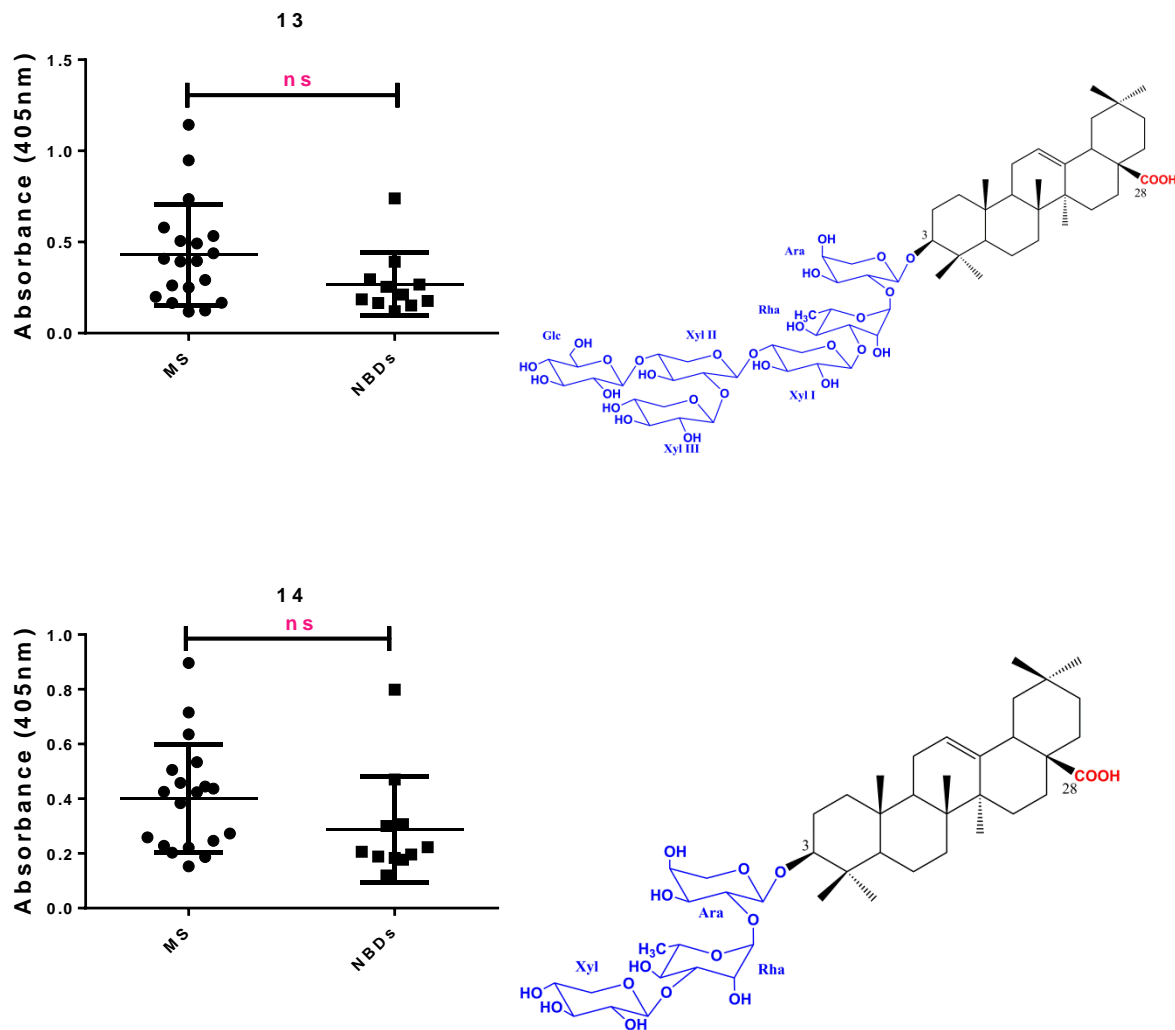


Figure 74: Data distribution of IgM antibody responses to saponin **13** and **14** in MS sera and NBDs determined by ELISA. Data are reported as absorbance at 405nm of sera diluted 1:100. Statistical analysis was performed using Graph prism 6 software. Mann-Whitney tests were used to evaluate the predictive antibody values and two-tailed p values were calculated (P value < 0.001=****, P value > 0.001=**, P value >0.01=*)

The bidesmosidic saponin **16** shows a small difference in detecting Abs in MS sera compared to NBDs with a p value of 0.0138 (Figure 75). It appears that this glycoside is not able to recognize IgM in MS sera; the results are not significant and are in agreement with previous data obtained by Peroni et al, 2016 [33] where similar compounds were tested as putative antigens for MS.

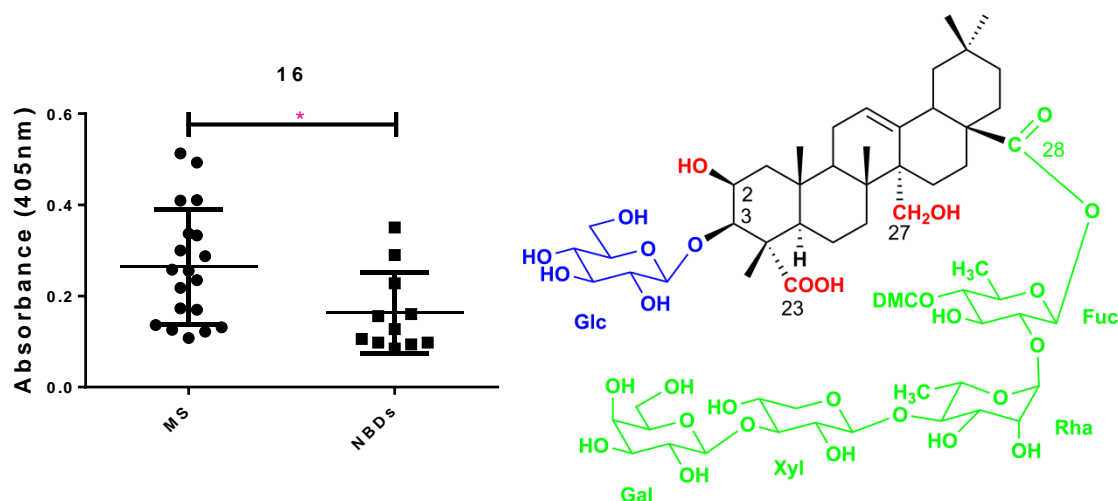


Figure 75: Data distribution of IgM antibody responses to saponin **16** in MS sera and NBDs determined by ELISA. Data are reported as absorbance at 405nm of sera diluted 1:100. Statistical analysis was performed using Graph prism 6 software. Mann-Whitney tests were used to evaluate the predictive antibody values and two-tailed p values were calculated (P value < 0.001=****, P value > 0.001=**, P value >0.01=*)

The triterpenic acid **17** which has no sugars was tested for the recognition of IgMs in MS sera. No relevant results were obtained (Figure 76). These data are in agreement with the relevant role of the glycosyl moiety for IgM recognition [33].

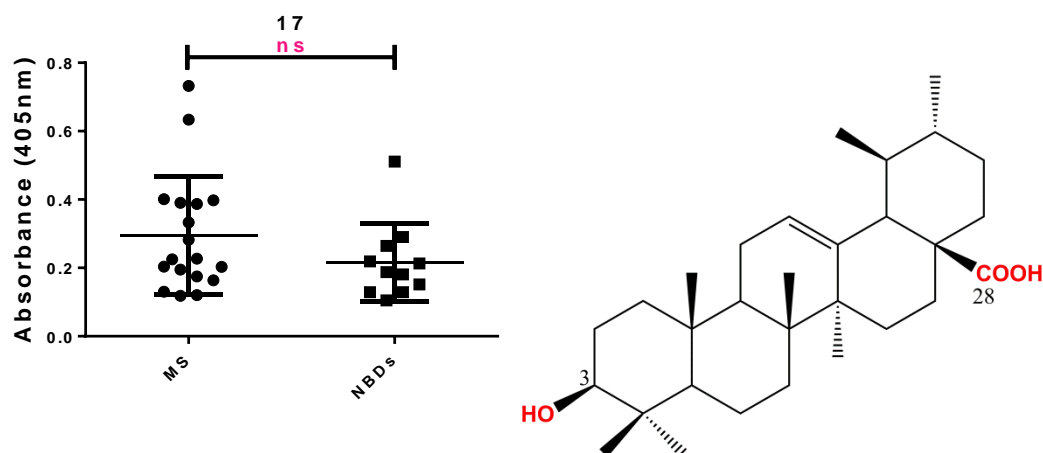


Figure 76: Data distribution of IgM antibody responses to ursolic acid **17** in MS sera and NBDs determined by ELISA. Data are reported as absorbance at 405nm of sera diluted 1:100. Statistical analysis was performed using Graph prism 6 software. Mann-Whitney tests were used to evaluate the predictive antibody values and two-tailed p values were calculated (P value < 0.001=****, P value > 0.001=**, P value >0.01=*)

Saponin **18** which has only one glucose moiety linked in C-3 position and different functions on the aglycone demonstrated a p value of 0.0061 (Figure 77). This compound is able to recognize IgMs in MS sera but the results are not statistically relevant according to the p value.

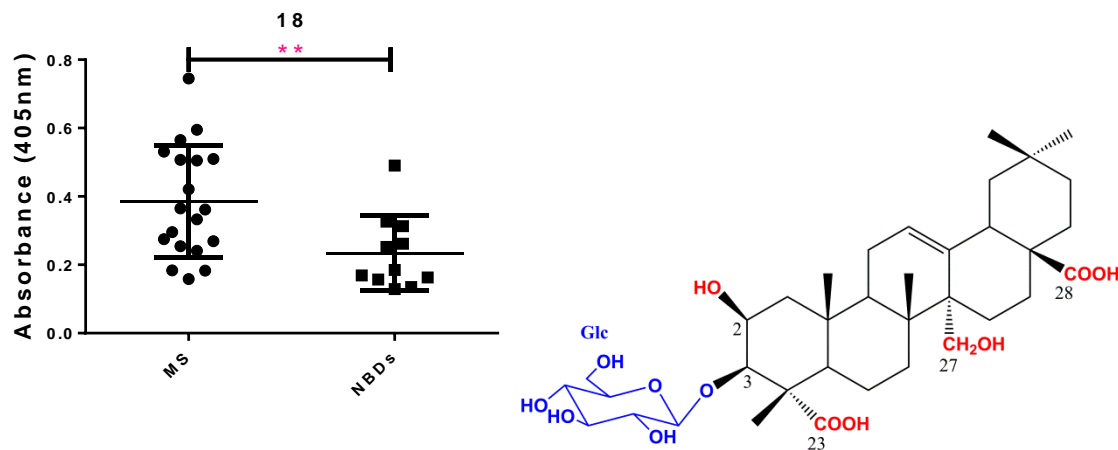


Figure 77: Data distribution of IgM antibody responses to saponin **18** in MS sera and NBDs determined by ELISA. Data are reported as absorbance at 405nm of sera diluted 1:100. Statistical analysis was performed using Graph prism 6 software. Mann-Whitney tests were used to evaluate the predictive antibody values and two-tailed p values were calculated (P value < 0.001=****, P value > 0.001=**, P value >0.01=*)

The only flavonoid glycoside **19** available was also tested. According to its structure, no significant results were obtained (Figure 78). In this case, we can hypothesize that the flavonoid-type aglycone may not allow the sugars to be exposed for the recognition.

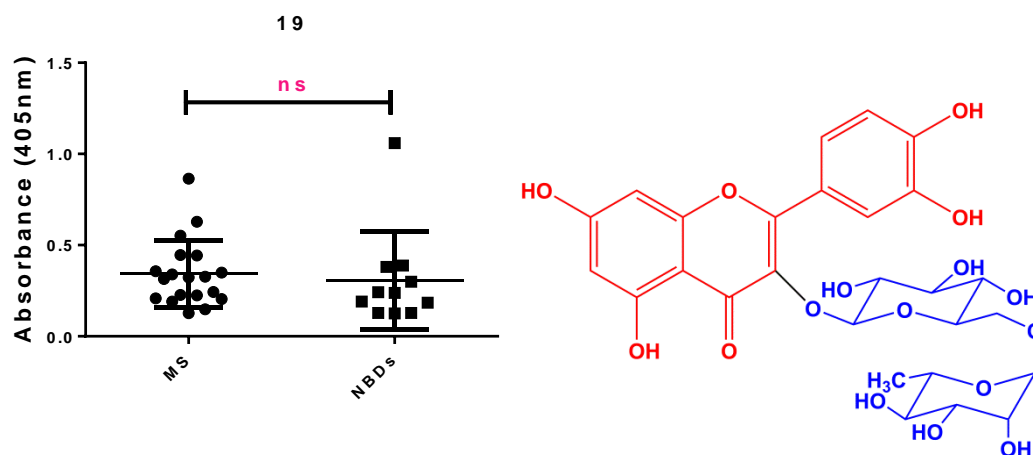


Figure 78: Data distribution of IgM antibody responses to rutoside **19** in MS sera and NBDs determined by ELISA. Data are reported as absorbance at 405nm of sera diluted 1:100. Statistical analysis was performed using Graph prism 6 software. Mann-Whitney tests were used to evaluate the predictive antibody values and two-tailed p values were calculated (P value < 0.001=****, P value > 0.001=**, P value >0.01=*)

We investigated a possible interaction between some of the natural isolated compounds and IgM antibodies in MS sera. According to these results, we can conclude that some saponins (**4**, **8**, **16** and **18**) are able to recognize IgMs in MS patients but the results are not statistically relevant compared to the synthetic peptide probe CSF114(Glc). Till now, the number of tested molecules is not sufficient but this study demonstrates the potential role of

natural compounds as mimetics of native antigens as previously hypothesized [33]. Further studies could be performed with new molecules in order to perform a statistically relevant structure/activity relationship study between IgMs and natural saponins isolated from plants. According to previous study, the glucosidic moiety, when present in the isolated compounds and not masked by the aglycone part, is fundamental for IgM recognition in Multiple Sclerosis.

3.2.3 Immunoenzymatic assays on Rett syndrome patient sera

3.2.3.1 Selection of Rett syndrome sera

Sera from 39 RTT patients collected at diagnosis and 22 healthy blood donors were obtained for diagnostic purposes and stored at -20°C until use. All patients and healthy donors gave their informed consent. RTT patients were previously diagnosed. Samples were pre-selected depending on their reactivity to CSF114(Glc). Antibody responses were determined in SP-ELISA.

3.2.3.2 SP-ELISA results

First of all, 19 RTT sera and 11 healthy blood donors were selected for our study. Samples were pre-selected depending on their reactivity to CSF114(Glc). Antibody responses were determined by ELISA and relevant results were obtained. Each compound interacted with IgMs but with different statistical significance. Therefore, we increased the number of RTT sera and healthy blood donors. Besides, samples were chosen depending on their reactivity to CSF114(Glc).

Below are shown only ELISA results obtained with 39 RTT sera and 22 normal blood donors. Experiments were carried out as described in the Experimental part. The sera were used in triplicate with a dilution of 1:100. Data distribution of IgM antibody responses to compounds **4**, **8**, **13**, **14**, **16**, **17**, **18** and **19** in the sera of RTT patients and normal blood donors (NBDs) determined by ELISA are herein presented:

Column scatter of data reported in Figure 79 serological results obtained in ELISA for all the compounds analyzed. All compounds presented lower mean values for NBDs than for RTT populations. These results highlighted the potential role of natural isolated compounds and ursolic acid **17** as mimetics of native antigens for specific RTT IgM antibody recognition. Two compounds (**8** and **17**) presented a similar performance as the glucopeptide CSF114(Glc) with significant differences between patients and controls (Mann-Whitney test, p value < 0.001).

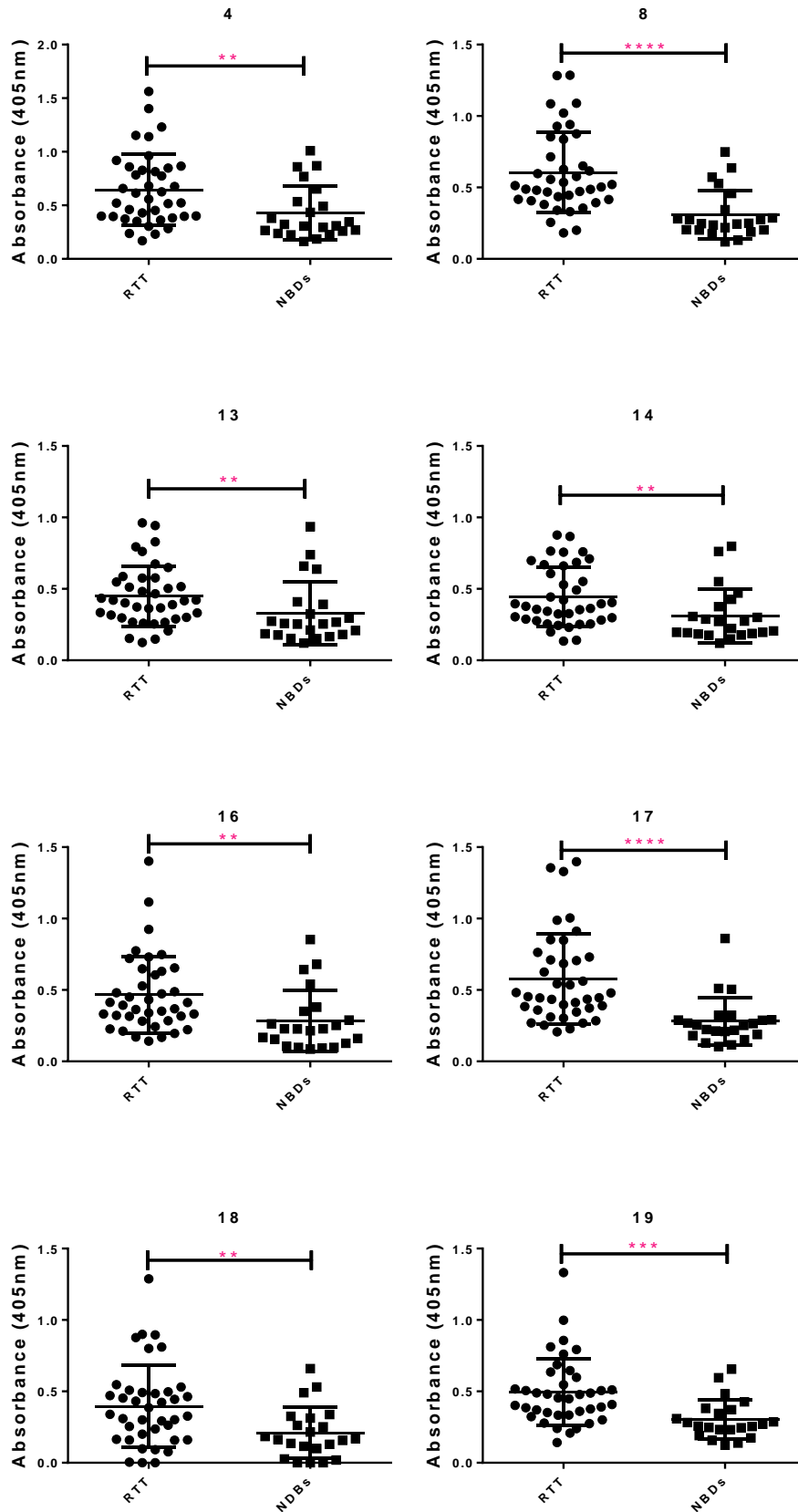


Figure 79: Data distribution of IgM antibody responses to compounds 4, 8, 13, 14, 16, 17, 18 and 19 in RTT sera and NBDs determined by ELISA. Data are reported as absorbance at 405nm of sera diluted 1:100. Statistical analysis was performed using Graph prism 6 software. Mann-Whitney tests were used to evaluate the predictive antibody values and two-tailed p values were calculated (P value < 0.001=****, P value > 0.001=**)

The receiver operating characteristic (ROC) analysis was employed to compare the discrimination power of the compounds, and the different cutoff values, sensitivity, specificity, and likelihood ratios were also calculated. Selected cutoff values, sensitivities and the rest of the other statistical parameters are summarized in Table 12.

Table 12. Values obtained from ROC analysis of glycosides **4**, **8**, **13**, **14**, **16**, **18** and **19** and ursolic acid **17** for the area under the curve (AUC), standard error (SE), the confidence interval (CI), p value, established cutoff, and the corresponding sensitivity, specificity and likelihood ratio.

Compound	AUC	SE	95% confidence interval	P value	Cutoff	Sensitivity (%)	Specificity (%)	Likelihood ratio
4	0.720	0.07	0.58-0.86	0.0044	>0.924	15.38	95.45	3.38
8	0.828	0.05	0.71-0.94	<0.0001	>0.649	28.21	95.45	6.20
13	0.712	0.07	0.56-0.85	0.0062	>0.766	10.26	95.45	2.25
14	0.717	0.07	0.57-0.86	0.0049	>0.684	17.95	90.91	1.97
16	0.749	0.07	0.61-0.88	0.0013	>0.709	15.38	95.45	3.38
17	0.852	0.05	0.74-0.95	<0.0001	>0.612	33.33	95.45	7.33
18	0.706	0.06	0.57-0.84	0.0077	>0.565	15.38	95.45	3.38
19	0.755	0.06	0.63-0.87	0.0005	>0.579	25.64	88.46	2.22

The characteristics of the curves, their shape and their underlying area provide evidence that the natural isolated glycosides and ursolic acid **17** are able to recognize RTT patients. The obtained values for glycosides **4**, **13**, **14**, **16**, **18** and **19** are in any case lower than those obtained with the glucopeptide CSF114(Glc) as a synthetic antigenic probe. However our results highlight the role of the N-glycosyl moiety in the antibody recognition. The diagnostic power of saponin **8** and ursolic **17** are higher than those presented by natural glycosides **4**, **13**, **14**, **16**, **18** and **19** and similar to the N-glycosylated peptide CFS114(Glc).

Moreover, we investigated the correlation between natural compounds and ursolic acid structures and their immunological reactivities with the CSF114(Glc) structure.

According to previous studies on CSF114(Glc) as antigenic probe for MS and RTT disease, our hypothesis is that the glucosyl moiety is involved in the recognition. That is why different natural compounds bearing different glycosyl moieties were tested. We suppose that the last sugar moiety in the oligosaccharidic chain is the most exposed for IgM recognition.

Saponins **4**, **13**, **14** and **18** which are monodesmosidic molecules with different oligosaccharidic chains linked in C-3 position as 3-*O*- α -L-rhamnopyranosyl-(1 \rightarrow 2)- β -D-xylopyranosyl-(1 \rightarrow 2)- β -D-glucuronopyranosyl, 3-*O*- β -D-xylopyranosyl-(1 \rightarrow 2)-[β -D-glucopyranosyl-(1 \rightarrow 4)]- β -D-xylopyranosyl-(1 \rightarrow 4)- β -D-xylopyranosyl-(1 \rightarrow 3)- α -L-rhamnopyranosyl-(1 \rightarrow 2)- α -L-arabinopyranosyloleanolic acid, 3-*O*- β -D-xylopyranosyl-(1 \rightarrow 3)- α -L-rhamnopyranosyl-(1 \rightarrow 2)- α -L-arabinopyranosyl and 3-*O*- β -D-glucopyranosyl respectively, showed similar results in spite of the difference of the sugars. They are able to recognise IgMs but according to their p value results they are not statistically relevant and are not as good as the synthetic probe CSF114(Glc).

The bidesmosidic saponin **16** showed similar results as saponins **4**, **13**, **14** and **18** in spite of its different structure. With this consideration in mind, we can interrogate ourself about the importance of the sugar chain in the recognition.

Moreover, the flavonoid glycoside **19** demonstrated a higher p value than triterpene saponins **4**, **13**, **14**, **16** and **18**. This compound has a different aglycone than saponins and one oligosaccharidic chain as α -L-rhamnopyranosyl-(1 \rightarrow 6)- α -L-glucopyranosyl. According to this result, we cannot explain the part of the molecule involved in the IgM recognition.

Concerning saponin **8** and ursolic acid **17** the results of ELISA are interesting and at the same time surprising. From a structural point of view, saponin **8** has the same oligosaccharidic chain as saponin **4** (3-*O*- α -L-rhamnopyranosyl-(1 \rightarrow 2)- β -D-xylopyranosyl-(1 \rightarrow 2)- β -D-glucuronopyranosyl) but their aglycone part is different: compound **8** has a secondary alcoholic function at C-23, one acetyl group at C-22, and one carboxylic group at C-30, while **4** has two secondary alcoholic functions at C-23 and C-30, and a rare ketone group at C-22. After p value comparison, saponin **8** demonstrated a better efficiency in IgM recognition than saponin **4**. According to these results, we can hypothesize on the possible role of the aglycone part in the recognition or in favouring the coating of the molecule on the ELISA plate and therefore exposure of the sugar moiety. Therefore, the most interesting result is up to now with ursolic acid **17**. This triterpenic acid has no sugars, only one hydroxyl group at C-3 position and one carboxylic group at C-28 position. These results, let us to hypothesize the possible role of the aglycone part in the recognition of IgM antibodies only in the case of RTT syndrome.

We investigated the possible role in antibody recognition of compounds **4, 8, 13, 14, 16, 17, 18** and **19** as mimetic of native antigens in the case of RTT syndrome. After performing immunoenzymatic assays, all the compounds displayed antibody recognition. We can conclude that these types of molecules are good candidates as mimetic antigens. Moreover, even if the number of tested molecules was not statistically significant, we discovered for the first time the possible role of the aglycone part in IgM recognition in Rett. These new results add a new molecule as possible probe to detect IgM antibodies in such complex disease that only recently has been proposed as an immune mediated disease [13]. More compounds without glycosylic part and with different triterpene-type aglycones could be in a near future selected and tested to confirm this hypothesis.

GENERAL CONCLUSION

GENERAL CONCLUSION

Saponins are amphiphilic glycosides, with many in vitro properties in various pharmacological fields. From a structural point of view, natural triterpene glycosides present an incredible variability of their aglycone and most of the time of their glycosyl moieties. According to this variability and previous collaboration, saponins demonstrated a potential role in detection of antibodies in multiple sclerosis. In the context of immune-mediated disease, the use of natural triterpene glycosides as mimetics of native antigens involving an immune response was investigated.

The aim of this PhD was to perform the extraction, purification and structural elucidation of saponins from plants in order to use natural isolated compounds as antigens for specific antibody recognition in some selected autoimmune diseases. The purpose is to find the best molecules, otherwise difficult to be synthesized, to detect new classes of antibodies.

The first chapter, deals with generalities on the immune system, autoimmunity, multiple sclerosis and rett syndrome. Then, a bibliographic study was realized to introduce and explain this research project.

In the second chapter, a bibliographic synthesis on the family and the genus of the studied plants was realized. Then, the personal phytochemical study including techniques, methods and results were presented. This work led to the isolation and purification of sixteen saponins. Their structures were elucidated using a detailed 600 MHz NMR analysis including 1D and 2D NMR (^1H , ^{13}C NMR, COSY, TOCSY, NOESY, HSQC, HMBC) experiments and mass spectrometry. In particular we characterized 3-*O*- α -L-rhamnopyranosyl-(1 \rightarrow 2)- β -D-xylopyranosyl-(1 \rightarrow 2)- β -D-glucuronopyranosyl-22,28-*O*-diacetylolean-12-ene-3 β ,16 β ,22 β ,28-tetrol (1), 3-*O*- α -L-rhamnopyranosyl-(1 \rightarrow 2)- β -D-glucopyranosyl-(1 \rightarrow 2)- β -D-glucuronopyranosyl-22-*O*-acetylolean-12-ene-3 β ,16 β ,22 β ,28-tetrol (2), 3-*O*- α -L-rhamnopyranosyl-(1 \rightarrow 2)- β -D-xylopyranosyl-(1 \rightarrow 2)- β -D-glucuronopyranosyl-22-*O*-acetyl-3 β ,22 β ,24-trihydroxyolean-12-en-30-oic acid (3), 3-*O*- α -L-rhamnopyranosyl-(1 \rightarrow 2)- β -D-xylopyranosyl-(1 \rightarrow 2)- β -D-glucuronopyranosyl wistariasapogenol A (wistariasaponin A) (4), 3-*O*- α -L-rhamnopyranosyl-(1 \rightarrow 2)- β -D-xylopyranosyl-(1 \rightarrow 2)- β -D-glucuronopyranosyl soyasapogenol B (wistariasaponin C) (5), 3-*O*- α -L-rhamnopyranosyl-(1 \rightarrow 2)- β -D-glucopyranosyl-(1 \rightarrow 2)- β -D-glucuronopyranosyl soyasapogenol B (azukisaponin V) (6), 3-*O*- β -D-xylopyranosyl-(1 \rightarrow 2)- β -D-glucuronopyranosyl-22-*O*-acetyl-3 β ,22 β ,24-trihydroxyolean-

12-en-30-oic acid (**7**), 3-*O*- α -L-rhamnopyranosyl-(1 \rightarrow 2)- β -D-xylopyranosyl-(1 \rightarrow 2)- β -D-glucuronopyranosyl-22-*O*-acetyl-3 β ,22 β ,24-trihydroxyolean-12-en-30-oic acid (**8**), 3-*O*- α -L-rhamnopyranosyl-(1 \rightarrow 2)- β -D-xylopyranosyl-(1 \rightarrow 2)- β -D-glucuronopyranosyl-22,28-*O*-diacetylolean-12-ene-3 β ,16 β ,22 β ,28-tetrol (**9**), 3-*O*- α -L-rhamnopyranosyl-(1 \rightarrow 2)- β -D-xylopyranosyl-(1 \rightarrow 2)- β -D-glucuronopyranosyl-olean-12-ene-3 β ,22 β ,24-triol (**10**) (Astragaloside VIII), 3-*O*- α -L-rhamnopyranosyl-(1 \rightarrow 2)- β -D-galactopyranosyl-(1 \rightarrow 2)- β -D-glucuronopyranosyl-22-*O*-acetyl-3 β ,22 β ,24-trihydroxyolean-12-en-30-oic acid (**11**) (Millettiasaponin A), 3-*O*- β -D-xylopyranosyl-(1 \rightarrow 2)-[β -D-xylopyranosyl-(1 \rightarrow 4)]- β -D-xylopyranosyl-(1 \rightarrow 4)- β -D-xylopyranosyl-(1 \rightarrow 3)- α -L-rhamnopyranosyl-(1 \rightarrow 2)- α -L-arabinopyranosyloleanolic acid (**12**), 3-*O*- β -D-xylopyranosyl-(1 \rightarrow 2)-[β -D-glucopyranosyl-(1 \rightarrow 4)]- β -D-xylopyranosyl-(1 \rightarrow 4)- β -D-xylopyranosyl-(1 \rightarrow 3)- α -L-rhamnopyranosyl-(1 \rightarrow 2)- α -L-arabinopyranosyloleanolic acid (**13**), 3-*O*- β -D-xylopyranosyl-(1 \rightarrow 3)- α -L-rhamnopyranosyl-(1 \rightarrow 2)- α -L-arabinopyranosyloleanolic acid (**14**), 3-*O*- β -D-glucopyranosyl-presenegenin-28-*O*- β -D-galactopyranosyl-(1 \rightarrow 3)- β -D-xylopyranosyl-(1 \rightarrow 4)- α -L-rhamnopyranosyl-(1 \rightarrow 2)-(3,4-di-*O*-acetyl)- β -D-fucopyranosyl ester (**15**) and 3-*O*- β -D-glucopyranosyl-presenegenin-28-*O*- β -D-galactopyranosyl-(1 \rightarrow 3)- β -D-xylopyranosyl-(1 \rightarrow 4)- α -L-rhamnopyranosyl-(1 \rightarrow 2)-[4-*O*-(*E*)-3,4-dimethoxycinnamoyl]- β -D-fucopyranosyl ester (**16**).

In the third chapter, eight compounds **4**, **8**, **13**, **14**, **16**, ursolic acid (**17**), tenuifolin (**18**) and rutoside (**19**) were selected for immunoenzymatic assays (ELISA) that were performed on multiple sclerosis and rett syndrome patient sera to detect antibodies. Natural isolated compounds, otherwise very difficult to be synthesized, were used as mimetics of native antigens involved in antibody response. IgM levels were measured in the case of MS and RTT sera and normal blood donors as controls. No relevant results were obtained in the case of MS but this study confirms the relevant role of the glucosyl moiety in antibody recognition in the case of this disease. Concerning Rett syndrome, interesting results were obtained. Each compound is able to recognize IgMs in different proportions. The most relevant results were obtained with compounds **8** and **17**, which differ for the presence or not of sugar moieties. In Rett syndrome, we demonstrated for the first time the new potential role of the aglycone in IgM recognition even if the number of tested molecules was not statistically significant.

In conclusion, isolated saponins from a structural point of view are good candidates as mimetics of native antigens (otherwise difficult to be synthesized) involved in antibody response.

ABBREVIATIONS

Ab	Antibodies
Ac	Acetyl
Ag	Antigen
AID	AutoImmune Disease
APC	Antigen-Presenting Cells
APG	Angiosperm Phylogeny Group
Api	Apiose
Ara	Arabinose
BCR	B Cell Receptor
CC	Column Chromatography
CI	Confidence Interval
CNS	Central Nervous System
COSY	COrelatedSpectroscopY
DEPT	Distortionless Enhancement by Polarization Transfer
DMC	DiMethoxyCinnamoyl
DNA	DesoxyriboNucleic Acid
ELISA	Enzyme-Linked Immunosorbent Assay
ESI	Electrospray Ionization
Fab	Fragment antigen-binding
FBS	Fetal Bovine Serum
Fc	Fragment crystallizable
Fuc	Fucose
Gal	Galactose
GC	Gas Chromatography
Glc	Glucose
GlcA	Glucuronic Acid
HMBC	Heteonuclear Multiple Bond Correlation
HPLC	High Performance Liquid Chromatography
HR-ESI	High Resolution Electropray Ionization
HSQC	Heteonuclear Single Quantum Correlation
HTPLC	High-Performance Thin-Layer Chromatography
IC	Inflammatory Cell

Ig	Immunoglobulin
MBP	Methyl-CpG-Binding Protein
MeCP2	Methyl-CpG-Binding Protein 2
MHC	Major Histocompatibility Complex
MPLC	Medium Pressure Liquid Chromatography
MRI	Magnetic Resonance Imaging
MS	Multiple Sclerosis
NBD	Normal Blood Donor
NMR	Nuclear Magnetic Resonance
NO	Nitric Oxide
NOESY	Nuclear Overhauser Effect Spectroscopy
OS	Oxydative Stress
Rha	Rhamnose
ROC	Receiver Operating Characteristic
ROESY	Rotating-frame Overhauser Effect Spectroscopy
RTT	Rett syndrome
SE	Standard Error
SP-ELISA	Solid-Phase ELISA
TCR	T Cell Receptor
TLC	Thin-Layer Chromatography
TOCSY	Total Correlation Spectroscopy
UV	Ultra-Violet
VLC	Vacuum Liquid Chromatography
Xyl	Xylose

LIST OF FIGURES AND TABLES

- Figure 1:** Function of the immune system
- Figure 2:** Pathological mechanisms of autoimmune diseases
- Figure 3:** Multiple sclerosis: destruction of the myelin sheath
- Figure 4:** Immune status and disease course in MS
- Figure 5:** MeCP2 is a multifunctional protein.
- Figure 6:** Indirect ELISA procedure
- Figure 7:** Phylogeny Fabales order
- Figure 8:** *Wisteria frutescens*
- Figure 9:** *W. floribunda* “macrobotrys” and *W. floribunda* “rosea”
- Figure 10:** *Polygala acicularis*
- Figure 11:** Phylogeny Dipsacales order
- Figure 12:** *Weigela florida* “rumba”
- Figure 13:** Triterpene skeleton: Oleanane (A), dammarane (B), ursane (C) and lupane (D)
- Figure 14:** Steroidic skeleton: spirostane (A) and furostane (B)
- Figure 15:** Most common osidic moieties found in saponins
- Figure 16:** Mechanism of electrospray ionization
- Figure 17:** Positive ESIMS of saponin 1
- Figure 18:** Significant NOE correlations in NOESY experiment of compound 1
- Figure 19:** General HSQC of saponin 1
- Figure 20:** HSQC anomers zone of saponin 1
- Figure 21:** HSQC spectrum of saponin 1
- Figure 22:** ROESY spectrum of saponin 1
- Figure 23:** Positive ESIMS of saponin 2
- Figure 24:** General HSQC spectrum of saponin 2
- Figure 25:** HSQC anomers zone of saponin 2
- Figure 26:** NOESY spectrum of saponin 2
- Figure 27:** Positive ESIMS of saponin 3
- Figure 28:** General HSQC of saponin 3
- Figure 29:** HSQC anomers zone of saponin 3
- Figure 30:** HSQC spectrum of saponin 3
- Figure 31:** ROESY spectrum of saponin 3
- Figure 32:** Structure of saponins 1-3

Figure 33: Structure of saponins 4-6

Figure 34: Negative ESIMS of saponin 7

Figure 35: Key HMBC and ROESY correlations for the aglycon of 7.

Figure 36: General HSQC of saponin 7

Figure 37: HSQC anomers zone of saponin 7

Figure 38: HSQC spectrum of saponin 7

Figure 39: HMBC spectrum of saponin 7

Figure 40: Structure of saponins 7-11

Figure 41: Positive ESIMS of saponin 12

Figure 42: General HSQC of saponin 12

Figure 43: HSQC anomers zone of saponin 12

Figure 44: HSQC spectrum of saponin 12

Figure 45: HMBC spectrum of saponin 12

Figure 46: Positive ESIMS of saponin 13

Figure 47: General HSQC spectra of saponin 13

Figure 48: HSQC anomers zone of saponin 13

Figure 49: HSQC spectrum of saponin 13

Figure 50: HMBC spectrum of saponin 13

Figure 51: Positive ESIMS of saponin 14

Figure 52: General HSQC spectrum of saponin 14

Figure 53: HSQC anomers zone of saponin 14

Figure 54: Sugar moieties of saponin 14

Figure 55: HMBC spectrum of saponin 14

Figure 56: NOESY spectrum of saponin 14

Figure 57: Structure of saponins 12-14

Figure 58: Positive ESIMS of saponin 15

Figure 59: General HSQC of saponin 15

Figure 60: HSQC spectrum of saponin 15

Figure 61: ROESY spectrum of saponin 15

Figure 62: Structure of saponins 15 and 16

Figure 63: Structure of ursolic acid (17)

Figure 64: Structure of prosapogenin tenuifolin (18)

Figure 65: *Sophora japonica*

Figure 66: Structure of rutoside (19)

Figure 67: Structure of saponins **4** and **8**

Figure 68: Structure of saponins **13** and **14**

Figure 69: Structure of saponin **16**

Figure 70: Structure of saponin **18**

Figure 71: Structure of the ursolic acid (**17**)

Figure 72: Structure of the rutoside (**19**)

Figure 73: Data distribution of IgM antibody responses to saponins **4** and **8** in MS sera and NBDs determined by ELISA.

Figure 74: Data distribution of IgM antibody responses to saponin **13** and **14** in MS sera and NBDs determined by ELISA.

Figure 75: Data distribution of IgM antibody responses to saponin **16** in MS sera and NBDs determined by ELISA.

Figure 76: Data distribution of IgM antibody responses to ursolic acid **17** in MS sera and NBDs determined by ELISA.

Figure 77: Data distribution of IgM antibody responses to saponin **18** in MS sera and NBDs determined by ELISA.

Figure 78: Data distribution of IgM antibody responses to rutoside **19** in MS sera and NBDs determined by ELISA.

Figure 79: Data distribution of IgM antibody responses to compounds **4, 8, 13, 14, 16, 17, 18** and **19** in RTT sera and NBDs determined by ELISA.

Table 1. Health promoting activities of saponins

Table 2a. Saponins isolated from *Weigela genus*

Table 2b. Saponins isolated from *Weigela genus*

Table 3a. Saponins isolated from *Polygala genus*

Table 3b. Saponins isolated from *Polygala genus*

Table 4. ^{13}C NMR and ^1H NMR data of the aglycones of compounds **1-3** in Pyridine- $d_5/\text{D}_2\text{O}$ (δ ppm, J in Hz)

Table 5. ^{13}C NMR and ^1H NMR data of the sugar moieties of compounds **1-3** in Pyridine- $d_5/\text{D}_2\text{O}$ (δ ppm, J in Hz)

Table 6. ^{13}C NMR and ^1H NMR data of compound **7** in Pyridine- d_5 (δ in ppm)

Table 7. ^{13}C NMR and ^1H NMR data of the sugar moiety of compound **7** in Pyridine- d_5 (δ in ppm)

Table 8. ^{13}C NMR and ^1H NMR data of the aglycones of compounds **12-14** in Pyridine- d_5 (δ in ppm, J in Hz)

Table 9. ^{13}C NMR and ^1H NMR data of the sugar moieties of compounds **12-14** in Pyridine- d_5 (δ in ppm, J in Hz)

Table 10. ^{13}C NMR and ^1H NMR data of the aglycones of compounds **15** and **16** in Pyridine- $d_5/\text{D}_2\text{O}$ (δ in ppm, J in Hz)

Table 11. ^{13}C NMR and ^1H NMR data of the sugar moieties and the 3,4-dimethoxycinnamoyl group of compounds **15** and **16** in Pyridine- $d_5/\text{D}_2\text{O}$ (δ in ppm, J in Hz)

Table 12. Values obtained from ROC analysis of glycosides **4, 8, 13, 14, 16, 18** and **19** and ursolic acid **17** for the area under the curve (AUC), standard error (SE), the confidence interval (CI), p value, established cutoff, and the corresponding sensitivity, specificity and likelihood ratio

BIBLIOGRAPHY

- [1] Aribi M (2017) Introductory Chapter: Immune system dysfunction and autoimmune diseases. In Aribi M (ed.), *Immunopathogenesis and Immune-based Therapy for Selected Autoimmune Disorders*. InTech.
- [2] Rentier C (2015) Autoimmune diseases: design, synthesis and immunological screening of post-translationally modified peptides to characterize autoantibodies in patients' sera. *PhD* (u Cergy Pontoise).
- [3] Régent A, Bussone G, Kaveri SV, Mouthon L (2009) Auto-immunité humorale et cellulaire: de la physiologie à la pathologie. *La Revue de Médecine Interne* **30**: H1-H8.
- [4] Salou M, Elong Ngono A, Garcia A, Michel L, Laplaud DA (2013) Immunité adaptative et physiopathologie de la sclérose en plaques. *La Revue de Médecine Interne* **34**: 479-486.
- [5] Sullivan MJL, Mikail S, Weinschenker B (1997) Coping with a diagnosis of multiple sclerosis. *Canadian Journal of Behavioural Science / Revue canadienne des sciences du comportement* **29**: 249-256.
- [6] Depaz R, Aboab J, Gout O (2013) Actualités dans le diagnostic et la prise en charge thérapeutique de la sclérose en plaques. *La Revue de Médecine Interne* **34**: 628-635.
- [7] Béthoux F (2005) Évaluation et sclérose en plaques. *Annales de Réadaptation et de Médecine Physique* **48**: 369-375.
- [8] Durand-Dubief F (2016) Les biomarqueurs de la sclérose en plaques en imagerie. *Neurophysiologie Clinique/Clinical Neurophysiology* **46**: 223.
- [9] Weiner HL (2009) The challenge of multiple sclerosis: How do we cure a chronic heterogeneous disease? *Annals of Neurology* **65**: 239-248.
- [10] (2009) Le syndrome de Rett. *Journal de Pédiatrie et de Puériculture* **22**: 48-49.
- [11] Zvereff V, Carpenter L, Patton D, Cabral H, Rita D, Wilson A, Anyane-Yeboa K, White L, Friedman KJ (2012) Molecular diagnostic dilemmas in Rett syndrome. *Brain and Development* **34**: 750-755.
- [12] De Felice C, Leoncini S, Signorini C, Cortelazzo A, Rovero P, Durand T, Ciccoli L, Papini AM, Hayek J (2016) Rett syndrome: An autoimmune disease? *Autoimmunity Reviews* **15**: 411-416.
- [13] Yang Y, Kucukkal TG, Li J, Alexov E, Cao W (2016) Binding analysis of Methyl-CpG Binding Domain of MeCP2 and Rett Syndrome mutations. *ACS Chemical Biology* **11**: 2706-2715.

- [14] Adkins NL, Georgel PT (2011) MeCP2: structure and function. *Biochemistry and Cell Biology* **89**: 1-11.
- [15] Gadalla KKE, Bailey MES, Cobb SR (2011) MeCP2 and Rett syndrome: reversibility and potential avenues for therapy. *Biochemical Journal* **439**: 1-14.
- [16] Bedogni F, Rossi RL, Galli F, Cobolli Gigli C, Gandaglia A, Kilstrup-Nielsen C, Landsberger N (2014) Rett syndrome and the urge of novel approaches to study MeCP2 functions and mechanisms of action. *Neuroscience & Biobehavioral Reviews* **46**: 187-201.
- [17] De Felice C, Signorini C, Leoncini S, Pecorelli A, Durand T, Valacchi G, Ciccoli L, Hayek J (2012) The role of oxidative stress in Rett syndrome: an overview. *Annals of the New York Academy of Sciences* **1259**: 121-135.
- [18] Wymann MP, Schneider R (2008) Lipid signalling in disease. *Nature Reviews Molecular Cell Biology* **9**: 162-176.
- [19] Kim SH, Turnbull J, Guimond S (2011) Extracellular matrix and cell signalling: the dynamic cooperation of integrin, proteoglycan and growth factor receptor. *Journal of Endocrinology* **209**: 139-151.
- [20] Nobile-Orazio E, Giannotta C (2011) Testing for anti-glycolipid IgM antibodies in chronic immune-mediated demyelinating neuropathies. *Journal of the Peripheral Nervous System* **16**: 18-23.
- [21] Miyahara K, Nouse K, Saito S, Hiraoka S, Harada K, Takahashi S, Morimoto Y, Kobayashi S, Ikeda F, Miyake Y (2013) Serum glycan markers for evaluation of disease activity and prediction of clinical course in patients with ulcerative colitis. *PLoS ONE* **8**: e74861.
- [22] Kaul A, Hutfless S, Liu L, Bayless TM, Marohn MR, Li X (2012) Serum anti-glycan antibody biomarkers for inflammatory bowel disease diagnosis and progression: A systematic review and meta-analysis. *Inflammatory Bowel Diseases* **18**: 1872-1884.
- [23] Alexander JS, Zivadinov R, Maghzi AH, Ganta VC, Harris MK, Minagar A (2011) Multiple sclerosis and cerebral endothelial dysfunction: Mechanisms. *Pathophysiology* **18**: 3-12.
- [24] Lolli F, Mazzanti B, Pazzagli M, Peroni E, Alcaro MC, Sabatino G, Lanzillo R, Brescia Morra V, Santoro L, Gasperini C (2005) The glycopeptide CSF114(Glc) detects serum antibodies in multiple sclerosis. *Journal of Neuroimmunology* **167**: 131-137.

- [25] Marta CB, Oliver AR, Sweet RA, Pfeiffer SE, Ruddle NH (2005) Pathogenic myelin oligodendrocyte glycoprotein antibodies recognize glycosylated epitopes and perturb oligodendrocyte physiology. *Proceedings of the National Academy of Sciences* **102**: 13992-13997.
- [26] Lolli F, Mulinacci B, Carotenuto A, Bonetti B, Sabatino G, Mazzanti B, D'Ursi AM, Novellino E, Pazzagli M, Lovato L (2005) An N-glycosylated peptide detecting disease-specific autoantibodies, biomarkers of multiple sclerosis. *Proceedings of the National Academy of Sciences* **102**: 10273-10278.
- [27] Real-Fernández F, Passalacqua I, Peroni E, Chelli M, Lolli F, Papini AM, Rovero P (2012) Glycopeptide-based antibody detection in multiple sclerosis by surface plasmon resonance. *Sensors* **12**: 5596-5607.
- [28] Carotenuto A, Alcaro MC, Saviello MR, Peroni E, Nuti F, Papini AM, Novellino E, Rovero P (2008) Designed glycopeptides with different β -Turn types as synthetic probes for the detection of autoantibodies as biomarkers of multiple sclerosis. *Journal of Medicinal Chemistry* **51**: 5304-5309.
- [29] Carotenuto A, D'Ursi AM, Mulinacci B, Paolini I, Lolli F, Papini AM, Novellino E, Rovero P (2006) Conformation–activity relationship of designed glycopeptides as synthetic probes for the detection of autoantibodies, biomarkers of multiple sclerosis. *Journal of Medicinal Chemistry* **49**: 5072-5079.
- [30] Nuti F, Peroni E, Real-Fernández F, Bonache MA, Le Chevalier-Isaad A, Chelli M, Lubin-Germain N, Uziel J, Rovero P, Lolli F (2010) Posttranslationally modified peptides efficiently mimicking neoantigens: A challenge for theragnostics of autoimmune diseases. *Biopolymers* **94**: 791-799.
- [31] Walvoort MTC, Testa C, Eilam R, Aharoni R, Nuti F, Rossi G, Real-Fernandez F, Lanzillo R, Brescia Morra V, Lolli F (2016) Antibodies from multiple sclerosis patients preferentially recognize hyperglucosylated adhesin of non-typeable *Haemophilus influenzae*. *Scientific Reports* **6**: 39430.
- [32] Papini AM, Nuti F, Real-Fernandez F, Rossi G, Tiberi C, Sabatino G, Pandey S, Leoncini S, Signorini C, Pecorelli A (2014) Immune dysfunction in Rett syndrome patients revealed by high levels of serum anti-N(Glc) IgM antibody fraction. *Journal of Immunology Research* **2014**: 1-6.
- [33] Peroni E, Real Fernández F, Gheri C, Nuti F, Mitaine-Offer AC, Lolli F, Lacaille-Dubois MA, Papini AM (2016) Natural triterpene glycosides for antibody recognition. *Planta Medica Letters* **3**: e2-e7.

- [34] Real-Fernández F, Rossi G, Lolli F, Papini AM, Rovero P (2015) Label-free method for anti-glucopeptide antibody detection in Multiple Sclerosis. *MethodsX* **2**: 141-144.
- [35] THE ANGIOSPERM PHYLOGENY GROUP (2009) An update of the Angiosperm Phylogeny Group classification for the orders and families of flowering plants: APG III: APG III. *Botanical Journal of the Linnean Society* **161**: 105-121.
- [36] www.mobot.org
- [37] Ibáñez MD, Martínez M, Sánchez JJ, Fernández-Caldas E (2003) Legume cross-reactivity. *Allergol Immunopathol (Madr)* **31**: 151-161.
- [38] Gulewicz P, Martinez-Villaluenga C, Kasprowicz-Potocka M, Frias J (2014) Non-nutritive compounds in Fabaceae family seeds and the improvement of their nutritional quality by traditional processing – a Review. *Polish Journal of Food and Nutrition Sciences* **64**: 75-89.
- [39] <http://www.tropicos.org/Name/40026522>
- [40] Jiang Y, Chen X, Lin H, Wang F, Chen F (2011) Floral scent in *Wisteria*: chemical composition, emission pattern, and regulation. *Journal of the American Society for Horticultural Science*, **136**: 307-314.
- [41] Li J, Jiang JH, Fu CX, Tang SQ (2014) Molecular systematics and biogeography of *Wisteria* inferred from nucleotide sequences of nuclear and plastid genes: Phylogenetics and biogeography of *Wisteria*. *Journal of Systematics and Evolution* **52**: 40-50.
- [42] Lacaille-Dubois MA, Mitaine-Offer AC (2005) Triterpene saponins from Polygalaceae. *Phytochemistry Reviews* **4**: 139-149.
- [43] Lacaille-Dubois MA, Delaude C, Mitaine-Offer AC (2013) Triterpenoid saponins: A focus on Polygalaceae. In Ramawat KG, Mérillon J-M (eds.), *Natural Products* 3205-3223. Springer Berlin Heidelberg, Berlin, Heidelberg.
- [44] Delaude C (1971) Étude comparative des saponines extraites de deux Polygalacées africaines. Le *Securidaca longependunculata* Fres. var. *parvifolia* et le *Polygala acicularis* Oliv. *Bulletin de la Société Royale des Sciences de Liège* **40**: 397-405.
- [45] Botineau M (2010) Botanique systématique et appliquée des plantes à fleurs. Lavoisier, Paris.
- [46] FOBS, Friends of the Botanical Gardens, Sheffield, 2015, <http://www.fobssheffield.co.uk/weigelas.html>.
- [47] Rezgui A, Mitaine-Offer AC, Miyamoto T, Tanaka C, Delemasure S, Dutartre P, Lacaille-Dubois MA (2016) Oleanolic acid and hederagenin glycosides from *Weigela stelzneri*. *Phytochemistry* **123**: 40-47.

- [48] Hostettman K and Marston A (1995) Saponins: chemistry and pharmacology of natural products. Cambridge, UK: Cambridge University Press: 1-174
- [49] Randriamampianina L, Offroy A, Mambu L, Randrianarivo R, Rakoto D, Jeannoda V, Djediat C, Puiseux Dao S, Edery M (2013) Marked toxicity of *Albizia bernieri* extracts on embryo–larval development in the medaka fish (*Oryzias latipes*). *Toxicol* **64**: 29-35.
- [50] Tian F, Zhang X, Tong Y, Yi Y, Zhang S, Li L, Sun P, Lin L, Ding J (2005) PE, a new sulfated saponin from sea cucumber, exhibits anti-angiogenic and anti-tumor activities in vitro and in vivo. *Cancer Biology Therapy* **4**: 874-882.
- [51] Hwang IH, Kim DW, Kim SJ, Min BS, Lee SH, Son JK, Kim CH, Chang HW & Na M (2011) Asterosaponins isolated from the starfish *Asterias amurensis*. *Chemical and Pharmaceutical Bulletin* **59**: 78-83.
- [52] Luo JG, Chen X, Kong LY (2011) Three new triterpenoid saponins from *Dianthus superbis*. *Chemical and Pharmaceutical Bulletin* **59**: 518-521.
- [53] Laurençon L, Sarrazin E, Chevalier M, Prêcheur I, Herbette G, Fernandez X (2013) Triterpenoid saponins from the aerial parts of *Solidago virgaurea alpestris* with inhibiting activity of *Candida albicans* yeast-hyphal conversion. *Phytochemistry* **86**: 103-111.
- [54] Bruneton J, (2009) Pharmacognosie, phytochimie, plantes médicinales. 4^{ème} éd : Tec et Doc, Editions médicales internationales – Lavoisier, Paris : 810-868.
- [55] Singh B, Singh JP, Singh N, Kaur A (2017) Saponins in pulses and their health promoting activities: A review. *Food Chemistry* **233**: 540-549.
- [56] Konoshima T, Kozuka M, Haruna M, Ito K, Kimura T (1989) Studies on the constituents of leguminous plants. XI. The structures of new triterpenoids from *Wistaria brachybotrys* Sieb. et Zucc. *Chemical and Pharmaceutical Bulletin* **37**: 1550-1553.
- [57] Konoshima T, Kozuka M, Haruna M, Ito K, Kimura T, Tokuda H (1989) Studies on the constituents of leguminous plants. XII. The structures of new triterpenoid saponins from *Wistaria brachybotrys* SIEB. et ZUCC. *Chemical and Pharmaceutical Bulletin* **37**: 2731-2735.
- [58] Kinjo J, Fujishima Y, Saino K, Tian R, Nohara T (1995) Five new triterpene glycosides from *Wisteria brachybotrys* (Leguminosae). *Chemical and Pharmaceutical Bulletin* **43**: 636-640.
- [59] Konoshima T, Kozuka M (1991) Constituents of leguminous plants, XIII. New triterpenoid saponins from *Wistaria brachybotrys*. *Journal of Natural Products* **54**: 830-836.
- [60] Murayama T, Kasahara A, Shiono Y, Ikeda M (2003) Structure elucidation of a triterpene glycoside isolated from *Weigela hortensis*. *Nature Medicine* **57**: 181-184.

- [61] Song YL, Zeng KW, Shi TX, Jiang Y, Tu PF (2013) Sibiricasaponins A–E, five new triterpenoid saponins from the aerial parts of *Polygala sibirica* L. *Fitoterapia* **84**: 295-301.
- [62] De Leo M, Peruzzi L, Granchi C, Tuccinardi T, Minutolo F, De Tommasi N, Braca A (2017) Constituents of *Polygala flavescens* ssp. *flavescens* and their activity as inhibitors of human lactate dehydrogenase. *Journal of Natural Products* **80**: 2077-2087.
- [63] Ho CS, Lam CWK, Chan MHM, Cheung RCK, Law LK, Lit LCW, Ng KF, Suen MWM, Tai HL (2003) Electrospray ionisation mass spectrometry: principles and clinical applications. *The Clinical Biochemist Reviews* **24**: 3-12.
- [64] Hara S, Okabe H, Mihashi K (1987) Gas-liquid chromatographic separation of aldose enantiomers as trimethylsilyl ethers of methyl 2-(polyhydroxyalkyl)-thiazolidine-4(R)-carboxylates. *Chemical and Pharmaceutical Bulletin* **35**: 501-506.
- [65] Kitagawa I, Wang H, Saito M, Yoshikawa M (1983) Saponin and sapogenol. XXXIII. Chemical constituents of the seeds of *Vigna angularis* (Willd.) Ohwi et Ohashi. (3). Azukisaponins V and VI. *Chemical and Pharmaceutical Bulletin* **31**: 683-688.
- [66] Champy AS, Mitaine-Offer AC, Miyamoto T, Tanaka C, Papini AM, Lacaille-Dubois MA (2017) Structural analysis of oleanane-type saponins from the roots of *Wisteria frutescens*: Oleanane-type saponins from *Wisteria frutescens*. *Magnetic Resonance in Chemistry* **55**: 595-600.
- [67] Uchiyama T, Furukawa M, Isobe S, Makino M, Akiyama T, Koyama T, Fujimoto Y (2003) New oleanane-type triterpene saponins from *Millettia speciosa*. *Heterocycles*, **60**: 655-661.
- [68] Benchadi W, Haba H, Lavaud C, Harakat D, Benkhaled M (2013) Secondary metabolites of *Astragalus cruciatus* Link. and their chemotaxonomic significance. *Records of Natural Products*, **7**: 105-113.
- [69] Birjatinder S, Joga S, Singh MV (2014) Ethno medicinal, pharmacological properties and chemistry of Fabaceae family. *Journal of Medical Pharmaceutical and Allied Sciences*, **02** : 24-28.
- [70] Kinjo J, Udayama M, Okawa M, Nohara T (1999) Study of structure-hepatoprotective relationships of oleanene-type triterpenoidal glucuronides obtained from several fabaceous plants on rat primary hepatocyte cultures. *Biological and Pharmaceutical Bulletin*, **22**: 203-206.
- [71] Abbas F, Zayed R (2005) Bioactive saponins from *Astragalus suberi* L. growing in Yemen. *Zeitschrift für Naturforschung*, **60c**: 813-820.

- [72] Ionkova I, Shkondrov A, Krasteva I, Ionkov T (2014) Recent progress in phytochemistry, pharmacology and biotechnology of *Astragalus* saponins. *Phytochemistry Reviews*, **13**: 343-374.
- [73] Tantry M A, Khan I A (2013) Saponins from *Glycine max* Merrill (soybean). *Fitoterapia*, **87** : 49-56.
- [74] Tava A, Scotti C, Avato P (2011) Biosynthesis of saponins in the genus *Medicago*. *Phytochemistry Reviews*, **10**: 459-469.
- [75] Zhang HX, Sun G, Gu JL, Du ZZ (2017) New sweet-tasting oleanane-type triterpenoid saponins from “Tugancao” (*Derris eriocarpa* How). *Journal of Agricultural and Food Chemistry*, **65**: 2357-2363.
- [76] Zhang D, Miyase T, Kuroyanagi M, Umehara K, Noguchi H (1996) Nine New Triterpene saponins, polygalasaponins XXXIII-XLI from the roots of *Polygala fallax* HEMSL. *Chemical and Pharmaceutical Bulletin* **44**: 2092-2099.
- [77] Miyase T, Saitoh H, Shiokawa K, Ueno A (1995) Six new presenegenin glycosides, reiniosides A-F, from *Polygala reinii* root. *Chemical and Pharmaceutical Bulletin* **43**: 466-472.
- [78] Mitaine-Offer AC, Miyamoto T, Khan IA, Delaude C, Lacaille-Dubois MA (2002) Three new triterpene saponins from two species of *Carpolobia*. *Journal of Natural Products* **65**: 553-557.
- [79] Yoshikawa M, Murakami T, Ueno T, Kadoya M, Matsuda H, Yamahara J, Murakami N (1995) E-senegasaponins A and B, Z-senegasaponins A and B, Z-senegins II and III, New type inhibitors of ethanol absorption in rats from *Senegae Radix*, the roots of *Polygala senega* L. var *Latifolia* TORREY et GRAY. *Chemical and Pharmaceutical Bulletin* **43**: 350-352.
- [80] Paniwnyk L, Beaufoy E, Lorimer JP, Mason TJ (2001) The extraction of rutin from flower buds of *Sophora japonica*. *Ultrasonics Sonochemistry* **8**: 299-301.
- [81] Dar MA, Tabassum N (2012) Rutin potent natural thrombolytic agent. *International Current Pharmaceutical Journal* **1**: 431-435.
- [82] Ganeshpurkar A, Saluja AK (2017) The pharmacological potential of rutin. *Saudi Pharmaceutical Journal* **25**: 149-164.

LIST OF PERSONAL COMMUNICATIONS AND PUBLICATIONS

Publications:

- 1) Structural analysis of oleanane-type saponins from the roots of *Wisteria frutescens*
Anne-Sophie Champy, Anne-Claire Mitaine-Offer, Tomofumi Miyamoto, Chiaki Tanaka, Anna-Maria Papini and Marie-Aleth Lacaille-Dubois
Magnetic Resonance in Chemistry 2017, 55, 595-600.
- 2) Triterpene saponins from *Wisteria floribunda* “macrobotrys” and “rosea”
Anne-Sophie Champy, Anne-Claire Mitaine-Offer, Thomas Paululat, Anna-Maria Papini and Marie-Aleth Lacaille-Dubois
Natural Product Communications 2017, 12, 1573-1576.
- 3) Oleanane-type glycosides from the roots of *Weigela florida* “rumba” (Bunge) A. DC. and evaluation of their antibody recognition
Anne-Sophie Champy, Feliciano Real Fernandez, Anne-Claire Mitaine-Offer, Tomofumi Miyamoto, Chiaki Tanaka, Anna-Maria Papini, Marie-Aleth Lacaille-Dubois. Submitted to Fitoterapia

International presentations:

- 1) (Poster) Champy A-S, Mitaine-Offer A-C, Miyamoto T and Lacaille-Dubois M-A, Two new triterpenoid saponins from the roots of *Wisteria frutescens*, 2nd international symposium AFERP-STOLON: Biodiversity and natural substances, Lyon (France), 15th-17th July 2015, P72
- 2) (Poster) Champy A-S, Real Fernandez F, Mitaine-Offer A-C, Papini A-M, Lacaille-Dubois M-A, Natural triterpene saponins to recognize autoantibodies in immune-mediated diseases, PhD day, Florence (Italy), 27th may 2016
- 3) (Poster) Champy A-S, Mitaine-Offer A-C, Paululat T, Papini A-M, Lacaille-Dubois M-A, Oleanane-type saponins from the roots of *Wisteria floribunda macrobotrys*, 9th Joint Natural Products Conference 2016, Copenhagen (Denemark), 24th-27th July 2016, published in Planta Med., 2016, 82 (S01): S1-S381, DOI: 10.1055/s-0036-1596324
- 4) (Oral communication) Champy A-S, Mitaine-Offer A-C, Real Fernandez F, Paululat T, Papini A-M, Lacaille-Dubois M-A, Natural triterpene saponins to recognize autoantibodies in immune-mediated diseases, Natural Products in Health, Agro-food and Cosmetics, Villeneuve d’Ascq (France), 28th June – 1st July 2017

- 5) (Poster) Champy A-S, Mitaine-Offer A-C, Real Fernandez F, Paululat T, Papini A-M, Lacaille-Dubois M-A, Natural triterpene saponins to recognize autoantibodies in immune-mediated diseases, 5th international symposium of AFERP in Angers (France), 17th-19th july **2017**

National presentations:

- 1) (Poster) Champy A-S, Mitaine-Offer A-C, Papini A-M, Miyamoto T and Lacaille-Dubois M-A, Glycosylated natural triterpene saponins for autoantibody recognition, *Forum des jeunes chercheurs (FJC)*, Dijon (France), 18th-19th june **2015**
- 2) (Oral communication) Champy A-S, Conference on standards and controls of essential oil in aromatherapy for an university degree in Dijon (France), 10th march **2016**
- 3) (Oral communication) Champy A-S, Mitaine-Offer A-C, Real Fernandez F, Paululat T, Papini A-M, Lacaille-Dubois M-A, Natural saponins used as antigens to recognize autoantibodies in immune-mediated diseases, *Forum des jeunes chercheurs (FJC)*, Dijon (France), 15th-16th june **2017**

Structural analysis of oleanane-type saponins from the roots of *Wisteria frutescens*

Keywords: 2D NMR; Triterpene glycosides; *Wisteria frutescens*; Fabaceae

Introduction

The Fabaceae family is represented by numerous genera, which contains approximately 19,500 species distributed around the world.^[1] The particularity of this family is to live in symbiosis with bacteria that live in gall and assimilating atmospheric nitrogen.^[2] *Wisteria* (also spelled *Wistaria*) is a genus of woody vines with alternate pinnately compound leaves and a large inflorescence of pendulous, showy purple, blue, or white flowers.^[3] Previous phytochemical studies were published on some *Wisteria* species: Triterpene saponins were isolated from the knots and vines of *Wisteria brachybotrys*^[4–7] and the leaves of *Wisteria sinensis* yielded flavonoid derivatives and triterpenes.^[8,9] Moreover, lectins from *Wisteria floribunda* were used for detection of tumor antigens with specific sugar chain and for diagnosis of cancer.^[10] *Wisteria frutescens* (L.) Poir., also known as 'American *Wisteria*', is a toxic plant native to the United States. Its pods, seeds, and bark contain toxic principles, a glycoside named wisterin and a resin.^[3] In this paper, we report about the isolation of six oleanane-type saponins from the roots of *W. frutescens*. Their structures were established by a detailed 600 MHz NMR analysis including 1D and 2D NMR (¹H, ¹³C NMR, COSY, TOCSY, NOESY, HSQC, and HMBC) experiments and mass spectrometry as two previously undescribed triterpenoid saponins (**1–2**) (Fig. 1) and four known ones: 3-*O*- α -L-rhamnopyranosyl-(1 \rightarrow 2)- β -D-xylopyranosyl-(1 \rightarrow 2)- β -D-glucuronopyranosyl-22-*O*-acetyl-3 β ,22 β ,24-trihydroxyolean-12-en-30-oic acid (**3**) (wistariasaponin G),^[6] 3-*O*- α -L-rhamnopyranosyl-(1 \rightarrow 2)- β -D-xylopyranosyl-(1 \rightarrow 2)- β -D-glucuronopyranosyl wistariasapogenol A (wistariasaponin A),^[5] 3-*O*- α -L-rhamnopyranosyl-(1 \rightarrow 2)- β -D-xylopyranosyl-(1 \rightarrow 2)- β -D-glucuronopyranosyl soyasapogenol B (wistariasaponin C),^[5] and 3-*O*- α -L-rhamnopyranosyl-(1 \rightarrow 2)- β -D-glucopyranosyl-(1 \rightarrow 2)- β -D-glucuronopyranosyl soyasapogenol B (azukisaponin V).^[11] The structural analysis of the native form of wistariasaponin G is described for the first time.

Results and Discussion

The saponins **1–3** were isolated from an aqueous-ethanolic extract of the roots of *W. frutescens* by various solid/liquid chromatographic methods: vacuum liquid chromatography (VLC) on normal and reverse phase RP-18 silica gel, medium pressure liquid chromatography (MPLC), and size exclusion chromatography on Sephadex LH-20 (GE Healthcare Bio-Sciences AB, Uppsala, Sweden).

The HR-ESIMS (positive-ion mode) spectrum of compound **1** established its molecular formula as C₅₁H₈₀O₂₀ with a pseudo-molecular peak at *m/z* 1035.5150 [M + Na]⁺ (calcd 1035.5141). Its

ESIMS (negative-ion mode) displayed a quasi-molecular ion peak at *m/z* 1011 [M – H][–], indicating a molecular weight of 1012.

The ¹H NMR spectrum of the aglycone part of **1** displayed signals assignable to seven angular methyl groups at δ_{H} 0.75, 0.85, 0.98, 1.01, 1.07, 1.22, and 1.28 (3H s, each), one olefinic proton at δ_{H} 5.28 (1H, br t, *J* = 3.0, H-12), three oxygen bearing methine protons at δ_{H} 3.23 (1H, dd, *J* = 12.0, 3.8 Hz, H-3_{ax}), 4.53 (1H, dd, *J* = 12.4, 4.0 Hz, H-16_{ax}), and 6.10 (1H, br s, H-22_{eq}), and one primary alcoholic function at δ_{H} 4.23 (1H, d, *J* = 12.4 Hz, H-28_{aeq}), 4.86 (1H, d, *J* = 12.4 Hz, H-28_{beq}) (Table 1). In the ¹³C NMR spectrum, signals at δ_{C} 170.3 and 171.1 suggested two ester functions. Furthermore, HMBC correlations at δ_{H} 2.01 (3H, s)/ δ_{C} 171.1 and δ_{H} 2.09 (3H, s)/ δ_{C} 170.3 revealed the presence of two acetyl groups. An HMBC cross-peak at δ_{H} 1.65 (1H, dd, *J* = 13.3, 4.0 Hz, H-15_{eq})/ δ_{C} 141.7 (C-13) and a COSY correlation between δ_{H} 1.65 (1H, dd, *J* = 13.3, 4.0 Hz, H-15_{eq}), 2.24 (1H, dd, *J* = 13.3, 12.4 Hz, H-15_{ax}), and 4.53 (1H, dd, *J* = 12.4, 4.0 Hz, H-16_{ax}) allowed the location of a secondary alcoholic function at the C-16 position. An HMBC correlation between a deshielded signal at δ_{H} 4.23 (1H, d, *J* = 12.4 Hz, H-28_{aeq}) and δ_{C} 66.4 (C-16) proved the location of the primary alcoholic function at C-28. Other HMBC correlations of δ_{H} 1.07 (3H, s, H₃-30_{ax}) and 0.85 (3H, s, H₃-29_{eq}) with δ_{C} 37.7 (C-21) and a COSY correlation between δ_{H} 1.74 (H-21_{ax}) and 6.10 (1H, br s, H-22_{eq}) confirmed the location of another secondary alcoholic function at C-22. The configurations of C-3 and C-16 of the aglycone were determined by the correlations observed in the NOESY spectrum between H-3 α -axial and H₃-23 α -equatorial, and between H-16 α -axial and H₃-27 α -axial, respectively. The α -equatorial orientation of H-22 was deduced by its coupling constant as a br s and by the NOESY connectivity with α -axial H-16. The structure of the aglycone of **1** was thus recognized to be the unusual olean-12-ene-3 β ,16 β ,22 β -28-tetrol, a stereoisomer of the camelliagenin A (Table 2).^[12] The deshielded values of H-22_{eq} at δ_{H} 6.10 and H-28_{aeq} and H-28_{beq} at δ_{H} 4.23, 4.86, respectively, suggested an acetylation at these two positions (Table 1). The HMBC correlation between δ_{H} 4.23 (H-28_{aeq}) and δ_{C} 171.1 (OCO) allowed the location of the first acetyl group at C-28 and thus the location of the other acetyl group at C-22.

The HSQC spectrum of **1** displayed signals of three anomers at δ_{H} 5.53 (1H, d, *J* = 7.3 Hz)/ δ_{C} 102.1, 4.83 (1H, d, *J* = 6.9 Hz)/104.8, and 6.20 (1H, br s)/101.6. The ring protons of the monosaccharide residues were assigned starting from the readily identifiable anomeric protons by means of the ¹H-¹H COSY, TOCSY, HSQC, and HMBC experiments and by gas chromatography (GC) (Experimental section). Units of one β -D-glucuronopyranosyl (GlcA), one β -D-xylopyranosyl (Xyl), and one α -L-rhamnopyranosyl (Rha) were thus identified (Table 3). The monodesmosidic structure was suggested by the HMBC cross-peak at δ_{H} 4.83 (1H, d, *J* = 6.9 Hz, GlcA-1)/ δ_{C}

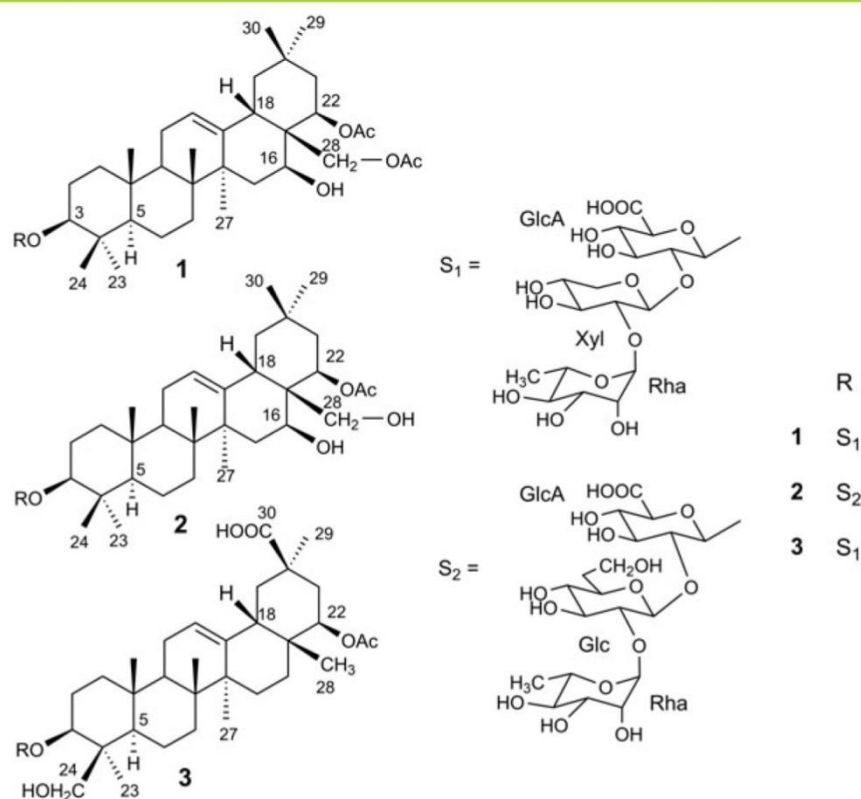


Figure 1. Structures of compounds **1–3**.

89.6 (C-3) and the NOESY cross-peak at δ_{H} 4.83 (1H, d, $J = 6.9$ Hz, GlcA-1)/ δ_{H} 3.23 (1H, dd, $J = 12.0, 3.8$ Hz, H-3_{ax}). Other HMBC correlations at δ_{H} 4.23 (1H, dd, $J = 8.0, 6.9$ Hz, GlcA-2)/ δ_{C} 102.1 (Xyl-1), and at δ_{H} 4.14 (1H, dd, $J = 8.8, 7.3$ Hz, Xyl-2)/ δ_{C} 101.6 (Rha-1) suggested a α -L-rhamnopyranosyl-(1 \rightarrow 2)- β -D-xylopyranosyl-(1 \rightarrow 2)- β -D-glucuronopyranosyl sequence (Table 3; Figs 1 and 2).

The monosaccharides obtained by acid hydrolysis of **1** were identified by comparison on thin-layer chromatography (TLC) with authentic samples as glucuronic acid, xylose, and rhamnose. The absolute configurations of the sugars were determined to be D for GlcA and Xyl and L for Rha by GC analysis according to a method previously described.^[13] The large $^1J_{\text{H-1,C-1}}$ value of the Rha (167 Hz) confirmed that the anomeric proton was equatorial (α -pyranoid anomeric form). The relatively large $^3J_{\text{H-1,H-2}}$ value of GlcA and Xyl (6.9 and 7.3 Hz, respectively) in their pyranose form indicated their β anomeric orientation. The same protocol was used for the identification of the monosaccharides of **2** and **3**.

On the basis of the previous results, the structure of **1** was elucidated as the new 3-O- α -L-rhamnopyranosyl-(1 \rightarrow 2)- β -D-xylopyranosyl-(1 \rightarrow 2)- β -D-glucuronopyranosyl-22,28-O-diacetylolean-12-ene-3 β ,16 β ,22 β ,28-tetrol (**1**).

The HR-ESIMS (positive-ion mode) spectrum of compound **2** showed a pseudo-molecular ion peak at m/z 1023.5269 [$\text{M} + \text{Na}$]⁺ (calcd 1023.5141) ascribable to the molecular formula $\text{C}_{50}\text{H}_{80}\text{O}_{20}$. Its ESIMS (positive-ion mode) displayed a quasi-molecular ion peak at m/z 1023 [$\text{M} + \text{Na}$]⁺, indicating a molecular weight of 1000.

The ^1H NMR spectrum of the aglycone part of **2** displayed signals assignable to seven angular methyl groups at δ_{H} 0.74, 0.83, 0.92,

1.01, 1.03, 1.22, and 1.28 (3H, s, each), one olefinic proton at δ_{H} 5.22 (1H, br t, $J = 3.1$, H-12), three oxygen bearing methine protons at δ_{H} 3.21 (1H, dd, $J = 11.9, 3.6$ Hz, H-3_{ax}), 4.53 (1H, dd, $J = 12.5, 4.1$ Hz, H-16_{ax}), and 6.24 (1H, br s, H-22_{eq}), and one free primary alcoholic function at δ_{H} 4.25 (1H, d, $J = 12.3$ Hz, H-28_{aeq}), 4.93 (1H, d, $J = 12.3$ Hz, H-28_{b_{eq}})/ δ_{C} 63.0. In the ^{13}C NMR spectrum, a signal at δ_{C} 170.2 suggested an ester function and a HSQC correlation at δ_{H} 2.07 (3H, s)/ δ_{C} 21.0 revealed the presence of only one acetyl group. These signals suggested that the aglycone of **2** is a 22-O-acetylated derivative of the aglycone of **1** (Table 1, Fig. 1).

The HSQC spectrum of **2** displayed signals of three anomers at δ_{H} 4.81 (1H, d, $J = 7.1$ Hz)/ δ_{C} 104.8, 5.50 (1H, d, $J = 7.4$ Hz)/ δ_{C} 101.9, and 6.18 (1H, br s)/ δ_{C} 101.6. According to the same protocol as for compound **1**, units of one β -D-glucuronopyranosyl, one β -D-glucopyranosyl, and one α -L-rhamnopyranosyl were identified (Table 3). NOESY correlations were mainly used to establish the structure of the oligosaccharidic chain, between δ_{H} 4.81 (1H, d, $J = 7.1$ Hz, GlcA-1)/ δ_{H} 3.21 (1H, dd, $J = 11.9, 3.6$ Hz, H-3_{ax}), δ_{H} 5.50 (1H, d, $J = 7.4$ Hz, Glc-1)/ δ_{H} 4.44 (1H, dd, $J = 8.1, 7.1$ Hz, GlcA-2), and δ_{H} 6.18 (1H, br s, Rha-1)/ δ_{H} 4.12 (1H, dd, $J = 8.4, 7.4$ Hz, Glc-2) (Table 3, Fig. 1).

The structure of the new natural compound **2** was thus established as 3-O- α -L-rhamnopyranosyl-(1 \rightarrow 2)- β -D-glucopyranosyl-(1 \rightarrow 2)- β -D-glucuronopyranosyl-22-O-acetylolean-12-ene-3 β ,16 β ,22 β ,28-tetrol (**2**).

The HR-ESIMS (positive-ion mode) spectrum of compound **3** established its molecular formula as $\text{C}_{49}\text{H}_{76}\text{O}_{20}$ with a pseudo-molecular peak at m/z 1007.4881 [$\text{M} + \text{Na}$]⁺ (calcd 1007.4828). Its

Table 1. ^{13}C NMR and ^1H NMR data of the aglycones of compounds **1-3** in Pyridine- d_5 / D_2O (δ ppm, J in Hz)

Position	1		2		3	
	δ_{C}	δ_{H}	δ_{C}	δ_{H}	δ_{C}	δ_{H}
1	38.6	0.82 (1H, m) 1.34 (1H, m)	38.7	0.78 (1H, m) 1.33 (1H, m)	38.5	0.79 (1H, m) 1.29 (1H, m)
2	26.1	1.81 (1H, m) 2.33 (1H, m)	26.1	1.92 (1H, m) 2.25 (1H, m)	26.2	1.86 (1H, m) 2.45 (1H, m)
3	89.6	3.23 (1H, dd, 12.0, 3.8)	90.6	3.21 (1H, dd, 11.9, 3.6)	90.9	3.37 (1H, dd, 12.0, 3.7)
4	39.4	—	39.4	—	43.7	—
5	55.5	0.67 (1H, br d, 10.8)	55.5	0.65 (1H, br d, 10.5)	55.9	0.79 (1H, br d, 10.8)
6	18.3	1.22 (1H, m) 1.39 (1H, m)	18.2	1.18 (1H, m) 1.39 (1H, m)	18.4	1.21 (1H, m) 1.52 (1H, m)
7	32.3	1.20 (1H, m) 1.40 (1H, m)	32.8	1.20 (1H, m) 1.40 (1H, m)	32.5	1.17 (1H, m) 1.38 (1H, m)
8	40.0	—	39.9	—	39.8	—
9	47.3	1.46 (1H, dd, 14.0, 7.0)	47.0	1.46 (1H, dd, 14.0, 6.9)	47.3	1.48 (1H, dd, 13.9, 6.8)
10	36.3	—	36.5	—	36.1	—
11	23.5	1.66 (1H, m) 1.75 (1H, m)	23.8	1.70 (1H, m) 1.74 (1H, m)	23.7	1.62 (1H, m) 1.68 (1H, m)
12	123.3	5.28 (1H, br t, 3.0)	122.3	5.22 (1H, br t, 3.1)	123.1	5.46 (1H, br t, 3.0)
13	141.7	—	141.5	—	144.5	—
14	42.8	—	43.1	—	41.7	—
15	36.5	1.65 (1H, dd, 13.3, 4.0) 2.24 (1H, dd, 13.3, 12.4)	37.0	1.72 (1H, dd, 13.4, 4.1) 2.17 (1H, dd, 13.4, 12.5)	25.9	1.70 (1H, m) 1.88 (1H, m)
16	66.4	4.53 (1H, dd, 12.4, 4.0)	68.0	4.53 (1H, dd, 12.5, 4.1)	26.2	0.96 (1H, m) 1.80 (1H, m)
17	46.7	—	46.2	—	36.0	—
18	43.1	2.57 (1H, dd, 13.4, 3.4)	42.2	2.38 (1H, dd, 13.0, 3.0)	44.5	2.84 (1H, dd, 12.8, 3.6)
19	45.8	1.18 (1H, dd, 13.6, 3.4) 1.91 (1H, dd, 13.6, 13.4)	46.3	1.16 (1H, dd, 13.3, 3.0) 1.86 (1H, dd, 13.3, 13.0)	41.7	1.72 (1H, dd, 13.2, 3.6) 2.30 (1H, dd, 13.2, 12.8)
20	29.9	—	30.0	—	43.7	—
21	37.7	1.74 (overlapped) 2.86 (1H, br d, 13.6)	37.6	1.75 (overlapped) 2.90 (1H, br d, 14.0)	35.2	1.63 (overlapped) 2.81 (1H, br d, 13.6)
22	71.3	6.10 (1H, br s)	70.2	6.24 (1H, br s)	78.1	4.77 (1H, br s)
23	27.9	1.22 (3H, s)	28.0	1.22 (3H, s)	22.5	1.39 (3H, s)
24	16.7	0.98 (3H, s)	16.2	1.01 (3H, s)	62.6	3.35 (1H, d, 11.2) 4.20 (overlapped)
25	15.2	0.75 (3H, s)	15.1	0.74 (3H, s)	15.2	0.59 (3H, s)
26	16.7	1.01 (3H, s)	16.3	0.92 (3H, s)	16.5	0.83 (3H, s)
27	27.3	1.28 (3H, s)	27.2	1.28 (3H, s)	26.3	1.23 (3H, s)
28	64.7	4.23 (1H, d, 12.4) 4.86 (1H, d, 12.4)	63.0	4.25 (1H, d, 12.3) 4.93 (1H, d, 12.3)	21.1	0.91 (3H, s)
29	33.4	0.85 (3H, s)	34.0	0.83 (3H, s)	29.9	1.26 (3H, s)
30	26.9	1.07 (3H, s)	27.9	1.03 (3H, s)	180.5	—
at C-22						
COCH_3	170.3	—	170.2	—	170.9	—
CH_3CO	21.1	2.09 (3H, s)	21.0	2.07 (3H, s)	21.1	2.09 (3H, s)
at C-28						
COCH_3	171.1	—	—	—	—	—
CH_3CO	20.9	2.01 (3H, s)	—	—	—	—

ESIMS (positive-ion mode) displayed a quasi-molecular ion peak at m/z 1007 $[\text{M} + \text{Na}]^+$, indicating a molecular weight of 984.

The NMR signals of compound **3** sugar portion were superimposable to those of **1** (Table 3). Moreover, the oligosaccharidic chain 3-*O*- α -L-rhamnopyranosyl-(1 \rightarrow 2)- β -D-xylopyranosyl-(1 \rightarrow 2)- β -D-glucuronopyranosyl was linked at the C-3 position of the aglycone according to the NOESY cross-peak at δ_{H} 3.37 (1H, dd, $J=12.0, 3.7$ Hz, H-3_{ax})/ δ_{H} 4.79 (1H, d, $J=6.9$ Hz, GlcA-1). The ^1H

NMR spectrum area corresponding to the aglycone part of **3** showed six tertiary methyl groups as singlets at δ_{H} 0.59, 0.83, 0.91, 1.23, 1.26, 1.39, (3H, s, each), one olefinic proton at δ_{H} 5.46 (1H, br t, $J=3.0$ Hz, H-12), three oxygen bearing methine protons at δ_{H} 3.37 (1H, dd, $J=12.0, 3.7$ Hz, H-3_{ax}) and 4.77 (1H, br s, H-22_{eq}), and one free primary alcoholic function at δ_{H} 3.35 (1H, d, $J=11.2$ Hz, H-24_{ax}), 4.20 (H-24_{ax})/ δ_{C} 62.6. In the ^{13}C NMR spectrum, a signal at δ_{C} 180.5 suggested a free carboxylic acid group and another

Table 2. Key HMBC (H→C) and NOESY correlations of the aglycone of compound **1** (δ_{H} , ppm)

Position	1		
	δ_{H}	HMBC (H→C)	NOESY
H-3 _{ax}	3.23		GlcA1, H ₃ -23 _{eq} , H-5 _{ax}
H-5 _{ax}	0.67	C-4, C-6, C-9, C-10, C-25, C-24	H-9 _{ax} , H-3 _{ax} , H ₃ -23 _{eq}
H-9 _{ax}	1.46	C-1, C-5, C-8, C-10, C-11, C-14, C-25	H-5 _{ax}
H-16 _{ax}	4.53	C-15, C-17, C-28	H ₃ -27 _{ax} , H-22 _{eq} , H-21 _{ax}
H-18 _{ax}	2.57	C-13, C-16, C-17, C-19, C-28	H ₂ -28 _{eq} , H-12
H-21 _{ax}	1.74	C-22, C-20, C-29	H-22 _{eq} , H-16 _{ax}
H-21 _{eq}	2.86		H-21 _{ax}
H-22 _{eq}	6.10	C-16, C-17, C-18, C-20, C-21	H-16 _{ax} , H-21 _{ax}
H ₃ -23 _{eq}	1.22	C-3, C-4, C-5, C-24	H-3 _{ax} , H-5 _{ax} , H-9 _{ax}
H ₃ -24 _{ax}	0.98	C-3, C-4, C-5, C-23	H ₃ -25 _{ax}
H ₃ -25 _{ax}	0.75	C-1, C-5, C-9, C-10	H ₃ -26 _{ax} , H ₃ -24 _{ax}
H ₃ -26 _{ax}	1.01	C-7, C-8, C-9, C-14	H ₃ -25 _{ax} , H ₂ -28 _{eq}
H ₃ -27 _{ax}	1.28	C-8, C-13, C-14, C-15	H-16 _{ax} , H-9 _{ax}
H-28 _{ax}	4.23	C-16, C-17, C-18	H-18 _{ax} , H ₃ -26 _{ax} , H-28 _b _{eq}
H-28 _b _{eq}	4.86	C-16, C-17, C-18	H ₃ -26 _{ax}
H ₃ -29 _{eq}	0.85	C-19, C-20, C-21, C-30	H-21 _{ax} , H ₃ -30 _{ax}
H ₃ -30 _{ax}	1.07	C-19, C-20, C-21, C-29	H ₃ -29 _{eq} , H-18 _{ax}

signal at δ_{C} 170.9, an ester function. The HSQC correlation at δ_{H} 2.09 (3H, s)/ δ_{C} 21.1 confirmed the presence of one acetyl group.

An HMBC correlation between δ_{H} 0.91 (3H, s, H₃-28_{eq}) and δ_{C} 78.1 (C-22) allowed the location of one secondary alcoholic function at C-22. The deshielded value of the C-22 signal was in accordance with an acetylation as described in the previous compounds **1** and **2**. In the same way, a HMBC cross-peak at δ_{H} 1.39 (3H, s, H₃-23_{eq}) and δ_{C} 62.6 (C-24) placed the primary alcoholic function at the C-24 position. NOESY correlations between H₃-23 α -equatorial and H-3 α -axial and H-5 α -axial confirmed the location of the CH₂OH group at the 24 β -axial position. The configuration of C-22 was determined by the connectivity observed in the NOESY spectrum between H-22 α -equatorial and H₃-27 α -axial. The lack of NOESY correlations between H₃-30_{ax} and H-18_{ax} and H₃-28_b_{eq} suggested the location of the carboxylic acid group at the C-30 position. The structure of the aglycone was thus recognized as an acetylated derivative of the 3 β ,22 β ,24-trihydroxyolean-12-en-30-oic acid (Table 1, Fig. 1).

On the basis of these results and the literature data, the structure of compound **3** was elucidated as 3-*O*- α -L-rhamnopyranosyl-(1→2)- β -D-xylopyranosyl-(1→2)- β -D-glucuronopyranosyl-22-*O*-acetyl-3 β ,22 β ,24-trihydroxyolean-12-en-30-oic acid (**3**). This saponin, named wistariasaponin G, was already isolated from *W. brachybotrys*, but its structural analysis was performed after methylation.^[6] For the first time, we have described the structural elucidation of its native form.

Experimental

General experimental procedures

Optical rotations values were recorded on a AA-10R automatic polarimeter (Optical Activity LTD, Ramsey, U.K.). HR-ESIMS (positive-ion mode) and ESIMS (positive- and negative-ion mode) were carried out on a Bruker micrOTOF mass spectrometer. A R.E.U.S ultrasonic apparatus (Contes, France) was used for the extraction. Isolations of compounds were carried out using column chromatography on Sephadex LH-20 (550 × 20 mm, GE Healthcare Bio-

Sciences AB, Uppsala, Sweden) and VLC on reversed-phase RP-18 silica gel (75–200 μ m, Silicycle (Quebec City (Quebec, Canada)). MPLC was performed on silica gel 60 (Merck (Darmstadt, Germany), 15–40 μ m) with a Gilson M 305 pump (25 SC head pump, M 805 manometric module), a Büchi glass column (460 × 25 mm and 460 × 15 mm), and a Büchi precolumn (110 × 15 mm). TLC (Silicycle) and high-performance TLC (Merck) were carried out on precoated silica gel plates 60 F₂₅₄, solvent system CHCl₃/MeOH/H₂O/AcOH (60:32:7:1 and 70:30:5:1). The spray reagent for saponins was vanillin reagent (1% vanillin in EtOH/H₂SO₄, 50:1).

Nuclear magnetic resonance spectra

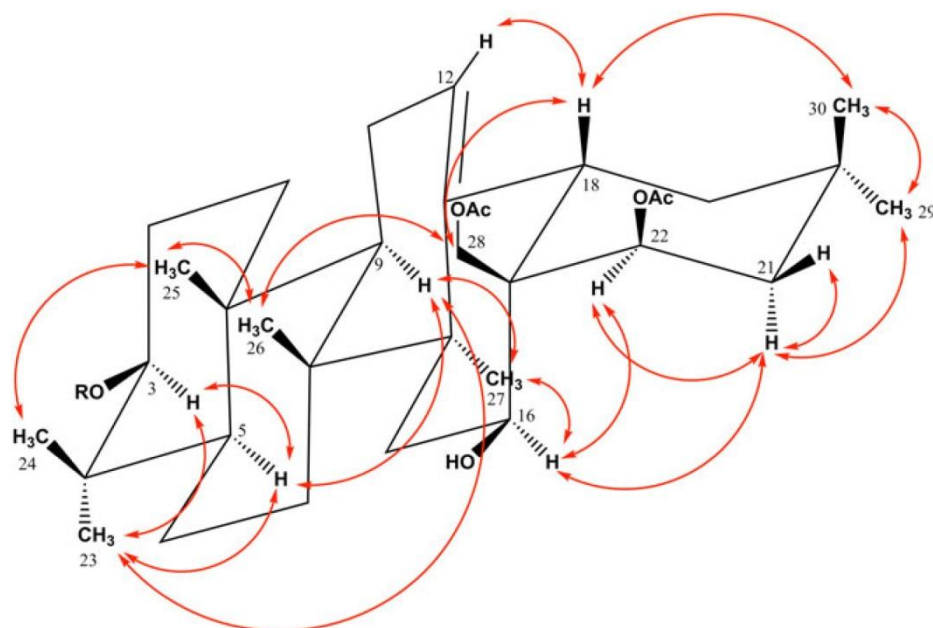
Spectra were performed using a Varian INOVA 600 (Agilent Technologies, California, USA) at the operating frequency of 600 MHz. The operating conditions were as follows: ¹H: frequency, 600 MHz; sweep width, 8 kHz; sampling point, 66 k; spectral width, 7804 Hz, accumulation, 32 pulses; and temperature, 304 K. ¹³C: frequency, 150 MHz; sweep width, 32 kHz; sampling point, 160 k; spectral width, 30,000 Hz, accumulation, 8000 pulses; and temperature, 304 K. Each samples (4–7 mg) were dissolved in C₅D₅N/D₂O (20/1, 200 μ l) using 5-mm micro-sample tube (SHIGEMI Co., Ltd., Japan). Chemical shifts were referenced to solvent signal (δ_{H} 7.22, δ_{C} 123.87). Conventional pulse sequences were used for gMQF-COSY, TOCSY, NOESY, gHSQC, and gHMBC. The mixing time in the NOESY experiment was set to 500 ms. TOCSY spectra were acquired using the standard MLEV17 spin-locking sequence and 60-ms mixing time. TOCSY, NOESY, and HSQC spectra were recorded using phase-sensitive mode. The size of the acquisition data matrix was 2048 × 256 words in f2 and f1, respectively, and zero filling up to 2 k in f1 was made prior to Fourier transformation. Sine-bell or Shifted sine-bell window functions, with the corresponding shift optimized for every spectrum, were used for resolution enhancement, and baseline correction was applied in both dimensions.

Plant material

Wisteria frutescens was provided in 2011 from Botanic® (Quéigny, France). A voucher specimen (N° 20111002) was deposited in the

Table 3. ^{13}C NMR and ^1H NMR data of the sugar moieties of compounds **1-3** in Pyridine- d_5/D_2O (δ ppm, J in Hz)

Position	1		2		3	
	δ_{C}	δ_{H}	δ_{C}	δ_{H}	δ_{C}	δ_{H}
GlcA-1	104.8	4.83 (1H, d, 6.9)	104.8	4.81 (1H, d, 7.1)	104.7	4.79 (1H, d, 6.9)
2	78.4	4.23 (1H, dd, 8.0, 6.9)	77.8	4.44 (1H, dd, 8.1, 7.1)	77.3	4.17 (1H, dd, 8.1, 6.9)
3	75.7	4.22 overlapped	75.9	4.22 (1H, dd, 8.1, 7.0)	75.7	4.22 overlapped
4	73.8	4.12 (1H, dd, 8.3, 6.9)	73.5	4.10 (1H, dd, 8.3, 7.0)	73.7	4.13 (1H, dd, 8.3, 6.9)
5	78.4	4.44 (1H, d, 8.3)	78.0	4.42 (1H, d, 8.3)	77.8	4.42 (1H, d, 8.3)
6	172.7	—	173.0	—	172.8	—
Xyl-1	102.1	5.53 (1H, d, 7.3)			102.2	5.42 (1H, d, 7.4)
2	77.5	4.14 (1H, dd, 8.8, 7.3)			78.4	4.19 (1H, dd, 8.5, 7.4)
3	78.7	4.07 (1H, dd, 8.8, 7.6)			78.8	3.99 (1H, dd, 8.5, 6.9)
4	70.5	4.31 m			70.3	4.31 m
5	66.3	3.47 (1H, dd, 11.2, 10.2) 4.24 (1H, dd, 11.2, 5.3)			66.3	3.38 (1H, dd, 11.9, 9.5) 4.29 (1H, dd, 11.9, 5.2)
Glc-1			101.9	5.50 (1H, d, 7.4)		
2			78.1	4.12 (1H, dd, 8.4, 7.4)		
3			78.2	4.08 (1H, t, 9.1)		
4			70.6	4.28 (1H, t, 9.0)		
5			77.4	3.80 m		
6			62.6	4.05 (1H, dd, 10.5, 4.5) 4.52 (1H, dd, 10.5, 1.7)		
Rha-1	101.6	6.20 (1H, br s)	101.6	6.18 (1H, br s)	101.7	6.14 (1H, br s)
2	71.8	4.66 (1H, br s)	72.0	4.68 (1H, br s)	71.8	4.67 (1H, br s)
3	71.9	4.63 (1H, dd, 9.2, 2.5)	72.0	4.62 (1H, dd, 9.0, 2.5)	71.9	4.61 (1H, dd, 9.1, 2.4)
4	73.8	4.27 (1H, t, 9.2)	73.8	4.26 (1H, t, 9.0)	73.3	4.27 (1H, t, 9.1)
5	69.1	4.91 (1H, dq, 9.2, 6.6)	69.0	4.95 (1H, dq, 9.0, 6.2)	68.9	4.92 (1H, dq, 9.1, 6.0)
6	18.5	1.71 (1H, d, 6.6)	18.0	1.70 (1H, d, 6.2)	18.4	1.72 (1H, d, 6.0)

**Figure 2.** Significant NOE correlations in NOESY experiment of compound **1**.

herbarium of the Laboratory of Pharmacognosy, Université de Bourgogne Franche-Comté, Dijon, France.

Extraction and isolation

The dried, powdered roots of *W. frutescens* (150 g) were extracted by ultrasound three times with EtOH-H₂O (7/3, 3 × 1 l) for 1 h. After evaporation of the solvent under vacuum, the resulting extract (1.2 g) was submitted to VLC (RP-18 silica gel, H₂O, MeOH/H₂O 30:70, 50:50, 70:30, and MeOH). The fraction eluted with 50:50 MeOH/H₂O (272.1 mg) was fractionated by column chromatography (Sephadex LH-20, MeOH) to give a fraction rich in saponins (74.7 mg), which was submitted to a MPLC on silica gel 60 (15–40 μm, CHCl₃/MeOH/H₂O 70:30:5; 60:32:7). Seven fractions (F1–F7) and a pure compound (**1**, 5.2 mg) were obtained. The remaining fractions were fractionated again by successive MPLC on silica gel RP-18 (MeOH/H₂O 25:75 to 40:60 and MeOH) to give compounds **2** (4.0 mg), **3** (8.1 mg), and wistariasaponin A (13.2 mg). The VLC fraction eluted with 70:30 MeOH/H₂O (104.7 mg) was submitted to a MPLC on silica gel 60 (15–40 μm, CHCl₃/MeOH/H₂O 70:30:5) yielding wistariasaponin C (5 mg) and azukisaponin V (5.1 mg).

Acid hydrolysis and GC analysis

Each compound (3 mg) was hydrolyzed with 2 N aq. CF₃COOH (5 ml) for 3 h at 95 °C. After extraction with CH₂Cl₂ (3 × 5 ml), the aq. layer was repeatedly evaporated to dryness with MeOH until neutral and then analyzed by TLC over silica gel (CHCl₃/MeOH/H₂O 8:5:1) by comparison with authentic samples. Furthermore, the residue of sugars was dissolved in anhydrous pyridine (100 μl), and L-cysteine methyl ester hydrochloride (0.06 mol/l) was added. The mixture was stirred at 60 °C for 1 h, then 150 μl of HMDS-TMCS (hexamethyldisilazane/trimethylchlorosilane 3:1) was added, and the mixture was stirred at 60 °C for another 30 min. The precipitate was centrifuged off, and the supernatant was concentrated under a N₂ stream. The residue was partitioned between *n*-hexane and H₂O (0.1 ml each), and the hexane layer (1 μl) was analyzed by GC.^[13] The absolute configurations were determined by comparing the retention times with thiazolidine derivatives prepared in a similar way from standard sugars (Sigma-Aldrich, St. Louis, MO, USA).

Spectroscopic data

3-*O*- α -L-rhamnopyranosyl-(1 \rightarrow 2)- β -D-xylopyranosyl-(1 \rightarrow 2)- β -D-glucopyranosyl-22,28-*O*-diacetylolean-12-ene-3 β ,16 β ,22 β ,28-tetrol (**1**): white amorphous powder; $[\alpha]_D^{25} = +21.1$ (c 0.90, MeOH); ¹H and ¹³C NMR data (600 and 150 MHz, pyridine-*d*₅/D₂O) (Tables 1 and 3); HR-ESIMS (positive-ion mode): *m/z* 1035.5150 ([M + Na]⁺, calcd for C₅₁H₈₀O₂₀Na, 1035.5141); ESIMS (negative-ion mode): *m/z* 1011 ([M – H][–]).

3-*O*- α -L-rhamnopyranosyl-(1 \rightarrow 2)- β -D-glucopyranosyl-(1 \rightarrow 2)- β -D-glucuronopyranosyl-22-*O*-acetylolean-12-ene-3 β ,16 β ,22 β ,28-tetrol (**2**): white amorphous powder; $[\alpha]_D^{25} = +19.8$ (c 0.80, MeOH); ¹H and ¹³C NMR data (600 and 150 MHz, pyridine-*d*₅/D₂O) (Tables 1 and 3); HR-ESIMS (positive-ion mode): *m/z* 1023.5269 ([M + Na]⁺, calcd for C₅₀H₈₀O₂₀Na, 1023.5141); ESIMS (positive-ion mode): *m/z* 1023 ([M + Na]⁺).

3-*O*- α -L-rhamnopyranosyl-(1 \rightarrow 2)- β -D-xylopyranosyl-(1 \rightarrow 2)- β -D-glucuronopyranosyl-22-*O*-acetyl-3 β ,22 β ,24-trihydroxyolean-12-ene-30-oic acid (**3**): white amorphous powder; $[\alpha]_D^{25} = -30.6$ (c 0.60,

MeOH); ¹H and ¹³C NMR data (600 and 150 MHz, pyridine-*d*₅/D₂O) (Tables 1 and 3); HR-ESIMS (positive-ion mode): *m/z* 1007.4881 ([M + Na]⁺, calcd for C₄₉H₇₆O₂₀Na, 1007.4828); ESIMS (positive-ion mode): *m/z* 1007 ([M + Na]⁺).

Conflict of Interest

The authors declare that they have no conflict of interest.

Anne-Sophie Champy,^{a,c,d} Anne-Claire Mitaine-Offier,^a Tomofumi Miyamoto,^b Chiaki Tanaka,^b Anna-Maria Papini^{c,d,e} and Marie-Aleth Lacaille-Dubois^{a*}

^aLaboratoire de Pharmacognosie, EA 4267, FDE, UFR Sciences de Santé, Université de Bourgogne Franche-Comté, BP 87900, 21079, Dijon Cedex, France

^bGraduate School of Pharmaceutical Sciences, Kyushu University, Fukuoka 812-8582, Japan

^cInterdepartmental Laboratory of Peptide and Protein Chemistry and Biology, University of Florence, 50019, Sesto Fiorentino, Italy

^dDepartment of Chemistry "Ugo Schiff", University of Florence, 50019, Sesto Fiorentino, Italy

^eLaboratory of Chemical Biology EA 4505 & PeptLab@UCP, University of Cergy-Pontoise, 95031, Cergy-Pontoise Cedex, France

*Correspondence to: Marie-Aleth Lacaille-Dubois, Laboratoire de Pharmacognosie, EA 4267, FDE, UFR Sciences de Santé, Université de Bourgogne Franche-Comté, BP 87900, 21079 Dijon Cedex, France.
E-mail: m-a.lacaille-dubois@u-bourgogne.fr

Received: 27 May 2016; Revised: 26 October 2016; Accepted: 1 November 2016

References

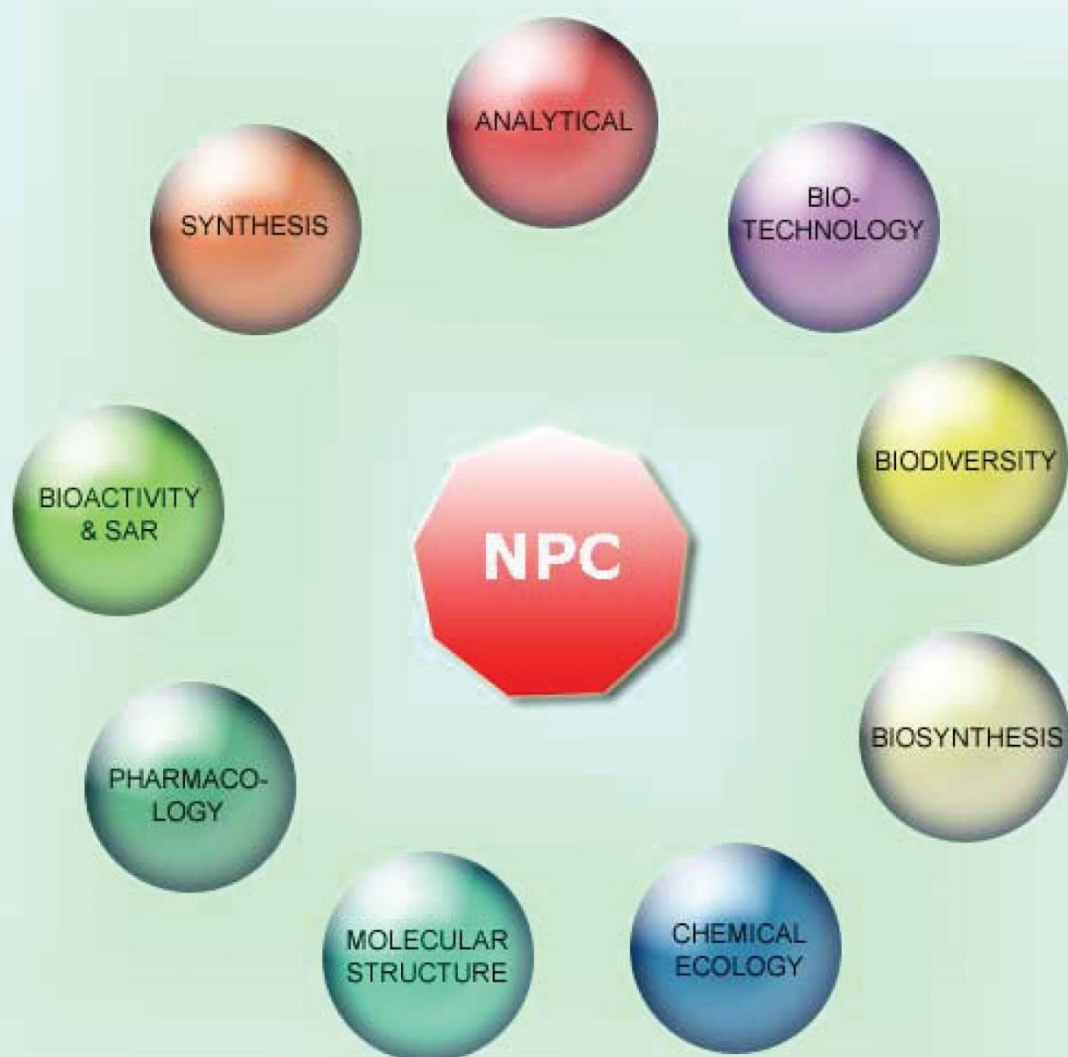
- [1] F. Dupont, J.-L. Guignard, *Botanique*, 15^{ème} éd. edn, Elsevier Masson, Issy-Les-Moulineaux, France, **2012**, pp. 163–170.
- [2] A. Marouf, J. Reynaud, *La botanique de A à Z*, Dunod, Paris, France, **2007**, pp. 106.
- [3] W. Gibbons, R. R. Hayes, J. L. Thomas, *Poisonous Plants and Venomous Animals of Alabama and Adjoining States*, The University of Alabama Press, Tuscaloosa and London, **1990**, pp. 120–121.
- [4] T. Konoshima, M. Kozuka, M. Haruna, K. Ito, T. Kimura. *Chem. Pharm. Bull.* **1989**, *37*, 1550–1553.
- [5] T. Konoshima, M. Kozuka, M. Haruna, K. Ito, T. Kimura, H. Tokuda. *Chem. Pharm. Bull.* **1989**, *37*, 2731–2735.
- [6] T. Konoshima, M. Kozuka, M. Haruna, K. Ito. *J. Nat. Prod.* **1991**, *54*, 830–836.
- [7] J. Kinjo, Y. Fujishima, K. Saino, R.-H. Tian, T. Nohara. *Chem. Pharm. Bull.* **1995**, *43*, 636–640.
- [8] A. M. Dawidar, L. M. Salih, E. M. Keshk, M. Abdel-Mogib. *Res. J. Pharm., Biol. Chem. Sci.* **2015**, *6*, 1327–1336.
- [9] M. A. Mohamed, M. M. Hamed, A. M. Abdou, W. S. Ahmed, A. M. Saad. *Molecules* **2011**, *16*, 4020–4030.
- [10] T. Kaneko, Y. Ide, *Lectins from Wisteria floribunda, Soybean, Lens culinaris and Trichosanthes japonica for Detection of Tumor Antigens with Specific Sugar Chain and for Diagnosis of Cancer*, PCT Int. Appl., Patent, Japan, **2013**, pp. 45.
- [11] I. Kitagawa, H. K. Wang, M. Saito, M. Yoshikawa. *Chem. Pharm. Bull.* **1983**, *31*, 683–688.
- [12] A. K. Chakravarty, B. Das, S. C. Pakrashi. *Phytochemistry* **1987**, *26*, 2345–2349.
- [13] S. Hara, H. Okabe, K. Mihashi. *Chem. Pharm. Bull.* **1987**, *35*, 501–506.

Supporting information

Additional supporting information may be found in the online version of this article at the publisher's web site.

NATURAL PRODUCT COMMUNICATIONS

An International Journal for Communications and Reviews Covering all
Aspects of Natural Products Research



Volume 12. Issue 10. Pages 1529-1672. 2017
ISSN 1934-578X (printed); ISSN 1555-9475 (online)
www.naturalproduct.us

EDITOR-IN-CHIEF

DR. PAWAN K AGRAWAL

Natural Product Inc.
7963, Anderson Park Lane,
Westerville, Ohio 43081, USA
agrawal@naturalproduct.us

EDITORS

PROFESSOR ALEJANDRO F. BARRERO

Department of Organic Chemistry, University of Granada,
Campus de Fuente Nueva, s/n, 18071, Granada, Spain
afbarre@ugr.es

PROFESSOR MAURIZIO BRUNO

Department STEBICEF,
University of Palermo, Viale delle Scienze,
Parco d'Orleans II - 90128 Palermo, Italy
maurizio.bruno@unipa.it

PROFESSOR VLADIMIR I. KALININ

G.B. Elyakov Pacific Institute of Bioorganic Chemistry,
Far Eastern Branch, Russian Academy of Sciences,
Pr. 100-letya Vladivostoka 159, 690022,
Vladivostok, Russian Federation
kalininv@piboc.dvo.ru

PROFESSOR YOSHIHIRO MIMAKI

School of Pharmacy,
Tokyo University of Pharmacy and Life Sciences,
Horinouchi 1432-1, Hachioji, Tokyo 192-0392, Japan
mimakiy@ps.toyaku.ac.jp

PROFESSOR STEPHEN G. PYNE

Department of Chemistry, University of Wollongong,
Wollongong, New South Wales, 2522, Australia
spyne@uow.edu.au

PROFESSOR MANFRED G. REINECKE

Department of Chemistry, Texas Christian University,
Forts Worth, TX 76129, USA
m.reinecke@tcu.edu

PROFESSOR WILLIAM N. SETZER

Department of Chemistry, The University of Alabama in Huntsville,
Huntsville, AL 35809, USA
wsetzer@chemistry.uah.edu

PROFESSOR PING-JYUN SUNG

National Museum of Marine Biology and Aquarium
Checheng, Pingtung 944
Taiwan
pjsung@nmmba.gov.tw

PROFESSOR YASUHIRO TEZUKA

Faculty of Pharmaceutical Sciences, Hokuriku University,
Ho-3 Kanagawa-machi, Kanazawa 920-1181, Japan
y-tezuka@hokuriku-u.ac.jp

PROFESSOR DAVID E. THURSTON

Institute of Pharmaceutical Science
Faculty of Life Sciences & Medicine
King's College London, Britannia House
7 Trinity Street, London SE1 1DB, UK
david.thurston@kcl.ac.uk

HONORARY EDITOR

PROFESSOR GERALD BLUNDEN

The School of Pharmacy & Biomedical Sciences,
University of Portsmouth,
Portsmouth, PO1 2DT U.K.
axu64@dsl.pipex.com

ADVISORY BOARD

Prof. Giovanni Appendino
Novara, Italy

Prof. Norbert Arnold
Halle, Germany

Prof. Yoshinori Asakawa
Tokushima, Japan

Prof. Vassaya Bankova
Sofia, Bulgaria

Prof. Roberto G. S. Berlinck
São Carlos, Brazil

Prof. Anna R. Bilia
Florence, Italy

Prof. Geoffrey Cordell
Chicago, IL, USA

Prof. Fatih Demirci
Eskişehir, Turkey

Prof. Francesco Epifano
Chieti Scalo, Italy

Prof. Ana Cristina Figueiredo
Lisbon, Portugal

Prof. Cristina Gracia-Viguera
Murcia, Spain

Dr. Christopher Gray
Saint John, NB, Canada

Prof. Dominique Guillaume
Reims, France

Prof. Duvvuru Gunasekar
Tirupati, India

Prof. Hisahiro Hagiwara
Niigata, Japan

Prof. Judith Hohmann
Szeged, Hungary

Prof. Tsukasa Iwashina
Tsukuba, Japan

Prof. Leopold Jirovetz
Vienna, Austria

Prof. Phan Van Kiem
Hanoi, Vietnam

Prof. Niel A. Koorbanally
Durban, South Africa

Prof. Chiaki Kuroda
Tokyo, Japan

Prof. Hartmut Laatsch
Gottingen, Germany

Prof. Marie Lacaille-Dubois
Dijon, France

Prof. Shoen-Sheng Lee
Taipei, Taiwan

Prof. M. Soledade C. Pedras
Saskatoon, Canada

Prof. Luc Pieters
Antwerp, Belgium

Prof. Peter Proksch
Düsseldorf, Germany

Prof. Phila Raharivelomanana
Tahiti, French Polynesia

Prof. Stefano Serra
Milano, Italy

Dr. Bikram Singh
Palampur, India

Prof. Leandros A. Skaltsounis
Zografou, Greece

Prof. John L. Sorensen
Manitoba, Canada

Prof. Johannes van Staden
Scottsville, South Africa

Prof. Valentin Stonik
Vladivostok, Russia

Prof. Winston F. Tinto
Barbados, West Indies

Prof. Sylvia Urban
Melbourne, Australia

Prof. Karen Valant-Vetschera
Vienna, Austria

INFORMATION FOR AUTHORS

Full details of how to submit a manuscript for publication in Natural Product Communications are given in Information for Authors on our Web site <http://www.naturalproduct.us>.

Authors may reproduce/republish portions of their published contribution without seeking permission from NPC, provided that any such republication is accompanied by an acknowledgment (original citation)-Reproduced by permission of Natural Product Communications. Any unauthorized reproduction, transmission or storage may result in either civil or criminal liability.

The publication of each of the articles contained herein is protected by copyright. Except as allowed under national "fair use" laws, copying is not permitted by any means or for any purpose, such as for distribution to any third party (whether by sale, loan, gift, or otherwise); as agent (express or implied) of any third party; for purposes of advertising or promotion; or to create collective or derivative works. Such permission requests, or other inquiries, should be addressed to the Natural Product Inc. (NPI). A photocopy license is available from the NPI for institutional subscribers that need to make multiple copies of single articles for internal study or research purposes.

To Subscribe: Natural Product Communications is a journal published monthly. 2017 subscription price: US\$2,595 (Print, ISSN# 1934-578X); US\$2,595 (Web edition, ISSN# 1555-9475); US\$2,995 (Print + single site online); US\$595 (Personal online). Orders should be addressed to Subscription Department, Natural Product Communications, Natural Product Inc., 7963 Anderson Park Lane, Westerville, Ohio 43081, USA. Subscriptions are renewed on an annual basis. Claims for nonreceipt of issues will be honored if made within three months of publication of the issue. All issues are dispatched by airmail throughout the world, excluding the USA and Canada.

Triterpene Saponins from *Wisteria floribunda* “macrobotrys” and “rosea”Anne-Sophie Champy^{a,c,d}, Anne-Claire Mitaine-Offer^a, Thomas Paululat^b, Anna-Maria Papini^{c,d,e} and Marie-Aleth Lacaille-Dubois^{a*}^aLaboratoire de Pharmacognosie, PEPITE EA 4267, UFR des Sciences de Santé, Université de Bourgogne Franche-Comté, BP 87900, 21079 Dijon cedex, France^bUniversität Siegen, OC-II, Naturwissenschaftlich-Technische Fakultät, Adolf-Reichwein-Str.2, D-57076, Siegen, Germany^cInterdepartmental Laboratory of Peptide and Protein Chemistry and Biology, University of Florence, 50019 Sesto Fiorentino, Italy^dDepartment of Chemistry “Ugo Schiff”, University of Florence, 50019 Sesto Fiorentino, Italy^eLaboratory of Chemical Biology EA 4505 & PeptLab@UCP, University of Cergy-Pontoise, 95031 Cergy-Pontoise cedex, France

m-a.lacaille-dubois@u-bourgogne.fr

Received: June 13th, 2017; Accepted: September 8th, 2017

Five oleanane-type saponins were isolated from two cultivars of *Wisteria floribunda* (Willd.) DC. (Fabaceae): From the roots of *Wisteria floribunda* “macrobotrys”, one new oleanane derivative elucidated as 3-*O*-β-D-xylopyranosyl-(1→2)-β-D-glucuronopyranosyl-22-*O*-acetyl-3β,22β,24-trihydroxyolean-12-en-30-oic acid, and two known glycosides, and from the roots of *Wisteria floribunda* “rosea”, two known ones. Their structures were elucidated by a detailed 600 MHz NMR analysis including 1D and 2D NMR (¹H, ¹³C, COSY, TOCSY, ROESY, HSQC, HMBC) experiments and mass spectrometry. Chemotaxonomic conclusions were proposed.

Keywords: 2D NMR, Oleanane-type glycosides, *Wisteria floribunda* “macrobotrys”, *Wisteria floribunda* “rosea”, Fabaceae.

Wisteria Nutt. (also spelled *Wistaria* Spreng. [1]) is a genus of woody vines of the Fabaceae family, very appreciated in horticulture for a garden use. From a phytochemical point of view, triterpene saponins were previously isolated from different species as *W. brachybotrys* Sieb. & Zucc., and *W. frutescens* (L.) Poir. [2-6]. As part as our phytochemical study of the *Wisteria* genus, two cultivars of *W. floribunda* (Willd.) DC., “rosea” and “macrobotrys”, were studied. *W. floribunda*, also called the “Japanese *Wisteria*”, occurs in Japan and Korea [7,8]. Ten flavonoids were previously isolated and identified from the flowers [9]. The cultivar “rosea” differs mainly by its pink flowers contrary to “macrobotrys” with huge purple and white flowers grapes, which can measure until one meter. In this paper, we report about the isolation and characterization of five saponins from these horticultural species. Their structures were elucidated by a detailed 600 MHz NMR analysis including 1D and 2D NMR (¹H, ¹³C, COSY, TOCSY, ROESY, HSQC, HMBC) experiments and mass spectrometry. From the roots of *W. floribunda* “macrobotrys”, a previously undescribed saponin was isolated and its structure was elucidated as 3-*O*-β-D-xylopyranosyl-(1→2)-β-D-glucuronopyranosyl-22-*O*-acetyl-3β,22β,24-trihydroxyolean-12-en-30-oic acid (1), together with two known ones previously isolated from *W. frutescens*, 3-*O*-α-L-rhamnopyranosyl-(1→2)-β-D-xylopyranosyl-(1→2)-β-D-glucuronopyranosyl-22-*O*-acetyl-3β,22β,24-trihydroxyolean-12-en-30-oic acid (2) and 3-*O*-α-L-rhamnopyranosyl-(1→2)-β-D-xylopyranosyl-(1→2)-β-D-glucuronopyranosyl-22,28-*O*-diacetylolean-12-ene-3β,16β,22β,28-tetrol (3) [2]. From the roots of *W. floribunda* “rosea”, two known saponins were identified as 3-*O*-α-L-rhamnopyranosyl-(1→2)-β-D-xylopyranosyl-(1→2)-β-D-glucuronopyranosyl-olean-12-ene-3β,22β,24-triol (4)

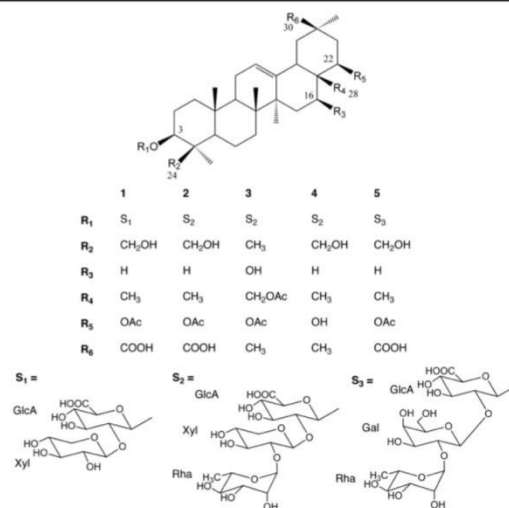


Figure 1: Structure of compounds 1-5.

(Astragaloside VIII) [10], and 3-*O*-α-L-rhamnopyranosyl-(1→2)-β-D-galactopyranosyl-(1→2)-β-D-glucuronopyranosyl-22-*O*-acetyl-3β,22β,24-trihydroxyolean-12-en-30-oic acid (5) (Millettiasaponin A) [11].

Compound 1 was isolated from an aqueous-ethanolic extract of the roots of *W. floribunda* “macrobotrys” by various solid/liquid chromatographic methods: Vacuum Liquid Chromatography (VLC)

Table 1: ^{13}C NMR and ^1H NMR data of compound **1** in Pyridine- d_5 (δ in ppm).

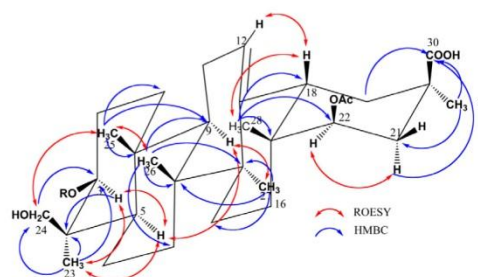
Position	δ_{C}	δ_{H} (J in Hz)
Aglycon		
1	38.8	0.91 (m), 1.47 (m)
2	26.2	1.94 (m), 2.49 (m)
3	89.9	3.46
4	44.0	-
5	56.2	0.88 (br d, $J = 10.5$)
6	18.7	1.43 (m), 1.66 (m)
7	32.8	1.26 (m), 1.45 (m)
8	39.9	-
9	47.5	1.58 (d, $J = 14.0, 6.8$)
10	36.4	-
11	23.8	1.78 m, 1.82 m
12	123.3	5.46 (br t, $J = 3.0$)
13	144.0	-
14	41.7	-
15	26.1	1.78 (m), 1.90 (m)
16	25.9	0.98 (m), 1.76 (m)
17	36.0	-
18	44.0	2.82 (dd, $J = 12.8, 3.4$)
19	41.5	1.79 (dd, $J = 13.5, 3.4$), 2.22 (dd, $J = 13.5, 12.8$)
20	40.6	-
21	35.0	1.74 (dd, $J = 13.6, 3.0$), 2.69 (brd, $J = 13.6$)
22	77.8	4.75 (br s)
23	22.6	1.36 (s)
24	62.7	3.48 (d, $J = 11.2$), 4.25 (d, $J = 11.2$)
25	15.4	0.82 (s)
26	16.7	0.91 (s)
27	26.2	1.26 (s)
28	21.2	0.93 (s)
29	29.7	1.27 (s)
30	179.2	-
Acetyl at C-22		
CO	170.2	-
CH ₃	21.1	2.07 (s)
GlcA-1		
2	104.3	4.77 d (7.6)
3	81.1	4.00 dd (8.4, 7.6)
4	78.2	4.11 dd (8.4, 8.0)
5	73.4	3.97
6	75.0	3.98
7	174.7	-
Xyl-1		
2	105.2	5.21 d (6.9)
3	75.4	3.84
4	78.0	3.83
5	70.4	4.02
	66.8	3.47 (dd, $J = 12.0, 10.0$), 4.22 (dd, $J = 12.0, 5.6$)

Overlapped proton signals are reported without designated multiplicity.

on normal and reverse phase RP-18 silica gel, Medium Pressure Liquid Chromatography (MPLC), size exclusion Column Chromatography on Sephadex LH-20 (CC), and High Performance Liquid Chromatography (HPLC).

The HR-ESIMS (positive-ion mode) of **1** established its molecular formula as $\text{C}_{43}\text{H}_{66}\text{O}_{16}$ with a pseudo-molecular ion peak at m/z 861.4268 $[\text{M} + \text{Na}]^+$ (calcd 861.4249). Its ESIMS (negative-ion mode) displayed a quasi-molecular ion peak at m/z 837 $[\text{M} - \text{H}]^-$, indicating a molecular weight of 838.

The ^1H NMR spectrum of the aglycon part displayed signals assignable to six angular methyl groups as singlets at δ_{H} 0.82 (H_3 -25), 0.91 (H_3 -26), 0.93 (H_3 -28), 1.26 (H_3 -27), 1.27 (H_3 -29), 1.36 (H_3 -23), one olefinic proton at δ_{H} 5.46 (br t, $J = 3.0$ Hz) (H-12), two oxygen-bearing methine protons at δ_{H} 3.46 (H-3) and 4.75 (br s) (H-22), and one primary alcoholic function at δ_{H} 3.48 (d, $J = 11.2$ Hz), 4.25 (d, $J = 11.2$ Hz) (H_2 -24) (Table 1). A signal in the ^{13}C NMR spectrum at δ_{C} 179.2 suggested a carbonyl function of a free carboxylic acid group. Another one at δ_{C} 170.2 suggested a

**Figure 2:** Key HMBC and ROESY correlations for the aglycon of **1**.

carbonyl function of an acetyl group, which was confirmed by a HMBC cross-peak at δ_{H} 2.07 (s)/ δ_{C} 170.2, and a HSQC correlation at δ_{H} 2.07 (s)/ δ_{C} 21.1. The HMBC correlation between an angular methyl group at δ_{H} 1.36 (s, H_3 -23) and δ_{C} 89.9 (C-3), allowed the location of the first secondary alcoholic function at C-3.

The second one was located at C-22, by observation of a HMBC correlation at δ_{H} 0.93 (s, H_3 -28)/ δ_{C} 77.8 (C-22). The deshielded chemical shift of H-22 at δ_{H} 4.75 suggested an acetylation at the C-22 position. In the HMBC spectrum, a cross-peak between δ_{H} 1.36 (H_3 -23) and δ_{C} 62.7 (C-24) allowed the location of the primary alcoholic function at C-24 position. More correlations were observed between δ_{H} 1.27 (s, H_3 -29), 1.74 (dd, $J = 13.6, 3.0$, H-21), and 1.79 (dd, $J = 13.5, 3.4$, H-19), and δ_{C} 179.2, to find the location of the free carboxylic group at the C-30 position. The lack of ROESY correlations between H_3 -30 β_{ax} and H-18 β_{ax} and H₃-28 β_{eq} suggested the location of the carboxylic acid group at the C-30 position. The configuration of C-3 was determined by the interactions observed in the ROESY spectrum between H-3 α -axial and H_3 -23 α -equatorial. Moreover, the multiplicity of the H-22 at δ_{H} 4.75 as a (br s), confirmed the α -equatorial orientation of the H-22. The structure of the aglycon of **1** was thus recognized to be the 22-*O*-acetyl-3 β ,22 β ,24-trihydroxyolean-12-en-30-oic acid, previously described in *W. frutescens* [2], *W. brachybotrys* [5], and *Milletia speciosa* Champ. ex Benth. [11] (Table 1, Figures 1 and 2).

In the osidic region, the HSQC spectrum of **1** displayed two anomeric signals at δ_{H} 4.77 (d, $J = 7.6$ Hz)/ δ_{C} 104.3 and δ_{H} 5.21 (d, $J = 6.9$ Hz)/ δ_{C} 105.2. The ring protons of the monosaccharide residues were assigned starting from the readily identifiable anomeric protons by means of the ^1H - ^1H COSY, TOCSY, HSQC, and HMBC experiments. The monosaccharides obtained by acid hydrolysis of **1** were identified by comparison on TLC with authentic samples as glucuronic acid (GlcA) and xylose (Xyl). The absolute configurations of the sugars were determined to be D for GlcA and Xyl by GC analysis according to a method previously described [12]. The relatively large $^3J_{\text{H-1,H-2}}$ value of the GlcA and Xyl (7.6, 6.9 Hz) in their pyranose form indicated a β anomeric orientation for GlcA and Xyl. Units of one β -D-glucuronopyranosyl and one β -D-xylopyranosyl were thus identified (Table 1). The 3-*O*-heterosidic linkage was suggested by a HMBC cross-peak δ_{H} 4.77 (d, $J = 7.6$ Hz, GlcA-1)/ δ_{C} 89.9 (C-3), and a ROESY cross-peak at δ_{H} 4.77 (GlcA-1)/ δ_{H} 3.46 (H-3). The HMBC correlations at δ_{H} 5.21 (d, $J = 6.9$ Hz, Xyl-1)/ δ_{C} 81.1 (GlcA-2) and the ROESY correlation at δ_{H} 5.21 (Xyl-1)/ δ_{H} 4.00 (dd, $J = 8.4, 7.6$, GlcA-2) proved a β -D-xylopyranosyl-(1 \rightarrow 2)- β -D-glucuronopyranosyl sequence (Table 1, Figure 1).

On the basis of the above results, the structure of **1** was elucidated as 3-*O*- β -D-xylopyranosyl-(1 \rightarrow 2)- β -D-glucuronopyranosyl-22-*O*-acetyl-3 β ,22 β ,24-trihydroxyolean-12-en-30-oic acid (**1**).

A literature survey of other *Wisteria* species [2-6, 13,14] and other genera of the Fabaceae [15] such as *Astragalus* L. [16-18], *Glycine* Willd. [19] or *Medicago* L. [20] for example, showed that monodesmosidic oleanane-type saponins with glucuronic acid linked at the C-3 position are very common to this family. More specifically, the sequence 3-*O*- β -D-glucuronopyranosyl-22-*O*-acetyl-3 β ,22 β ,24-trihydroxyolean-12-en-30-oic acid is found in saponins isolated from *Wisteria* [2,5], *Derris* Wall. [21], and *Millettia* Wight & Arn. [11] genera, which belong to the subfamily Faboideae. This may represent a chemotaxonomic marker of this subfamily.

Experimental

General experimental procedures: Optical rotation values were recorded on a AA-10R automatic polarimeter (Optical Activity LTD). The 1D and 2D spectra (^1H and ^{13}C NMR, ^1H - ^1H COSY, TOCSY, ROESY, HSQC and HMBC) were performed using a Varian VNMR-S 600 MHz spectrometer equipped with 3 mm triple resonance inverse and 3 mm dual broadband probeheads. Spectra are recorded in pyridine-*d*₅. Solvent signals were used as internal standard (pyridine-*d*₅: $\delta_{\text{H}} = 7.21$, $\delta_{\text{C}} = 123.5$ ppm), and all spectra were recorded at T = 35°C. The carbon type (CH₃, CH₂, CH) was determined by DEPT and coupling constants (*J*) were measured in Hz. HRESIMS (positive-ion mode) were carried out on a Bruker micrOTOF spectrometer and ESIMS (negative-ion mode) on a Finnigan LCQ Deca. A R.E.U.S. ultrasonic apparatus was used for the extraction (US frequency 24 KHz, Power 200 W). Compound isolations were carried out using column chromatography (CC) on Sephadex LH-20 (550 mm x 20 mm, GE Healthcare Bio-Sciences AB), and vacuum liquid chromatography (VLC) on reversed-phase RP-18 silica gel (75-200 μm , Silicycle) and silica gel 60 (Merck, 60-200 μm). Medium-pressure liquid chromatography (MPLC) was performed on silica gel 60 (15-40 μm , Merck) with a Gilson M 305 pump (25 SC head pump, M 805 manometric module), a Büchi glass column (460 mm x 25 mm and 460 mm x 15 mm), and a Büchi precolumn (110 mm x 15 mm). MPLC was performed on reversed-phase RP-18 silica gel (75-200 μm , Silicycle) with a Gilson Pump Manager C-605, having two pumps (2x Büchi pump modul C-601). HPLC was performed on a 1260 Agilent instrument, equipped with a degasser, a quaternary pump, an autosampler, and an UV detector at 210 nm. Chromatographic separation for analytical part was carried out on a C18 column (250 mm x 4.6 mm id, 5 μm ; Phenomenex LUNA) at room temperature and protected by a guard column. The mobile phase constituted of (A) 0.01% (v/v) aqueous trifluoroacetic acid and (B) acetonitrile delivered at 1 ml/min according to the gradient 1: 0-20 min 20% B - 55% B, and the gradient 2: 0-20 min 20% B - 80% B. The injection volume was 10 μl at the concentration of 1 mg/ml. Semi preparative part: Chromatographic separation was carried out on a C-18 column (250 mm x 10 mm id, 5 μm ; Phenomenex LUNA) at room temperature and protected by a guard column. The gradient was the same at 3 ml/min. The injection volume was 0.3 ml at the concentration of 10 mg/ml. Thin-layer chromatography (TLC, Silicycle) and high-performance thin-layer chromatography (HPTLC, Merck) were carried out on precoated silica gel plates 60F₂₅₄, solvent system CHCl₃/MeOH/H₂O (60:32:7, 60:35:8 and 60:35:10 lower phase). The spray reagent for saponins was vanillin reagent (1% vanillin in EtOH/H₂SO₄, 50:1).

Plant material: The two plants were provided in 2015 from Botanic® (Quéigny, France). Voucher specimens, N°20151001 for *W. floribunda* "macrobotrys" and N°20151002 for *W. floribunda* "rosea", were deposited in the herbarium of the Laboratory of

Pharmacognosy, Université de Bourgogne Franche-Comté, Dijon, France.

Extraction and isolation of saponins from *W. floribunda* "macrobotrys": The dried powdered roots (122 g) were extracted by an ultrasonic method three times with EtOH-H₂O (75/35, 3 x 1 L) for 1 h. After evaporation of the solvent under vacuum, the resulting extract (23.4 g) was submitted to VLC (RP-18 silica gel, H₂O, MeOH/H₂O 50:50 and MeOH). The fraction eluted with 50:50 MeOH/H₂O (3g) was fractionated by CC (Sephadex LH-20, MeOH) to give four fractions (F1-F4). F1 (810 mg), rich in saponins, was submitted to a VLC on silica gel 60 (CHCl₃/MeOH/H₂O 70:30:5; 60:32:7; 64:40:8). Ten fractions (f1-f10) were obtained. Fraction f4 (139.3mg) was submitted to a MPLC (silicagel 60, CHCl₃/MeOH/H₂O 70:30:5), yielding seven fractions. One of these (61mg) was submitted to successive semi-preparative HPLC (H₂O/ACN, gradient 1, 20 min) to obtain saponin **2** (12.2 mg). Remaining fractions were collected together according to their TLC profile, and were submitted to MPLC (silicagel 60, CHCl₃/MeOH/H₂O 65:35:10, lower phase) to give saponin **1** (9.5mg), and successive HPLC (H₂O/ACN, gradient 2, 20 min) to give saponin **3** (10.0 mg).

Extraction and isolation of saponins from *W. floribunda* "rosea": The dried powdered roots (79 g) were extracted by an ultrasonic method three times with EtOH-H₂O (75/35, 3 x 1 L) for 1 h. After evaporation of the solvent under vacuum, the resulting extract (4.1 g) was submitted to a VLC on silica gel 60 (CHCl₃/MeOH/H₂O 65:35:10, lower phase) to obtain sixteen fractions (F1-F16). F3 and F8 were submitted to MPLC (silicagel 60, CHCl₃/MeOH/H₂O 65:35:10, lower phase) to give several fractions. Remaining fractions were collected together according to their TLC profile, and were submitted to successive MPLC on normal phase silicagel (CHCl₃/MeOH/H₂O 65:35:10, lower phase) and reversed-phase RP-18 silicagel (MeOH/H₂O 30:70 to 45:55) to give saponins **4** (7.5 mg) and **5** (8.7mg).

Acid hydrolysis and GC analysis: Each compound (3 mg) was hydrolyzed with 2N aq. CF₃COOH (5 mL) for 3 h at 95 °C. After extraction with CH₂Cl₂ (3 x 5 mL), the aq. layer was repeatedly evaporated to dryness with MeOH until neutral, and then analyzed by TLC over silica gel (CHCl₃/MeOH/H₂O 8:5:1) by comparison with authentic samples. Furthermore, the residue of sugars was dissolved in anhydrous pyridine (100 μL), and L-cysteine methyl ester hydrochloride (0.06 mol/L) was added. The mixture was stirred at 60 °C for 1 h, then 150 μL of HMDS-TMCS (hexamethyldisilazane/trimethylchlorosilane 3:1) was added, and the mixture was stirred at 60 °C for another 30 min. The precipitate was centrifuged off, and the supernatant was concentrated under a N₂ stream. The residue was partitioned between *n*-hexane and H₂O (0.1 mL each), and the hexane layer (1 μL) was analyzed by GC [12]. The absolute configurations were determined by comparing the retention times with thiazolidine derivatives prepared in a similar way from standard sugars (Sigma-Aldrich).

3-*O*- β -D-xylopyranosyl-(1 \rightarrow 2)- β -D-glucuronopyranosyl-22-*O*-acetyl-3 β ,22 β ,24-trihydroxyolean-12-en-30-oic acid (1**)**
White amorphous powder.

$[\alpha]_{\text{D}}^{25}$: -28.0 (*c* 0.60, MeOH)

^1H and ^{13}C NMR (600 and 150 MHz, pyridine-*d*₅): Table 1
HR-ESIMS (positive-ion mode): *m/z* 861.4268 [M + Na]⁺ (calcd C₄₃H₆₆NaO₁₆ 861.4249); ESIMS (negative-ion mode) *m/z* 837 [M - H]⁻.

References

- [1] <http://www.tropicos.org/Name/40026522>
- [2] Champy A-S, Mitaine-Offer A-C, Miyamoto T, Tanaka C, Papini A-M, Lacaille-Dubois M-A. (2017) Structural analysis of oleanane-type saponins from the roots of *Wisteria frutescens*. *Magnetic Resonance in Chemistry*, **55**, 595-600.
- [3] Konoshima T, Kozuka M, Haruna M, Ito K, Kimura T. (1989) Studies on the constituents of Leguminous plants. XI. The structure of new triterpenoids from *Wisteria brachybotrys* SIEB. *et* ZUCC. *Chemical and Pharmaceutical Bulletin*, **37**, 1550-1553.
- [4] Konoshima T, Kozuka M, Haruna M, Ito K, Kimura T, Tokuda H. (1989) Studies on the constituents of Leguminous plants. XII. The structure of new triterpenoids from *Wisteria brachybotrys* SIEB. *et* ZUCC. *Chemical and Pharmaceutical Bulletin*, **37**, 2731-2735.
- [5] Konoshima T, Kozuka M, Haruna M, Ito K. (1991) Constituents of Leguminous plants. XIII. New triterpenoid saponins from *Wisteria brachybotrys*. *Journal of Natural Products*, **54**, 830-836.
- [6] Kinjo J, Fujishima Y, Saino K, Tian R-H, Nohara T. (1995) Five new triterpene glycosides from *Wisteria brachybotrys* (Leguminosae). *Chemical and Pharmaceutical Bulletin*, **43**, 636-640.
- [7] Jiang Y, Chen X, Lin H, Wang F, Chen F. (2011) Floral scent in *Wisteria*: chemical composition, emission pattern, and regulation. *Journal of the American Society for Horticultural Science*, **136**, 307-314.
- [8] Li J, Jiang J-H, Fu C-X, Tang S-Q. (2014) Molecular systematic and biogeography of *Wisteria* inferred from nucleotide sequences of nuclear and plastid genes. *Journal of Systematics and Evolution*, **52**, 40-50.
- [9] Ono M, Iwashina T. (2015) Quantitative flavonoid variation accompanied by change of flower colors in *Edgeworthia chrysantha*, *Pittosporum tobira* and *Wisteria floribunda*. *Natural Product Communications*, **10**, 413-416.
- [10] Benchadi W, Haba H, Lavaud C, Harakat D, Benkhaled M. (2013) Secondary metabolites of *Astragalus cruciatus* Link. and their chemotaxonomic significance. *Records of Natural Products*, **7**, 105-113.
- [11] Uchiyama T, Furukawa M, Isobe S, Makino M, Akiyama T, Koyama T, Fujimoto Y. (2003) New oleanane-type triterpene saponins from *Millettia speciosa*. *Heterocycles*, **60**, 655-661.
- [12] Hara S, Okabe H, Mihashi K. (1987) Gas-liquid chromatographic separation of aldose enantiomers as trimethylsilyl ethers of methyl 2-(polyhydroxyalkyl)-thiazolidine-4(R)-carboxylates. *Chemical and Pharmaceutical Bulletin*, **35**, 501-506.
- [13] Tai B H, Trung T N, Nhiem N X, Ha D T, Phuong T T, Thu N B, Luong H V, Bae K H, Kim Y H. (2011) Chemical components from the fruit peels of *Wisteria floribunda* and their effects on rat aortic vascular smooth muscle cells. *Bulletin of the Korean Chemical Society*, **32**, 2079-2082.
- [14] Mohamed M A, Hamed M M, Abdou A M, Ahmed W S, Saad A M. (2011) Antioxidant and cytotoxic constituents from *Wisteria sinensis*. *Molecules*, **16**, 4020-4030.
- [15] Birjatinder S, Joga S, Singh MV. (2014) Ethno medicinal, pharmacological properties and chemistry of Fabaceae family. *Journal of Medical Pharmaceutical and Allied Sciences*, **02**, 24-28.
- [16] Kinjo J, Udayama M, Okawa M, Nohara T. (1999) Study of structure-hepatoprotective relationships of oleanane-type triterpenoid glucuronides obtained from several fabaceous plants on rat primary hepatocyte cultures. *Biological and Pharmaceutical Bulletin*, **22**, 203-206.
- [17] Abbas F, Zayed R. (2005) Bioactive saponins from *Astragalus suberi* L. growing in Yemen. *Zeitschrift für Naturforschung*, **60c**, 813-820.
- [18] Ionkova I, Shkondrov A, Krasteva I, Ionkov T. (2014) Recent progress in phytochemistry, pharmacology and biotechnology of *Astragalus* saponins. *Phytochemistry Reviews*, **13**, 343-374.
- [19] Tantry M A, Khan I A. (2013) Saponins from *Glycine max* Merrill (soybean). *Fitoterapia*, **87**, 49-56.
- [20] Tava A, Scotti C, Avato P. (2011) Biosynthesis of saponins in the genus *Medicago*. *Phytochemistry Reviews*, **10**, 459-469.
- [21] Zhang H-X, Sun G, Gu J-L, Du Z-Z. (2017) New sweet-tasting oleanane-type triterpenoid saponins from "Tugancao" (*Derris eriocarpa* How). *Journal of Agricultural and Food Chemistry*, **65**, 2357-2363.

Pseudoalteromone C: a Novel Ubichromenol Derivative from Bacterium <i>Pseudoalteromonas</i> sp. CGH2XX Isolated from the Cultured-type Octocoral <i>Lobophytum crassum</i> Yu-Hsin Chen, Wu-Fu Chen, Juan-Cheng Yang, Mei-Chin Lu, Jimmy Kuo, Jui-Hsin Su, Ching-Feng Weng, Yang-Chang Wu and Ping-Jyun Sung	1615
Non-alkaloid Constituents from <i>Mahonia bealei</i> Bui Van Thanh, Nguyen Thi Van Anh, Do Hoang Giang, Nguyen Hai Dang, Luu Dam Ngoc Anh, Bui Van Huong, Ngo Duc Phuong and Nguyen Tien Dat	1619
Zingerone Suppresses the Shedding of Endothelial Protein C Receptor In-Chul Lee, Dae Yong Kim and Jong-Sup Bae	1623
Suppressive Effects of Sulforaphane on TGFBIp-mediated Sepsis In-Chul Lee and Jong-Sup Bae	1627
Enzyme-treated Asparagus Extract (ETAS) Enhances Memory in Normal Rats and Induces Neurite-outgrowth in PC12 Cells Tomoko Koda, Jun Takanari, Kentaro Kitadate and Hideki Imai	1631
<i>In Vivo</i> and <i>In Vitro</i> Evidence for the Antihyperuricemic, Anti-inflammatory and Antioxidant Effects of a Traditional Ayurvedic Medicine, Triphala Vilasinee Hirunpanich Sato, Bunleu Sungthong, Narawat Nuamnaichati, Prasob-orn Rinthong, Supachoke Mangmool and Hitoshi Sato	1635
Comparison of Volatiles of <i>Sideritis caesarea</i> Specimens Collected from Different Localities in Turkey Tuğba Günbatan, Betül Demirci, İlhan Gürbüz, Fatih Demirci and Ayşe Mine Gençler Özkan	1639
Chemical Composition of Essential Oil among Seven Populations of <i>Zanthoxylum armatum</i> from Himachal Pradesh: Chemotypic and Seasonal Variation Vinod Bhatt, Sushila Sharma, Neeraj Kumar, Upendra Sharma and Bikram Singh	1643
Composition, <i>in vitro</i> Antibacterial and Anti-mildew Fungal Activities of Essential Oils from Twig and Fruit Parts of <i>Eucalyptus citriodora</i> Yu-Chang Su, Kuang-Ping Hsu and Chen-Lung Ho	1647
Antibacterial, Antiviral, Antioxidant and Antiproliferative Activities of <i>Thymus guyonii</i> Essential Oil Assia Zeghib, Ahmed Kabouche, Souheila Laggoune, Claude-Alain Calliste, Alain Simon, Philippe Bressolier, Mahjoub Aouni, Jean-Luc Duroux and Zahia Kabouche	1651
Chemoinformatic Investigation of Antibiotic Antagonism: The Interference of <i>Thymus glabrescens</i> Essential Oil Components with the Action of Streptomycin Budimir S. Ilić, Dragoljub L. Miladinović, Branislava D. Kocić, Boban R. Spalović, Marija S. Marković, Hristina Čolović and Dejan M. Nikolić	1655
Insecticidal Effect of Essential Oils Against Fall Webworm (<i>Hypantria cunea</i> Drury (Lepidoptera: Arctiidae)) Temel Gokturk, Saban Kordali and Ayse Usanmaz Bozhuyuk	1659

Natural Product Communications

2017

Volume 12, Number 10

Contents

<u>Original Paper</u>	<u>Page</u>
Fungal Biotransformation of Cyclademol and Antimicrobial Activities of Its Metabolites Ismail Kiran, Özge Özşen, K. Hüsnü Can Başer and Fatih Demirci	1529
Quantitative Analysis and Pharmacological Effects of <i>Artemisia ludoviciana</i> Aqueous Extract and Compounds Isabel Rivero-Cruz, Gerardo Anaya-Eugenio, Araceli Pérez-Vásquez, Ana Laura Martínez and Rachel Mata	1531
Guaiane Sesquiterpenes from the Rhizome of <i>Curcuma xanthorrhiza</i> and Their Inhibitory Effects on UVB-induced MMP-1 Expression in Human Keratinocytes Ji-Hae Park, Mohamed Antar Aziz Mohamed, Nhan Nguyen Thi, Kyeong-Hwa Seo, Ye-Jin Jung, Sabina Shrestha, Tae Hoon Lee, Jiyoung Kim and Nam-In Baek	1535
Further Guaianolides from <i>Chrysophthalmum montanum</i> Perihan Gürbüz and Şengül D. Doğan	1539
Anti-allergic and Cytotoxic Effects of Sesquiterpenoids and Phenylpropanoids Isolated from <i>Magnolia biondii</i> Thi Tuyet Mai Nguyen, Thi Thu Nguyen, Hyun-Su Lee, Bomi Lee, Byung Sun Min and Jeong Ah Kim	1543
Metabolomic and Proteomic Analysis of the Response of <i>Angelica acutiloba</i> after Herbivore Attack Risa Kato, Yusuke Morita, Atsutoshi Ina, Yoshiaki Tatsuo, Takayuki Tamura, Yasuhiro Tezuka and Ken Tanaka	1547
Two New Abietane-type Diterpenes from the Bark of <i>Cryptomeria japonica</i> Chi-I Chang, Chien-Chih Chen, Che-Yi Chao, Horng-Huey Ko, Hsun-Shuo Chang, Sheng-Yang Wang, Jih-Jung Chen, Cheng-Chi Chen and Yueh-Hsiung Kuo	1553
Complete Structure Elucidation of New Steviol Glycosides Possessing 9 Glucose Units Isolated from <i>Stevia rebaudiana</i> Indra Prakash, Sangphyo Hong, Gil Ma, Cynthia Bunders, Krishna P. Devkota, Romila D. Charan, Catherine Ramirez and Tara M. Snyder	1557
Cytotoxic Activities of Different Iranian Solanaceae and Lamiaceae Plants and Bioassay-Guided Study of an Active Extract from <i>Salvia lachnocalyx</i> Hossein H. Mirzaei, Omidreza Firuzi, Ian T. Baldwin and Amir Reza Jassbi	1563
Synthesis and Cytotoxic Evaluation of Betulin-Triazole-AZT Hybrids Dang Thi Tuyet Anh, Le Nhat Thuy Giang, Nguyen Thi Hien, Dinh Thi Cuc, Nguyen Ha Thanh, Nguyen Thi Thu Ha, Pham The Chinh, Nguyen Van Tuyen and Phan Van Kiem	1567
A Novel Cycloartane Triterpenoid Bisdesmoside from <i>Actaea vaginata</i> Qiongyu Zou, Meichun Wu, Yindi Zhu, Jinping Shen, Guoxu Ma, Xudong Xu, Gui Chen, Li Zhang, Zijian Zhao, Dizhao Chen and Haifeng Wu	1571
Triterpene Saponins from <i>Wisteria floribunda</i> “macrobotrys” and “rosea” Anne-Sophie Champy, Anne-Claire Mitaine-Offier, Thomas Paululat, Anna-Maria Papini and Marie-Aleth Lacaille-Dubois	1573
Magnumosides B₃, B₄ and C₃, Mono- and Disulfated Triterpene Tetraosides from the Vietnamese Sea Cucumber <i>Neothyridium (= Massinium) magnum</i> Alexandra S. Silchenko, Anatoly I. Kalinovsky, Sergey A. Avilov, Vladimir I. Kalinin, Pelageya V. Andrijaschenko, Pavel S. Dmitrenok, Ekaterina A. Chingizova, Svetlana P. Ermakova, Olesya S. Malyarenko and Tatyana N. Dautova	1577
Chemical Analysis of the Edible Mushroom <i>Tricholoma populinum</i>: Steroids and Sulfinyladenosine Compounds Bernadett Kovács, Zoltán Béni, Miklós Dékány, Orsolya Orbán-Gypapai, Izabella Sinka, István Zupkó, Judit Hohmann and Attila Ványolós	1583
A New Steroidal Glycoside Granuloside C from the Starfish <i>Choriaster granulatus</i>, Unexpectedly Combining Structural Features of Polar Steroids from Several Different Marine Invertebrate Phyla Natalia V. Ivanchina, Timofey V. Malyarenko, Alla A. Kicha, Anatoly I. Kalinovsky, Pavel S. Dmitrenok and Valentin A. Stonik	1585
A Novel Cytotoxic Physalin from <i>Physalis angulata</i> Jia-Jia Fan, Xia Liu, Xi-Long Zheng, Hai Yu Zhao, Huan Xia and Yi Sun	1589
Efficient Bioproduction of Mycosporine-2-glycine, Which Functions as Potential Osmoprotectant, using <i>Escherichia coli</i> Cells Tanutchai Patipong, Takashi Hibino, Rungaroon Waditee-Sirisattha and Hakuto Kageyama	1593
Anti-inflammatory Effect of Discretamine, a Protoberberine Alkaloid Isolated from <i>Duguetia moricandiana</i> Danilo Eduardo Costa Vieira Lemos, Luiz Henrique Agra Cavalcante-Silva, Éssia de Almeida Lima, Adriano Francisco Alves, Ana Silvia Suassuna Carneiro Lúcio, José Maria Barbosa-Filho and Sandra Rodrigues Mascarenhas	1595
Asymmetric Synthesis of Tetrahydroisoquinoline Alkaloids Using Ellman's Chiral Auxiliary Y. Vikram Reddy, Dhanraj. O. Biradar, B. Jagan Mohan Reddy, Aravinda Rathod, M. Himabindu and B. V. Subba Reddy	1599
Chemical Constituents of the Aerial Parts of <i>Santolina chamaecyparissus</i> and Evaluation of Their Antioxidant Activity Fatıha Labed, Milena Masullo, Antonietta Cerulli, Fadila Benayache, Samir Benayache and Sonia Piacente	1605
Phenolic Composition of Leaf extracts of <i>Ailanthus altissima</i> (Simaroubaceae) with Antibacterial and Antifungal Activity Equivalent to Standard Antibiotics Danijela Poljuha, Barbara Sladonja, Ivana Šola, Slavica Dudaš, Josipa Bilić, Gordana Rusak, Katlego E Motlhatlego and Jacobus N Eloff	1609
Synthesis of an Antileukemic Pyrone from <i>Alternaria phragmospora</i> Yang Qu and George A. Kraus	1613

Continued inside backcover